Advancing ecosystem understanding: Identifying the drivers of habitat degradation, species distributions and species vulnerabilities in East African grasslands.

Joris Hendrik Wiethase

Doctor of Philosophy

University of York
Department of Biology

December 2023

Abstract

Environments are changing at an accelerated rate, as a consequence of human activity. Many questions remain unanswered regarding the drivers of this change in the landscape, the mechanisms by which species are affected, and patterns of consequential species vulnerabilities. Here I use remote sensing and machine learning to investigate pathways of savannah degradation; use Bayesian species distribution models with data integration to test predictors of range shifts in savannah birds; and evaluate a common climate change vulnerability assessment framework based on simulated data and foundational concepts. I find that the most degraded savannah sites are those that decline in resistance over time and tend to exhibit lower rainfall and higher human and livestock density. However, I show that the same sites do not lose their recovery potential, giving hope for their eventual restoration under correct management. I find that degradation has increased across the whole landscape, and that this increase was lowest for national parks and wildlife management areas, underlining the effectiveness of these management strategies for mitigating current degradation trends. Next, I find little support for broad trait-range shift relationships across taxa, for either local extinctions, local colonisations, or total change. This calls into question the usefulness of traits in vulnerability assessments of taxa, where they are applied to wider taxonomic groups. However, I also identify strong species-specific relationships among the results, suggesting that more research into those individual species might reveal important trait relationships. Finally, I show that vulnerability frameworks based on separately assessed species sensitivity, exposure, and adaptive capacity, such as many trait-based approaches, are fundamentally unable to accurately predict true vulnerability of species. I showcase how recent advances in species distribution modelling can be applied to develop revised vulnerability metrics.

Acknowledgements

I would like to sincerely thank my supervisors, Prof. Colin Beale and Prof. Sue Hartley, for the help, support and guidance they have provided throughout the years. I could not have wished for better mentors; their dedication and patience through the many stages of my PhD have helped me thrive in this position, and for this I will always be grateful.

I would also like to thank my Training Advisory Panel member, Dr. Kelly Redeker. He has been incredibly supportive every step of the way, and his advice always helped steer my work in the right direction.

My thanks go to the Whole Organism Ecology group, and later the Leverhulme Centre for Anthropocene Biodiversity. The many discussions, in meetings or through personal conversations, have been instrumental in providing context to my work and helped me look at problems from a different perspective.

I am extremely grateful for the funding I received from the Natural Environment Research Council through the ACCE doctoral training program, without it this work would not have been possible.

I would like to thank my family, whose support has been limitless over the years. My parents, who helped me pursue a career in science from an early age, and who patiently listened to me trying to explain my PhD research; my grandparents, especially Klaus who I know would be proud to see me complete this PhD, and who I loved sharing stories of fieldwork and research with; my siblings who never hesitated to support me in any way they could.

Finally, my partner Hannah. Without her help and encouragement early on, I would undoubtedly not be where I am today. Through Covid lockdowns and the highs and lows of my PhD, she was at my side with unwavering positivity and support, and I will forever be grateful.

Author's declaration

I declare that this thesis is a presentation of original work and I am the sole author. This work has not previously been presented for a degree or other qualification at this University or elsewhere. All sources are acknowledged as references.

This thesis involved collaboration with Colin Beale (C.M.B.), Kelly Redeker (K.R), Sue Hartley (S.E.H.), Rob Critchlow (R.C.), Charles Foley (C.F.), Lara Foley (L.F.), Elliot Kinsey (E.J.K.), Brenda Bergman (B.B.), Boniface Osujaki (B.O.), Zawadi Mbwambo (Z.M.), Paul Baran Kirway (P.B.K.), Philip Mostert (P.S.M.), Chris Cooney (C.C.) and Bob O'Hara (R.B.O.).

Chapter 2 is a re-formatted version of the following published journal paper:

> **Wiethase**, J. H., Critchlow, R., Foley, C., Foley, L., Kinsey, E. J., Bergman, B. G., Osujaki, B., Mbwambo, Z., Kirway, P.B., Redeker, K.R., Hartley, S.E. & Beale, C. M. (2023). Pathways of degradation in rangelands in Northern Tanzania show their loss of resistance, but potential for recovery. Scientific Reports, 13(1), 2417. https://doi.org/10.1038/s41598-023-29358-6

R.C., C.M.B., C.F., L.F., E.J.K., and B.B. conceived and designed the data collection; R.C., B.O., Z.M., and P.B.K. participated in collecting the data; J.H.W. analysed the data and interpreted the results; J.H.W., R.C. and C.M.B. drafted the manuscript; J.H.W. finalised the manuscript; R.C., C.M.B., E.J.K., B.B., K.R., S.E.H., C.F. and L.F. provided input to the manuscript.

Chapter 3 is a re-formatted version of the following published journal paper:

> **Wiethase**, J. H., Mostert, P.S., Cooney, C., O'Hara, R.B. & Beale, C. M. (2024). Spatio-temporal integrated Bayesian species distribution models reveal lack of broad relationships between traits and range shifts. Global Ecology and Biogeography, e13819. https://doi.org/10.1111/geb.13819

J.H.W. and C.M.B. conceived the study; J.H.W. analysed the data and interpreted the results; J.H.W. wrote the manuscript; C.M.B., P.S.M. and R.B.O. provided input to the data analysis and interpretation of results; C.M.B., P.S.M., R.B.O. and C.C. provided input to the manuscript text.

Chapter 4 is written as for publication with the intention of submission.

J.H.W. and C.M.B. conceived the study; J.H.W. analysed the data and interpreted the results; J.H.W. wrote the manuscript. C.M.B provided input to the manuscript text.

All chapters are reproduced in full in this thesis, with minor formatting alterations to published versions.

Contents

List of tables xiii

List of figures xvi

1 Chapter 1: General Introduction **1**

1.1 Climate change and habitat alteration in the Anthropocene . 2

1.2 Impacts on habitat quality 4

1.3 Savannahs as case studies of habitat impacts 5

1.4 Impacts on species 7

1.4.1 Range shifts of species 8

1.4.2 Vulnerability assessments of species 10

1.5 Analytical advances 15

1.5.1 Remote sensing, with applications in machine learning 15

1.5.2 Species distribution modelling 17

1.6 Tanzania as a case study 21

1.7 Aims and structure of thesis 23

2 Chapter 2: Pathways of Degradation **25**

2.1 Abstract 25

2.2 Introduction 26

- 2.3 Methods 31
  - 2.3.1 Study area 32
  - 2.3.2 Choice of degradation parameters 33
  - 2.3.3 Baseline ground surveys 34
  - 2.3.4 Survey site stratification 37
  - 2.3.5 Estimating degradation parameters, using machine learning 39
  - 2.3.6 Data analysis 42
- 2.4 Results 45
  - 2.4.1 Model performance 45
  - 2.4.2 Spatial patterns 46
  - 2.4.3 Time series analysis 48
- 2.5 Discussion 55
- 2.6 Code availability 62
- 2.7 Acknowledgements 62

3 Chapter 3: Traits and Range Shifts 64

- 3.1 Abstract 64
- 3.2 Introduction 66
- 3.3 Methods 74
  - 3.3.1 Bird data 76
  - 3.3.2 Environmental covariates 77
  - 3.3.3 Estimating species ranges 78
  - 3.3.4 Mesh specification, prior choice & model evaluation 82
  - 3.3.5 Species traits 84
  - 3.3.6 Quantifying range shifts 85
  - 3.3.7 Trait-range shift relationship 89

3.4 Results 91
3.4.1 Ecological generalisation 94
3.4.2 Movement ability 94
3.4.3 Exposure-related trait 95
3.4.4 Sensitivity 95
3.4.5 Individual species associations 95
3.5 Discussion 98
3.6 Conclusion 108
3.7 Data availability 109
3.8 Acknowledgements 109

4 Chapter 4: Climate Change Vulnerability 110

4.1 Highlights 110
4.2 Abstract 111
4.3 Introduction 112
4.4 Methods 119
4.4.1 Objective 1: Reduce the SEAC framework to foundational concepts 120
4.4.2 Objective 2: Quantify true vulnerability 121
4.4.3 Objective 3: Empirical example showcasing potential improvements to vulnerability assessments 123
4.5 Results & Discussion 125
4.5.1 Quantifying vulnerability following the SEAC approach 125
4.5.2 Quantifying true vulnerability 130
4.5.3 Emergent shortcomings of separately assessed sensitivity, exposure and adaptive capacity 133
4.5.4 The case for correlative assessments 134

4.5.5 Improved correlative assessments using advances in SDM methods . . . 135
4.5.6 Empirical example: Savannah birds in Tanzania . . . 136
4.6 Conclusion . . . 140
4.7 Data availability . . . 142
4.8 Acknowledgements . . . 142

5 Chapter 5: General Discussion 143
5.1 Summary of thesis findings . . . 143
5.2 Degradation and recovery in East African savannahs . . . 145
5.3 Predictors of species responses to Anthropocene change . . 148
5.4 Prioritising species for conservation in the Anthropocene . . 151
5.5 Limitations and future directions . . . 152
5.5.1 Prospects for analytical improvements . . . 152
5.5.2 Evaluation by comparison . . . 154
5.6 Concluding remarks . . . 155

Appendices 158

A Appendix 1: Supplementary material for Chapter 2 158
A.1 Supplementary Tables . . . 159
A.2 Supplementary Figures . . . 162

B Appendix 2: Supplementary material for Chapter 3 166
B.1 Supplementary Tables . . . 167
B.2 Supplementary Figures . . . 170
B.3 Methods expanded . . . 179
B.3.1 Integrated model formulation . . . 179

B.3.2 Underlying process model 180
B.3.3 Observation models 183

C Appendix 3: Supplementary material for Chapter 4 185

C.1 Supplementary Figures 186

References 188

List of Tables

2.1 Model performance of the different classifiers evaluated for the prediction of a bare ground (BG) and invasive & toxic plants (ITP) index. Values represent averages across 10 random splits of the training partition, with standard deviation. 'Final performance' represents the performance against the holdout partition. 46

2.2 Parameter estimates and their 95% credible intervals for INLA model results predicting the rate of bare ground scores over time. Positive estimates correspond with positive rates of bare ground scores, and negative estimates with negative rates of bare ground scores. Parameters with credible intervals that do not overlap zero (bold) may be considered well supported by these Bayesian models. 55

3.1 Overview of the traits included in the analysis of range shifts. Sensitivity and niche breadth were derived from the integrated species distribution model, and corresponded to the environmental covariates included in the model formula (highest temperature, annual rainfall, longest dry spell duration, bare ground cover, human footprint). Niche breadth was calculated as the range of covariate values where P(presence) 0.5, while sensitivity was calculated as the percentage of model variation explained by the covariate. Mean dorsal reflectance was adapted from data published in Cooney et al. 2022 (Cooney et al. 2022). All other traits were derived from the AVONET database (Tobias et al. 2022). 'Kipp's distance' describes the distance between the tip of the first secondary feather and the tip of the longest primary feather. 86

A.1 Predictor variables used as input for the svr classifier. *L7* Landsat 7 product, *L8* Landsat 8 product, *B1-7* band number in Landsat 7 or 8 products. GEE: Google Earth Engine. . . 159

A.2 Data layers used in creating the rangeland-only mask. 160

A.3 Total area covered (including non-rangeland), and number of pixels used in the land use analysis in the different land use designation sites considered in the study. NP: National Park (NP), WMA: Wildlife Management Area, CCRO: Certificate of Customary Right of Occupancy, NONE: No official management/protection scheme. 161

B.1 Environmental covariates included in the species distribution models used to estimate species ranges. Covariates were summarised for the given time frames using a median. 167

B.2 Taxonomy of the species included in the trait-range shift regression analysis. Numbers in column names represent the total number of unique values in each taxonomic group. Also included are total numbers of detections in the raw observation data, for each species, and each observation data source(eBird and Tanzania Bird Atlas). Taxonomy derived from the National Center for Biotechnology Information (NCBI) database using the 'taxize' package in R (Chamberlain et al. 2013). . 168

B.3 Samples sizes, as the number of individual species, corresponding to the different levels of categorical traits included in the analyses. Based on a total of 57 study species. 169

List of Figures

2.1 Location of the study area and sites for the baseline vegetation survey in April–May 2016 (blue circles) and April 2018 (orange diamonds). Background shading represents terrain elevation, derived from Shuttle Radar Topography Mission data (Farr et al. 2007). Areas not falling into the National Park (NP), Wildlife Management Area (WMA), or Certificate of Customary Right of Occupancy (CCRO) designation were included in the study under the 'NONE' category. The map was created using QGIS 3.14 (QGIS Development Team 2022). 36

2.2 Conceptual overview of the steps involved in creating annual maps of predicted degradation scores for the study area. The map was created using R 3.2.2 (R Core Team 2016), and the flowchart was created using Adobe Illustrator Version 23.0.3 (Adobe Systems Incorporated 2022). 42

2.3 Map of normalized bare ground index scores in the study area, averaged for the years 2018–2020. Areas of high bare ground cover receive higher scores (max index = 1) and are coloured yellow, areas of low bare ground cover have lower scores (max index = -1) and are coloured purple. Gaps in the data (coloured white) are areas removed by the masking layer. The map was created using QGIS 3.14 (QGIS Development Team 2022). 47

2.4 Normalized bare ground index scores over time – areas of high bare ground cover receive higher scores. A) Split by land use designation (black: No official management/protection scheme (NONE), orange: Certificate of Customary Right of Occupancy (CCRO), blue: Wildlife Management Area (WMA), cyan: National Park (NP)) and B) Split by bare ground percentile, based on the median degradation scores of the final three years of the time series (2018-2020). Whiskers represent 95% confidence intervals around the median. Outliers are not shown. The dashed gray line in the background indicates annual median rainfall (November to October), based on CHIRPS version 2 data retrieved for the study area (Funk et al. 2015). 49

2.5 Changes in normalized bare ground index scores during the four years of greatest increase in bare ground cover, Split by bare ground percentile, based on the median degradation scores of the final three years of the time series (2018-2020). Positive numbers along the y axis signify an increase in bare ground cover, while negative numbers signify a decrease. Whiskers represent 95% confidence intervals around the median. Outliers are not shown. All contrasts were statistically different in the ANOVA tests, unless otherwise indicated. n.s.: not significant. 50

2.6 Recovery in bare ground scores following the four years of largest degradation. Split by bare ground percentile, based on the median degradation scores of the final three years of the time series (2018-2020). A) *Absolute recovery*, positive numbers along the y axis signify an increase in bare ground, while negative numbers signify a decrease in bare ground. Blue diamonds indicate annual rainfall (November to October) based on CHIRPS version 2 (Funk et al. 2015) data. B) *Relative recovery*, the proportion of decline that returns in the recovery year. A value of 1 = total recovery, 0 = no recovery, <0 = continued decline, >1 net improvement. Whiskers represent 95% confidence intervals around the median. Outliers are not shown. All contrasts were statistically different in the ANOVA tests. 52

2.7 Effect plots showing the correlations between covariates and the rate of change in bare ground cover across the time period. A) Human population density, B) Mean annual rainfall, C) Livestock density and D) Land use designation. 54

3.1 Overview of the main analytical steps conducted in the analysis. R-INLA: R package for implementing the integrated nested Laplace approximation. TZ Atlas: Tanzania Bird Atlas. Colour schemes correspond to methodological groups. Blue: Species distribution model components and inputs. Yellow: Species distribution model and outputs. Orange: Traits derived from literature. Green: Trait-range shift analysis and output. 75

3.2 Overview of range shifts observed in the study. A) Raw presence and absence data and posterior median probability of presence estimates for example species in the study. Red points/squares on the raw observations plots show raw species detections, while black points/squares show nondetections. Points represent eBird data records, and squares represent Bird Atlas records. The colour gradient in the model estimates plots shows the probability of presence as estimated by the model, with more yellow colours signifying a higher probability of presence. Dark blue and dark purple colour outlines highlight the amount of range shifts corresponding to the example species. Dark blue: Kori bustard (*Ardeotis kori*); dark purple: Von der Decken's hornbill (*Tockus deckeni*).*(continued on following page)* 93

3.2 *(continued caption)* B) Relative change factor for range shifts of individual species between the time periods of 1980-1999 and 2000-2020, separated into total range change, meaningful contraction scores, and meaningful expansion scores. Values on the y-axis are presented on the linear scale. A relative change factor of 1 corresponds to no meaningful change for contractions or expansions (area lost or gained equal to area of chance transitions), and no change for total range change (range in 1980-1999 equal to range in 2000-2020). A relative change factor of 2 corresponds to a doubling of area, and a factor of 0.5 to a halving of area. 94

3.3 Parameter estimates and their 95% credible intervals for INLA model results predicting three measures of range shifts: Total range change, meaningful contraction scores, and meaningful expansion scores. Figures A-C are derived from models including human footprint, longest dry spell duration, hottest temperature, annual rainfall, and bare ground cover as niche breadth scores (highlighted in orange). Figures D-F are derived from models including that same set of variables as sensitivity scores (highlighted in blue). Parameters with credible intervals that do not overlap zero, or credible intervals of other factor levels for categorical variables, may be considered as strong effects in the Bayesian models, and are highlighted in green. For categorical parameters, this signifies that a trait level within a category is statistically different from the reference level. The reference levels are: "Migratory ability: Low", "Locomotory niche: Insessorial" and "Trophic level: Carnivore". 97

3.4 Selected effect plots showing the correlations between covariates and different measures of range shifts. All effect plots can be accessed in the supplementary material (suppl. figures B.4-B.9). Boxplots represent categorical covariates, while scatter plots represent continuous variables. Numbers on x-axis labels represent sample sizes for levels of categorical variables. Values on the y-axis are presented on the linear scale. A score of 1 indicates that changes are exactly as expected by chance (area gained or lost equal to the area of high uncertainty transitions), and a value of 2 indicates that there are twice as many meaningful expansions or contractions as expected by chance. A score of 0.5 indicates 50% fewer transitions occurred than expected by chance. Black points are drawn on the raw data provided to the models, red dashed lines, as well as red points with red error bars are posterior model estimates derived from linear combinations. The rug plots visualise the density of the data points. ΔX is the change along units on the x-axis that corresponds with a ΔY change of units on the y-axis. 98

4.1 A) Overview of the vulnerability framework based on sensitivity, exposure, and adaptive capacity (SEAC), based on Foden et al. (2019). a) Sensitivity is defined as intrinsic to the species. While many definitions exist, they ultimately relate to the niche shape of a species. b) Exposure is defined as the extrinsic change in the environment, current or projected. c) Adaptive capacity is defined as species characteristics that mediate the impact of sensitivity and exposure on the persistence of a species, such as dispersal ability. Vulnerability is defined as the overlap of sensitivity, exposure and adaptive capacity. B) Overview of two commonly used strategies for deriving vulnerability from SEAC components, with frameworks used in practical applications. 116

4.2 Overview of the SEAC vulnerability approaches reduced to the simplest case (A), and vulnerability derived following principles of trait-based assessments (B). A) Niche shapes for four exemplar species based on simulated data, with varying slope, breadth and position of the mean (centre of curve plateau) in the spatial temperature gradient. Niche breadth represents the range of values along the x-axis for which the probability of presence is 0.5 or higher. B) Quantification of the components of the SEAC framework for each of the exemplar species, with vulnerability measurements akin to trait-based approaches. Background colours for exposure, sensitivity and adaptive capacity measurements correspond to colour panels in Figure 1. 126

4.3 The simple example, applied to geography. *(continued on following page)* 131

4.3 *(continued caption)* A) Species range maps were derived by applying the niche curves from Figure 2A to a simulated temperature field that included spatial autocorrelation. The colour gradient represents the probability of presence, ranging from 0 (not present) to 1 (present). The range sizes are calculated as the sum of all pixel-level suitability scores. B) Range maps after exposure of +4. C) Range change after exposure of +4, highlighting areas of transitions (red: colonisation, green: extinction), as well as areas of continued presence (blue), where no change in range occurred. Areas of continued absence are used as an opacity mask, with those areas fully transparent. D) Vulnerability scores calculated as log-proportional change in range size after exposure of +4. For easier interpretation, scores are labelled as relative change, where 0 represents no overall change in range size, 0.5 represents a halving, and 2 represents a doubling of size. Species D experienced large losses under some simulations, leading to several very small scores; scores were limited to those between -3 and 1 on the log scale for visualisation purposes. The line colours correspond to the colours used in Figure 2A. Box plots and density curves are based on 100 different simulations of the spatial temperature field. 132

4.4 *Empirical example for the application of recent advances in distribution modelling to climate change vulnerability assessments. (continued on following page)* 138

4.4 *(continued caption)* A) Example species, showing the current range estimates as well as change in climatically suitable area for Tanzania, under future climate scenarios SSP2-4.5 and SSP5-8.5. Suitability change maps contain a transparency layer based on quantile values emphasizing pixels where larger changes occurred. B) Species ranked by final vulnerability scores, averaged across the two climate scenarios. Scores are labelled as relative change, where 0 represents no overall change in suitable area, 0.5 represents a halving, and 2 represents a doubling. Highlighted in the photos are the species with a breeding range in Tanzania showing the largest increase (*Turdus tephronotus*) as well as the largest decrease (*Rhodophoneus cruentus*) in climatically suitable area. Photo credits: "Bare-eyed Thrush (5529613751)" by Eleanor Briccetti, CC BY-SA 2.0, via Flickr. "Rosy Patched Bush Shrike, Samburu NR, Kenya" by ChrisHodgesUK, CC BY-SA 3.0, own work. No changes made to original photos. 139

A.1 Conceptual overview of the steps involved in creating annual composite maps for the study area. 162

A.2 Validation of degradation scores, observed vs. predicted on 25% of sites not included in modelling for bare ground and number of invasive & toxic plants. Based on the final model, fine-tuned during cross-validation. Dashed lines are trend lines from a linear model on the data. 163

A.3 Yearly maps of invasive & toxic plant (ITP) cover, based on predictions from the machine learning model. Darker colors correspond to lower ITP cover. The maps were created using R 3.2.2R Core Team 2016. 164

A.4 Yearly maps of bare ground index, based on predictions from the machine learning model, not normalized. Darker colors correspond to a lower bare ground index. The maps were created using R 3.2.2R Core Team 2016. 165

B.1 Plots visualising the effect of the choice of constant sampling effort on the predicted range sizes of species. A) Range size estimates for the 57 species included in the study for the two time periods (1980-1999, 2000-2020), under different sampling effort constants, derived as different quantile values of overall sampling effort. Points are coloured based on the relative rank of each species by range size. Dashed lines connect the range size values within each species. B) Box plots based on r-square values for each species, derived from the four separate range size values of each species in panel A. Average r-square values suggest highly linear relationships for both time periods. *(continued on following page)* 170

B.1 *(continued caption)* C) Box plots based on the average change in relative range size rank for each species, as sampling effort is varied. Average range change values suggest little to no relative rank change driven by variation in the sampling effort constant. 171

B.2 Parameter estimates and their 95% credible intervals for INLA model results predicting three measures of range shifts: Total range change, meaningful contraction scores, and meaningful expansion scores. Results derived from models containing a phylogenetic random intercept term of family nested in order. Figures A-C are derived from models including human footprint, longest dry spell duration, hottest temperature, annual rainfall, and bare ground cover as niche breadth scores (highlighted in orange). Figures D-F are derived from models including that same set of variables as sensitivity scores (highlighted in blue). *(continued on following page)* 171

B.2 *(continued caption)* Parameters with credible intervals that do not overlap zero, or credible intervals of other factor levels for categorical variables, may be considered as strong effects in the Bayesian models, and are highlighted in green. For categorical parameters, this signifies that a trait level within a category is statistically different from the reference level. The reference levels are: "Migratory ability: Low", "Locomotory niche: Insessorial" and "Trophic level: Carnivore". 172

B.3 Parameter estimates and their 95% credible intervals for INLA model results predicting three measures of range shifts: Total range change, meaningful contraction scores, and meaningful expansion scores. Alternative outputs after removing 11 species containing improperly estimated niche shapes (human footprint niche breadth: 8 cases, dry spell duration niche breadth: 3 cases, rainfall niche breadth: 1 case). Parameters with credible intervals that do not overlap zero, or credible intervals of other factor levels for categorical variables, may be considered as strong effects in the Bayesian models, and are highlighted in green. For categorical parameters, this signifies that a trait level within a category is statistically different from the reference level. The reference levels are: "Migratory ability: Low", "Locomotory niche: Insessorial" and "Trophic level: Carnivore". 172

B.4 Effect plots showing the correlations between covariates and total range change, for models containing sensitivity to environmental covariates. Boxplots represent categorical covariates, while scatter plots represent continuous variables. Numbers on x-axis labels represent sample sizes for levels of categorical variables. A score of 1 indicated that no range changes occurred, and a value of 2 indicated that the range size doubled, compared to the initial range. Black points are drawn on the raw data provided to the models, red dashed lines, as well as red points with red error bars are posterior model estimates derived from linear combinations. The rug plots visualise the density of the data points. 173

B.5 Effect plots showing the correlations between covariates and meaningful extinction scores, for models containing sensitivity to environmental covariates. Boxplots represent categorical covariates, while scatter plots represent continuous variables. Numbers on x-axis labels represent sample sizes for levels of categorical variables. A score of 1 indicated that changes were exactly as expected from chance (area lost equal to the area of high uncertainty transitions), and a value of 2 indicated that there were twice as many extinctions as expected by chance. A score of 0.5 indicated 50% fewer transitions occurred than expected by chance. Black points are drawn on the raw data provided to the models, red dashed lines, as well as red points with red error bars are posterior model estimates derived from linear combinations. The rug plots visualise the density of the data points. 174

B.6 Effect plots showing the correlations between covariates and meaningful colonisation scores, for models containing sensitivity to environmental covariates. Boxplots represent categorical covariates, while scatter plots represent continuous variables. Numbers on x-axis labels represent sample sizes for levels of categorical variables. A score of 1 indicated that changes were exactly as expected by chance (area colonised equal to the area of high uncertainty transitions), and a value of 2 indicated that there were twice as many colonisations as expected by chance. A score of 0.5 indicated 50% fewer transitions occurred than expected by chance. Black points are drawn on the raw data provided to the models, red dashed lines, as well as red points with red error bars are posterior model estimates derived from linear combinations. The rug plots visualise the density of the data points. 175

B.7 Effect plots showing the correlations between covariates and total range change, for models containing niche breadth for environmental covariates. Boxplots represent categorical covariates, while scatter plots represent continuous variables. Numbers on x-axis labels represent sample sizes for levels of categorical variables. A score of 1 indicated that no range changes occurred, and a value of 2 indicated that the range size doubled, compared to the initial range. Black points are drawn on the raw data provided to the models, red dashed lines, as well as red points with red error bars are posterior model estimates derived from linear combinations. The rug plots visualise the density of the data points. 176

B.8 Effect plots showing the correlations between covariates and meaningful extinction scores, for models containing niche breadth for environmental covariates. Boxplots represent categorical covariates, while scatter plots represent continuous variables. Numbers on x-axis labels represent sample sizes for levels of categorical variables. A score of 1 indicated that changes were exactly as expected from chance (area lost equal to the area of high uncertainty transitions), and a value of 2 indicated that there were twice as many extinctions as expected by chance. A score of 0.5 indicated 50% fewer transitions occurred than expected by chance. Black points are drawn on the raw data provided to the models, red dashed lines, as well as red points with red error bars are posterior model estimates derived from linear combinations. The rug plots visualise the density of the data points. 177

B.9 Effect plots showing the correlations between covariates and meaningful colonisation scores, for models containing niche breadth for environmental covariates. Boxplots represent categorical covariates, while scatter plots represent continuous variables. Numbers on x-axis labels represent sample sizes for levels of categorical variables. A score of 1 indicated that changes were exactly as expected by chance (area colonised equal to the area of high uncertainty transitions), and a value of 2 indicated that there were twice as many colonisations as expected by chance. A score of 0.5 indicated 50% fewer transitions occurred than expected by chance. Black points are drawn on the raw data provided to the models, red dashed lines, as well as red points with red error bars are posterior model estimates derived from linear combinations. The rug plots visualise the density of the data points. 178

C.1 Effect of range of autocorrelation in the simulated spatial temperature field on true vulnerability rankings of the example species A, B, C and D. *(continued on following page)* 186

C.1 *(continued caption)* Box plots and density plots are based on vulnerability scores calculated as log-proportional change in range size after exposure of +4 (derived from 100 different simulations of the spatial temperature field). For easier interpretation, scores are labelled as relative change, where 0 represents no overall change in range size, 0.5 represents a halving, and 2 represents a doubling of size. Species D experienced large losses under some simulations, leading to several very small scores; scores were limited to those between -3 and 1 on the log scale for visualisation purposes. Box plots and density curves are based on 100 different simulations of the spatial temperature field. Heat maps show the simulated spatial temperature field under different specifications of the range of the autocorrelation (0.5, 1, 2.5, 5). 187

1

Chapter 1: General Introduction

General introduction to the central topics of the thesis

We live in a time of rapid environmental change (Theobald et al. 2020). After decades of anthropogenic habitat alteration and climate change, we are now inching closer to an official definition of this new epoch: the Anthropocene (Waters et al. 2022). As ecologists, we aim to make sense of how living things have responded to these past changes and try to anticipate how they will change in the future. Who loses, who profits, and how does this link to economic and societal needs? Decades of ecological research on ecosystem interactions have brought us closer to answering these questions, but much remains to be resolved. In this thesis, I aim to advance our understanding of the effects of environmental change, by investigating three main topics: (1) causes of habitat degradation in rangelands, (2) predictors of species range shifts and (3) species vulnerabilities to future climate change. To test the underlying questions empirically, I use data from East African grasslands, a biome that has experienced both, recent accelerated habitat alteration and changing climatic conditions.

First, I start by summarising trends of climate change and habitat alteration in the Anthropocene, globally as well as specifically in East Africa, where this thesis is focused. I then give an overview of how these changes can impact habitat quality, as well as species, with a focus on species range shifts and vulnerabilities. Moving on from ecological concepts, I summarise recent analytical advances that are crucial to answering the questions posed in this thesis, namely advances in remote sensing and species distribution modelling. Next, I introduce the study system: East African grasslands in Tanzania, followed by a brief background on recent and projected environmental change in the region and socioeconomic impacts. Finally, I present the aims of the thesis and give the overall structure of the thesis.

1.1 Climate change and habitat alteration in the Anthropocene

Anthropogenic climate change has been a defining feature of the last decades. The most recent evidence suggests that global surface temperatures have now warmed by 1.09°C compared to pre-industrial levels, putting an estimated 3.3 to 3.6 billion people at severe risk due to climate change. In the latest IPCC report, evidence gathered projects a higher than 50% chance that global warming will meet or exceed 1.5°C in the short-term, even if greenhouse gas emissions are reduced to an extremely low level. This warming will lead to more climate hazards and risks to ecosystems and human populations, and although these risks can be diminished if warming is reduced, they cannot be completely eradicated (Pörtner et al. 2022). Alongside climatic shifts, vegetation communities have undergone a restructuring globally, as a consequence of human expansion, exacerbating the negative effects of climate change. While anthropogenic land use change has been a reality for millennia, as a consequence of hunting, farming and pastoralism (Ellis et al. 2021), modern changes are accelerated (McNeill 2016; Theobald et al. 2020), e.g. with a nearly 10% increase in cropland area observed over the last 16 years (Potapov et al. 2022). This trend is predicted to continue (Powers et al. 2019), with changes in the near future including an additional 10.4% global decrease of forests projected by the end of the century (Addae et al. 2023), and a 1.4 times increase in global urban cover projected by 2050 (Zhou et al. 2019).

In East Africa, where this thesis is focused, temperatures have increased in the last 50 years by approximately 0.7°C–1°C, with the most noticeable temperature increases observed in the central and northern areas (Camberlin 2018). This trend of heating is projected to continue (Dosio 2017; Ayugi et al. 2021). In addition, the number and intensity of dangerously hot days and heat waves are set to increase considerably (Das et al. 2023). Historically, rainfall patterns in the region distinguish two main seasons, the "short rains", typically lasting from October to November, and the "long rains", typically between March and May (Nicholson 2017). However, short-term precipitation in equatorial East Africa has shown a consistent increase since the 1960s (Manatsa et al. 2013; Nicholson 2015; Nicholson 2017), while long-season rainfall in East Africa has declined continuously over the last decades (Lyon et al. 2012; Liebmann et al. 2017; Nicholson 2017). At the same time, the frequency of droughts has been on the rise since 2005 (Gebremeskel Haile et al. 2019). As for future rainfall patterns, with 1.5°C and 2°C global warming, models predict increased mean annual rainfall in the eastern parts of East Africa (Nikulin et al. 2018) and more frequent heavy rainfall events (Finney et al. 2020; Ogega et al. 2020; Li et al. 2021). This climatic trend is leading to a projected yield decline of major crops of up to 72% in the region, threatening the livelihood of millions of people (Adhikari et al. 2015). All of these trends highlight a growing need to understand the impact on ecosystems and species. This understanding forms the foundation for predicting future trends and guiding conservation and mitigation efforts.

1.2 Impacts on habitat quality

Impacts on vegetation communities can manifest in a variety of ways, from a change in composition and consequential ecosystem functioning to a complete loss of structure and biomass. While compositional changes in communities through species turnover over time is a natural aspect of ecosystems (Diamond et al. 1977; Lindholm et al. 2021), there is strong evidence to suggest that this is happening more frequently as a consequence of human activity (Daskalova et al. 2020; Dornelas et al. 2023), leading to economic impacts. What is considered habitat degradation, or reduction in habitat quality, ultimately depends on the observer: for example, the encroachment of woody plants in savannahs may increase diversity in vegetation structure, leading to higher species richness of savannah birds (Andersen et al. 2019). This might be perceived as a positive by naturalists, but simultaneously reduces the grazing potential from a pastoralist's point of view. However, a complete and unintentional loss of biomass is rarely desired from any point of view, with such changes being arguably the most drastic outcomes of habitat alteration. While a complete loss of an ecosystem is usually followed by replacement with another through succession (e.g. Rahmonov et al. 2010; Pang et al. 2018), this can have unwanted consequences, such as local extinctions of species (Sih et al. 2000), or loss of ecosystem services (Walz et al. 2021). Examples include the loss of forests due to frequent fires (Tyukavina et al. 2022), the desertification of forests (Nwilo et al. 2020), or the global loss of grasslands due to fragmentation and overgrazing (Hoekstra et al. 2005). Grasslands are now one of the most threatened biomes globally (Bardgett et al. 2021), with large declines projected in Africa (Moncrieff et al. 2016; Kumar et al. 2021). Depending on the type of grassland, up to 46% of the total area has been converted from the natural state to human-dominated land, threatening biodiversity and ecological functioning (Hoekstra et al. 2005).

1.3 Savannahs as case studies of habitat impacts

Savannahs are ecosystems characterised by a mix of grasses and trees, covering some 20 percent of the earth's terrestrial surface (Scholes et al. 1997; Lehmann et al. 2011). Due to their dynamic nature (Skarpe 1992; Touboul et al. 2018), they are an ideal case study of how anthropogenic changes can impact habitat quality and composition.

On the one extreme, savannahs can be seen as primarily open grasslands with few trees, while on the other, they are characterised by a high density of woody vegetation, interspersing the grassy surface (Scholes et al. 1997). For millennia, human activities such as planned fires and pastoralist grazing have directly shaped savannah structure (Scholes et al. 1997), alongside indirect effects from activities such as hunting. As fires or grazing become more frequent, savannahs transition to a more open state (Skarpe 1991; Dantas et al. 2013; Beckett et al. 2022), while the hunting of large herbivores like elephants may increase woody cover through a reduction of damage to trees (Skarpe 1991; Owen-Smith et al. 2019).

The past decades have seen pressures on savannahs far exceeding historic levels, due to a combination of a growing human population and consequential demand for food (Midgley et al. 2015; Lind et al. 2020), and the effects of climate change (Vågen et al. 2016; Stevens et al. 2017). A negative outcome is a transition from wooded to open savannah, and finally from open savannah to bare soil (Hill et al. 2020b). This transition is often accompanied by the encroachment of thorny, unpalatable bushes or toxic plants, a consequence of local land-use alterations like fire suppression and heavy grazing, further exacerbated by changing rainfall patterns, elevated CO_2, and changing soil nutrients (Belayneh et al. 2017). The increase in woody bushes impacts grazing potential (Smit et al. 2015), and reduces biodiversity (Pellegrini et al. 2016; Andersen et al. 2019). From a pastoralist's point of view, the ultimate outcome of these transitions is a severe degradation of the savannah, as a vanishing of grazeable biomass.

In a review study, Gibson (2009) collated evidence for grassland degradation, including savannah, on a global scale, identifying conversion to agriculture, fragmentation, and invasion of non-native species as the main causes of grassland loss. Recent advances in remote sensing have provided further evidence. Hill et al. (2020a) found that global grasslands have experienced positive trends of fractional bare soil cover between 2001 and 2018, and identified East Africa as one of the core areas for this development. In the Maasai Mara, one of East Africa's most iconic grasslands, Li et al. (2020) found that more than half of unprotected grasslands have been converted to bare soil since 1985.

1.4 Impacts on species

As climates are shifting and ecosystems are changing, the life history of species might be affected, with potential impacts on the species' persistence. Species extinctions, whether directly or indirectly caused by human activities, are the most worrying outcomes. Although the start of a Sixth Mass Extinction brought about by humans is still being debated (Cowie et al. 2022), it is generally accepted that biodiversity is changing as a consequence of recent human actions, and extinction rates are likely outpacing speciation rates (Dornelas et al. 2023). Future predictions are reason for more concern: Latest climate projections see an additional >10% of species becoming endangered in one-third of the land area in the near future, under the very likely 1.5°C warming of atmospheric temperatures, alongside a 9% increase in species at very high risk of extinction, far exceeding natural background rates (IPCC 2023). Under a scenario where temperatures increase by 4.0°C, the percentage of species at threat of extinction more than doubles (IPCC 2023). It is therefore crucial and timely to increase our understanding of how species are impacted.

1.4.1 Range shifts of species

In studies on environmental impacts on species, a primary focus is how a species' range changes. The range can be defined as the species distribution in geographical space and is determined by the species' traits, which define the type of conditions that promote survival and reproduction (Kirkpatrick et al. 1997). Such traits might include behavioural strategies that help regulate climatic conditions (e.g. Baldwin 1974), morphology that allows for successful nutrient acquisition (e.g. Grant 2017), or phenology that allows successful reproduction under changed seasons, resulting in optimal offspring fitness (e.g. Forchhammer et al. 1998; Visser et al. 2006). When conditions change enough to impact survival and reproduction, range changes usually follow.

There are two important dimensions of range change, namely range size and geographical location. While the two are not independent (i.e. species may shift geographically and simultaneously increase or decrease their range size), implications for conservation and management differ.

In terms of range size, species might experience a decrease due to a failure to move to more suitable habitat after conditions change. At its most extreme, the ultimate outcome of this trend is the complete extinction of a species. A recent example of this is the bramble cay, which has become known as the first recent mammalian extinction due to anthropogenic climate change (Gynther et al. 2016). Decreases in range size are of particular interest in assessments of extinction risk such as the Red List of the International Union for Conservation of Nature (IUCN)(Vié et al. 2009), which attempt to predict the likelihood of this ultimate outcome, and rank species according to their extinction threat level. It is hypothesised that range size links to extinction risk through resource availability, and there is evidence to suggest that this link is preserved across multiple taxa (Chichorro et al. 2019). However, the relationship between extinction risk and range size is not trivial, since actual population size may be related to range size in a non-linear fashion (Zurell et al. 2023).

Analogously, species may increase their range size: If conditions adjacent to the historic range become more suitable, and species are able to successfully disperse into these new areas while maintaining their original range, the outcome is a range expansion. Examples include the range expansion of deer in Great Britain, following decades of reforestation efforts (Ward 2005). In the literature, changes in range size are frequently assessed in relative terms, e.g. as the area newly colonised, relative to the initial range size (Yalcin et al. 2017).

In terms of geographic range location, both range size decrease and increase ultimately constitute a location change, and hence range shift. While these examples often maintain populations in the historical core range, at its most extreme, species may move fully to more suitable habitats after the loss of the historic range.

Analysing past trends in range shifts has helped researchers to increase the understanding of ecological processes shaping ecosystems, especially in response to climate change. There is now a large body of evidence showing poleward and altitudinal range shifts of species globally as a direct consequence of climate change, with species tracking their required climatic conditions with varying degree and speed (Parmesan et al. 1999; Hickling et al. 2006; Chen et al. 2011; Mason et al. 2015; Parmesan et al. 2023), with some species lagging behind (Devictor et al. 2008; Bertrand et al. 2011; La Sorte et al. 2012), putting them at risk of extinction. Estimates of future range shifts, under different scenarios of projected climatic change, can be used to establish new protected areas, based on their projected capability to harbour species in the future (Hannah et al. 2007).

There are still many questions unanswered when it comes to the processes that drive species range shifts, or range size declines. While species appear to track climatic conditions, on average, there is a great amount of inter-specific variation, with species-specific trends diverging from the general pattern (Chen et al. 2011; Howard et al. 2023). Theory suggests that traits should explain this variation, with traits like dispersal ability determining if a species can successfully shift its range. However, a growing body of research is calling into question the existence of broad generalising patterns. Recent review studies failed to find consistent links between species traits and range shifts, preserved across taxa, with often opposing trends identified in different studies, and poor explanatory power overall (MacLean et al. 2017; Beissinger et al. 2021; Howard et al. 2023).

1.4.2 Vulnerability assessments of species

Species extinctions have been a consistent characteristic of life on Earth (Raup et al. 1982; McKinney 1997). Rapid anthropogenic changes of environments in the Anthropocene, coupled with a greater understanding of the extent of current biodiversity loss, have resulted in a sense of responsibility to prevent any further such trends, where possible (Cowie et al. 2022). The sheer number of species threatened now or in the future, combined with limited allocated resources (Wiedenfeld et al. 2021), makes it impossible to prevent the extinction of all vulnerable species. An important goal in conservation is, therefore, the identification of species most in need of protection, allowing the prioritisation of species or habitats for conservation action (Brooks et al. 2006; Pullin et al. 2013). At the centre of such research lies the question of a species' vulnerability. As environments are changing, some species might emerge as winners and thrive under new conditions, while others might emerge as losers, with negative outcomes to their persistence. Vulnerability aims to describe the risk of negative outcomes for species. When quantified, it can be used to prioritise the species most in need of conservation efforts. Perhaps the earliest example of such assessments are the "red books", first commissioned in the 1960s by the IUCN, which eventually evolved into the IUCN Red List, arguably the most comprehensive and impactful register of threatened species (Rodrigues et al. 2006; Vié et al. 2009). Under IUCN guidelines, the threat level of species is assigned to one of 8 categories, using different criteria based on current range size and range and population trends over time (Betts et al. 2020). Originally borrowed from the field of natural hazards research, climate vulnerability assessments have been developed complementary to the Red List classification, and have been implemented in IPCC reports since 2007 (Foden et al. 2019).

In these applications, vulnerability is defined as the combination of a species' sensitivity to environmental changes, exposure to such changes, and adaptive capacity (from hereon the 'SEAC framework') (Foden et al. 2019). Exposure is mainly expressed by the amount of historic or future change in an environmental variable experienced across a species' observed range and is strictly extrinsic (Foden et al. 2019). Sensitivity is less uniformly defined but is considered intrinsic to the species (Foden et al. 2019). It has been quantified in a number of ways, including species' physiological traits (Gardali et al. 2012; Foden et al. 2013), climate niche size (Rinnan et al. 2019), observed range (Dickinson et al. 2014), or future range loss (Wilsey et al. 2019; Kling et al. 2020; Valencia et al. 2020). Ultimately, since sensitivity is inherent to the species, all definitions reduce to the species' fundamental niche. In the traditional SEAC framework, sensitivity and exposure are defined independently of each other, meaning that exposure is quantified as an equal pressure across species ranges (e.g. Wilsey et al. 2019; Bateman et al. 2020; Kling et al. 2020; Thurman et al. 2020), and relationships with species-level sensitivities are disregarded. In practice, however, the two are often defined as dependent, for example when sensitivity is measured as the potential future range change given exposure to projected climate change (e.g. Wilsey et al. 2019). Adaptive capacity is generally defined as the ability of species to avoid negative impacts of environmental change through adaptation (Bateman et al. 2020; Thurman et al. 2020). Such adaptation might be dispersal ability, and a species exhibiting high adaptive capacity will disperse more effectively to suitable habitat when experiencing environmental pressures, that is, it will populate a larger fraction of the suitable range than a species with low adaptive capacity would.

Range shifts are generally expected to occur where sensitivity and exposure overlap, mediated by adaptive capacity (Purvis et al. 2005). A species might persist in place where exposure to a pressure is high, but its specific sensitivity to that pressure is low, or where exposure and sensitivity are high, but adaptive capacity is also high, and similarly shift in space where high exposure coincides with high sensitivity, as well as high dispersal ability. Different vulnerability assessment frameworks exist that aim to quantify this overlap of sensitivity, exposure, and adaptive capacity. Broadly, they can be grouped into trait-based, mechanistic, and correlative/trend-based approaches (see Foden et al. 2019 for a detailed overview). In short, trait-based vulnerability assessments aim to measure the components of vulnerability through trait frameworks, tallying the number and degree of species characteristics that might correspond to each. In practice, authors quantify to what degree the traits overlap by taking the product of weighted means (e.g. Hare et al. 2016; Albouy et al. 2020; Fremout et al. 2020; McClure et al. 2023), the sum (e.g. Haji et al. 2023), or creating a more complex weighted score (e.g. Cianfrani et al. 2018; Rinnan et al. 2019; Ramos et al. 2022). This approach allows relatively rapid assessments but requires detailed knowledge of species traits that is not available for many species. Mechanistic approaches aim to assess vulnerability as a function of environmental processes, based on a deep understanding of the physiological characteristics of the ecosystem and species (Foden et al. 2019). Correlative or trend-based approaches utilise species distribution models (SDMs) at their core, quantifying vulnerability components based on observed and projected species distributions, or environmental suitability (Foden et al. 2019). Instead of tallying sensitivity, exposure, and adaptive capacity individually, a single vulnerability score is created that encompasses all three concepts. While their application is restricted to species where observation data exist, there is evidence to suggest that they outperform purely trait-based approaches in terms of their predictive power (Wheatley et al. 2017).

Vulnerability assessments based on the SEAC framework have been used in a number of different applications, such as habitat prioritisation for protection, or identifying species most in need of conservation action (e.g. Albouy et al. 2020; Coldrey et al. 2022). With the increase of species vulnerability research has come a better understanding of the shortcomings of the SEAC framework. For example, while exposure and sensitivity are relatively straightforward to quantify, adaptive capacity is more abstract, leading to some authors excluding it altogether (e.g. Gardali et al. 2012). Furthermore, climate suitability, which often forms the basis of correlative assessments, has been shown to be a poor predictor of range shifts (Howard et al. 2023), calling into question the validity of vulnerability assessments based on climate suitability alone. Potentially indicative of wider issues, studies have highlighted poor agreement in vulnerability rankings of the same sets of species if different assessments based on the SEA framework were utilised (Lankford et al. 2014; Still et al. 2015; Wheatley et al. 2017). As a consequence of the shortcomings of the SEAC framework, some authors have suggested moving away from this quantification of vulnerability entirely, instead adopting methodologies that focus on directly measuring species responses, such as distribution changes (Fortini et al. 2017a).

1.5 Analytical advances

We live in an age of big data (Brown et al. 2010), and paired with increasing computational power, this has led to analytical advances in ecology, such as in the field of machine learning (Borowiec et al. 2022) and remote sensing Guo et al. 2020. Researchers have benefited from this trend, with greater availability of satellite data (Ma et al. 2015; Hemati et al. 2021) as well as citizen science observations (Sullivan et al. 2014), together with advances in species distribution modelling (Franklin 2023), providing exciting new avenues to test species-environment relationships.

1.5.1 Remote sensing, with applications in machine learning

Starting in 1972 with the Landsat 1 program, satellites have gathered spectral data on a global scale (Wulder et al. 2019). Remote sensing of the environment is based on the utilization of a range of different wavelengths, each transmitting different layers of information. Combining wavelengths provides additional functionality, for example, a combination of red, green, and blue spectra results in naturally-coloured satellite images, while a combination of near-infrared and red spectra results in the NDVI index of vegetation greenness (Wynne et al. 2011), an index used in countless studies in ecology (Pettorelli et al. 2011). Recent decades have brought about a growing number of satellite programs, such as the Sentinel program of the European Space Agency (ESA)(Phiri et al. 2020), providing additional information at an increasingly fine scale. Simultaneously, many more remote sensing products have become freely available (Hemati et al. 2021). Remote sensing data is characterised by a high density of information, typically being collected in the form of thousands of pixels, in multiple time layers, quickly leading to large data files. Increasing computational power, and freely available platforms such as Google Earth Engine (Gorelick et al. 2017) have made it feasible to access these data without special hardware. All of this has led to a steadily increasing uptake of remote sensing data within the broader research community, and ecological studies more specifically. Common applications include analysing the connectivity of landscapes (Bishop-Taylor et al. 2018), management strategies such as fire regimes (Szpakowski et al. 2019), or tracking environmental change like deforestation or desertification (Chowdhury 2006; Albalawi et al. 2013).

The high density of information in remote sensing products lends itself to data-hungry methodologies such as machine learning (Lary et al. 2016; Maxwell et al. 2018). Broadly, machine learning allows users to identify patterns in vast amounts of data, and hence effective classification of satellite imagery (Maxwell et al. 2018). Commonly used algorithms for remote sensing include random forest, an ensemble method that generates multiple decision trees from subsets of training data and variables (Belgiu et al. 2016), or support vector machines, a non-parametric statistical learning technique (Mountrakis et al. 2011). Many of these machine learning methods are now being used to provide new global data products, such as downscaled climate data (e.g. CHELSA: Karger et al. 2017), the human footprint index (Theobald et al. 2020) or land classification products (Castelluccio et al. 2015).

Perhaps one of the most important applications of remote sensing products for ecologists lies in the field of species distribution modelling, where satellite products provide crucial context to species observations in the landscape (Leitão et al. 2019).

1.5.2 Species distribution modelling

Species distribution models have long been a key tool in ecology (Franklin 2023). At their core, they match geographical coordinates of species observations with environmental variables, to estimate the species-environment relationship, or niche space (Elith et al. 2009). This relationship is then utilised to project the estimated species occurrence onto the landscape. Knowing where species occur at one point in time provides crucial information about the habitat requirements of species. For example, the spatial occurrence can help infer required climatic conditions at the local microclimate or regional macroclimate scale (Lembrechts et al. 2019), habitat heterogeneity requirements such as vertical structure (Moudrý et al. 2023), or co-occurrence with other species, such as pollinators (Giannini et al. 2013) or species of prey (Trainor et al. 2014). If tracked across multiple time points, SDMs allow us to identify population dynamics, such as range shifts (e.g. Bond et al. 2011), biodiversity trends (Rodríguez et al. 2007), or community turnover (Wisz et al. 2013), with implications for species and community vulnerabilities and conservation management. In fact, SDMs are one of the most widely used tools in vulnerability assessments (Foden et al. 2019). Due to their spatially explicit nature and flexibility, they have been central to conservation planning (Angelieri et al. 2016; Villero et al. 2017). In the context of global anthropogenic change, SDMs are an increasingly used tool for projecting the potential impacts of climate projections on species, especially in regards to suitability (Araújo et al. 2019b).

Challenges remain in the field of distribution modelling of species. Key among them is the question of exactly what type of niche SDMs are estimating (Franklin 2023). The traditional Hutchinsonian niche concept distinguishes between the fundamental niche of species, i.e. the environmental conditions that would allow a species to persist indefinitely, as well as the realised niche, i.e. the subset of environmental conditions in which the species actually exists, as a result of competitive exclusion (Hutchinson 1957). If SDMs were to capture the fundamental niche characteristics of a species fully, this would greatly benefit conservation planning, allowing us for example to predict the possible impact of future climate change on distributions with great accuracy, or forecast range shifts of invasive species (Tingley et al. 2014; Jiménez et al. 2022). However, this is complicated by the fact that the dispersal of species is often limited by factors such as physical barriers (Goldberg et al. 2007; Caplat et al. 2016). Additionally, behavioural adaptation can allow species to persist in areas where pressures exceed physiological limits, such as utilising thermal refuges to avoid heat exposure (Milling et al. 2018), resulting in realised niches potentially exceeding the fundamental niche (Pulliam 1988). SDMs might therefore capture only a fraction of the potential distribution of species, leading to inaccurate niche estimates (Anderson 2013). Due to the high potential value of estimating the fundamental niche, efforts have been made to expand SDMs beyond a single geographical region and time period, ultimately increasing the range of environmental conditions included in the niche estimation. Methods include the addition of palaeontological records (Jones et al. 2019) or individuals colonising habitats far outside the historical range (Beaumont et al. 2009; Gallien et al. 2012). The availability of global climate data products and observation data reaching back decades provides an additional avenue: SDMs that include a temporal structure, i.e. model species distributions within multiple time slices, can help move closer to characterising the fundamental niche, relating species observations to changing environments over time, and hence a wider range of environmental conditions (Myers et al. 2015).

More generally, the basic methodology behind SDMs has been criticised. Traditionally, SDMs depend on a large amount of observation data to produce reliable estimates, restricting them to well-studied species (Boitani et al. 2011). Furthermore, quantifying uncertainty in predictions is often omitted, leading to potentially misleading distribution estimates (Beale et al. 2012). Spatial autocorrelation can further bias SDM outputs, violating the statistical assumption of independency in residuals (Dormann et al. 2007; Miller 2012) - observations that are closer together spatially tend to be more similar by nature (Tobler 1970; Koenig 1999). Due to the potential for biased results if unaccounted for, this has remained an important consideration in SDMs (Beale et al. 2010; Faisal et al. 2010; Naimi et al. 2011; Radosavljevic et al. 2014; Gaspard et al. 2019). A recent review found nearly half of the SDMs applied in studies in the last 20 years deficient in terms of model adequacy, leading to the development of standards for SDMs (Araújo et al. 2019a).

The immense value that SDMs provide has led to a constantly evolving field, striving to overcome some of the traditional challenges posed by the

SDM methodology (Franklin 2023). Starting in the 1990s with the development of the Markov chain Monte Carlo (MCMC) method (Gilks et al. 1995), Bayesian statistics have provided a compelling solution for quantifying uncertainty in SDMs. In Bayesian models, prior information can be specified in the modelling process, leading to flexibility in dealing with the complex issues of spatial data, and consequentially more realistic results, i.e. estimates closely matching known distributions (Blangiardo et al. 2015; Redding et al. 2017; Martínez-Minaya et al. 2018). MCMC played a large role in making these types of analyses possible, approximating probability distributions by constructing a Markov chain (Andrieu et al. 2008). However, shortcomings included long computation times and validity of results reliant on the convergence of the Markov chain (Taylor et al. 2014). 2009 saw the publication of the Integrated Nested Laplace Approximation (INLA) (Rue et al. 2009), an alternative method for Bayesian spatial models, with similar accuracy to MCMC, but much improved computational speed (Blangiardo et al. 2013). This is achieved through the utilisation of approximation and integration techniques as opposed to Markov chain construction (Taylor et al. 2014).

INLA is constantly being developed and new features added, with the most significant addition for SDMs being the Stochastic Partial Differential Equation (SPDE) (Lindgren et al. 2011). By utilising a triangulated mesh for approximations, a key advantage of the SPDE is computational efficiency. The user constructs this mesh through a range of parameters like triangle size and angle, balancing computational cost and model performance (Righetto et al. 2020). Providing a solution to the problem of autocorrelation, the SPDE quantifies variation in the observations that cannot be explained by the fixed effects of the model and assigns it to a spatial random effect. Two hyperparameters, namely range and marginal variance (sigma), exert control over this spatial random effect. The range determines the smoothness of the spatial field, i.e., the distance between the high and low points, while the variance dictates the amplitude of these peaks and troughs. This allowed modellers to improve SDM estimates by accounting for unexplained effects and autocorrelation issues in a flexible way (Lezama-Ochoa et al. 2020; Fichera et al. 2023), while also reducing overprediction issues outside species distribution ranges (Engel et al. 2022). One of the latest additions to INLA is the method of model-based data integration (Isaac et al. 2020). Observation data frequently come in different formats, traditionally necessitating observations to be pooled, subsequently leading to the loss of information. Model-based data integration provides a solution to this problem, maximising the amount of information retained from each data set (Isaac et al. 2020; Morera-Pujol et al. 2023). Since INLA is a relatively new method, frameworks for processes like model selection and evaluation are still being established. This includes, for example, the selection of appropriate triangulated mesh parameters based on conditional predictive ordinate (CPO) scores, a score derived from leave-one-out-cross-validation, utilising posterior sampling without the need to re-fit the model (Rivera et al. 2019; Righetto et al. 2020).

1.6 Tanzania as a case study

All of the data and analyses in this thesis are focused on Tanzania, East Africa. Tanzania is a country roughly the size of France, situated just below the Equator. The biome with the largest national cover is the savannah, a grassland biome known for its rich biodiversity and dynamic environmental characteristics. However, grasslands (which include savannahs) are experiencing a declining trend as a consequence of climate change globally (Parmesan et al. 2023). Under the Representative Concentration Pathway 4.5 (RCP4.5) climate forecast model, which considers moderate greenhouse gas emissions and assumes CO_2 concentrations will stabilize by the year 2100, the extent of African savannahs is projected to decrease significantly, with an approximately 50% loss by the year 2070 (Moncrieff et al. 2016), transitioning into closed canopy systems. Tanzania has become a key area of this trend of savannah loss (Hill et al. 2020a; Nzunda 2022). At the same time, Tanzania has experienced the effects of climate change, with increasing temperatures (Ayugi et al. 2021) and more extreme rainfall over the past decades (Shongwe et al. 2011; Dunning et al. 2018; Ongoma et al. 2018), alongside one of the highest projected increases in extreme heat events in East Africa (Das et al. 2023). It is situated in one of the hotspot areas of high human vulnerability to climate change (IPCC 2023), and is experiencing widespread land degradation (Kirui 2016). These trends combined are threatening the persistence of the unique fauna inhabiting Tanzania's grasslands, as well as the thousands of people whose livelihoods depend on this biome. As a consequence, research in this area is both timely and relevant, and current and projected future trends render it an ideal case study site.

1.7 Aims and structure of thesis

The overall aims of this thesis are to advance our understanding of ecosystem processes revolving around habitat degradation and species distribution shifts, as well as species vulnerability concepts. Here, I focus on Tanzania as the geographical area, but the implications of my findings have wider geographical reach.

Chapter 2: Pathways of degradation in rangelands in Northern Tanzania show their loss of resistance, but potential for recovery
Effective management of grasslands relies on an understanding of the processes that lead to degradation. Using remote sensing data coupled with machine learning methods and field survey data, I investigate long-term trends of grassland conditions in Tanzania, to identify if degradation stems from a loss of resistance or loss of recovery. Correlating degradation rates with a range of environmental variables, I identify factors associated with decreasing grassland conditions.

Chapter 3: Spatio-temporal integrated Bayesian species distribution models reveal lack of broad relationships between traits and range shifts.
Climate change is leading to increasing rates of global range shifts. While traits have been proposed as important factors, recent research has called this into question. By developing species distribution models that overcome traditional analytical challenges in studies of range dynamics, I test the relationship between traits and range shifts empirically. I base this on 40 years of grassland bird observation data from 57 species in Tanzania. I provide evidence that will go towards resolving the trait-range shift relationship while

showcasing methodological advances that can be utilised in future studies.

Chapter 4: Separately assessed sensitivity, exposure and adaptive capacity inadequately represent species vulnerability to climate change Climate change vulnerability assessments are important for conservation prioritisation, but studies have shown contradictory vulnerability rankings when different approaches are applied to the same species. By reducing assessments to foundational concepts using simulated examples, I critically evaluate a commonly used framework. In addition, I showcase how recently developed species distribution models can aid vulnerability assessments.

2

Chapter 2: Pathways of Degradation

Pathways of degradation in rangelands in Northern Tanzania show their loss of resistance, but potential for recovery

2.1 Abstract

Semi-arid rangelands are identified as at high risk of degradation due to anthropogenic pressure and climate change. Through tracking timelines of degradation we aimed to identify whether degradation results from a loss of resistance to environmental shocks, or loss of recovery, both of which are important prerequisites for restoration. Here we combined extensive field surveys with remote sensing data to explore whether long-term changes in grazing potential demonstrate loss of resistance (ability to maintain function despite pressure) or loss of recovery (ability to recover following shocks). To monitor degradation, we created a bare ground index: a measure of grazeable vegetation cover visible in satellite imagery, allowing for machine learning based image classification. We found that locations that ended up the most degraded tended to decline in condition more during years of widespread degradation but maintained their recovery potential. These results suggest that resilience in rangelands is lost through declines in resistance, rather than loss of recovery potential. We show that the long-term rate of degradation correlates negatively with rainfall and positively with human population and livestock density, and conclude that sensitive land and grazing management could enable restoration of degraded landscapes, given their retained ability to recover.

2.2 Introduction

Covering 47% of the terrestrial surface, rangelands are home to one third of the global population, many of whom are pastoralists who depend on rangelands to meet their daily need for shelter, water and food (Asner et al. 2004; Millenium Ecosystem Assessment Board 2005; Lind et al. 2020). Rangelands are also home to diverse ecosystems, including iconic wilderness areas such as the Serengeti and Ngorongoro. Because rangelands develop in semi-arid areas and are primarily used for grazing, they are often perceived as highly vulnerable to changes in rainfall and anthropogenic pressures (Hoffman et al. 2008; Joyce et al. 2013). With evidence of growing loss and degradation within rangelands and other semi-arid regions, the UN established the Convention to Combat Desertification (UNCCD) in 1996 (Stringer et al. 2007). Although a primary concern that led to the UNCCD were a series of Sahelian droughts that have now ended, concern about loss of rangelands and increasing degradation among the remaining rangeland areas has continued (Vågen et al. 2016; Stevens et al. 2017). If we are to effectively combat degradation within rangelands, it is important that we understand the drivers of mechanisms by which degradation occurs.

The UNCCD identifies Africa as particularly vulnerable, estimating that land degradation is affecting more than half the continent's population (Muñoz et al. 2019). Here, rangelands are synonymous with savanna, a biome defined by the presence of C4 grasses, generally occurring in regions with rainfall between 450 mm and 1500 mm per year and often maintained by fire (Bond et al. 2005; Lehmann et al. 2011; Staver et al. 2011). The savanna biome encompasses several habitats, from open grasslands to deciduous woodlands. A key aspect of savanna ecosystems is their high temporal and spatial heterogeneity, a factor that necessitates mobility in human and wildlife populations to exploit patchy resources (Fuhlendorf et al. 2017; Liao et al. 2020). Societal and land use constraints limit the ability of populations to move when conditions become temporarily unsuitable, and sustained grazing alters the dynamics of savannas, reducing their ability to sustain grazing (Galvin 2009; López-i-Gelats et al. 2016).

Heavy, year-round grazing in savannas reduces grazing potential (i.e. quantity of vegetation palatable to grazers) through two pathways that result in either land invaded by toxic and unpalatable plants, including bush encroachment (Obiri 2011; Stevens et al. 2017), or in bare ground experiencing soil loss (Kioko et al. 2012). Rangeland degradation has been defined as a long-term decline in productivity resulting in rangelands unsuitable for grazing (Kotiaho et al. 2018), rather than short-term declines driven by temporal variability of environmental conditions (e.g. rainfall, grazing pressure). Such degradation has been linked to rainfall patterns (Western et al. 2015), and might be exacerbated by climate-change driven changes in annual rainfall variability, already widely observed across African savannas (Dai 2011). At either end of the savanna rainfall gradient, continued precipitation change may interact with pressures like grazing in a way that leads to permanent loss of savannas. Further research into the relationship of these interacting factors with long-term trends of degradation is needed to better understand their importance for sustainable rangeland management.

Degradation and loss of savannas is already a primary driver of poverty and displacement of human populations in Africa. With a rapidly growing human population (averaging a growth rate of 2.2% per year in Africa, Holechek et al. 2017), the anthropogenic demands on savannas are growing, while the pressures from climate change are simultaneously mounting (Midgley et al. 2015; Lind et al. 2020). In a recent study, Hill et al. (2020b) identified East Africa as a focal point for increases in bare ground cover, and recommended investigating these trends at a finer spatial scale. In order to meet growing demands from humans and their livestock in the face of potentially deteriorating environmental conditions we must identify how to increase sustainability of savanna use.

Resistance and recovery are two processes that underpin sustainable use of ecological resources (Lake 2013), particularly in environments that normally function within cycles of change. Together, these processes define the 'resilience' of a system (Hodgson et al. 2015). Resistance describes the ability of an ecosystem to continue to maintain function (such as the provision of grazing) despite external pressures, while recovery describes the internal processes that pull a system back towards the pre-disturbed state (Hodgson et al. 2015). In this context, ‘shocks’ are referred to as any event in the environment that leads to reductions in rangeland condition beyond the typical, interannual oscillation around the baseline state of rangeland health. Such events might include extreme droughts, or heavy rain resulting in floods. It is important to distinguish between resistance and recovery because management aimed at increasing recovery might be different to that designed to increase resistance. For example, in rangelands, resistance may be increased by promoting a high diversity of grass species or a particularly beneficial grass community composition (Tilman et al. 1994), while recovery may require, in addition, temporal variation in grazing pressure, for example through temporary grazing exclusion (Fedrigo et al. 2018).

It is unclear whether the recent trend in savanna degradation is driven by reduced recovery potential, a decline in resistance, or both (Ruppert et al. 2015). Observing the long-term trends of rangeland condition, quantified by a degradation index, helps reveal the mechanisms behind eventual degradation of habitats: If degradation is driven by a loss of recovery, areas that become degraded will show the same short-term response (i.e. reduction in rangeland condition) to external shocks as comparable sites, but would be expected to recover more slowly, and potentially insufficiently, before the next shock occurs. Alternatively, if degradation is driven by a loss of resistance, areas that become degraded will show a greater initial response to shocks, and will therefore be less likely to have recovered to pre-shock conditions before another shock occurs, despite similar recovery rates to more resistant areas. Recovery and resistance are not mutually exclusive, and may interact with land management or rainfall conditions to generate different relative impacts in different areas. Quantifying the relative effects of resistance and recovery is important to identify management priorities for savannas (Ruppert et al. 2015).

The rangelands of Northern Tanzania are typical of many African savannas. They are home to significant populations of pastoralists (Homewood 2004; Lind et al. 2020) and hold globally important wildlife populations (Caro et al. 2016), yet there is widespread concern about their loss and degradation (Bollig et al. 1999). Wildlife numbers are falling and poverty is high: degradation has been identified as a key contributor to this problem (Veldhuis et al. 2019) but is not ubiquitous. Across Northern Tanzanian rangelands there is considerable variation in the degree of degradation and in anthropogenic and environmental drivers of degradation. For example, in our study area, rainfall varies from 400 to 900 mm (Nicholson 2017), human population from 5 to 35 people per km^2 (*2012 Population and Housing Census* 2013) and livestock densities up to 250 head of cattle per km^2 (Kiffner et al. 2016). These landscape conditions are also moderated by a variety of conservation-related land use restrictions. The combination of all of these interacting components makes Northern Tanzania an ideal location to study the processes that shape recovery and resistance in rangeland dynamics.

Here we combine field data on vegetation structure with high-resolution satellite data gathered over the last two decades (a period spanning two severe droughts) to identify the drivers of degradation within Northern Tanzanian rangelands. Our aims were to (1) test whether long-term changes in grazing potential demonstrate loss of resistance, loss of recovery, or both, and (2) identify how spatial variation in land use designation, human and livestock density, and rainfall patterns impact degradation pathways at a fine spatial scale. We hypothesize that drier areas experience higher rates of degradation, and we expect both livestock and human population density to be positively correlated with degradation. We predict that long-term rates of degradation correspond to the degree to which grazing is managed by official land use designation, with areas that have the most grazing restrictions (i.e. national parks) exhibiting the lowest increases in degradation. Finally, we hypothesize that loss of recovery and loss of resistance both contribute to long term degradation patterns.

2.3 Methods

To test whether loss of resistance or recovery is the primary mechanism driving degradation in Northern Tanzanian rangelands, we (a) chose key parameters that defined degradation within our study area, (b) quantified variation in degradation across the landscape, and (c) evaluated how degradation changed at specific locations over time. We evaluated bare ground cover and the number of invasive & toxic plants (ITP), measured as the abundance of three key plant species, as candidates for degradation parameters. We used field survey data gathered in 2016 and 2018, across sampling sites stratified throughout the study region, to train a machine learning algorithm. Using this algorithm, we estimated degradation parameters for the years 2000 to 2020, based on Landsat satellite images and rainfall data, taking into account seasonal variation of vegetation productivity. Subsets of survey data were used to ground truth and test model outputs. We then tested whether estimated degradation outcomes correlated with spatial maps of anthropogenic and environmental variation. When considering long-term trends in degradation, we accounted for the effects of temporal and spatial variation in annual rainfall.

2.3.1 Study area

The study area consisted of 30,300 km^2 of the Tarangire-Manyara ecosystem and Maasai Steppe of northern Tanzania (Fig. 2.1). This is a semi-arid ecosystem, dominated by Acacia-Commiphora woodland (Msoffe et al. 2007). Annual rainfall is bimodal (rains in November to January and March to May) with large inter-annual variability (Foley et al. 2010). The 20 years considered in this study covered multiple positive and negative phases of Indian Ocean Dipole (IOD) and the El Niño–Southern Oscillation (ENSO), which represent large scale climate processes that impact rainfall in East Africa (Kebacho 2021). Notable droughts in the study region were recorded in 2003-4 and 2016-17, when average rainfall was around 50% below average (Foley, unpublished data). The period between October 2019 – January 2020 was the wettest recorded in East Africa in over two decades (Wainwright et al. 2021). The stratified sampling locations fell into areas of four different land use strategies. These included, in descending order according to the degree of grazing restrictions:

- NP: Two national parks (Tarangire, established 1970, and Lake Manyara, established 1960, where grazing is outlawed, but some illegal grazing persists, Abukari et al. 2018).
- WMA: Four wildlife management areas (WMAs) (Enduimet, Randilen,

Burunge and Makame), established beginning in 2003 (Kaswamila 2012). WMAs primarily give communities the rights to manage wildlife on their lands, as well as grazing activities, but all activities are managed by a WMA board.

- CCRO: Areas secured by the Certificate of Customary Right of Occupancy (CCRO) initiative (NTRI 2016), a relatively new intervention implemented beginning in 2015, whereby communities retain land ownership and decide on land use practices.
- NONE: Land not covered under any official management/protection scheme.

2.3.2 Choice of degradation parameters

Since this study focused on rangeland habitats, we chose degradation parameters from a grazing potential perspective. We followed the Intergovernmental Science-Policy Platform on Biodiversity and Ecosystem Services (IPBES) definition of rangeland degradation, as "persistent loss of vegetation productivity cover, especially of those plants which support herbivores." (Kotiaho et al. 2018). Our proposed parameters consisted of an index of bare ground cover (absence of grazeable vegetation cover) and the number of individual ITP, which replace plants palatable to herbivores. The latter consisted of three key plant species, all native to the area, but behaving like invasive plants: *Ipomea hildebrantii*, an evergreen woody shrub that can significantly decrease grass biomass production (Mworia et al. 2008; Manyanza et al. 2021); *Solanum campylacanthum*, a thorny shrub which has been shown to be highly toxic to livestock (Thaiyah et al. 2011); and *Dichrostachys cinerea*, a fast growing tree species that accounts for the majority of bush encroachment in African savannas (Roques et al. 2001).

2.3.3 Baseline ground surveys

We used ground survey data to train and validate remote sensing estimates of degradation. To select survey sites across the study area (Fig. 2.1), we stratified the ecosystem to ensure data collection from a complete representative selection of land cover, vegetation quality and rainfall levels. This survey stratification also allowed manageable sampling and route planning for accessing sites across the ecosystem. The strata were based on combinations of rainfall, mean annual NDVI (vegetation greenness) for the year 2015, and land cover type (grassland and woodland) (see section 'Survey site stratification' for details). We chose April and May as the sampling months since this coincided with the end of the wet season and consequential peak vegetation growth, enabling plant species identification (Riginos et al. 2010). We randomly selected 250 cells evenly across all strata to sample using a basic vegetation survey, with the centre of each 500 m cell selected as the focal sampling point for the vegetation survey. Neighbouring cells were excluded. Some 43 target cells were unsuitable (e.g. recently cleared crops) or inaccessible, resulting in 208 cells sampled between April and May 2016. To increase the geographic spread of sampling locations, during April 2018 additional 48 vegetation surveys were carried out across the ecosystem, three of which targeted areas containing *D. cinerea*. This allowed us to train the machine learning algorithm on a wider range of values, improving the performance when applied over the full study region. The total number of survey locations used in the analysis was 256.

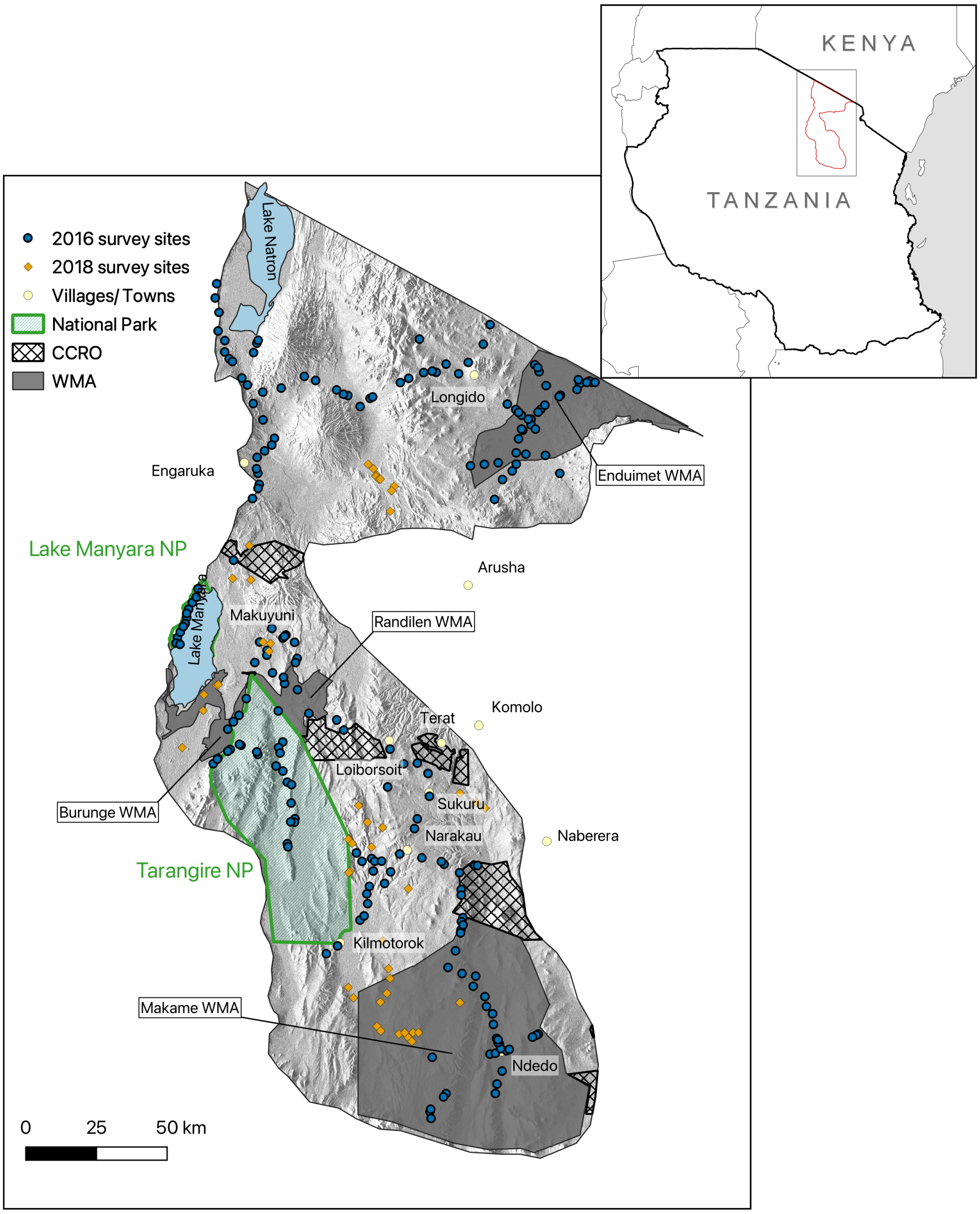
KENYA
TANZANIA
2016 survey sites
2018 survey sites
Villages/ Towns
National Park
CCRO
WMA
Lake Natron
Longido
Enduimet WMA
Engaruka
Lake Manyara NP
Arusha
Lake Manyara
Makuyuni
Randilen WMA
Komolo
Terat
Loiborsoit
Sukuru
Burunge WMA
Narakau
Naberera
Tarangire NP
Kilmotorok
Makame WMA
Ndedo
0
25
50 km

Figure 2.1: Location of the study area and sites for the baseline vegetation survey in April–May 2016 (blue circles) and April 2018 (orange diamonds). Background shading represents terrain elevation, derived from Shuttle Radar Topography Mission data (Farr et al. 2007). Areas not falling into the National Park (NP), Wildlife Management Area (WMA), or Certificate of Customary Right of Occupancy (CCRO) designation were included in the study under the 'NONE' category. The map was created using QGIS 3.14 (QGIS Development Team 2022).

At each survey site (Fig. 2.1), we collected data based on the Monitoring Rangeland Health guide (Riginos et al. 2010), which is designed for rapid vegetation and degradation assessments with minimal equipment. Measurements were taken at sampling points every five meters along four 25 m transects extending north, east, south and west, resulting in a 50 x 50 m cross, diagonally covering a plot of 35 x 35 m. At every sampling point, measurements were recorded at 5 notches along a 1 m measuring stick, leading to a total of 100 individual data points (25 for each of the four 25 m transects). The following measurements were quantified: (1) The number of invasive and/or toxic rangeland species (*I. hildebrantii*, *S. campylacanthum* and *D. cinerea*), as a total count of stems at the survey site across all sampling points. (2) The percentage of bare ground, as the percentage of notches falling onto bare ground, across sampling points at the survey site. Measures of plant density and bare ground were not mutually exclusive, e.g. a count of one plant of *D. cinerea* could coincide with a high percentage of bare ground at a given sampling point, in the absence of ground vegetation.

2.3.4 Survey site stratification

We used remote sensing data (MODIS), accessed and downloaded using the Google Earth Engine (GEE) cloud computing platform (Gorelick et al. 2017), to stratify vegetation survey locations. This stratification allowed us to collect samples over a range of different environmental conditions. The MODIS products included: MOD13A1 (Didan 2015), a 16-day Normalized Difference Vegetation Index (NDVI) composite (a measure of vegetation productivity), at a 500 m resolution from which we calculated the mean NDVI value per grid cell from all 2015 data; MCD12Q1 (Friedl et al. 2019), a land cover product providing five annual classification layers for global land cover at a 500m resolution. Land cover per grid cell was calculated at the most common annual BIOME-Biogeochemical Cycles (BGC) classification between 2001 and 2013; MOD09A1 (Vermote 2015), an 8-day land surface reflectance product, downloaded for May 2015–April 2016.We further retrieved rainfall data at 0.05° resolution for the years 2000–2020 from CHIRPS version 2 (Funk et al. 2015), a quasi-global dataset, ranging from 50°S to 50°N, that combines satellite imagery with rainfall station data to create a gridded rainfall time series. We calculated mean rainfall for the period 2000–2020, interpolated to the same resolution as the MODIS data. For each 8-day MODIS reflectance tile, we interpolated single missing values in all seven bands due to cloud cover based on the average of the preceding and succeeding tiles. Where there were cells with two or three successive missing values, these were replaced by linear interpolation using the 'na.approx()' function in the ‘zoo’ package (Zeileis et al. 2005) in R 3.2.2 (R Core Team 2016). The sample stratification resulted in a design that spanned a wide rainfall gradient, from 360 mm to 1095 mm total annual rainfall.

2.3.5 Estimating degradation parameters, using machine learning

We obtained remotely sensed satellite data for the machine learning regression from Landsat through Google Earth Engine, at 30 m resolution, which closely matched the 35 m vegetation survey plots. We combined Landsat 5, 7 and 8 products (courtesy of the U.S. Geological Survey) to maximise data coverage for our study period and region. For Landsat 7 products, the scan line correction device failed in May 2003, leading to a 22% loss in values for each scene (Scaramuzza et al. 2005). A gap-filling function was applied in GEE to mitigate this. For each Landsat product, we calculated per-pixel cloud scores and only included pixels with less than 10% cloud cover.

Based on the Landsat images, we calculated yearly indices that had the potential to indicate patterns of rangeland degradation at 30 m resolution. All composites were created starting in November the previous year, and ending in October of the given year used for predictions, to capture the seasonality in the region. Vegetation indices are used as a quantitative measure of vegetation productivity; we therefore calculated the enhanced vegetation index (EVI), an index that is optimised for areas with high productivity and variations in soil brightness (Huete et al. 2002). Next, we calculated a bare soil index (BSI) based on a formula introduced by Rikimaru et al., which combines the NDVI and normalised difference built-up index (Rikimaru et al. 2002), and has been used in similar studies (Diek et al. 2017). We calculated the modified soil-adjusted vegetation index (MSAVI), a vegetation index with increased dynamic range over NDVI, and reduced soil background bias (Qi et al. 1994).

We used harmonic regression to calculate trend variables (magnitude, phase) for EVI, BSI, and MSAVI. This allowed us to capture the seasonal change of vegetation indices (i.e. variation in plant phenologies), a quantification that can improve the predictive power of classifiers (Adams et al. 2020), and was lacking from the yearly averages used for the remaining indices. Finally, we included the total yearly rainfall at the pixel level, based on CHIRPS data, to account for the potentially strong effect rainfall might have on the chosen degradation parameters. Recognising that the amount of grass present at the end of a rainy season is influenced both by the severity of the preceding dry season and the total rainfall across the previous rainy season, we computed annual rainfall from May in the previous calendar year, to the end of April in the focal year. Supplementary Figure A.1 provides a conceptual overview of the steps involved in creating the composite layers. Supplementary Table A.1 gives a summary of all predictor variables used to train the model algorithm. To minimise unnecessary computations, a mask layer was created that excluded any data for non-savanna habitat. Supplementary Table A.2 gives an overview of data products and parameters used to create the mask.

Supervised Machine learning regression algorithms were trained and evaluated in GEE. The surface survey data were joined with predictor variables at the respective sampling locations and years (2016 or 2018), and randomly split into a holdout testing partition (25%) and training partition (75%). The training partition was used for repeated random cross-validation, using ten repeats, and 75%-25% splits for training and validation subsets. Model performance was evaluated using the average r-squared value and RMSE with standard deviation for observed vs. predicted results, across all ten repeats.

Model parameters were tuned in GEE, and the final, best performing model was evaluated against the testing holdout partition, previously unseen by the model. This workflow provided us with an unbiased approach to evaluate the models ability to generalize, and avoid overfitting (Nwanganga et al. 2020). The predictor variables had very different ranges, and were standardised to improve model performance. The bare ground cover values were skewed towards zero, and an improved model performance was achieved by log-transforming the response: log(x+1). The final model for the classification was trained using all of the ground truth data available. Different classification algorithms were evaluated. Random forest (RF) and support vector regression (SVR) with radial kernel and nu parameter were chosen since they are known to perform well in remote sensing applications (Adam et al. 2014). The accuracy performance of one over the other differs between studies (Adam et al. 2014; Mansour et al. 2016; Hunter et al. 2020), warranting a direct comparison. While less often used in remote sensing studies, gradient boosting trees (GBT) have outperformed SVR and RBF algorithms on some occasions (Yang et al. 2018; Pham et al. 2020), and it was therefore included in the comparison. The resulting predictions were back-transformed from the log scale to the original scale for bare ground scores and scaled using the 2016 mean and standard deviation. Final prediction maps were visualised in GEE for every year, to check for abnormalities. Figure 2.2 gives a conceptual overview of all steps involved in predicting degradation scores, based on the annual composite maps.

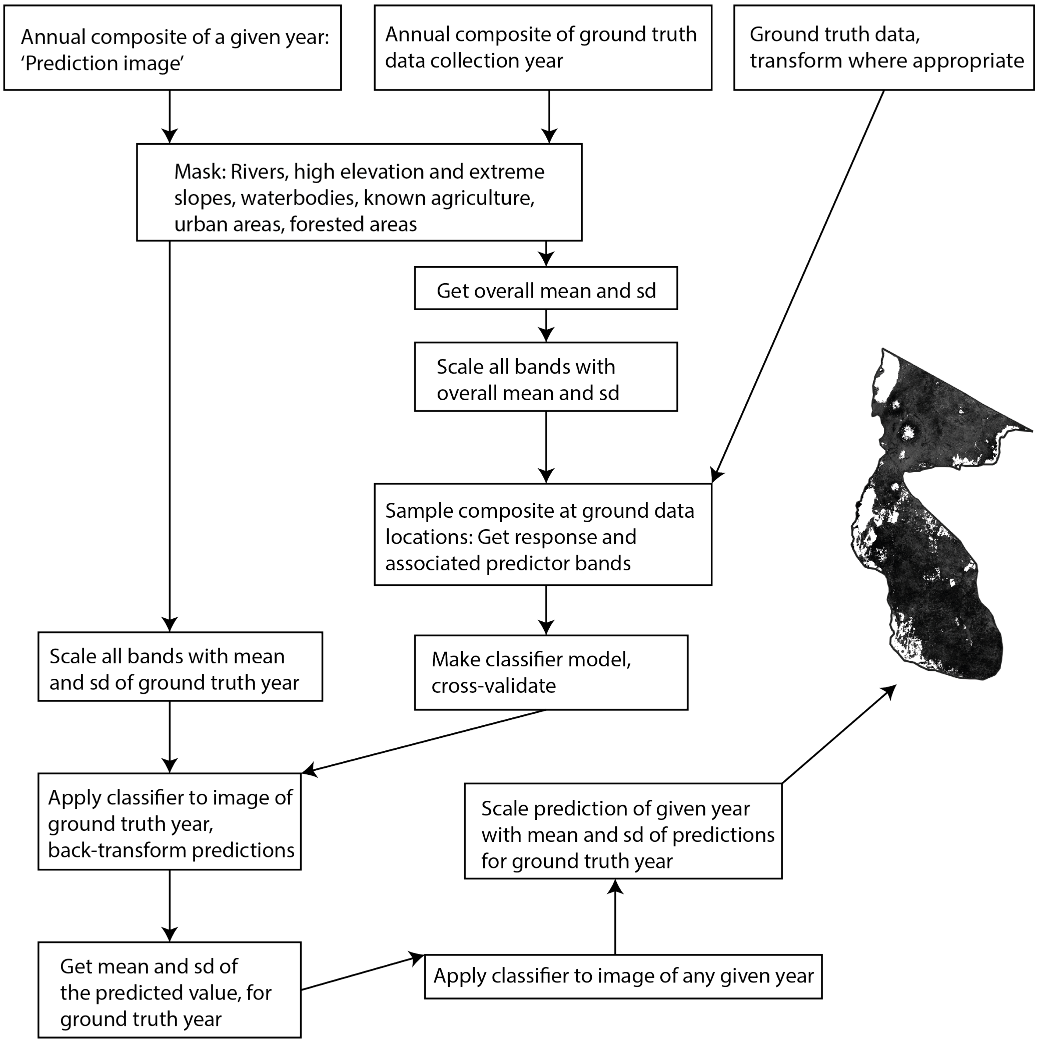
Annual composite of a given year: 'Prediction image'
Annual composite of ground truth data collection year
Ground truth data, transform where appropriate
Mask: Rivers, high elevation and extreme slopes, waterbodies, known agriculture, urban areas, forested areas
Get overall mean and sd
Scale all bands with overall mean and sd
Sample composite at ground data locations: Get response and associated predictor bands
Scale all bands with mean and sd of ground truth year
Make classifier model, cross-validate
Apply classifier to image of ground truth year, back-transform predictions
Scale prediction of given year with mean and sd of predictions for ground truth year
Get mean and sd of the predicted value, for ground truth year
Apply classifier to image of any given year

Figure 2.2: Conceptual overview of the steps involved in creating annual maps of predicted degradation scores for the study area. The map was created using R 3.2.2 (R Core Team 2016), and the flowchart was created using Adobe Illustrator Version 23.0.3 (Adobe Systems Incorporated 2022).

2.3.6 Data analysis

Estimates were made at a 30 m resolution to match the 35 m vegetation plots, but aggregated to 200 m resolution for further analyses using a median. This aggregation reduces stochastic noise potentially arising from extreme values across the 200 m pixels (i.e. very high degradation pixels neighbouring very low degradation pixels), at the cost of ignoring fine-scale patterns. We argue, however, that degradation from a grazing perspective is most meaningful if observed at a scale above 30 m resolution and across the larger scales at which grazing decisions are made. To test hypotheses about resistance and recovery, we normalized degradation scores between 0 and 1, and divided the savanna landscape into three even-sized classes identifying the most, least, and medium degraded areas, based on the median degradation scores of the final three years of the time series (2018–2020). If loss of resistance underpins degradation, we anticipated that sites that are most degraded by the end of the time series would show bigger changes during years with large declines in degradation. If lack of recovery underpins degradation we anticipated that the first year of recovery following a large decline would see smaller recoveries in the most degraded areas. As recovery could be measured in absolute or relative terms (i.e. number of units recovered, or proportion of decline recovered) we considered both quantifications. We used two-way ANOVAs in R to statistically compare classes. We estimated the marginal means for covariates based on the model using the 'emmeans' package (Lenth 2021), and conducted Tukey's post hoc tests for pairwise comparisons. It should be noted that, due to the large sample sizes in these comparisons, traditional statistical significance becomes almost inevitable (Royall 1986).

To test hypotheses regarding the mechanisms leading to degradation, we computed the pixel-wise linear rate of degradation parameters at a 200 m resolution across the entire time series (long-term trend), taking into account the annual variation of rainfall when calculating the slope. We fitted a spatially-explicit hierarchical Bayesian regression model using Integrated Nested Laplace Approximation (INLA) with the Stochastic Partial Differential Equation (SPDE) approach in the package 'R-INLA' (Rue et al. 2009; Lindgren et al. 2015; Bakka et al. 2018) in R. INLA offers a fast, flexible alternative to Markov-Chain Monte-Carlo methods for fitting complex regression models and allows us to estimate the effects of spatial covariates while accounting for the non-independence of spatial data (Lobora et al. 2017). The model correlated the long-term rate of degradation to human population density for 2017 (from the Landscan dataset, Bright et al. 2018), livestock density for the year 2010 (measured in Tropical Livestock Units based on cattle, goats, and sheep, data from the Gridded Livestock of the World database, FAO, Gilbert et al. 2018), the land use designation (NP, WMA, CCRO, and NONE) as a categorical variable, and total annual rainfall (from the CHIRPS data). Including rainfall as a covariate explicitly accounted for the spatial variation in rainfall, a variable that drives large amounts of variation in grassland productivity (Yang et al. 2008; Guo et al. 2012), and would likely mask trends if unaccounted for. The statistical power of the regression analysis was related to the number of pixels considered. Supplementary Table A.3 gives an overview of the sample sizes used for the land use designation analysis.

Initial models revealed that the estimated range of the spatial autocorrelation was very small, requiring a very fine mesh resolution to fit a smooth SPDE. We created a simple spatial mesh at the point locations using the 'inla.mesh.create' function in 'INLA', covering the study region and extending beyond the border (using the default settings), to avoid boundary effects of the SPDE. We cross-validated the fit of the model by visually inspecting probability integral transform (PIT) values (Wang et al. 2018).

2.4 Results

2.4.1 Model performance

The random forest (RF) model slightly outperformed support vector regression (SVR) for predicting the bare ground scores during cross-validation but performed considerably worse on the holdout partition (Table 2.1), and SVR was chosen for the final classifier model for the bare ground index. Gradient boosting trees performed best on the holdout partition for predicting the number of invasive & toxic plants (ITP), but considerably worse than SVR and RF during cross-validation. SVR performed better than RF during cross-validation, but performed slightly worse than RF on the holdout partition (Table 2.1), and RF was chosen for the final classifier model for the number of ITP. See Supplementary Figure A.2 for validation plots of the final models. When visualizing the prediction maps for the number of ITP, we observed inter-annual variation far greater than plausible for relatively slow-growing woody plants (see Supplementary Fig. A.3), suggesting that the model did not sufficiently differentiate ITP from the remaining vegetation. We therefore excluded this parameter from further analysis and focused on bare ground cover only.

Table 2.1: Model performance of the different classifiers evaluated for the prediction of a bare ground (BG) and invasive & toxic plants (ITP) index. Values represent averages across 10 random splits of the training partition, with standard deviation. 'Final performance' represents the performance against the holdout partition.

Classifier	Response	RMSE	R^2	Final performance
Random Forest	BG	0.16 (± 0.02)	0.41 (± 0.10)	RMSE: 0.17, R^2: 0.33
	ITP	48 (± 8)	0.53 (± 0.70)	RMSE: 46, R^2: 0.57
Gradient Boosting Tree	BG	0.21 (± 0.02)	0.38 (± 0.1)	RMSE: 0.20, R^2: 0.31
	ITP	57 (± 12)	0.42 (± 0.11)	RMSE: 51, R^2: 0.60
Nu SVR	BG	0.17(± 0.02)	0.38 (± 0.11)	RMSE: 0.15, R^2: 0.43
	ITP	48 (± 9)	0.59 (± 0.11)	RMSE: 65, R^2: 0.54

2.4.2 Spatial patterns

Maps of bare ground index scores showed expected spatial patterns. We found lower bare ground cover in Tarangire and Lake Manyara national parks, as well as in the forests surrounding the peaks in the north of the study area (Fig. 2.3).

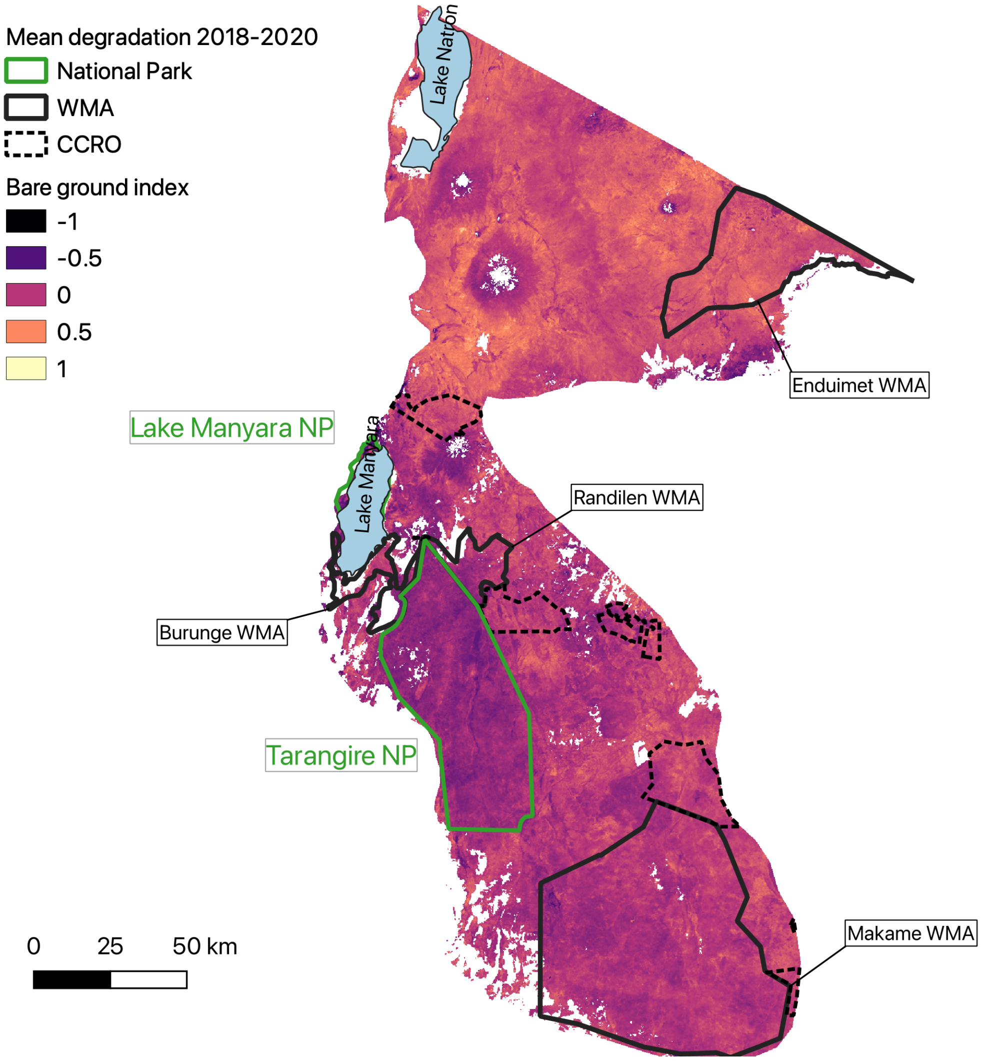
Mean degradation 2018-2020
National Park
WMA
CCRO
Bare ground index
-1
-0.5
0
0.5
1
Lake Natron
Enduimet WMA
Lake Manyara NP
Lake Manyara
Randilen WMA
Burunge WMA
Tarangire NP
Makame WMA
0
25
50 km

Figure 2.3: Map of normalized bare ground index scores in the study area, averaged for the years 2018–2020. Areas of high bare ground cover receive higher scores (max index = 1) and are coloured yellow, areas of low bare ground cover have lower scores (max index = -1) and are coloured purple. Gaps in the data (coloured white) are areas removed by the masking layer. The map was created using QGIS 3.14 (QGIS Development Team 2022).

2.4.3 Time series analysis

Annual rainfall in the study area was variable and corresponded to recorded rainfall extremes. During the drought years of 2003–2004, rainfall in the study area remained at a lower level, and rainfall dipped during the drought of 2016–2017 (Fig. 2.4). The extreme rainfall of 2020 had a strong impact in the study area, with the year exhibiting highest recorded rainfall during the timeline (Fig. 2.4). We found clear year-to-year variation in bare ground scores (Fig. 2.4). Consistent land use designation effects were visible throughout the timeline (Fig.2.4A). In most years, national parks showed lower bare ground scores than any other land use designation, with notable exceptions in years of high rainfall (e.g. 2001, 2020). Land that would eventually become CCROs or WMAs often had similarly high bare ground scores to land in the 'NONE' category (Fig. 2.4A). Areas that were classified as having most, least and medium bare ground scores at the end of the timeline maintained the same classification throughout the study period (Fig. 2.4B). Recovery years were frequently associated with high annual rainfall (eg. 2001, 2018, 2020) (Fig. 2.4).

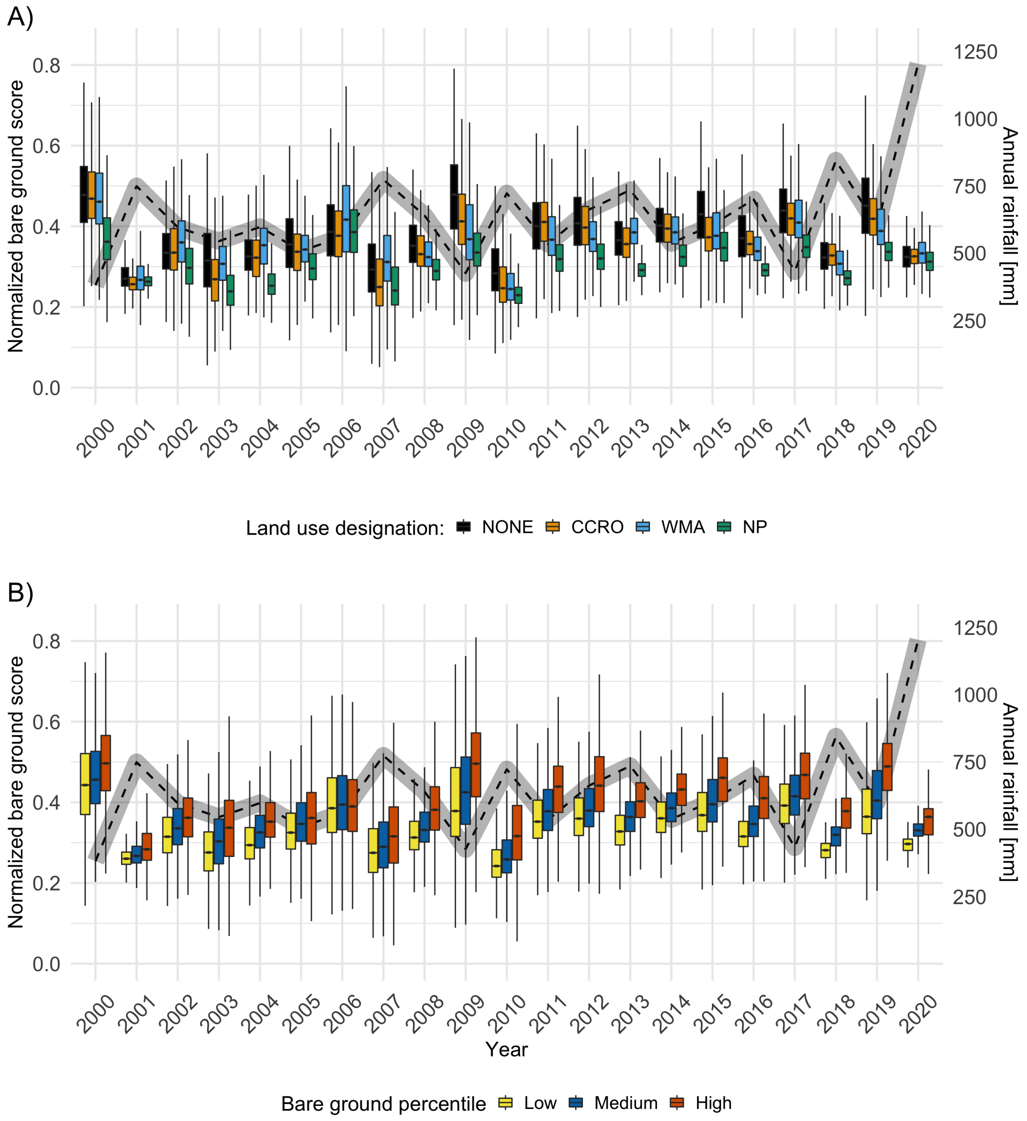

Figure 2.4: Normalized bare ground index scores over time – areas of high bare ground cover receive higher scores. A) Split by land use designation (black: No official management/protection scheme (NONE), orange: Certificate of Customary Right of Occupancy (CCRO), blue: Wildlife Management Area (WMA), cyan: National Park (NP)) and B) Split by bare ground percentile, based on the median degradation scores of the final three years of the time series (2018-2020). Whiskers represent 95% confidence intervals around the median. Outliers are not shown. The dashed gray line in the background indicates annual median rainfall (November to October), based on CHIRPS version 2 data retrieved for the study area (Funk et al. 2015).

To assess resistance, we focused on the four years with the largest increase in bare ground scores (2002, 2009, 2011 and 2019). We found that cells in the high bare ground percentile increased in bare ground cover more, on average, than other cells in three of the four years assessed (Fig. 2.5). Similarly, lowest bare ground percentiles in 2018–2020 also showed the lowest average increase in bare ground in three of the four years (Fig. 2.5).

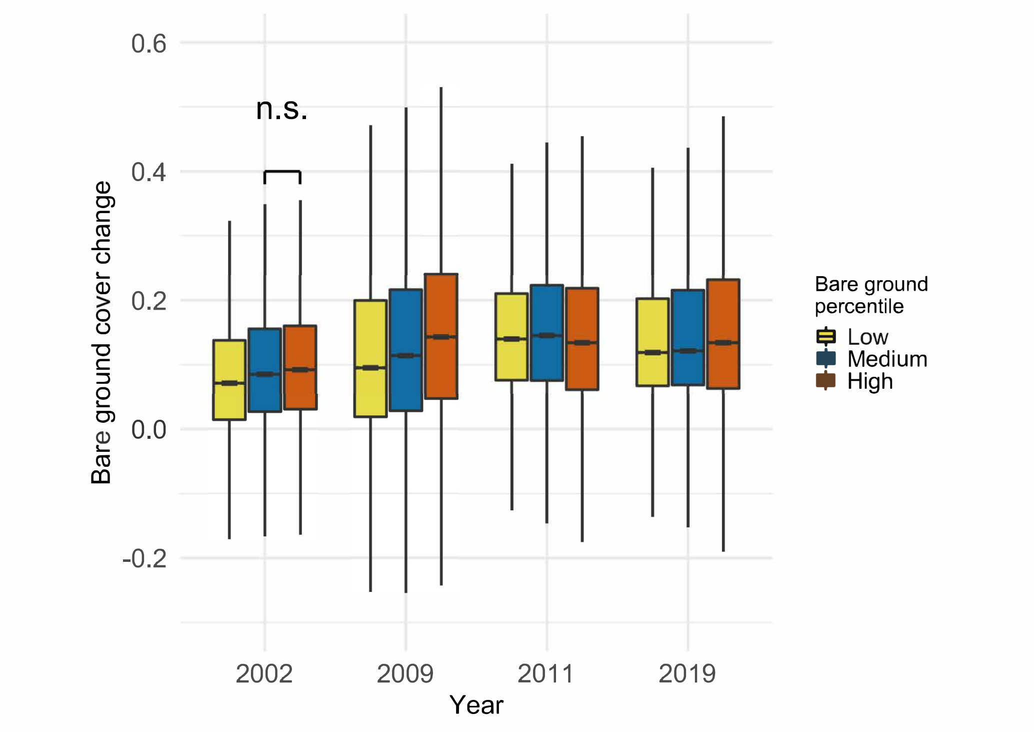

Figure 2.5: Changes in normalized bare ground index scores during the four years of greatest increase in bare ground cover, Split by bare ground percentile, based on the median degradation scores of the final three years of the time series (2018-2020). Positive numbers along the y axis signify an increase in bare ground cover, while negative numbers signify a decrease. Whiskers represent 95% confidence intervals around the median. Outliers are not shown. All contrasts were statistically different in the ANOVA tests, unless otherwise indicated. n.s.: not significant.

Looking at the recovery year following large declines, we found that cells ending in the highest bare ground percentile exhibited lower absolute and relative recovery than other cells in the driest recovery year (2003) (Fig. 2.6). In the remaining years, cells in the ultimately highest bare ground percentile showed higher absolute recovery than other cells, and the difference increased with higher annual rainfall (Fig. 2.6A). In terms of relative recovery, cells in the ultimately highest bare ground percentile showed the same trend of higher recovery in wetter years, and were the only cells with median net improvement in the wettest year (2020) (Fig. 2.6B).

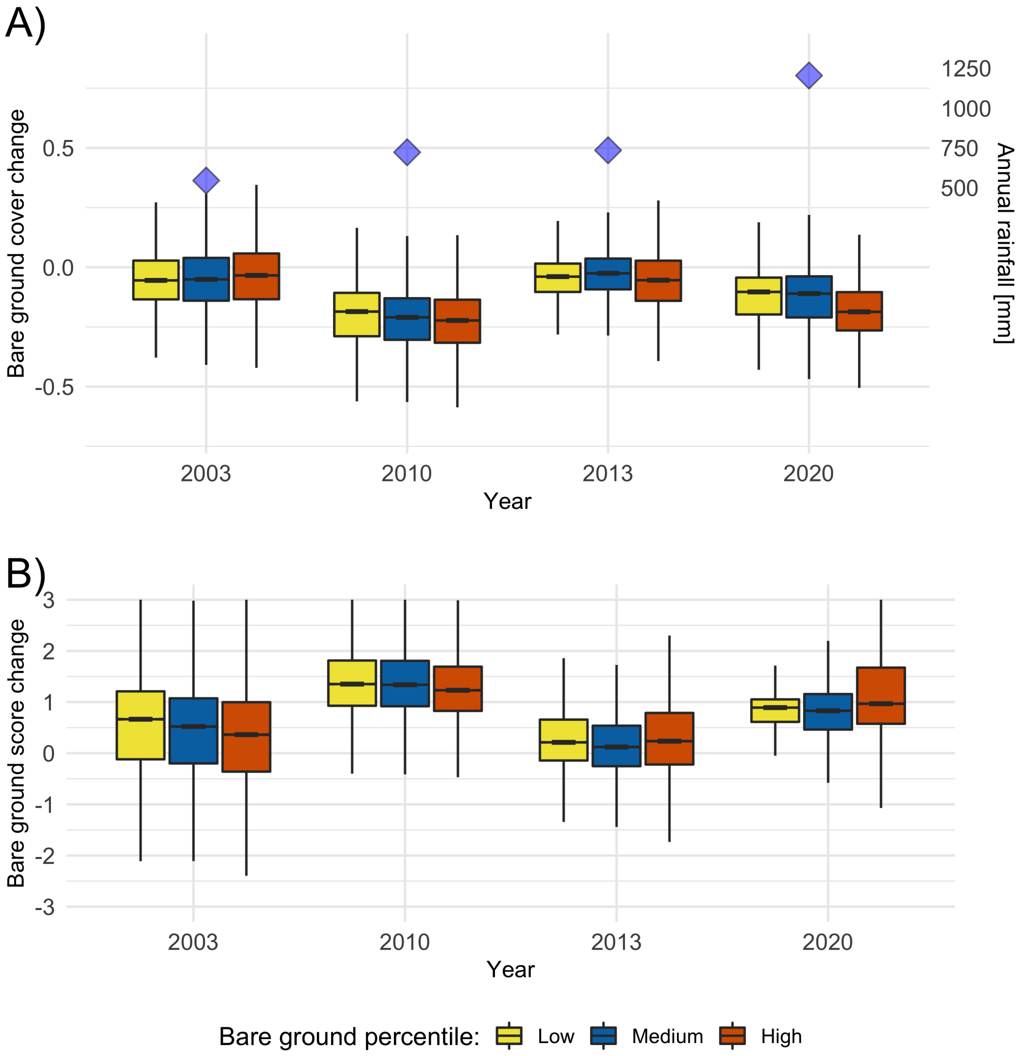

Figure 2.6: Recovery in bare ground scores following the four years of largest degradation. Split by bare ground percentile, based on the median degradation scores of the final three years of the time series (2018-2020). A) *Absolute recovery*, positive numbers along the y axis signify an increase in bare ground, while negative numbers signify a decrease in bare ground. Blue diamonds indicate annual rainfall (November to October) based on CHIRPS version 2 (Funk et al. 2015) data. B) *Relative recovery*, the proportion of decline that returns in the recovery year. A value of 1 = total recovery, 0 = no recovery, <0 = continued decline, >1 net improvement. Whiskers represent 95% confidence intervals around the median. Outliers are not shown. All contrasts were statistically different in the ANOVA tests.

Formal statistical analysis of the cell-specific change of bare ground scores between 2000 and 2020 showed significant effects of all covariates (Fig. 2.7, Table 2.2). We found evidence that mean annual rainfall had the strongest effect on the long-term trend of bare ground scores compared to the other covariates in the model, with drier areas showing steeper increases in bare ground scores than wetter areas (Fig. 2.7B). We found increases of bare ground scores over the last 20 years in all areas, independent of land use designation (Fig. 2.7, Table 2.2). The bare ground cover change in land that had been designated as CCROs by the end of the time period was no different from land in the NONE category, while national parks and WMAs had a lower rate of increase in bare ground than NONE (Fig. 2.7D). Both human population density and livestock density had small correlations with the change of bare ground scores, such that areas with higher human density, as well as more livestock, experienced increasing bare ground cover rates (Fig. 2.7A, C).

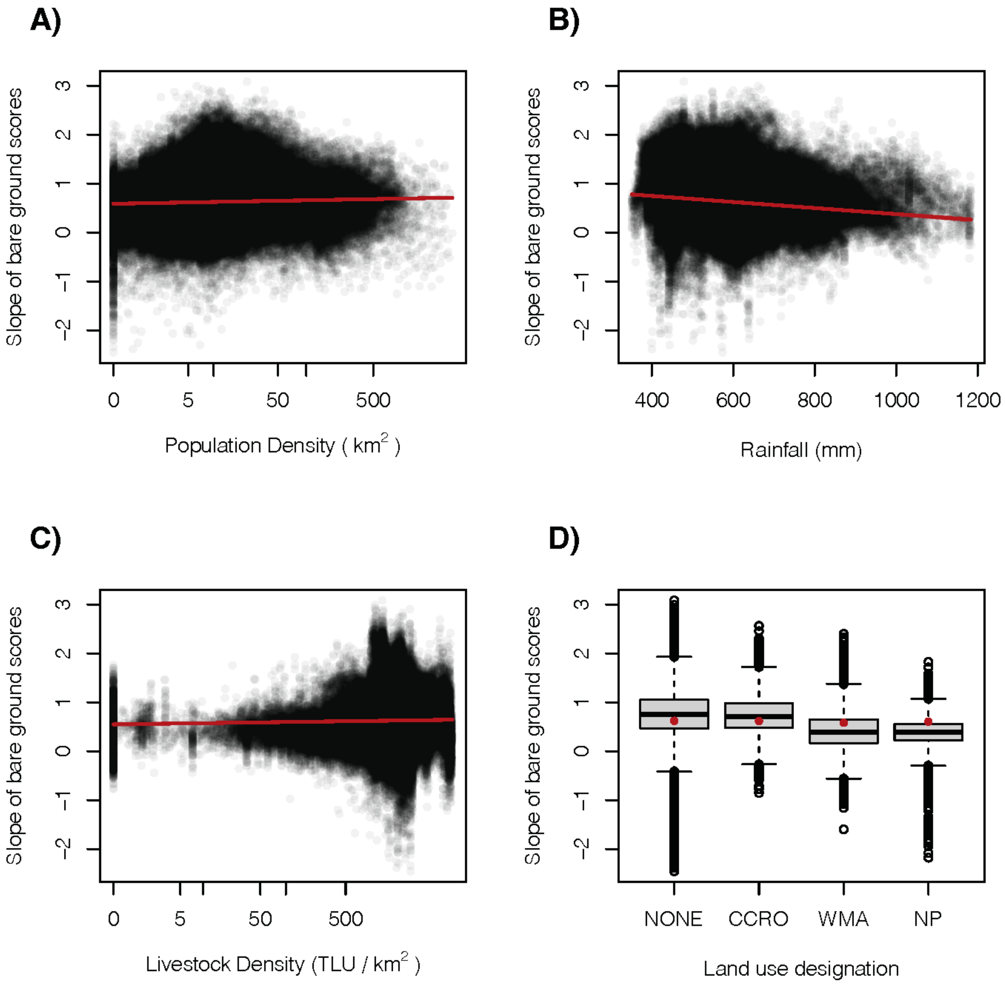

Figure 2.7: Effect plots showing the correlations between covariates and the rate of change in bare ground cover across the time period. A) Human population density, B) Mean annual rainfall, C) Livestock density and D) Land use designation.

Table 2.2: Parameter estimates and their 95% credible intervals for INLA model results predicting the rate of bare ground scores over time. Positive estimates correspond with positive rates of bare ground scores, and negative estimates with negative rates of bare ground scores. Parameters with credible intervals that do not overlap zero (bold) may be considered well supported by these Bayesian models.

Parameter	Estimate	Credible intervals
Intercept	**0.621**	**(0.611, 0.631)**
Human population density	**0.015**	**(0.011, 0.015)**
Rainfall	**-0.052**	**(-0.059, -0.045)**
Livestock density	**0.015**	**(0.008, 0.023)**
Designation: CCRO	-0.004	(-0.017, 0.008)
Designation: NP	**-0.04**	**(-0.056, -0.025)**
Designation: WMA	**-0.018**	**(-0.028, -0.009)**

2.5 Discussion

We found evidence that, in our study area, degradation seems to result primarily from a loss of resistance to change, not a lack of recovery. Land identified in the highest bare ground percentile by the end of the time period experienced slightly larger declines in condition in most years of widespread annual decline, but maintained recovery potential throughout. Absolute recovery in ultimately more degraded sites (i.e. sites in the highest bare ground percentile during the last three years of the time period) was actually slightly greater in all but the driest recovery year. Our results show that, as one shock rapidly follows another, sites that are ultimately degraded do not have time to fully recover between shocks. Sites with ultimately highest bare ground scores would have had to repeatedly exhibit net improvement to balance out the increased decline, but this degree of recovery only occurred during years of high rainfall. As we explicitly included annual rainfall in our models, we do not consider that large-scale climatic processes on the decadal scale can explain our overall findings. It should be noted that our estimated degradation scores exhibited significant variation, leading to small median effects. Nonetheless, we observed consistent patterns across years, suggesting that these trends go beyond statistical noise.

Although there is much in the ecological literature that defines separate concepts for resistance and recovery (Côté et al. 2010; Lake 2013; Hodgson et al. 2015), our results provide evidence that, in this area, repeated environmental shocks are a driver of bare ground cover. However, defining recovery will require more than measuring improvements in our bare ground index. The conceptualization of degradation as delivered through a repeated process of shock followed by partial recovery is important because it gives hope for eventual restoration of these rangelands. Although it seems unlikely that ecological shocks are to decline in frequency given global perturbations of the climate system (O'Loughlin et al. 2012; Ongoma et al. 2018), the fact that recovery potential remains suggests that reducing factors that decrease resistance to change could allow rapid recovery. Indeed, the ability to recover quickly from year to year has long been at the core of traditional management of these rangelands: heavy use over a few years could lead to severe local degradation, but nomadic people moved away for a few years allowing natural recovery (Homewood et al. 1987; Scoones 1995). Today, such movements are increasingly restricted by fragmentation of rangelands, mainly through increasing agriculture (Goldman et al. 2013; Selemani et al. 2014), rendering it necessary for pastoralists to remain in what may otherwise have been only temporarily degraded sites (Sallu et al. 2010; Middleton 2018), resulting in declining grassland productivity and increased degradation (Oba et al. 1987; Western et al. 2015; Russell et al. 2018).

Under the current prediction of overall increased rainfall in East Africa (Ongoma et al. 2018; Girvetz et al. 2019), the increased recovery potential with higher rainfall could give hope for the eventual restoration of these rangelands. However, rainfall predictions for the region are complex. Historically, long season rainfall in East Africa has declined (Lyon et al. 2012; Liebmann et al. 2017). Future climate change is predicted to lead to more intense rainfall on individual days during the long rain season (Shongwe et al. 2011; Dunning et al. 2018; Ongoma et al. 2018) and increasing rainfall during the short rain season (Rowell et al. 2015; Dunning et al. 2018), but also an increase in dry days (Vizy et al. 2012) and frequency and duration of droughts (Nicholson 2017; Gebremeskel Haile et al. 2019). Overall, studies predict an increased frequency of high rainfall events associated with storms over Africa, linked to climate change (Kendon et al. 2019; Finney et al. 2020). It is currently unclear how these changing patterns will affect rangeland recovery potential. Due to the temporal resolution of our study, considering total annual rainfall only, we are lacking this insight into the finer scale rainfall patterns driving bare ground cover change. The clear association of rangeland recovery with total rainfall during our study period suggests that temporal variation in rainfall does not yet override the spatial effect of total annual rainfall, but the relationship with rainfall patterns should be explored to evaluate the future risk to rangeland recovery posed by climate change in East Africa. Furthermore, the spatial pattern of rainfall in relation to recovery should be considered. Rainfall in savanna grasslands is characterized by a high spatial patchiness (Prins et al. 1988). Our study related recovery to rainfall averaged over the whole study area, disregarding local trends, and thus the finer scale responses to rain. Our results are applicable at the wider scale, but more research is needed to confirm the relationship between rainfall and recovery at the regional scale of management areas.

The general association of rangeland recovery with rainfall highlights a potential caveat of studies including bare ground as a parameter: while bare ground is the most visible expression of resistance and recovery on a wider landscape scale (enabling coarse satellite analyses), it is also potentially misleading, because of the high sensitivity to rainfall. Even rangeland well on its path to degradation (resulting from loss of resistance and/or recovery potential) may show a flush of growth following high rainfall events, leading to short-term variability of bare ground estimates. It is therefore crucial to account for rainfall, as it was done here: i) use rainfall to inform estimates of bare ground cover, ii) consider the long-term trends of bare ground, after factoring out temporal variation in rainfall, and iii) account for spatial variation in rainfall when analysing spatial patterns of bare ground cover. But even where rainfall is accounted for, the use of bare ground alone may present problems. In the context of recovery, for example, we registered a rangeland as 'recovered' if vegetation cover had sufficiently increased, even though this might be through fast-growing invasive or toxic species, rather than palatable grasses. For this bias to lead to false conclusions, however, such invasive and toxic plants would have to be more dominant than grazeable vegetation, during times of regrowth, across the hundreds of pixels considered for this study. Surveys suggest that the majority of these invasives are still low in numbers in the region (Ngondya et al. 2017), although this might become a greater risk in the future.

We succeeded in generating classified maps of bare ground scores from Landsat images since 2000. Formal validation confirmed pixel-level correlations between observed and predicted test regions for both parameters of interest, bare ground and ITP, but further evaluation based on expected year-to-year variation only validated predictions of bare ground. Using satellite imagery to identify specific vegetation types, particularly at a taxonomic level, has long been a challenge in the field of remote sensing, requiring data at higher resolution than used in this study (Mansour et al. 2016; Hunter et al. 2020). With the establishment of the Sentinel-2 program, providing imagery with high spatial (10 m) and temporal (5-day) resolution (Drusch et al. 2012), researchers have increasingly overcome this challenge, particularly through the use of time series analyses, utilizing images at peak vegetation intensity (Rapinel et al. 2019; Hunter et al. 2020). However, data are not available before 2015, making these data unsuitable for the analysis of longer term trends, as are expected in savanna habitats. The final generated landscape level patterns of bare ground cover in our study were consistent with known land use patterns. Our bare ground scores showed considerable variation year to year, which is consistent with known patterns of inter-annual variation in grass productivity in semi-arid savannas (Wonkka et al. 2016; Li et al. 2020). We found evidence for increases in bare ground scores across the study area, particularly in the driest areas, exactly as reported elsewhere (Vierich et al. 1990; Fynn et al. 2000; Wang et al. 2020), and in line with the large scale increases in bare ground observed in East African grasslands over the last two decades (Hill et al. 2020b).

We found the expected positive relationship between human density and degradation (Vierich et al. 1990; Holechek et al. 2017). Furthermore, we found that increases in bare ground cover were positively correlated with livestock density. While this result corroborates the negative relationship between high grazing intensity and grass biomass observed in African savannas (Western et al. 2015), the relatively low spatial resolution of the FAO product used to estimate livestock density (Gilbert et al. 2018) lends only limited interpretability to this finding. Under the current predictions of continued growth in human population and demand for livestock products, however, this potential pressure on rangelands is unlikely to decrease. The signs of lower increases of bare ground cover in WMAs and national parks point to their effectiveness in mitigating large scale declines. Finally, we found no evidence for reduced bare ground increases in land that became CCROs. CCROs are a relatively new tool being promoted to enable the effective management of rangelands by local communities (Huggins 2016; Stein et al. 2016; Alananga et al. 2019), so it may seem surprising that these areas do not show improvements during the final years, especially as our analysis accounts for differences in rainfall and human population density that may differ between sites. In practice, however, CCROs are not in themselves a solution to the problem of degradation: although they establish areas dedicated for grazing, they do not yet provide sufficient management guidance around that grazing (Alananga et al. 2019). Consequently, once established they may generate grazing honeypots that increase degradation locally, rather than resolve the problems associated with poor land use. However, several CCROs are now engaged in sustainable grazing and management schemes, which might lead to a future reduction of degradation in these areas. Our results show that the ability of these sites to recover if effectively managed is undiminished, which speaks to the potential effectiveness of sustainable management schemes in CCROs. Establishing responsible community management may well be the first step that is needed if degradation is to be reduced. Continued monitoring of rangeland conditions in these areas is needed to establish the effectiveness of these new management strategies. It should be added that the list of CCROs included for the study area is not exhaustive: Due to the time-consuming process involved in establishing these areas, not all boundaries were available at the time of analysis.

Future research should include measurements of finer-scale qualities of rangeland health, to overcome some of the caveats highlighted in this study. Such measurements could include species composition of the vegetation cover, plant traits related to palatability, individual resistance and recovery capacity of plants, or soil properties (e.g. composition, compaction). The latter could provide important insights into the mechanisms of grassland degradation and recovery at a finer spatial scale, given its influence on water retention (Hall et al. 1977), soil erosion (Moore et al. 1990; Cotler et al. 2006), and soil microbial activity (Bach et al. 2010). Additional management techniques could be considered, such as the frequency of fires, an important historic and contemporary management strategy in the region (Butz 2009). These variables may reveal a more complete picture of the pathways to degradation, and enable more effective rangeland management strategies. If the qualities underlying rangelands resistant to degradation are identified, they could be targeted in order to further promote rangeland resistance in the face of greater shocks and stress.

2.6 Code availability

The code used in Google Earth Engine can be accessed online using the following link: https://doi.org/10.6084/m9.figshare.24581922.v2.
R code for the data analysis can be accessed online using the following link: https://doi.org/10.6084/m9.figshare.24581967.v3.

2.7 Acknowledgements

The research was part of the Northern Tanzanian Rangelands Initiative and funded by USAID through their Endangered Ecosystem Northern Tanzania Initiative (AID-621-A-15-00004), and implemented by The Nature Conservancy. This study received research approval from the Tanzanian Commission for Science and Technology (permit numbers 2016-80-NA-92-43, 2016-81-NA-92-43, 2016-97-NA-92-43, 2017-143-ER-92-43 and 2017-147-ER-92-43).

Permission for research in communities was obtained from relevant local and district authorities. We are extremely grateful to support from the

Tanzania National Parks Authority (TANAPA) and Tanzania Wildlife Management Authority (TAWA) for allowing access to rangelands throughout the study area. We would also like to acknowledge the field and support team - Dr. Alex Lobora, Jumanne Ramadhani (Tanzania Wildlife Research Institute), John Mkindi and Mustafa Hassanali.

3

Chapter 3: Traits and Range Shifts

Spatio-temporal integrated Bayesian species distribution models reveal lack of broad relationships between traits and range shifts

3.1 Abstract

Aim: Climate change and habitat loss or degradation are some of the greatest threats that species face today, often resulting in range shifts. Species traits have been discussed as important predictors of range shifts, with the identification of general trends being of great interest to conservation efforts. However, studies reviewing relationships between traits and range shifts have questioned the existence of such generalized trends, due to mixed results and weak correlations, as well as analytical shortcomings. The aim of this study was to test this relationship empirically, using analytical approaches that account for common sources of bias when assessing range trends.

Location: Tanzania, East Africa.

Time period: 1980-1999 and 2000-2020.

Major taxa studied: 57 savannah specialist birds found in Tanzania, belonging to 26 families and 11 orders.

Methods: We applied recently developed integrated spatio-temporal species distribution models in R-INLA, combining citizen science and bird Atlas data to estimate ranges of species, quantify range shifts, and test the predictive power of traditional trait groups, as well as exposure-related and sensitivity traits. We based our study on 40 years of bird observations in East African savannahs, a biome that has experienced increasing climatic and non-climatic pressures over recent decades. We correlated patterns of change with species traits using linear regression models.

Results: We find indications of relationships identified by previous research, but low average explanatory power of traits from an ecological perspective, confirming the lack of meaningful general associations. However, our analysis finds compelling species-specific results.

Main conclusions: We highlight the importance of individual assessments while demonstrating the usefulness of our analytical approach for analyses of range shifts.

Keywords

Climate change, data integration models, eBird, range shifts, savannahs, species distribution models, species traits

3.2 Introduction

Climate change is posing an increasing threat to the survival of many species and is expected to result in the loss of species at the local or global level (Urban 2015; Wiens 2016; Panetta et al. 2018). Non-climatic factors, such as anthropogenic land use change, are further threatening species through degradation of habitat, changes in land cover, and fragmentation (Haddad et al. 2015; Horváth et al. 2019; Strien et al. 2019). Populations of species can persist despite these changes if they show plastic or evolutionary change (Hoffmann et al. 2011), or simply move to other locations. While micro-evolutionary adaptation to climate change can occur over relatively short periods of time, recent examples are mainly of species with short life cycles, such as fruit flies (Balanyá et al. 2006) or field mustard (Franks et al. 2007). There is increasing evidence for micro-evolutionary adaptation in taxa with longer life cycles, such as birds (Karell et al. 2011), but the effectiveness of this mitigation is unclear. One of the best-documented responses is range shifts where species distributions change to track suitable environments. There is mounting evidence for range shifts across taxa, at a global scale, accelerated by anthropogenic climate change (Davis et al. 2001; Parmesan et al. 2003; Colwell et al. 2008; Chen et al. 2011; Pörtner et al. 2022). Under future climate change scenarios, these range shifts are projected to continue (Thuiller 2004; Williams et al. 2018). Where species are unable to emigrate the outcome can be drastic, with the first climate-driven mammalian extinction recently documented (Gynther et al. 2016). Conversely, some species that redistribute effectively may benefit from environmental changes (Tayleur et al. 2016), establishing populations in new areas. Considerable unexplained variation in species range shifts as a consequence of climate change has been recorded, with authors proposing non-climatic variables such as species interactions or traits as possible explanations (Williams et al. 2018; McCain et al. 2021). Accurately quantifying range shifts and identifying the underlying drivers are crucial steps towards gaining a better understanding of the causes of such variation, ultimately enabling us to identify the most vulnerable species and inform conservation efforts (Foden et al. 2019).

The vulnerability of species to external pressures affects their ability to adapt to environmental change. Such vulnerability is characterised by the intersection of exposure and sensitivity to change, and adaptive capacity (Dawson et al. 2011; Foden et al. 2019). Exposure is typically defined as the amount of historic or future change in an environmental variable experienced across a species' observed range (Foden et al. 2019). At the species level, it can be quantified relative to a species trait (e.g. habitat suitability: Gardali et al. 2012; Alabia et al. 2018, drought threshold and climate suitability: Aubin et al. 2018). Sensitivity describes the degree to which species might be impacted by environmental change and is considered intrinsic to the species (Foden et al. 2019). It is commonly estimated through a species' physiological traits (Gardali et al. 2012; Foden et al. 2013). Adaptive capacity is generally defined as the ability of a species to cope with the negative impacts of environmental change (Bateman et al. 2020; Thurman et al. 2020). Such adaptation includes dispersal ability, and a species exhibiting high adaptive capacity may colonise newly suitable habitat more effectively when experiencing environmental pressures than a species with low adaptive capacity. Range shifts are generally expected to occur where sensitivity and exposure overlap (Purvis et al. 2005). One species may be able to persist in areas where it is heavily exposed to a certain change because it is not particularly sensitive to it, while another species may be highly sensitive to the pressure, but lacks the ability to disperse to a different location, leading to a negative range shift, or range contraction. In cases where exposure and sensitivity are both high and dispersal ability is also high, the species may shift its range into new areas, where they are suitable. Species vulnerabilities and resulting range shifts are therefore closely tied to species traits, i.e. the physiology, behaviour, and life history (Foden et al. 2013; Triviño et al. 2013; Pearson et al. 2014). As traits are, by definition, the only way by which species interact with the environment it is ultimately necessary that they explain vulnerability to climate change, and many vulnerability assessments are generated partially or wholly from species trait information (Foden et al. 2019).

There has long been an interest in identifying coherent groupings of traits associated with species range shifts across a wider taxonomic range (Lavergne et al. 2004; Van Der Veken et al. 2007). Such a generalisation would be a powerful tool for predicting the effects of future environmental change across many species, while also helping to identify the most vulnerable species based on their known traits (Garcia et al. 2014; Pearson et al. 2014; Aubin et al. 2018). In an effort to establish standardised and comparable trait groupings, Estrada et al. (2016) developed a traits framework, identifying broad categories of traits that might explain observed range shifts. Among these categories, they highlighted ecological generalisation and movement ability as being the most important predictors. Ecological generalisation refers to the ability of a species to use a variety of resources in the environment (Estrada et al. 2016), which can be expressed by a broad behavioural lifestyle (e.g. locomotory niche while foraging), wide trophic niche, or ability to tolerate a wide range of climatic variables or habitat structures. Species that are strongly represented in this trait group would be expected to show lower sensitivity to environmental change, as well as a higher adaptive capacity, leading to colonisation of new habitats and therefore larger range shifts (Angert et al. 2011; Buckley et al. 2012; Estrada et al. 2016). Movement ability refers to the ability to travel beyond the natal region (Estrada et al. 2016). In birds, higher movement ability may be associated with larger body size and longer wings, or high migratory ability, providing physiological prerequisites for covering longer distances, and thereby enabling larger range shifts (Angert et al. 2011; Buckley et al. 2012). Conversely, high migratory ability may lead to higher fidelity to established migration sites and therefore fewer range expansions (Bensch 1999), while a larger body size can be associated with reduced reproductive potential (Saether 1988), potentially hindering establishment in new areas and therefore range expansions (MacLean et al. 2017). The increasing availability of trait databases spanning whole taxonomic groups, such as AVONET for birds (Tobias et al. 2022), has facilitated testing the relationships between such trait categories and range shifts empirically. Meta-analyses of studies linking traditional traits with range shifts found considerable conflicting evidence for trait effects between taxonomic groups, for most traits categories considered, and weak predictive power overall (MacLean et al. 2017; Beissinger et al. 2021). Moreover, validation of climate risk assessment methods shows trait-based methods to have poor predictive ability (Wheatley et al. 2017). This led to the conclusion that traits might be surprisingly poor predictors of range shifts and not suitable contributions to climate change vulnerability assessments, unless analytical shortcomings were tested and addressed (Beissinger et al. 2021).

To further investigate the predictive power of traits, Beissinger and Riddell (2021) called for better inclusion of exposure-related traits in analyses of range shifts. Traditional trait groups considered as predictors of range shifts, such as ecological generalisation and movement ability, tend to correspond to the adaptive capacity or sensitivity of species, and might therefore not be sufficiently explaining trends. Exposure-related traits should in theory capture the positive relationship between species exposure and range shifts (Beissinger et al. 2021). Proposed exposure-related traits include morphologies that influence heat transfer, such as the plumage colouration of birds (Beissinger et al. 2021). In addition, a more direct measure of sensitivity to different environmental pressures may be an informative trait group. Species sensitivity definitions have been criticised as being ambiguous (Fortini et al. 2017b). Correlative species distribution models (SDMs) may present a solution to this problem. Since they quantify the probability of presence under different environmental conditions, they reflect a species' relationship with the environment more directly, and sensitivity may simply be quantified as the degree of influence of environmental variables on a species' occurrence.

Studies have discussed issues in quantifying species ranges as a potential weakness of analyses of range shifts (Şekercioğlu et al. 2008; Yalcin et al. 2017; Beissinger et al. 2021). Indeed, empirical studies are difficult due to the nature of observation data used to quantify range shifts. Common issues include lack of available data, non-standard survey protocols and observer bias, auto-correlation issues due to the spatial nature of the data, and imperfect detection (Beale et al. 2010; Faisal et al. 2010; Araújo et al. 2019a; Beissinger et al. 2021). The increasing availability of citizen science observations has helped fill data gaps (Feldman et al. 2021), but these data are often collected in different formats and come with a variety of sampling biases to account for (Isaac et al. 2015; Zhang 2020), making it challenging to include them in analyses. In recent years, SDMs have gained popularity, due to their ability to overcome many of the issues in estimating species ranges (Kéry et al. 2013; Franklin 2023). The extension to spatio-temporal SDMs has shown promising results for estimating range shifts, representing the probability of transitions between time periods, taking into account spatial and temporal changes in sampling effort (Beale et al. 2013; Bled et al. 2013; Grattarola et al. 2023). The recent development of the Integrated Nested Laplace Approximation (INLA) method and its associated R-INLA package (Lindgren et al. 2015; Bakka et al. 2018) has made it possible to develop and run complex Bayesian SDMs with drastically reduced computation times, but similar accuracy, compared to other methods (Blangiardo et al. 2013), while accounting for common issues like spatial clumping and sparse data (Redding et al. 2017). R-INLA is continuously being developed, with the addition of the Stochastic Partial Differential Equation (SPDE) allowing efficient modelling of spatial autocorrelation (Lindgren et al. 2011), further enabling robust assessment of range shifts. The recent development of an INLA framework for data integration allows combining different data sources of species occurrence, potentially improving predictions for species with poor data availability

(Sadykova et al. 2017; Isaac et al. 2020; Grattarola et al. 2023; Morera-Pujol et al. 2023).

At the core of these SDMs is the estimation of the species' niche shape. These models correlate observed occurrences of species with environmental factors, determining conditions favouring or inhibiting their presence. However, species distributions may be influenced more by dispersal constraints, like geographical barriers, than physiological limits. This leads SDMs to often reflect the realized niche rather than the fundamental niche (Franklin 2023). For more accurate predictions under future climate scenarios, SDMs strive to approximate the fundamental niche (Peterson 2001; Booth 2017). To enhance this estimation, efforts include expanding SDMs beyond single regions or time frames, incorporating broader environmental conditions through methods like adding paleontological data (Jones et al. 2019) or observations of species in new habitats (Beaumont et al. 2009; Gallien et al. 2012). The availability of global climate data products and observation data reaching back decades provides an additional avenue: SDMs that include a temporal structure, i.e. model species distributions within multiple time slices, can help move closer to characterising the fundamental niche, relating species observations to changing environments over time, and hence a wider range of environmental conditions (Myers et al. 2015).

The aim of this study was to apply recently developed integrated spatio-temporal SDMs in R-INLA to estimate ranges of species, quantify range shifts, and test the predictive power of traditional trait groups, as well as sensitivity traits and an exposure-related trait. In terms of range shifts, we focused on changes in range size, a key dimension of distribution change (Yalcin et al.

2017). We based our study on 40 years of bird observations in East African savannahs. Increasing anthropogenic pressure in the form of inappropriate grazing regimes has led to accelerated conversion to bare ground in the region (Hill et al. 2020a), resulting in a drastic change in habitat structure. Additionally, rainfall has become more intense on individual days (Shongwe et al. 2011; Dunning et al. 2018; Ongoma et al. 2018), while the number of dry days and frequency and duration of droughts has increased (Vizy et al. 2012; Nicholson 2017; Gebrechorkos et al. 2019b; Gebremeskel Haile et al. 2019). Under current climate change scenarios, these trends are predicted to become more extreme (Finney et al. 2020; Ogega et al. 2020; Li et al. 2021). Savannah birds are known to be sensitive to these changes (e.g. Dean et al. 2001; Beale et al. 2013). Previous studies have identified bare ground as one of the key predictors of savannah bird ranges since reproductive behaviour as well as foraging strategies are commonly tied to the grass structure (Fisher et al. 2010; Schaub et al. 2010). Rainfall has been shown to directly influence savannah bird populations, due to its ties to food availability and grassland productivity (Dean 1997; Lloyd 1999; Dean et al. 2001). Due to a long-running bird observation program, the Tanzania Bird Atlas, observations are available for four decades, providing enough time to observe meaningful range shifts, as well as pronounced environmental changes. Based on Tanzania Bird Atlas data, Beale et al. (2013) provided empirical evidence that Tanzanian savannah birds have shifted their ranges over the last four decades, due to a combination of climate and habitat change, making them an ideal study group. Here, we tested the following hypotheses: (1) Range shifts are positively associated with ecological generalisation; (2) range shifts are positively correlated with movement ability; (3) range shifts are positively correlated with exposure-related traits; and (4) range shifts are positively correlated with sensitivity traits.

3.3 Methods

We estimated range shifts using spatio-temporal models in the R-INLA package that integrated citizen science and bird Atlas data, and accounted for sampling effort and autocorrelation. We derived species-specific occurrence-environment relationships, informed by the observed temporal change of distributions. We correlated traits, derived from trait databases and model outputs, with observed range shifts, using robust regression models. Figure 3.1 provides an overview of the main analytical steps included in the data analysis. A full description of the spatio-temporal integrated model is provided in the supplementary information file of this document.

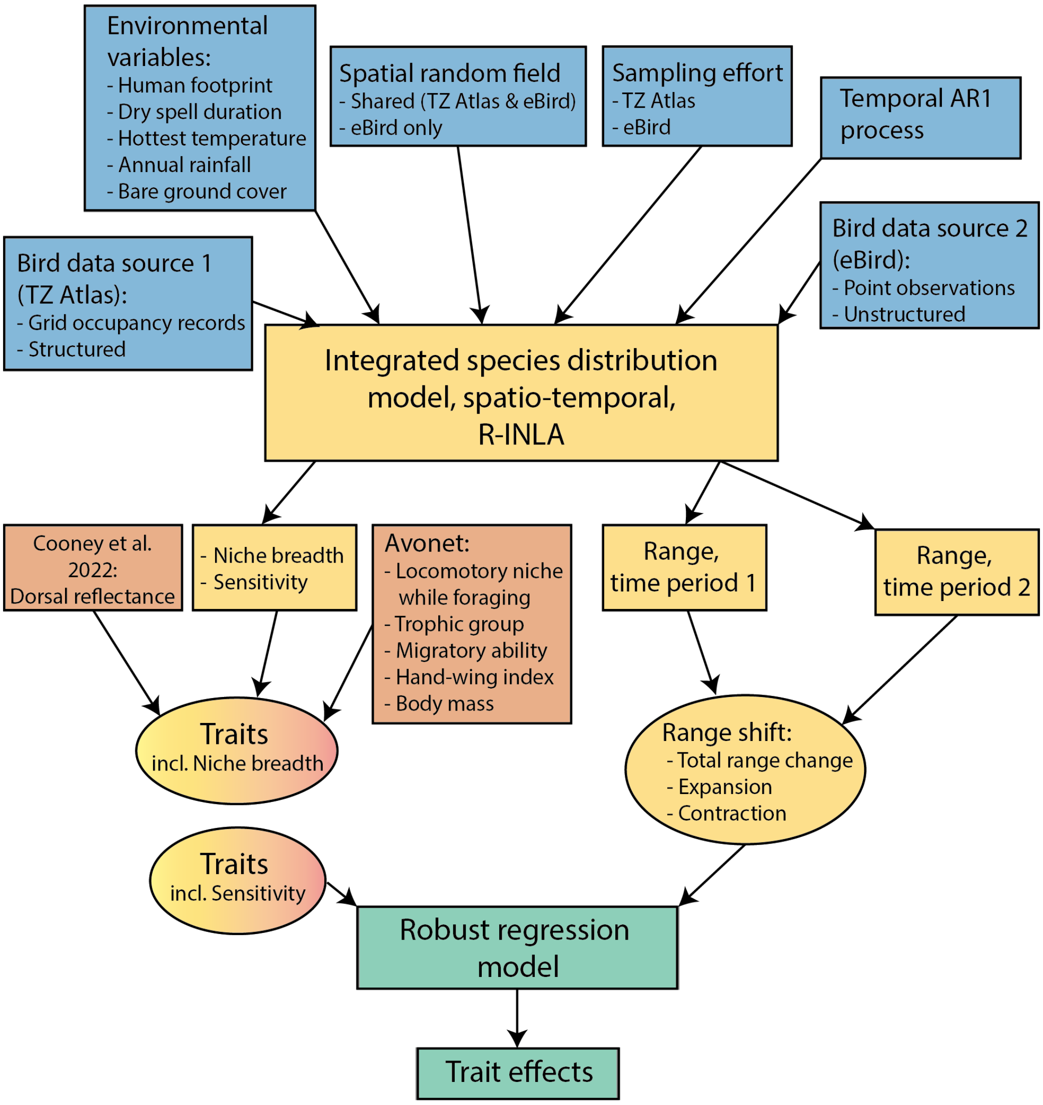
Environmental variables:
- Human footprint
- Dry spell duration
- Hottest temperature
- Annual rainfall
- Bare ground cover
Spatial random field
- Shared (TZ Atlas & eBird)
- eBird only
Sampling effort
- TZ Atlas
- eBird
Temporal AR1 process
Bird data source 1 (TZ Atlas):
- Grid occupancy records
- Structured
Bird data source 2 (eBird):
- Point observations
- Unstructured
Integrated species distribution model, spatio-temporal, R-INLA
Cooney et al. 2022: Dorsal reflectance
- Niche breadth
- Sensitivity
Avonet:
- Locomotory niche while foraging
- Trophic group
- Migratory ability
- Hand-wing index
- Body mass
Range, time period 1
Range, time period 2
Traits incl. Niche breadth
Range shift:
- Total range change
- Expansion
- Contraction
Traits incl. Sensitivity
Robust regression model
Trait effects

Figure 3.1: Overview of the main analytical steps conducted in the analysis. R-INLA: R package for implementing the integrated nested Laplace approximation. TZ Atlas: Tanzania Bird Atlas. Colour schemes correspond to methodological groups. Blue: Species distribution model components and inputs. Yellow: Species distribution model and outputs. Orange: Traits derived from literature. Green: Trait-range shift analysis and output.

3.3.1 Bird data

We obtained bird observation data from the Tanzania Bird Atlas, as well as citizen science data from the Cornell Laboratory of Ornithology citizen science database eBird (Sullivan et al. 2009). The Atlas dataset contains over 1 million bird observations, collected by volunteer and professional ornithologists since the 1960s. It consists of systematically gathered records, summarized into quarter-degree squares (approx 50 x 50 km at the equator). Due to the systematic nature of sampling, the Atlas dataset provides broad geographic coverage of Tanzania (Beale et al. 2013). Observer effort and spatial and temporal coverage are variable but contained in the metadata. eBird is a steadily growing resource for citizen science bird observations, increasingly used in scientific studies. Data were retrieved on May 2021 for Tanzania, and filtered following best practices (Strimas-Mackey et al. 2023). This included filtering the eBird records to retain only complete checklists, defined as containing all species seen on a given outing, as well as only those records that were reviewed and approved by a volunteer reviewer. We included only those records that had associated effort, and only included observations that spanned less than 15 km, lasted between 5 and 360 minutes, and involved 30 observers or fewer, due to declining detection rates in larger groups (Strimas-Mackey et al. 2023). Because of the unstructured nature of eBird records, spatial coverage of Tanzania is considerably reduced compared to the Atlas data, and observations are biased spatially, e.g. towards roads (Zhang 2020). To account for spatial variation, we only included records that contained associated GPS locations. Both Atlas and eBird records were filtered to those records that fall inside the Tanzania country boundary, using the 'gIntersection' function in the R package 'rgeos' (Bivand et al. 2017). We chose to focus on savannah specialists, since they are, in this region, the most likely group to show detectable responses to climate change (for a discussion see Beale et al. 2013), while also being well represented in both Atlas and eBird data. We based our choice of species on a published list of Tanzanian savannah specialist birds (Beale et al. 2013). After initial filtering steps, we retained 91 species that were considered candidates for the SDMs.

3.3.2 Environmental covariates

Several environmental covariates were included in the models, accessed and processed through Google Earth Engine (Gorelick et al. 2017). To reflect climatic variables, we chose factors that are known to affect grassland bird demographics. These included variables related to rainfall (annual rainfall (Sicacha-Parada et al. 2021), median annual dry spell duration as the number of continuous days with less than 1 mm of rainfall (Brawn et al. 2016)), and annual maximum temperature. We derived rainfall data from the CHIRPS version 2 dataset (Funk et al. 2015) and calculated the dryspell duration using the Google Earth Engine cloud computing platform (Gorelick et al. 2017). We accessed temperature data from the 'Climatologies at high resolution for the earth's land surface areas' (CHELSA) version 2.1 data product (Karger et al. 2017). To reflect habitat alteration, we included a measure of bare ground cover, derived from Landsat images using a machine learning algorithm (Wiethase et al. 2023). As a measure of anthropogenic pressure, we included a human footprint layer, which quantifies the amount of anthropogenic alteration of habitats (Venter et al. 2016). These environmental variables also reflected the recent environmental change experienced in the region, which include changes to dry spell duration and rainfall (Lyon et al. 2012; Liebmann et al. 2017), increasing bare ground (Wiethase et al. 2023), increasing maximum temperatures (Daron 2018), and growing populations leading to increasing agriculture conversion and urbanisation (Bullock et al. 2021). All covariates were re-projected to the lowest resolution layer available, resulting in a pixel resolution of approximately 5 km. For a detailed overview of the covariates and data sources see suppl. table B.1.

3.3.3 Estimating species ranges

We estimated ranges at approx. 28 km resolution using separate integrated distribution models for each species. This coarser resolution allowed us to run the distribution models at greater computational efficiency while closely matching the resolution used in similar studies (Adde et al. 2021; Morera-Pujol et al. 2023). We followed the integrated SDM approach outlined in Isaac et al. (2020), which allowed us to integrate the eBird and Atlas data in a single model, despite their differences in sampling structure (Isaac et al. 2020). In short, model-based data integration retains the structure of each data set, while also accounting for weaknesses, such as sampling bias. This is achieved by specifying separate observation models for each data set. As part of the data integration process, environmental covariate layers corresponding to observation data were sampled at their 5 km resolution at point locations for the eBird data, and at the centroids of the squares for the Atlas data.

The model was implemented in a Bayesian framework in the "INLA" package version 23.04.24 (Lindgren et al. 2015; Bakka et al. 2018) using R version 4.2.3 (R Core Team 2021). INLA is an alternative to Markov chain Monte Carlo methods (MCMC) for approximate Bayesian inference, with similar accuracy but higher computational speed (De Smedt et al. 2015), at the cost of limited flexibility, as it is restricted to latent Gaussian models. We modelled the true species distribution as a Log-Gaussian Cox Process (Møller et al. 1998) with an intensity function that defined the expected intensity at a given location, given the environmental covariates and a Gaussian random field. The Gaussian random field aimed to account for spatial autocorrelation and unexplained effects, and was estimated using the SPDE for computational efficiency (Lindgren et al. 2011). For each species, we included a shared random field for both data sources, as well as a random field for eBird data alone, which accounted for unexplained variation in sampling effort unique to the eBird data (e.g. increased sampling along road networks). We modelled the intensity using a binomial model with a complementary log-log (cloglog) link function (see Adde et al. 2021). We included separate effort variables for each bird data set. For eBird data, this was the checklist duration, automatically recorded by the eBird application in minutes. For Atlas data, this was the number of unique days any birds had been reported from a cell within the survey periods. During the model call, we specified the "Laplace" strategy for approximations, and default integration strategy.

We modelled the relationship between environmental covariates and bird occurrence in a non-linear fashion using penalized regression splines (Beale et al. 2014), in accordance with the expectation of species existing in niche spaces. We avoided smoothing approaches that fit regression curves closely to the data (e.g. random walk models in INLA), following the sentiment that such smoothing can quickly lead to biologically implausible effects in SDMs (Hofner et al. 2011). This approach reflected our prior expectation that the probability of presence relates to environmental variables in an approximately monomodal way, representing a single continuous niche space. We fitted the relationship with restricted flexibility by using a small set of regression splines, based on thin-plate regression spline basis functions (adapted from steps provided in Crainiceanu et al. 2005). We selected control points for the regression splines based on the density distribution of covariate values covering the whole study area. In addition to the environmental fixed effects, we included the scaled coordinates as linear fixed effects in the model. This ensured that the spatial random effect fitted well in the case of species with very peripheral distributions (Beale et al. 2014).

Bird observation data and covariates were grouped into two time periods (time period 1: 1980-1999, time period 2: 2000-2020), and a temporal first-order autoregressive process (AR1) was integrated into the model structure. In AR1 models, the probability of presence in one time period is influenced by the probability of presence in the previous period. This overall model structure allowed us to estimate ranges at the two time periods while keeping the species-covariate relationships fixed, thereby reflecting the assumption that fundamental environmental limits of birds did not evolve during the time period (Radchuk et al. 2019). Simultaneously, this allowed us to better estimate the species occurrence-environment relationship, as this was influenced by the species ranges in two separate time periods, taking into account movement over time.

To derive pixel-level estimates closely related to the probability of presence produced by occupancy models, we projected posterior intensity estimates onto the study area under the assumption of constant high sampling effort (95 percentile value of overall sampling effort in the study), and we back-transformed these estimates to the probability scale. Our approach diverges from traditional occupancy models in a critical aspect. Under our framework, assuming an infinitely high sampling effort theoretically leads to a probability of presence of one (i.e., absolute certainty of presence) across all areas. In contrast, traditional occupancy models distinguish between the likelihood of presence and sampling effort, allowing for the possibility of absence regardless of sampling intensity. For the sake of readability and simplicity, we use the term "probability of presence" to describe our estimates from hereon out. We removed the estimates of the separate eBird random field from our final score. Fixing high sampling effort and removing the eBird specific random field allowed the underlying ecological process to be visualised without variations in observation intensity due to effort. Due to the nature of the model, projected ranges are sensitive to the choice of the sampling effort constant. We conducted a sensitivity analysis, to test our assumption that this relationship with constant sampling effort should be linear and with no bearing on the ranking of species. For this, we refitted models using 55, 65, 75 and 95 percentile values for effort, checked linearity of the resulting range sizes using R-squared values, and calculated the change in the relative ranking of species by range size across the different effort quantile values.

3.3.4 Mesh specification, prior choice & model evaluation

In INLA, the SPDE method for approximating the spatial random field achieves computational efficiency by utilising a computational mesh, i.e. a surface of triangles covering the study area (Lindgren et al. 2011; Lindgren et al. 2015). The specification of the spatial resolution of the mesh, i.e. the triangle size, has to be considered carefully, as growing research highlights the potential effect of this parameter on model results (Righetto et al. 2020; Dambly et al. 2023). In the absence of well established guidelines on choosing the optimal mesh size, we initially followed rules-of-thumb, i.e. basing first values for the mesh size on the estimated spatial range of model predictions (Bakka 2017). Following this, we opted to model bird distributions using a range of different mesh size specifications close to these initial values, for each of the study species, with triangle sizes of 0.55, 0.75, 1, 1.45 and 1.65 degrees (approximately 61, 84, 111, 161 and 183 km). Two hyperparameters, namely range and marginal variance (sigma), exert control over the spatial fields. The range determines the smoothness of the spatial field, i.e., the distance between the high and low points, while the variance dictates the amplitude of these peaks and troughs. In the Bayesian framework, prior values must be assigned to these hyperparameters. We adopted the Penalised Complexity (PC) priors framework, which is a technique that provides easy-to-interpret and modifiable priors (Simpson et al. 2017). PC priors are weakly informative, which allows the data to mainly dictate the posterior for each hyperparameter. For each combination of a species and mesh resolution, we chose a separate set of priors for either the shared or eBird random field. We chose the range and sigma priors relative to the spatial extent of the presence records of each individual species, as 0.5, 0.7 or 0.9 times the spatial extent, to test the effect of prior choice on model results. We set the probability that the range is below the chosen value, and the sigma is above the chosen value, to 50 percent. This combination of PC priors and mesh resolutions resulted in a sensitivity analysis containing 15 different model configurations per species, for a total of 1365 models. To evaluate the performance of each model, we calculated the logged negative sum of the conditional predictive ordinate scores (log-CPO), a recommended procedure for choosing the optimal mesh resolution (Righetto et al. 2020), where a lower score corresponds to the better fitting model. Additionally, we checked model outputs for visible convergence issues (e.g. regions with probability scores of 1 only and no spatial smoothness, or effect plots with abrupt drops to zero or 1 on the y axis), and derived the spatial range of the random field estimated by the model (where a range much larger than the total study area indicates poor estimation of the spatial effect). For each species, candidate models were those that passed visual convergence checks and showed successful estimation of the spatial effect, and the final model was chosen based on the lowest log-CPO score. For a final measure of model fit, we extracted model predictions at the bird observation points (eBird and Atlas) using the "extract" function in the package "terra" (Hijmans et al. 2023). We then compared model predictions with observed presence and absence data separately for each time period, and calculated the area under the receiver operating characteristic (ROC) curve (AUC), as well as sensitivity (proportion of correctly predicted presences) and specificity (proportion of correctly predicted absences) using the package "pROC" (Robin et al. 2011) in R. While AUC can be problematic when generating pseudo-absences with presence-only data (Lobo et al. 2008; Shabani et al. 2016), issues are reduced for detection/non-detection data as used in this study.

In addition to the PC priors, we specified Gaussian fixed effect priors, equally for all species. These parameters describe the slope of the relationship between the covariate and occurrence on the link function of the response, and are applied to the fixed effects of the model. We chose Gaussian priors on the fixed effects with 0 mean and precision of 1, suitable as a vague prior given the complementary log-log link function used here.

3.3.5 Species traits

We included traits broadly falling under the categories set out in Estrada et al. (2016), as well as an exposure-related trait and sensitivity (Estrada et al. 2016). Table 3.1 gives an overview of the traits and associated data sources. The sensitivity traits were quantified from the SDM estimates based on variance partitioning, broadly following Beale et al. (2014). This was the percentage of variation in presence probability explained by any of the environmental covariates alone. Sensitivity was therefore quantified in line with the IPCC definition, as the degree to which a species is affected by or susceptible to environmental change (IPCC 2007). Due to the fact that both sensitivity and range shift scores were derived from the same distribution models, an important consideration is the potential for the two variables to be inherently correlated with each other, i.e. with larger range shifts coinciding with higher sensitivities. If this were the case, we would expect to find consistent and statistically clear positive correlations between range shifts and sensitivity, an outcome that our analysis tested implicitly. Model-derived environmental niche breadth was quantified based on the estimated niche shape, as the range of values associated with a probability of presence above 50 percent. This quantification relied on the assumption of a single environmental niche. Where effect plots showed a probability of presence above 50 percent at low as well as high environmental values, this therefore indicated issues in estimating the niche shape. Since in those cases, the SDM still identified high presence associations with low and high environmental values regardless of the niche shape, we set the niche breadth to the maximum. Acknowledging that this is an imperfect solution, we quantified the extent of the issue and its effect on the final regression analysis. We expected the relationship between body mass and range shifts to be non-linear, meaning that a hypothetical difference of 5 grams body mass should play a larger role for small species than for large species (up to 8 kg body mass in this study). Hence, we transformed mass measurements using a natural log. All continuous traits were centred and scaled to a mean of zero and standard deviation of one.

3.3.6 Quantifying range shifts

We analysed the effect of traits on three measures of range shifts for each species: Total range change, and two transition scores (expansion, contraction). Due to the nature of the model (projections under an assumption of high constant sampling effort), these transition scores represented the change in estimated intensity. We calculated the measures of range shifts based on

Table 3.1: Overview of the traits included in the analysis of range shifts. Sensitivity and niche breadth were derived from the integrated species distribution model, and corresponded to the environmental covariates included in the model formula (highest temperature, annual rainfall, longest dry spell duration, bare ground cover, human footprint). Niche breadth was calculated as the range of covariate values where P(presence) 0.5, while sensitivity was calculated as the percentage of model variation explained by the covariate. Mean dorsal reflectance was adapted from data published in Cooney et al. 2022 (Cooney et al. 2022). All other traits were derived from the AVONET database (Tobias et al. 2022). 'Kipp's distance' describes the distance between the tip of the first secondary feather and the tip of the longest primary feather.

Mechanism	Trait	Description	Source
Ecological generalisation	Locomotory niche while foraging	Aerial, Terrestrial, Insessorial, Generalist	AVONET
	Trophic group	Omnivore, Herbivore, Carnivore	AVONET
	Niche specialisation	Niche breadth*	Model-derived
Movement ability/Site fidelity	Migratory ability	Low, Medium, High	AVONET
	Hand-wing index	(100*Kipp's distance)/Wing length	AVONET
	Body mass	Species average (gram)	AVONET
Exposure-related	Mean dorsal reflectance	300-700 nm	Cooney et al. 2022
Sensitivity	Sensitivity to environment*	Variation of presence probability explained	Model-derived

* Hottest temperature, annual rainfall, longest dry spell, bare ground cover, human footprint.

the pixel-level probability of presence in time period 1 ($P(presence)_{1980-1999}$) or time period 2 ($P(presence)_{2000-2020}$), using the sum of probabilities (presence or transitions) over all pixels i to derive a single measure that related to geographical area (total range size or range expanded/contracted). We calculated the total range change as the range size in time period 2 divided by the range size in time period 1 (3.1).

$$\text{Total range change} = \log\left(\frac{\sum_i P(\text{presence})_{\text{2000-2020, } i}}{\sum_i P(\text{presence})_{\text{1980-1999, } i}}\right) \tag{3.1}$$

We calculated the pixel-level probability of range contraction as the probability of presence in time period 2 multiplied by the probability of absence in time period 1, and calculated the sum over all pixels i to derive the expected total range lost (3.2).

$$\text{Range lost} = \sum_i ((1 - P(\text{presence})_{\text{2000-2020, } i}) \times P(\text{presence})_{\text{1980-1999, } i}) \tag{3.2}$$

We calculated the pixel-level probability of range expansion as the probability of absence in time period 1 multiplied by the probability of presence in time period 2, and calculated the sum over all pixels i to derive the expected total range gained (3.3).

$$\text{Range gained} = \sum_i ((1 - P(\text{presence})_{\text{1980-1999, } i}) \times P(\text{presence})_{\text{2000-2020, } i}) \tag{3.3}$$

Importantly, we normalised the transition metrics by a stochastic uncertainty score. It necessarily follows from the transition calculations above that in places where little to no change occurred, pixel-level contraction and expansion probabilities were highest if the probability of presence was 0.5 in both time periods (e.g. $(1 - 0.5) \times 0.5 > (1 - 0.1) \times 0.1 = (1 - 0.9) \times 0.9$). Initial testing revealed that such areas of high sustained stochasticity can inflate transition scores if not accounted for, producing misleading transition metrics. We therefore defined a stochastic uncertainty score, as the binomial variance in time period 1 (1980-1999) (3.4). Where the probability of presence was closest to 0.5 in both time periods (i.e. contraction or expansion scores were inflated due to high stochasticity), this uncertainty score was equal to the transition metrics, allowing effective normalisation by division. The sum of the uncertainty score over all pixels i represents the area of high stochastic uncertainty (3.4).

$$\text{Stochastic uncertainty score} = \sum_i \left(\left(1 - P(\text{presence})_{\text{1980-1999},\, i}\right) \times P(\text{presence})_{\text{1980-1999},\, i} \right) \quad (3.4)$$

The final, normalised transition scores (from hereon called 'Meaningful contraction' (3.5) and 'Meaningful expansion' (3.6)) represented the ecologically meaningful area gained or lost, beyond stochastic noise. All three final scores (total range change, meaningful contraction, meaningful expansion) were log-transformed, to scale proportional increases the same as proportional decreases. On the linear scale, a score of 1 indicated that changes were exactly as expected by chance (area gained or lost equal to the area of high uncertainty), and a value of 2 indicated that there were twice as many expansions or contractions as expected by chance. A score of 0.5 indicated 50 percent fewer transitions occurred than expected by chance.

$$\text{Meaningful contraction} = log\left(\frac{\text{Range lost}}{\text{Stochastic uncertainty score}}\right) \tag{3.5}$$

$$\text{Meaningful expansion} = log\left(\frac{\text{Range colonised}}{\text{Stochastic uncertainty score}}\right) \tag{3.6}$$

3.3.7 Trait-range shift relationship

For a statistical test of the trait-range shift relationship, we built additive linear Bayesian regression models with default priors in the R-INLA package (R version 4.3.1, R-INLA version 23.09.09). We chose robust regression models over more traditional methods since they effectively reduce the weight of outliers through a t distributed error structure (Wang et al. 2018). In essence, this was chosen to help capture broad underlying trends, decreasing the potential influence of outlier species. We fitted separate regression models with each of the three measures of range shifts as a response, and the species traits as explanatory variables. In the regression data set, each row represented range shift metrics and associated traits for an individual species in the study. Since higher sensitivity generally coincides with smaller niches (Rinnan et al. 2019), likely leading to a correlation between the two, we fitted separate models containing either sensitivity and all other traits as independent variables, or niche breadth and all other traits. This specification of model formulas led to a total of six separate linear models. We conducted cross-validation model checking to evaluate the goodness of fit of the models. For each model, this was based on the probability integral transform (PIT) values, a recommended method of Bayesian model criticism (Ferkingstad et al. 2017). For a well-fitting model, we expected uniformity in the distribution of PIT values, translating into a good match between observations and model predictions (Gneiting et al. 2007; Wang et al. 2018). We fitted posterior model estimates to the observation data using posterior marginals of linear combinations. This allowed us to conduct a final visual inspection for outliers that might be driving results despite the robust regression approach. Where such outliers were identified, we compared model results with and without the outlier included. We evaluated the statistical importance of traits based on the distance of posterior estimates from zero, taking into account 95% credible intervals. Where credible intervals did not overlap zero and were narrow, trait effects were considered especially well supported by the model. Due to the potential influence of phylogenetic relatedness on results (Angert et al. 2011), we first retrieved taxonomic information for our study species from the National Center for Biotechnology Information (NCBI) database using the 'taxize' package in R (Chamberlain et al. 2013). We then re-fitted the linear models specifying a random intercept term of family nested in order as an 'iid' model with default priors (Faraway 2016), and checked the influence on model results.

3.4 Results

Of the initial list of 91 savannah birds that we built SDMs for, 79 species were well supported based on model evaluation steps, while we failed to produce reliable estimates for 12 species, consequently discarded. Expert review of the model output confirmed plausible predicted ranges for all 79 species, reflecting expert knowledge of distributions and geographical boundaries. The average model AUC was 82.3 percent, suggesting the model output reflected the observation data well. Average dorsal reflectance values were not available for a set of 22 species, and we excluded these species from the regression analysis. The trait category of "Trophic level: Scavenger" contained only one species (White-backed vulture, *Gyps africanus*) and was therefore removed from the analysis. The final dataset contained a total of 57 species belonging to 26 families and 11 orders (suppl. table B.2). Supplementary table B.2 provides an overview of the number of detections for each species and observation data set, and supplementary table B.3 provides an overview of the sample sizes for each trait category. As expected, we found that range size estimates were sensitive to the choice of the effort constant. Testing revealed that range size estimates increased with effort in a highly linear way, with little change to the relative species ranks for most species (suppl. figure B.1). We found no discernible effect of including a random effect of phylogeny in the linear models (suppl. figure B.2), and the results presented here are based on the simpler models without random intercepts. We found cases of improperly estimated niche shapes in 11 of the 57 species. However, this was predominantly found for human footprint niche breadth (8 cases), followed by niche breadth of dry spell duration (3 cases) and rainfall (1 case). Re-running the models with the 11 species excluded revealed that the relevant model estimates were not affected (suppl. figure B.3).

Kori bustard (*Ardeotis kori*) showed one of the largest range contractions, disappearing from its Western range (Fig. 3.2A, 30 percent greater contraction than expected by chance). Among the species with the highest meaningful expansion scores was the Von der Decken's hornbill (*Tockus deckeni*), showing a westward range extension into miombo woodland areas (Fig. 3.2A, range gained 220 percent greater than expected by chance).

Total range changes varied between species and were predominantly positive (Fig. 3.2B), meaning that most species increased their range relative to the initial range size. In the case of the bare-eyed thrush (*Turdus tephronotus*), this expansion was as high as 3.9 times larger than what would be expected by chance. Overall, meaningful contractions rarely exceeded what was expected by chance, and were often lower than expected chance transitions. For a number of species, including Kori bustard, both contractions and expansions were considerably higher than total range changes (Fig. 3.2B). In those cases, large range losses in one region coincided with large gains in another (Kori bustard expanding its Southern range, Fig. 3.2A), highlighting the importance of considering more than total range change alone.

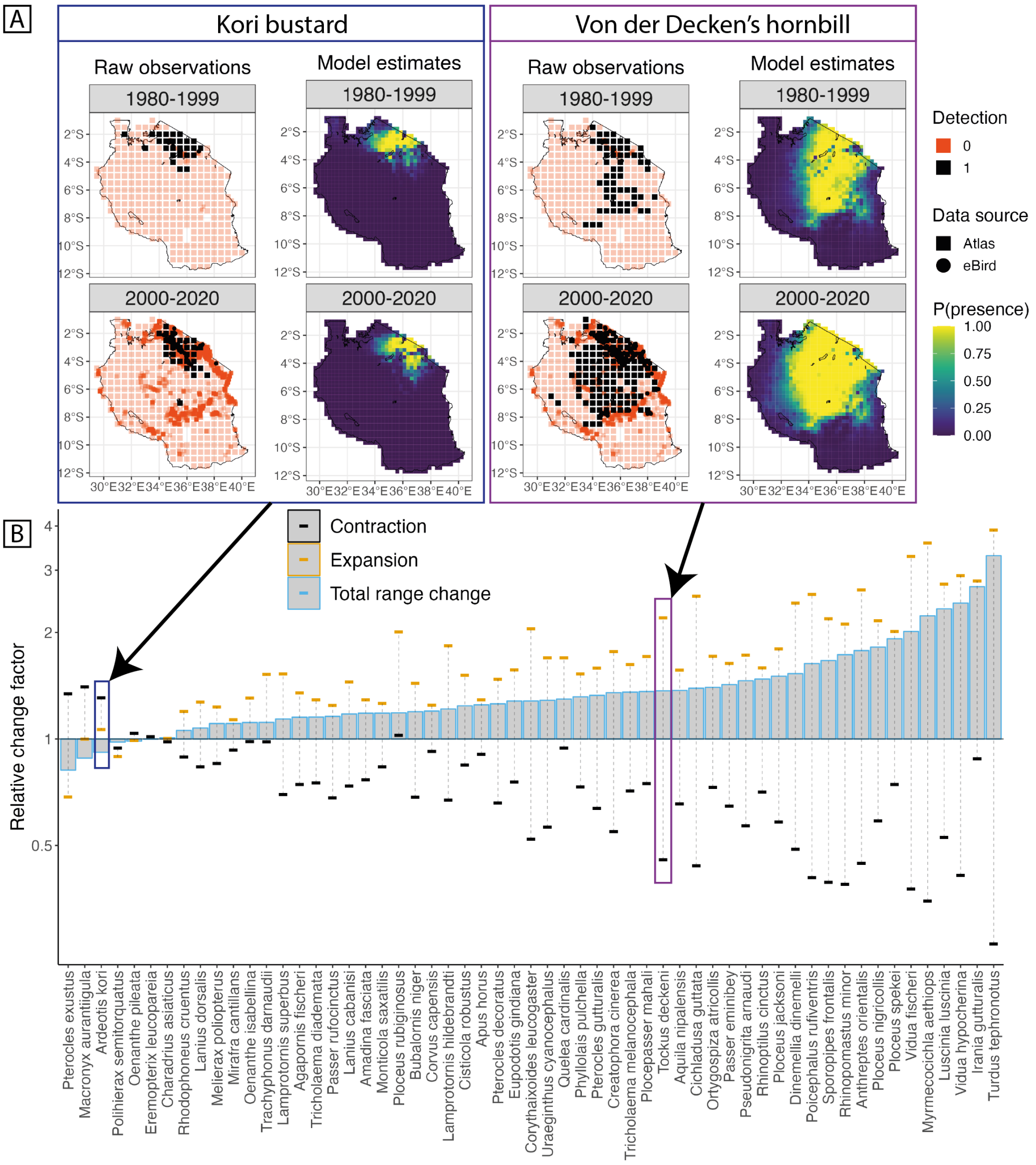

Figure 3.2: Overview of range shifts observed in the study. A) Raw presence and absence data and posterior median probability of presence estimates for example species in the study. Red points/squares on the raw observations plots show raw species detections, while black points/squares show nondetections. Points represent eBird data records, and squares represent Bird Atlas records. The colour gradient in the model estimates plots shows the probability of presence as estimated by the model, with more yellow colours signifying a higher probability of presence. Dark blue and dark purple colour outlines highlight the amount of range shifts corresponding to the example species. Dark blue: Kori bustard (*Ardeotis kori*); dark purple: Von der Decken's hornbill (*Tockus deckeni*).*(continued on following page)*

(continued caption) B) Relative change factor for range shifts of individual species between the time periods of 1980-1999 and 2000-2020, separated into total range change, meaningful contraction scores, and meaningful expansion scores. Values on the y-axis are presented on the linear scale. A relative change factor of 1 corresponds to no meaningful change for contractions or expansions (area lost or gained equal to area of chance transitions), and no change for total range change (range in 1980-1999 equal to range in 2000-2020). A relative change factor of 2 corresponds to a doubling of area, and a factor of 0.5 to a halving of area.

3.4.1 Ecological generalisation

We found a statistically significant increase in total range change in generalist foraging species (Fig.3.4A), driven by fewer contractions and more expansions (Fig.3.3). However, the statistical significance was barely conserved between models including niche breadth or sensitivity covariates (the group 'generalist' contained only three species), indicating a poor statistical signal, and limited interpretability (Fig.3.3). There was no clear association between any range shift metric and trophic level, as well as most measures of niche breadth (Fig.3.3). Hottest temperature niche breadth showed a statistically significant positive correlation with contractions, and a negative correlation with expansions (Fig.3.3 B, C). However, this effect was small, with e.g. an 11.9% increase in contractions for a 10°Celsius increase in niche breadth (Fig.3.4B).

3.4.2 Movement ability

We found no clear associations between migratory ability, body mass or hand-wing index and any range shift metric (Fig.3.3).

3.4.3 Exposure-related trait

Dorsal reflectance tended to be negatively associated with total range change, driven by fewer meaningful expansions, and more meaningful contractions(Fig.3.3). However, effect sizes were small, with e.g. a 1.8 % decrease in expansions for a 0.01 increase in plumage reflectance (Fig.3.4C). The correlation with total range change and contractions was statistically significant only for models including niche breadth covariates, indicating limited interpretability.

3.4.4 Sensitivity

We found no statistically significant relationships between any species sensitivities and range shift metrics (Fig.3.3D-F).

3.4.5 Individual species associations

Individual species showed strong associations, as remarkable range change values coupled with remarkable trait values. Some individual species showed a strong association between range shifts and sensitivity, with e.g. bare-eyed thrush (*T. tephronotus*) exhibiting a dry spell duration sensitivity of 0.25 (25 percent of model variation explained by dry spell duration) that coincided with a large expansion score of 3.9 times larger than expected by chance. Sensitivity to bare ground cover explained roughly 11 percent of variation in the distribution model of the horus swift (*Apus horus*). This was associated with an expansion roughly 21 percent larger than what would be expected by chance alone. Narrow niche breadth coincided with large declines in individual species. Chestnut-bellied sandgrouse (*Pterocles exustus*) showed one of the largest declines in the study, losing about 25 percent more of its range than expected by chance, while also exhibiting one of the narrowest niche breadths for human footprint. We observed similar declines in Kori bustard (*A. kori*), also associated with a relatively narrow human footprint niche.

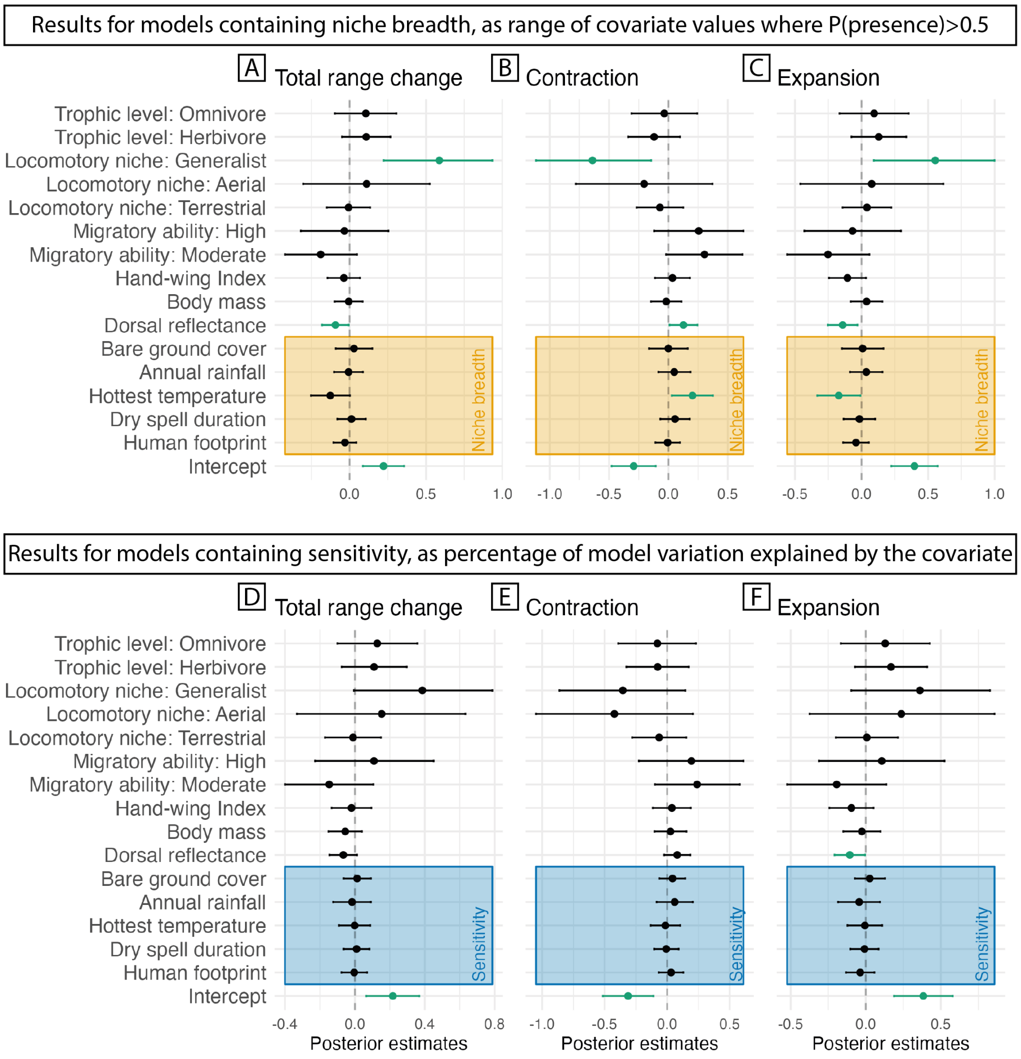

Figure 3.3: Parameter estimates and their 95% credible intervals for INLA model results predicting three measures of range shifts: Total range change, meaningful contraction scores, and meaningful expansion scores. Figures A-C are derived from models including human footprint, longest dry spell duration, hottest temperature, annual rainfall, and bare ground cover as niche breadth scores (highlighted in orange). Figures D-F are derived from models including that same set of variables as sensitivity scores (highlighted in blue). Parameters with credible intervals that do not overlap zero, or credible intervals of other factor levels for categorical variables, may be considered as strong effects in the Bayesian models, and are highlighted in green. For categorical parameters, this signifies that a trait level within a category is statistically different from the reference level. The reference levels are: "Migratory ability: Low", "Locomotory niche: Insessorial" and "Trophic level: Carnivore".

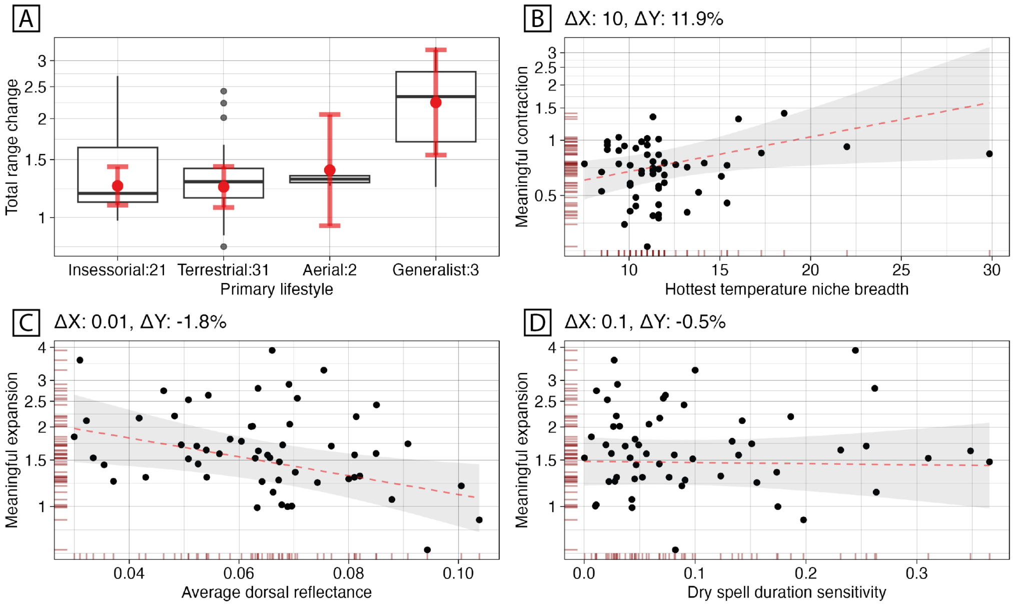

Figure 3.4: Selected effect plots showing the correlations between covariates and different measures of range shifts. All effect plots can be accessed in the supplementary material (suppl. figures B.4-B.9). Boxplots represent categorical covariates, while scatter plots represent continuous variables. Numbers on x-axis labels represent sample sizes for levels of categorical variables. Values on the y-axis are presented on the linear scale. A score of 1 indicates that changes are exactly as expected by chance (area gained or lost equal to the area of high uncertainty transitions), and a value of 2 indicates that there are twice as many meaningful expansions or contractions as expected by chance. A score of 0.5 indicates 50% fewer transitions occurred than expected by chance. Black points are drawn on the raw data provided to the models, red dashed lines, as well as red points with red error bars are posterior model estimates derived from linear combinations. The rug plots visualise the density of the data points. ΔX is the change along units on the x-axis that corresponds with a ΔY change of units on the y-axis.

3.5 Discussion

We succeeded in creating plausible species-specific range shift estimates of high agreement with observation data, taking into account sampling bias and unobserved effects, and reflecting known trends (e.g. range contraction of the kori bustard in East Africa, Senyatso et al. 2013). Our sensitivity analysis of effort used in model predictions supported the validity of our approximation of the probability of presence as derived in occupancy models. Furthermore, the lack of strong positive correlations between sensitivity traits and range shifts asserted that results were not driven by circularity between model-derived traits and range estimates. Our model of trait-range shift relationships indicated some trends similar to previous studies (e.g. Yang et al. 2020; Beissinger et al. 2021). However, despite considering a wide range of species traits, effects were small overall, even where statistically significant. This questions the ecological significance of these effects, adding to growing research identifying a lack of broad, generalising trends between most traits and range shifts across multiple taxa (Angert et al. 2011; Buckley et al. 2012; Reif et al. 2012; MacLean et al. 2017; Beissinger et al. 2021; Howard et al. 2023).

We found that savannah birds primarily showed positive total range changes, meaning that most species had larger ranges in the later time period, compared to the initial range. This change was generally a function of higher expansion rates. Tanzania has had a higher-than-average deforestation rate compared to the rest of Sub-Saharan Africa, with an estimated 0.9% annual decline in forest cover since 1995 (Nzunda et al. 2019). If some of these forests were converted into habitat suitable for colonisation by savannah bird species, this might help explain the high rates of expansions. However, patterns of change are complex, often resulting in increased cultivated land, and the rate of grassland loss being nine times higher than that of deforestation (Nzunda et al. 2019). Additionally, Tanzania has experienced increasing bush encroachment, further modifying habitat structure (Selemani 2018). Overall, the core species ranges appeared to be surprisingly stable, with most birds showing fewer contractions than what would be expected by chance. This might be especially surprising given the aforementioned rapid changes in Tanzanian grasslands over the past decades. More research is needed to link these patterns of land cover change to individual trends and habitat preferences of species, which are frequently unknown.

Contrary to our first hypothesis, we did not find broad, statistically clear positive associations between range shifts and most traits reflecting ecological generalisation in this study (i.e. trophic level, most niche breadth metrics), and effect sizes tended to be small. The finding of significantly higher total range changes in generalist feeding species is in line with previous research. As generalist species can exploit a wider range of food sources, they are thought to be more successful at colonising new habitats, and although ambiguous, evidence of this relationship exists in the literature (MacLean et al. 2017). The lack of an effect of niche breadth regarding rainfall suggests that studies of range shifts might not necessarily be more informed by the addition of hygric niches, as suggested in the literature (Beissinger et al. 2021). However, due to the taxonomic and geographical restrictions of this study, there is a need for additional work to confirm this.

The finding of more contractions and fewer expansions with wider hot temperature niches is surprising: as species with a wider niche breadth have the potential to tolerate more extreme hot temperatures, and the frequency of extreme heat days has increased in East Africa (Das et al. 2023), one might expect an opposite trend. However, maximum temperatures may simply not have increased enough yet in the area (although they are projected to increase in the future, Das et al. 2023) to impact species ranges in a way that leads to detectable associations with niche breadth, and given the small effect size, interpretability is limited. Alternatively, since species range responses can lag behind climatic change, not enough time might have passed for species to shift their ranges in response to temperature (Howard et al. 2023). The range shifts observed in this study might have been caused by factors affecting species survival faster than climate, such as land cover change (Sirami et al. 2008; Faurby et al. 2018).

The results of this study tended to disprove our second hypothesis regarding movement ability. Although previous studies found stronger migratory behaviour to be commonly associated with fewer range shifts in birds, attributed to their higher level of site fidelity to their home range (MacLean et al. 2017), no such pattern emerged in our results. Although a small effect, HWI tended to be negatively associated with range expansions. Previous work has identified HWI as being strongly positively correlated with dispersal ability across many bird taxa (Arango et al. 2022), meaning we would have expected to see more expansions as HWI increases. However, this effect may be confounded by the reproductive strategies of smaller birds with lower HWI. As they tend to exhibit higher reproductive rates and shorter generation times (Saether 1988), smaller birds might colonise new areas more successfully, resulting in more range expansions (MacLean et al. 2017). In fact, if we consider HWI as approximately proportional to body size, the negative correlation with range shifts found here is in agreement with multiple studies using birds (Brommer 2008; Yang et al. 2020; Beissinger et al. 2021).

Contrary to our third hypothesis, our results indicated that species with higher dorsal reflectance (i.e. lighter-coloured birds) tended to show lower total range changes, driven by fewer expansions, and more range contractions. Theory suggests that lighter-coloured birds should be better able to cope with higher heat loads, due to increased reflectivity (Medina et al. 2018). In a recent study on the Iberian Peninsula, including 96 bird species, researchers found that lighter birds were less geographically restricted from occupying hotter areas, having a wider thermal niche (Galván et al. 2018). Virtually all of East Africa has seen an increase in maximum temperatures of nearly 2 degrees Celsius (Gebrechorkos et al. 2019a), so it is surprising to see an indication of lower total range changes in lighter-coloured birds. However, as with the other trait effects, the degree of the correlation was small, limiting interpretability. If we assume a mechanistic relationship between dorsal reflectance and range change, our results suggest that the recent increase in temperatures is not yet high enough in Tanzanian savannahs to lead to a strong positive signal, limiting new expansions of thermally restricted species. However, it has been hypothesized that thermoregulatory behaviour is more important than plumage reflectance alone (Stuart-Fox et al. 2017), further calling into question the assumed positive relationship between reflectance and range shifts.

Our results indicated that relationships between range shifts and sensitivity traits were surprisingly weak, contrary to our fourth hypothesis. The human footprint is increasing globally at an accelerated pace, particularly in areas of high biodiversity, and East Africa is no exception (Venter et al. 2016). Reflective of human-made structures like urban areas, roads, agricultural land,

and other forms of developed land, this metric represents the most significant habitat alteration, virtually erasing natural features where human activities are most intense. While in Tanzania's savannahs, such areas may not have expanded sufficiently to cause widespread contractions in sensitive bird species, the human footprint layer includes factors known to lead to habitat fragmentation on a landscape scale, such as road networks and increasing agriculture. This kind of fragmentation has been shown to adversely affect the local survival of savannah bird species (Herkert 1994). A recent study found that the amount of anthropogenic infrastructure more generally negatively impacted bird functional diversity in an African savannah in and around the Kruger National Park, South Africa (Lerm et al. 2023). Continued monitoring of those species most sensitive to human footprint is therefore recommended, as simply not enough time may have passed since the landscape changed to cause a reduction in range. It is perhaps surprising that, on average, no strong associations with sensitivity to bare ground emerged. However, previous research found that, while land degradation such as an increase in bare ground was an important predictor of savannah bird ranges in Tanzania, this relationship likely occurred at fine spatial scales (Beale et al. 2013). By integrating eBird point data of higher spatial resolution, our study went towards analysing these finer scale patterns, although we allowed eBird resolutions of up to 15 km, a necessary condition to include a reasonable number of records. Overall, we summarized range changes over a fairly large spatial and temporal scale, and while this allowed us to investigate broad relationships, it is unlikely to reflect fine-scale relationships between land degradation and species ranges.

Although we were unable to identify meaningful general relationships across species between traits and range changes, it is important to note that some individual species showed strong associations between range shifts and traits, potentially indicative of ecological trends. Horus swift, for example, showed large range expansions coupled with high sensitivity to bare ground. As this is a species that relies on sandy riverbanks for nesting (Piot et al. 2021), it might have benefited from the trend of increasing bare ground in the region (Hill et al. 2020a), providing the conditions for additional breeding grounds. In the Von der Decken's hornbill, the large range increase was associated with relatively low sensitivity to temperature and length of dry days, potentially indicating mitigating traits underlying the expansion. The large decline coupled with a narrow human footprint niche in the chestnut-bellied sandgrouse, on the other hand, might highlight the species' challenge to persist under recent anthropogenic changes in Tanzania. As the species is both reliant on grassland and is being hunted, the decline might be indicative of the increased fragmentation and hunting pressure associated with increasing human pressure (Thiollay 2006). Similarly, the large decline in kori bustard coincided with a relatively narrow human footprint niche, with the species known to be threatened by hunting and habitat change (Mmassy 2017). Despite the absence of broad trends, these individual associations provide meaningful insights into species-environment relationships, and could inform vulnerability assessments and conservation efforts. Under the projection of increasing environmental change in East Africa (Moore et al. 2012; Dunning et al. 2018), these individual assessments will become more important in the region.

Our study demonstrates the potential of a spatio-temporally structured, integrated model in R-INLA to estimate range changes of species. The spatial random effects definition allowed us to capture dataset-specific observation bias, reducing the impact of common issues associated with citizen science records (Isaac et al. 2015). Additionally, it accounted for unexplained effects that weren't included in the model, hence reducing spatial autocorrelation issues commonly associated with species distribution models (Beale et al. 2010; Faisal et al. 2010; Beale et al. 2012; Beale et al. 2014). While this is a powerful method for accounting for bias, model results are, to an extent, sensitive to sample size (Simmonds et al. 2020). Our citizen-science data source, eBird, has experienced a rapid increase in popularity, leading to an increase in data availability (Sullivan et al. 2014). While users are able to submit observations retrospectively, such observations are outweighed by the constant inflow of new checklist submissions, leading to uneven sample sizes and effort between the two time periods in our study. This might potentially lead to false colonisation estimates if absences in the earlier time period are due to the species having been missed. However, the coverage of the Atlas grid surveys is extensive, leaving very few gaps across the study area, and the additional temporal autoregressive process included in the model structure helps alleviate any unevenness: where species were reported through eBird or Atlas records in the later time period, 2000-2020, the model assigned a probability of presence in the same places in 1980-1999, as a function of environmental conditions. A different case of inflated colonisation estimates may be presented through increased taxonomic awareness of species, and more reliable species identification through the availability of improved field guides. It is unlikely, however, that this source of bias would affect overall multi-taxa results. Finally, it should be noted that the lack of strong statistical associations might, to some degree, be a result of low statistical power in the analysis. While the relationship with continuous traits was supported by the full set of species, some levels of the categorical traits were represented by a small number of species, leading to low statistical precision. This warrants more investigation of these categorical traits, supported by higher statistical power. The hypotheses in our study, however, were driven by sets of traits containing both categorical and continuous variables (e.g. movement ability as migratory ability, but also HWI and body mass), reducing the effect of statistical power on the validity of inferences made in this study.

The set of traits included in this study was extensive, building on a trait framework designed to encompass the most important predictors of range shifts, and adding additional traits related to sensitivity and exposure, both important traits determining a species range (Foden et al. 2019). Species sensitivity has traditionally been challenging to assess, with definitions being criticized for being arbitrary and ambiguous (Fortini et al. 2017b). Our sensitivity measures directly quantified the degree to which a species' probability of presence is determined by different conditions in the environment. It is a potentially less ambiguous measure of sensitivity, arising from the realised species distribution. Such range-specific metrics have previously been proposed in the context of vulnerability assessments of species, for example in the form of "Range exposure" (Rose et al. 2023). Our quantification of sensitivity may be a valuable contribution to future studies. However, the aforementioned potential for circularity issues has to be considered, and since this sensitivity metric is only based on the realised niche, it likely paints an incomplete picture. Past studies included additional traits not considered in our analysis, for example, related to reproductive behaviour or additional physiological features (Estrada et al. 2016). However, many of these will strongly covary with the traits included in our study. Body mass, for example, correlates with clutch size and annual fecundity (Böhning-Gaese et al. 2000). Similarly, our model-derived sensitivity might reflect adaptive behaviour such as hiding in shade during the hottest hours of the day: a higher degree of successful adaptive behaviour would likely be correlated with lower sensitivity. Hence, our set of traits likely reflected other species' characteristics not explicitly included. Due to the lack of meaningful average associations between range shifts and any trait considered in our study, additional traits not explicitly included likely would not diverge markedly from this pattern. However, more research is needed to confirm this, and to test how transferable these results are to other taxonomic groups, such as plants where the synthesized associations between traits and range shifts appear less contradictory (Stahl et al. 2014; Beissinger et al. 2021).

Individual studies exist that found some traits to be predictive of range shifts across multiple bird species, such as an example for birds in China (Yang et al. 2020) and Europe (Estrada et al. 2018). Importantly though, the methodologies applied in these examples to assess range shifts diverged markedly from our study. In the case of Yang et al. (2020), range shifts were quantified on a simple binomial scale (1 or 0), significantly reducing nuance in the analysis. In the case of Estrada et al. (2018), range shifts were based on climate suitability models rather than observation data, which suffer from many of the methodological challenges we aimed to overcome in this study, such as unaccounted spatial autocorrelation or non-climatic effects (Beale et al. 2014; Gaspard et al. 2019). Notably, a recent publication on range shifts in European birds found directly contradictory results, with most traits having poor predictive power (Howard et al. 2023). This is indicative of the wider trend of inconsistent and weak results concerning the trait-range shift relationship identified in comprehensive reviews and meta-analyses, leading some authors to discourage the use of traits in conservation planning unless analytical shortcomings were addressed (Buckley et al. 2012; MacLean et al. 2017; Beissinger et al. 2021). Multiple possible reasons for this weak predictive ability of traits have been proposed (see Beissinger et al. (2021) for an overview). We believe that this study provides empirical evidence that analytical issues are an insufficient explanation of this trend.

3.6 Conclusion

The lack of trends across species between traits and range shifts identified in this study calls into question the usefulness of traits when analysing range shifts over higher taxonomic levels. The novel analytical techniques we used accounted for shortcomings identified in previous assessments of range shifts and further corroborated this result. While acknowledging the taxonomic and geographical restrictions of our study, we suggest that research into the effect of environmental change on range shifts of taxonomic groups may not necessarily benefit from the inclusion of traits. However, where individual species are considered, traits can provide important insights into the drivers of observed distribution changes.

3.7 Data availability

R code and data for the analysis can be accessed online using the following link: https://doi.org/10.5061/dryad.m63xsj47c.

3.8 Acknowledgements

This research was funded by the Natural Environment Research Council (NERC) through the Adapting to the Challenges of a Changing Environment Doctoral Training Partnership (ACCE DTP) program (grant number NE/S00713X). We are extremely grateful to Neil Baker for providing the Tanzania Bird Atlas data, as well as the volunteers who submitted their records to the Tanzania Bird Atlas. We also thank all eBird participants for submitting their observations to the eBird database.

4

Chapter 4: Climate Change Vulnerability

Separately assessed sensitivity, exposure and adaptive capacity inadequately represent species vulnerability to climate change

4.1 Highlights

- Vulnerability assessments based on separately estimated sensitivity, exposure and adaptive capacity are fundamentally unable to predict the true climate vulnerability of species

- Trait-based vulnerability assessments rely inherently on subjective definitions of sensitivity and disagree with correlative assessments

- Recent advancements in species distribution modelling can overcome analytical challenges in vulnerability assessments

4.2 Abstract

Climate change vulnerability assessments play a vital role in directing conservation resources to the species most in need of protection, ultimately preventing future extinctions. A popular assessment framework derives vulnerability from sensitivity, exposure and adaptive capacity (SEAC). Where these components are assessed separately, as in trait-based approaches, studies have highlighted poor predictive power and disagreement compared to methods based on species distribution modelling, which forego separate assessments. To identify possible sources for this, we critically evaluate this approach by reducing it to foundational concepts, using simulated examples. We find that the method of separately assessed SEAC is fundamentally unable to predict the true vulnerability of species and demonstrate how subjectivity is ingrained in trait-based approaches, leading to high uncertainty in vulnerability rankings. We therefore discourage the use of such assessments, but highlight the analytical challenges of alternative approaches based on distribution models. Using empirical data, we demonstrate how recent advances in distribution modelling can overcome these challenges, providing new avenues for climate vulnerability assessments of species.

Keywords

vulnerability assessments, climate change, species distribution modelling, species traits, trait-based vulnerability, species niches

4.3 Introduction

Species extinction is accelerating due to growing anthropogenic environmental change (Ceballos et al. 2015; Urban 2015). Mounting evidence suggests that these extinctions are outpacing speciation events (Dornelas et al. 2023), causing a global biodiversity crisis (Singh 2002), and leading some to conclude that we are at the beginning of a sixth mass extinction (Cowie et al. 2022; Ceballos et al. 2023). The latest report of the Intergovernmental Panel on Climate Change estimates an additional >10 percent of species becoming endangered in the near future, under the now almost inevitable scenario of a 1.5°C warming, alongside a 9 percent increase in species at very high risk of extinction, far exceeding background rates of extinction (Parmesan et al. 2023). The sheer number of species threatened now or in the future, combined with limited resources allocated to conservation (Wiedenfeld et al. 2021), means that effective prioritisation of species or habitats for conservation action is imperative (Brooks et al. 2006; Pullin et al. 2013).

Initially developed for natural hazards research in the context of risks to people and infrastructure, climate change vulnerability assessments (CCVAs) have been adopted by ecologists to assess species and habitat vulnerability from climate change (Foden et al. 2019). In this context, vulnerability is generally defined as "the degree to which a system is susceptible to, and unable to cope with, the adverse effects of climate change" (Intergovernmental Panel on Climate Change, 2007). Perhaps most prominently, CCVAs have been implemented by the International Union for Conservation of Nature (IUCN) for their Red List, classing species into different degrees of threat of extinction

(Collar 1996; Rodrigues et al. 2006). The accuracy of these classifications is important to effectively prioritise conservation efforts. Yet, considerable uncertainty exists regarding the reliability of existing methods of conducting CCVAs (Wheatley et al. 2017).

The framework underlying the majority of CCVAs is based on the concept that species vulnerability is a function of sensitivity, exposure, and adaptive capacity (SEAC) (Foden et al. 2013; Foden et al. 2019) (Fig. 4.1). Exposure is mainly expressed as the amount of past or future change in an environmental variable experienced across a species' observed range and is defined as extrinsic to the species (Foden et al. 2019). Examples include the rate of multidecadal change in past climate across a wider region (Kling et al. 2020), or the mean change of climate values between present and future in cells occupied by the species (Dickinson et al. 2014). Sensitivity is less uniformly defined but is traditionally considered intrinsic to the species in the SEAC framework, and describes the degree to which a species might be affected if it is exposed to climate change (Foden et al. 2019). Such intrinsic sensitivity might be defined by biological or life history traits, such as differences in the spawning cycle and adult mobility of fish species (McClure et al. 2023), or clutch size of birds (Reside et al. 2016), due to the relationship between clutch size and survival (Martin 2004). Adaptive capacity is generally defined as the ability of species to avoid negative impacts of environmental change through adaptation (Bateman et al. 2020; Thurman et al. 2020; Beever et al. 2023). This need not be limited to evolutionary adaptation but includes dispersal ability: a species exhibiting high adaptive capacity may disperse more effectively to suitable habitat when experiencing environmental pressures. In the SEAC framework, vulnerability results from the overlap of exposure, sensitivity and low adaptive capacity (Foden et al. 2013, Fig. 4.1A). Two species in a shared environment may experience the same climatic change (exposure), but differ in their sensitivity and hence would exhibit markedly different extinction risks, further mediated by their adaptive capacity.

Commonly used SEAC assessment types include trait-based and correlative/trend-based approaches (from hereon 'correlative') (Fig. 4.1B, see Foden et al. 2019 for a detailed overview). Mechanistic approaches are also used, although less frequently as they require a deep understanding of the physiological characteristics of the ecosystem and species (Foden et al. 2019).

In short, trait-based vulnerability assessments typically aim to separately assess the SEAC components of vulnerability through trait frameworks (from hereon 'separate SEAC'), tallying the number of species characteristics, as well as strength of association, that might correspond to each. To derive vulnerability, authors combine those components by multiplying weighted means of each (e.g. Morrison et al. 2015; Hare et al. 2016; Albouy et al. 2020; Fremout et al. 2020; McClure et al. 2023), taking the sum (e.g. Haji et al. 2023), or creating a more complex weighted score (e.g. Cianfrani et al. 2018; Rinnan et al. 2019; Ramos et al. 2022). Hence, this assumes a negative outcome where the SEAC components overlap unfavourably, rather than explicitly measuring the response. This approach allows relatively rapid assessments but requires expert knowledge of species traits and their role in mediating environmental impacts.

Correlative approaches can be based on abundance changes (e.g. Thomas et al. 2011), but more commonly, they use species distribution models (SDMs) at their core, in combination with global climate circulation models. Such studies typically quantify vulnerability as the projected change in climatically suitable areas (e.g. Still et al. 2015; Leão et al. 2021), hence estimating potential species responses directly. The SEAC components are not separately quantified but rather indirectly implicated in the process: sensitivity is represented by the modelled niche shape in the SDM, while adaptive capacity might be considered as indirectly accounted for by the species sensitivity (Williams et al. 2008; Dawson et al. 2011; Morrison et al. 2015; Fortini et al. 2017a). While the application of correlative assessments is restricted to species where observation data exist, there is evidence to suggest that they outperform purely trait-based approaches in terms of their predictive power (Wheatley et al. 2017).

Some overlap exists between the two approaches outlined here. For example, traits used in trait-based assessments can be derived from SDMs, such as the breadth of climate tolerances as the range of climatic variables covered by the estimated species range (Foden et al. 2013), or projected range loss (Wilsey et al. 2019). Conversely, traits have been integrated into correlative assessments to improve the predictive power, e.g. by including them as exacerbating factors (Thomas et al. 2011).

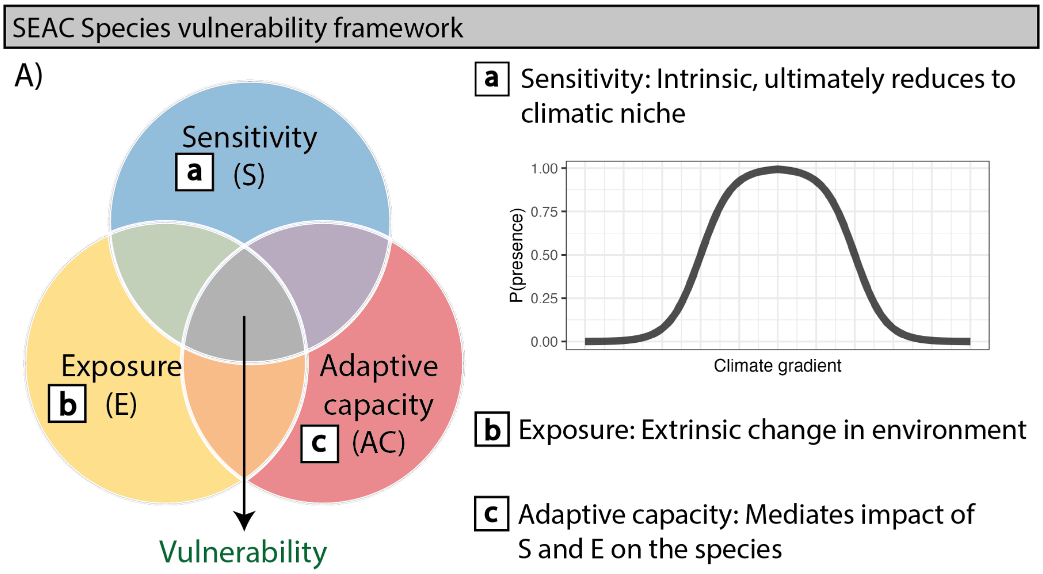
SEAC Species vulnerability framework
A)
Sensitivity
a (S)
Exposure
b (E)
Adaptive capacity
c (AC)
Vulnerability
a Sensitivity: Intrinsic, ultimately reduces to climatic niche
1.00
0.75
0.50
0.25
0.00
P(presence)
Climate gradient
b Exposure: Extrinsic change in environment
c Adaptive capacity: Mediates impact of S and E on the species

B)

Strategy	**Framework**
SEAC assessed separately	Trait-based approaches
SEAC implied in process	Correlative/trend-based approaches

Figure 4.1: A) Overview of the vulnerability framework based on sensitivity, exposure, and adaptive capacity (SEAC), based on Foden et al. (2019). a) Sensitivity is defined as intrinsic to the species. While many definitions exist, they ultimately relate to the niche shape of a species. b) Exposure is defined as the extrinsic change in the environment, current or projected. c) Adaptive capacity is defined as species characteristics that mediate the impact of sensitivity and exposure on the persistence of a species, such as dispersal ability. Vulnerability is defined as the overlap of sensitivity, exposure and adaptive capacity. B) Overview of two commonly used strategies for deriving vulnerability from SEAC components, with frameworks used in practical applications.

The approaches employed under the SEAC framework have attracted criticism over the years. For trait-based assessments, this is often based on the many nuanced and challenging decisions that go into the analysis. These include the choice of thresholds that determine the risk associated with particular traits (Foden et al. 2019), decisions of what traits constitute sensitivity vs. adaptive capacity (Fortini et al. 2017a), and the choice of method for combining the vulnerability components to derive the final score (Willis et al. 2015). Where trait-based and correlative assessments are combined, the weightings applied to combine the two components are difficult to determine objectively (Wheatley et al. 2017). Additionally, there are major sources of uncertainty in trait-based approaches, specifically when trying to link traits with climate change impacts (Foden et al. 2019). Trait-based approaches are grounded in an assumption that meaningful and causal links exist between the trait measures and the sensitivity of the species, but empirical evidence is lacking for many species, and observed links vary widely between taxonomic groups, leading to poor predictive ability (Wheatley et al. 2017).

Correlative approaches, on the other hand, are often criticised for not fully accounting for adaptive capacity, such as dispersal ability (Foden et al. 2019), or ignoring it altogether. Furthermore, exactly what type of niche SDMs are estimating is a topic of debate (Franklin 2023), with relevance to correlative vulnerability assessments. The traditional Hutchinsonian niche concept distinguishes between the fundamental niche of species (the environmental conditions that would allow a species to persist indefinitely) and the realised niche (the subset of environmental conditions in which the species exists, as a result of competitive exclusion) (Hutchinson 1957). If we believe that the SDM used for a given correlative assessment captures only the realised niche, estimates of vulnerability based on this might be biased towards higher sensitivity, and hence vulnerability. Where correlative assessments ignore non-climatic stresses related to climate change such as species interactions, they can confound the realised niche with the fundamental niche (Willis et al.

2015), and projections may fail to account for the dynamic nature of different species associations with the environment.

Since SDMs often play an important part in correlative assessments, vulnerability estimates rely on accurate SDM approaches. However, there are doubts about many methods widely applied today, such as climate suitability models based on SDMs. Since dispersal limitations can restrict species from colonising theoretically suitable habitats, suitability models paint an oversimplified picture of where species might occur, presenting suitability outside a species' actual range. The resulting overprediction could have negative consequences for conservation efforts, producing misleading prioritisation of areas that should be preserved, or erroneous estimates of climate change effects on species (Mendes et al. 2020; Velazco et al. 2020). An additional challenge is one of spatial autocorrelation, wherein the physical proximity of spatial observations violates the independence assumption of statistical tests - observations that are closer together spatially tend to be more similar by nature (Tobler 1970; Koenig 1999). Due to the potential for consistent overestimates of the importance of spatial covariates when spatial autocorrelation is unaccounted for, this remains an important consideration in SDMs (Beale et al. 2010; Faisal et al. 2010; Naimi et al. 2011; Beale et al. 2012; Radosavljevic et al. 2014; Gaspard et al. 2019), and therefore vulnerability assessments using them.

The net result of these forms of uncertainty in correlative and trait-based assessments is a poor agreement between different SEAC frameworks when applied to the same species (Lankford et al. 2014; Still et al. 2015; Wheatley et al. 2017). This suggests that a critical evaluation of SEAC-based vulnerability assessments is timely. In addition, promising new SDM methods in the shape of spatial Bayesian models are becoming available, which should be explored to a greater extent in the context of CCVAs. These methods avoid spatial overprediction and efficiently account for autocorrelation, thereby producing more realistic estimates (Blangiardo et al. 2015; Redding et al. 2017; Martínez-Minaya et al. 2018; Engel et al. 2022; Fichera et al. 2023). While still rarely used in the field of vulnerability assessments, recent research is showcasing their applicability for CCVAs (Wheatley et al. 2023).

In this study, we critically evaluate the SEAC vulnerability assessment framework. To do so, we first investigate the validity of vulnerability as a function of separate SEAC by reducing the SEAC framework to its foundational concepts (objective 1). We do this by simulating a one-dimensional example in the form of fundamental niche curves of species. We then expand this example to two-dimensional landscapes using a simulated spatial climate gradient, to quantify true species vulnerability from the perspective of correlative assessments (objective 2). Finally, we apply the correlative assessment to real-world data, showcasing recent advancements in species distribution modelling that can improve current vulnerability assessments (objective 3).

4.4 Methods

All analyses were conducted in R version 4.3.2 (R Core Team 2023). All plots were created using the 'ggplot2' package (Wickham 2011), supported by the 'tidyterra' package (Hernangómez 2023) for visualising spatial data, and the package 'viridis' (Garnier et al. 2023) for colour scales.

4.4.1 Objective 1: Reduce the SEAC framework to foundational concepts

To critically evaluate the SEAC framework, we simplify the breadth of definitions and assessment types applied by practitioners into foundational concepts. To do this, we first simulate the relationship between species and the environment in the simplest way, as a symmetrical unimodal one-dimensional curve (a combination of a logistic growth function and a logistic decay function) reflecting the fundamental niche, with species occurrence limited entirely by a single environmental gradient, temperature (Fig. 4.2A, equation 4.1).

$$\text{Niche curve} = \min\left(\frac{1}{1+e^{-\kappa(t-(\text{temp0}-\frac{\text{breadth}}{2}))}}, \frac{1}{1+e^{\kappa(t-(\text{temp0}+\frac{\text{breadth}}{2}))}}\right) \tag{4.1}$$

Where:

- t: The value of the climatic gradient (e.g. temperature).
- temp0: The mean value of the curve, determining the position of the curve along the x-axis.
- κ: The slope of the curve. A higher κ value results in a steeper transition, while a lower value leads to a more gradual slope.
- breadth: The breadth of the curve, as the range of x values where $y >= 0.5$.

The gradient is representative of all temperatures a species encounters in geographical space. In our simplest example, we therefore have a perfect understanding of the fundamental niche shape. We vary the shapes of the curves by changing the slope (steep or shallow), the location of the centre point of the curve, or mean (centre of temperature gradient at the x-axis, or marginal position), and the width of the curve (wide or narrow). We define the niche breadth as the range of temperature values along the x-axis at which the probability of presence is above 50 percent. Varying all three parameters (slope, position, breadth) allows us to capture key components of species niche shapes (Thuiller 2004).

4.4.2 Objective 2: Quantify true vulnerability

A key response in climate vulnerability assessments of species is the decrease in suitable area, and ultimately range size, following climatic change (e.g. Wilsey et al. 2019; Bateman et al. 2020; Leão et al. 2021). While recent research cautions that the link between range size and extinction risk should not be assumed (Zurell et al. 2023), there is mounting evidence that this link is preserved across multiple taxa (Rejmánek 2018; Chichorro et al. 2019; Van der Colff et al. 2023). Much work is focused on anticipating potential future range decreases of species as a metric of vulnerability (e.g. Lourenço-de-Moraes et al. 2019; Ruaro et al. 2019; Menéndez-Guerrero et al. 2020). We therefore choose the change in range size as the key metric for quantifying true climate vulnerability.

Since we have perfect knowledge of the fundamental niche shapes in our simulated example, we can calculate the true climate vulnerability based on the change in range size. To do so, we apply our simulated niche shapes from objective 1 to a simulated two-dimensional geographical extent of temperature values. We first create a two-dimensional matrix of spatial coordinates and introduce spatial autocorrelation using a Matérn covariance function in the 'fields' package (Nychka et al. 2021) to reflect different temperature zones in the environment. We then populate the matrix with random temperature values using the 'mvtnorm' package (Genz et al. 2009), and adjust the range of temperature values to match our one-dimensional example. We derive the species ranges by applying equation 4.1 to the populated temperature matrix.

In this simple spatial example, distributions are physically restricted to the bounding box, as they would be by geographical features such as coasts or mountain chains. Since we assume perfect dispersal ability and occurrence entirely limited by temperature, our suitability maps are equivalent to species ranges.

To quantify the true vulnerability of our example species, we calculate the change in range size, as the log-proportional difference in range size before and after exposure (equation 4.2). Through the log-transformation, we normalise expansions and contractions. By calculating the proportional change relative to the initial range, we account for the importance of range size in calculations of extinction risk. We apply the calculation to 100 different random simulations of the spatially autocorrelated temperature field.

$$\text{Climate vulnerability} = \log\left(\frac{\sum_i \text{Range size}_{\text{before\_exposure},\ i}}{\sum_i \text{Range size}_{\text{after\_exposure},\ i}}\right) \tag{4.2}$$

4.4.3 Objective 3: Empirical example showcasing potential improvements to vulnerability assessments

Species and environmental data

For an overview of species observation data and environmental data layers used to create the full distribution models, see Chapter 3. We accessed projections of future climate using the CMIP6 NASA Earth Exchange Global Daily Downscaled Projections product (Thrasher et al. 2022) at https://nex-gddp-cmip6.s3.us-west-2.amazonaws.com/index.html. The downloaded product had a spatial horizontal resolution of 0.25 degrees (approx. 28km). We selected this product rather than the 1km resolution Bioclim data (Karger et al. 2017), as this analysis required daily temporal resolution to calculate dry spell duration. We chose the GFDL-CM4 (USA) general circulation model, as it was identified as being less biased for the East African region than other models (Akinsanola et al. 2021). In terms of climate scenarios, we chose two different future pathways of societal development, or shared socioeconomic pathways (SSPs): SSP2-4.5 and SSP5-8.5 (O'Neill et al. 2017). Respectively, these represent a "middle-of-the-road" and "fossil-fueled development" scenario (O'Neill et al. 2017), and approximately correspond to Representative Concentration Pathway (RCP) 4.5 and 8.5 emission scenarios (Gidden et al. 2019).

Modelling species distributions

We built species distribution models in a Bayesian framework, using the "INLA" package version 23.04.24 (Lindgren et al. 2015; Bakka et al. 2018) in R version 4.2.3 (R Core Team 2021). Modelling steps followed those outlined in Wiethase et al. 2024. Broadly, this included data integration steps to combine observation data from two different sources (eBird and Tanzania Bird Atlas) in a single model, despite their differences in sampling structure (Isaac et al. 2020), and inclusion of a temporal component. The latter allowed us to estimate species' niche requirements based on two time periods (1980-1999 and 2000-2020), potentially providing more realistic estimates of the species' niches. The inclusion of a Gaussian random field allowed us to account for spatial autocorrelation and unexplained effects, as well as reduce overprediction issues, and was estimated using the Stochastic Partial Differential Equation (SPDE) for computational efficiency (Lindgren et al. 2011).

Estimating climate vulnerability

As in our simulated example of true vulnerability, we calculated the climate vulnerability score as the log-proportional change in climatically suitable area between the current and future time period (2000-2020 vs. 2055-2060). To do so, we first isolated model estimates of all climatic variables used in the model formula (average annual highest temperature of hottest month, average annual rainfall, average annual longest dryspell duration) using linear combinations, provided to the model structure during model fitting. These linear combinations let us quantify the contribution of sets of variables to the total model estimates, relative to other factors, without altering the fit of the model. We did this for each time period and temporally matched climate layers (2000-2020, 2055-2060: SSP2-4.5, 2055-2060: SSP5-8.5), and combined it with present-day spatial components (geographical coordinates, spatial random field). This combination was done on the linear scale, and values subsequently back-transformed to the probability scale. This allowed us to produce estimates controlled for spatial autocorrelation while simultaneously avoiding overprediction into areas far from current observations, using our best current knowledge of the underlying spatial processes shaping the distributions.

Suitability estimates for each pixel i were summed to derive the suitable area. The final vulnerability scores were derived as the climatically suitable area in the future proportional to the current one, log-transformed to scale proportional increases the same as proportional decreases (equation 4.3). Since the spatial component was equal for all estimates, this calculation removed the spatial effect from the final score, leaving us only with the change in the climate component.

$$\text{Climate vulnerability} = \log\left(\frac{\sum_i \text{Climate suitability}_{\text{2055-2060, } i}}{\sum_i \text{Climate suitability}_{\text{2000-2020, } i}}\right) \tag{4.3}$$

4.5 Results & Discussion

4.5.1 Quantifying vulnerability following the SEAC approach

To fulfil objective 1 and investigate the validity of vulnerability as a function of separate SEAC, we provide four contrasting hypothetical examples, species A, B, C and D (Fig. 4.2A). Species B, C and D exhibit the same slopes, which are steeper than that of species A. Species A, B and C exhibit the same centre point, which is less marginally positioned along the temperature gradient than the one in species D. Species A and B exhibit the same niche width, which is wider than species C and D.

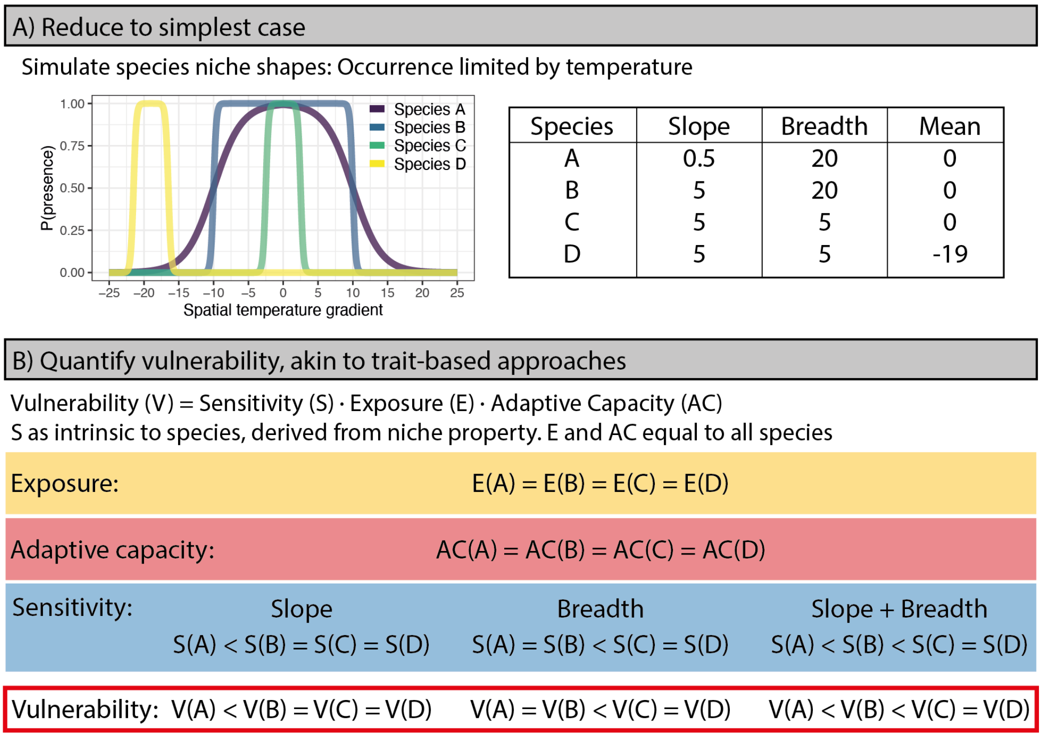
A) Reduce to simplest case
Simulate species niche shapes: Occurrence limited by temperature
P(presence)
1.00
0.75
0.50
0.25
0.00
−25 −20 −15 −10 −5 0 5 10 15 20 25
Spatial temperature gradient
Species A
Species B
Species C
Species D

Species	Slope	Breadth	Mean
A	0.5	20	0
B	5	20	0
C	5	5	0
D	5	5	-19

B) Quantify vulnerability, akin to trait-based approaches

Vulnerability (V) = Sensitivity (S) · Exposure (E) · Adaptive Capacity (AC)
S as intrinsic to species, derived from niche property. E and AC equal to all species

Exposure: E(A) = E(B) = E(C) = E(D)

Adaptive capacity: AC(A) = AC(B) = AC(C) = AC(D)

Sensitivity:	Slope	Breadth	Slope + Breadth
	S(A) < S(B) = S(C) = S(D)	S(A) = S(B) < S(C) = S(D)	S(A) < S(B) < S(C) = S(D)
Vulnerability:	V(A) < V(B) = V(C) = V(D)	V(A) = V(B) < V(C) = V(D)	V(A) < V(B) < V(C) = V(D)

Figure 4.2: Overview of the SEAC vulnerability approaches reduced to the simplest case (A), and vulnerability derived following principles of trait-based assessments (B). A) Niche shapes for four exemplar species based on simulated data, with varying slope, breadth and position of the mean (centre of curve plateau) in the spatial temperature gradient. Niche breadth represents the range of values along the x-axis for which the probability of presence is 0.5 or higher. B) Quantification of the components of the SEAC framework for each of the exemplar species, with vulnerability measurements akin to trait-based approaches. Background colours for exposure, sensitivity and adaptive capacity measurements correspond to colour panels in Figure 1.

In the SEAC framework, exposure is typically considered extrinsic to the species, independent of species' sensitivities (Foden et al. 2019), and is often quantified as the amount of climatic change experienced by a species.

Exposure is the least ambiguous component in the SEAC framework, with definitions being fairly consistent between studies (Foden et al. 2019). In practice, exposure is typically quantified over the existing range of species under consideration, e.g. calculated as climatic change in cells where the species have been observed (Dickinson et al. 2014), and is expected to be similar for species inhabiting the same sites (Loarie et al. 2009; Trisos et al. 2020). While this is an overly simplistic view of exposure in the environment (Riddell et al. 2021), it is one frequently used in the SEAC framework. In our simplest example of the niche curves, we assume the same climatic change across all values of the temperature gradient, representative of a fixed change across the geographical space. Following assumptions used in the SEAC framework, the exposure level is therefore equal for all four species (Fig. 4.2).

Adaptive capacity is defined as mitigating the effect of sensitivity and exposure, and in the geographical space in our example, it can result in contradictory effects. Where sensitivity and exposure are high, high capacity may lead to no change in probability of presence if species adapt to new conditions e.g. behaviourally, or it may lead to a large change if species disperse well. For simplicity, we assume that all four species exhibit the same adaptive capacity in the sense that they can disperse perfectly, i.e. that they fully shift their distributions following exposure (Fig. 4.2B).

Since sensitivity is defined as intrinsic to the species in the SEAC framework, we argue that this necessarily reduces to the shape of the fundamental niche curve in our simplest example (Fig. 4.1a). In practical vulnerability assessments, the niche shape is sometimes used directly to quantify sensitivity, for example as the niche breadth (Cianfrani et al. 2018; Rinnan et al. 2019), i.e. the range of environmental conditions at which the species thrives. Although niche position has also been used to define sensitivity (i.e. how much the required environmental conditions for a species deviate from the common conditions in a region, e.g. Cianfrani et al. 2018), we believe that this is not an intrinsic property of the species, but rather reflective of the specific environment surrounding the species' range.

Where sensitivity is not directly quantified from the niche curve, such as in trait-based assessments, we argue that frequently used traits such as those first outlined in Foden et al. (2013), ultimately also relate to properties of the curves demonstrated in Figure 4.2A. For example, habitat/microhabitat specialisation traits such as water-dependence of amphibian larvae (Foden et al. 2013) will relate to the breadth of favourable conditions encountered, with e.g. species C and D in the example being more specialised than species A and B, and therefore more sensitive (Fig. 4.2A). Traits related to environmental thresholds like temperatures, or dependence on environmental triggers such as conditions that start migration or hibernation, correspond to the slope of the simple curve, with highly dependent species exhibiting steep slopes. It follows that species B, C and D have narrower thresholds and higher dependency on triggers, and therefore higher sensitivity, than species A (Fig. 4.2A). For species dependent on interspecific interactions, such as the abundance of a specific prey source, the simple curve will reflect the environmental conditions favourable to prey occurrence. Finally, rarity traits can translate to geographically small range sizes, and are therefore assumed to tolerate a narrower range of environmental conditions, with species C and D considered rarer and therefore more sensitive than species A or B (Fig. 4.2A). Although rarity is considered a trait in the SEAC framework (Foden et al. 2013), we argue that rarity is an exacerbating factor in vulnerability rather than a true intrinsic species trait. In practice, sensitivity is often characterised by a suit of traits (e.g. Fremout et al. 2020; McClure et al. 2023). In our example, we might assess sensitivity based on a combined measure of niche slope and breadth. By assigning a value of 1 for the least sensitive species, and a value of 2 for the most sensitive species of each, species A would emerge as the least sensitive species with a value of 2, followed by species B at a sensitivity of 3, and species C and D at a sensitivity of 4.

We have demonstrated how frequently used assessments of sensitivity can be interpreted in relation to how they alter the slope and breadth of the niche curve. To quantify vulnerability using the SEAC methodology, we tally up the individually assessed measures of exposure, adaptive capacity and sensitivity. In our simple example, we set the first two to be equal for all species and thus the final vulnerability ranking depends entirely upon differences in assessed sensitivity.

If we define the sensitivity of species as a function of the slope of the niche curve, i.e. if we assume that species that experience steep thresholds in occupancy as a function of climate variables are most sensitive, species A would emerge as the least vulnerable, with the remaining species having equal vulnerability (Fig. 4.2B). It should be noted, however, that sensitivity may also be defined by shallow gradients rather than steep thresholds. This is because species with shallower relationships are likely to be affected over a broader range of the climatic gradient, unlike those with steeper relationships. If the climatic impacts are negative, we would expect declines in occupancy to occur across a much larger proportion of the range of species A, and extending into its core area. If we define sensitivity as a function of niche breadth, assuming that climatic specialisation drives sensitivity, species A and B emerge as equally vulnerable, and less vulnerable than species C and D (Fig. 4.2B). Finally, if we define sensitivity as a combined measure of niche slope and breadth and assume the two to be equally important, species A emerges as the least vulnerable, followed by species B, and finally species C and D as the most vulnerable, with equal scores (Fig. 4.2B).

This illustrates the value of considering vulnerability assessments in this abstract example: we are forced to be explicit about what sensitivity means in terms of the fundamental niche shape of species.

4.5.2 Quantifying true vulnerability

To fulfil objective 2 and quantify true species vulnerability, we evaluate our simulated spatial example. We see the slopes, niche breadths and centre points of the simulated fundamental curves reflected in the spatial pattern (Fig. 4.3). Species A exhibits smooth edges around areas of high probability of presence (i.e. gradual decrease from presence to absence) owing to its lower slope, while species B, C and D exhibit equally steep edges, changing abruptly from present to absent, due to their steep slopes (Fig. 4.3A). Species A and B have roughly equal range sizes in the region, larger than the range of species C, due to differences in niche breadth. Species D has a smaller range still, due to the additional marginal niche position in the region's climate space (Fig. 4.3A).

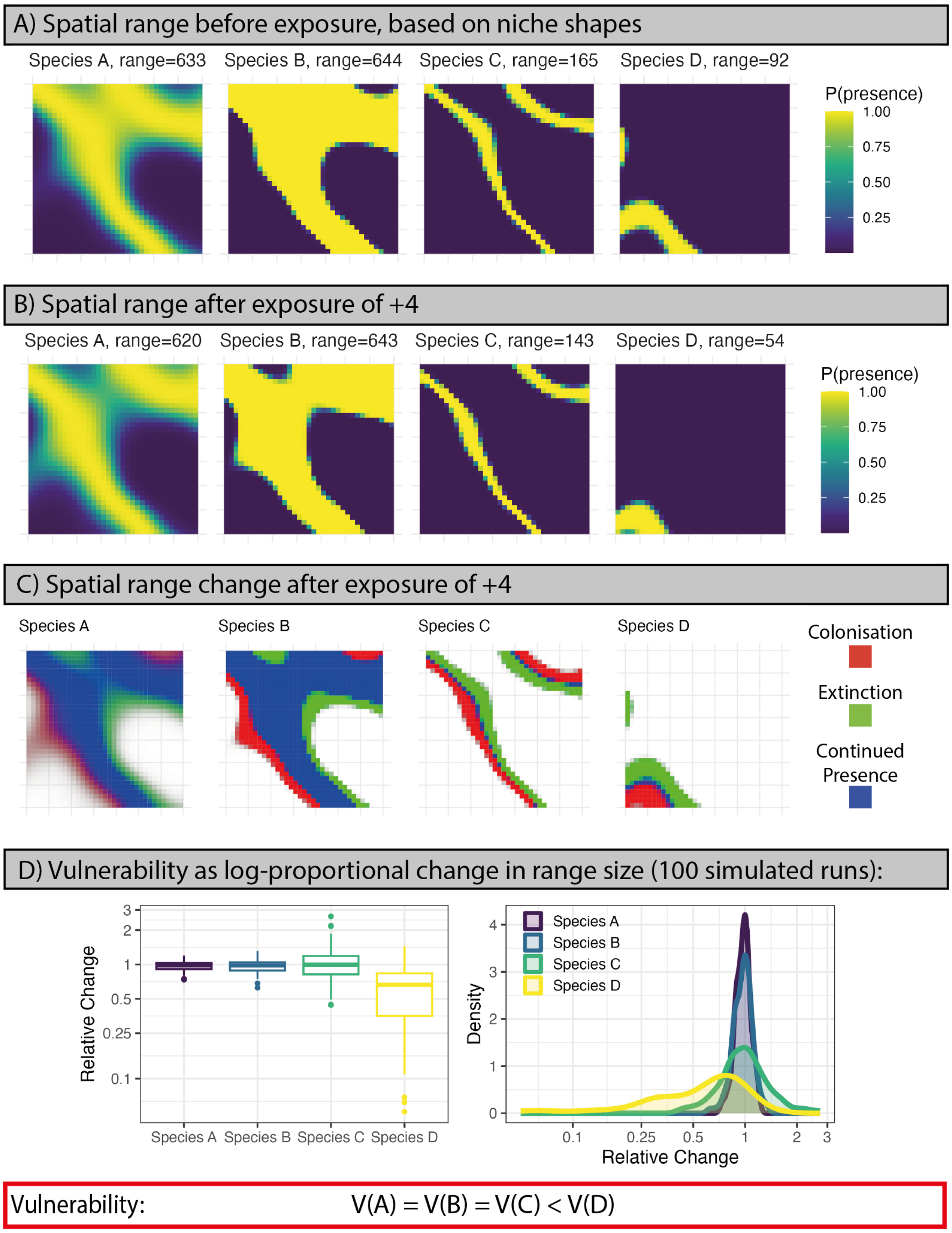

A) Spatial range before exposure, based on niche shapes

B) Spatial range after exposure of +4

C) Spatial range change after exposure of +4

D) Vulnerability as log-proportional change in range size (100 simulated runs):

Figure 4.3: The simple example, applied to geography. *(continued on following page)*

(continued caption) A) Species range maps were derived by applying the niche curves from Figure 2A to a simulated temperature field that included spatial autocorrelation. The colour gradient represents the probability of presence, ranging from 0 (not present) to 1 (present). The range sizes are calculated as the sum of all pixel-level suitability scores. B) Range maps after exposure of +4. C) Range change after exposure of +4, highlighting areas of transitions (red: colonisation, green: extinction), as well as areas of continued presence (blue), where no change in range occurred. Areas of continued absence are used as an opacity mask, with those areas fully transparent. D) Vulnerability scores calculated as log-proportional change in range size after exposure of +4. For easier interpretation, scores are labelled as relative change, where 0 represents no overall change in range size, 0.5 represents a halving, and 2 represents a doubling of size. Species D experienced large losses under some simulations, leading to several very small scores; scores were limited to those between -3 and 1 on the log scale for visualisation purposes. The line colours correspond to the colours used in Figure 2A. Box plots and density curves are based on 100 different simulations of the spatial temperature field.

As before, we assume equal exposure for all species. We introduce a constant exposure of +4 across all pixels in the spatial field and project species ranges again (Fig. 4.3B). In Figure 4.3C, we visualise the different transitions that occur, showing probabilities of local colonisations, extinctions or continued presence. As expected, the shallower slope of species A is reflected in the overall transition pattern, with probabilities of extinction reaching further into the core area of the species range (Fig. 4.3B). Species C and D, with their narrow niches, mainly show transitions, with only small areas of continued presence (Fig. 4.3B). Species D, with its marginal initial range, is further pushed towards the edge, leading to a complete loss of the North-Western distribution (Fig. 4.3B).

We find that species A-C exhibit equal vulnerability, with no average loss in range size. Species D, on the other hand, shows the highest vulnerability, losing nearly 40 percent of its range, on average (Fig. 4.3C). Testing the effect of the scale of spatial autocorrelation on this result, we visualise the contrasts for four different magnitudes of correlation and find the vulnerability ranking preserved across all variations (Suppl. Fig. 1).

4.5.3 Emergent shortcomings of separately assessed sensitivity, exposure and adaptive capacity

In applying the SEAC approach to our simple examples, sensitivity is an intrinsic property of the species and relates to the shape of the fundamental niche curve. Comparing our vulnerability scores derived using separate SEAC with the true vulnerability scores (as range change following climatic change), we find disagreement: the former distinguishes either species A and B, B and C, or A, B and C in terms of their vulnerability, while the latter does not distinguish either species, but assigns higher vulnerability to species D. This shows that, even with a perfect understanding of the niche shape, it is impossible to adequately capture true vulnerability using separate SEAC - the true population impacts as a consequence of species sensitivities and exposure are missed. We can therefore deem any niche-based vulnerability assessments that use separate SEAC to be fundamentally flawed.

As a consequence of this finding, the frequently used trait-based vulnerability assessment appears to be an inadequate method, not least because it is based on separate SEAC: our example shows how the final vulnerability ranking depends entirely on a subjective judgement of what sensitivity represents. We reduced sensitivity traits to two foundational components (niche breadth and slope) and using either alone or in combination results in contradictory vulnerability rankings. One might argue that this is only the case where adaptive capacity and exposure are equal for all species assessed (as in our scenario), and hence not a frequent occurrence. However, adaptive capacity is often not assessed in empirical studies as it is deemed to be implied in the chosen sensitivity traits. In those cases, exposure between species is equal where ranges overlap which still results in a final vulnerability ranking driven entirely by the chosen definition of sensitivity. Thus, the flaws we identify appear fundamentally ingrained in trait-based approaches.

4.5.4 The case for correlative assessments

We have demonstrated that vulnerability rankings based on separate SEAC, as commonly used in trait-based assessments, lead to incorrect results. In essence, our quantification of true vulnerability was analogous to methods used in correlative vulnerability assessments, with the crucial difference being perfect knowledge of the fundamental niche shape and adaptive capacity in our theoretical example. Several studies have identified contradictory results when applying both trait-based and correlative assessments simultaneously to the same species (Lankford et al. 2014; Still et al. 2015; Wheatley et al. 2017). We believe this is due to the inadequacy of separate SEAC, as well as the subjectivity that goes into quantifying sensitivity, with correlative assessments attempting to quantify true vulnerability more directly.

While there are many sources of bias and practical hurdles with species distribution models to consider in correlative assessments, they forego subjective decisions that are integral to separate SEAC and are instead driven by observation data. The challenge becomes one of analytical nature, not a fundamental misalignment of method with goal. As more observation records become available or methodological strides are made, existing SDMs can be improved. We live in an age of big data in macroecology (Wüest et al. 2020), steadily growing the amount of information available to SDMs.

4.5.5 Improved correlative assessments using advances in SDM methods

Recent developments in SDMs have shown promising results in overcoming analytical challenges in correlative assessments. Since the development of the Markov chain Monte Carlo (MCMC) methods (Gilks et al. 1995), Bayesian statistics have been applied in spatial ecology due to their flexibility in dealing with the complex issues of spatial data, leading to more realistic results (Blangiardo et al. 2015; Redding et al. 2017; Martínez-Minaya et al. 2018). In 2009, a new method for Bayesian modelling, the Integrated Nested Laplace Approximation (INLA), was publicised (Rue et al. 2009). Implemented in the programming language R, INLA showed similar accuracy to MCMC but lower computation times (Blangiardo et al. 2013) for the subset of problems that can be fitted using latent Gaussian models. INLA is an increasingly popular tool in ecology (e.g. Gutowsky et al. 2019; Niekerk et al. 2019; Rivera et al. 2019), with recent research showcasing its applicability to vulnerability assessments (Wheatley et al. 2023). The addition of the Stochastic Partial Differential Equations (SPDE) approach (Lindgren et al. 2011) enabled a computationally efficient characterisation of the spatial effect, allowing for the specification of a spatial random field. In essence, this allowed modellers to improve SDM estimates by accounting for unexplained spatial effects and auto-correlation issues (Fichera et al. 2023). In the context of climate vulnerability assessments, such unexplained effects might include non-climatic factors, such as species interactions. Additionally, random fields reduce over-prediction issues outside species distribution ranges by restricting estimates spatially (Engel et al. 2022). One of the latest additions to INLA is the method of model-based data integration (Isaac et al. 2020). Observation data frequently come in different formats, traditionally necessitating observations to be pooled, subsequently leading to the loss of information. Model-based data integration provides a solution to this problem, maximising the amount of information retained from each data set (Isaac et al. 2020). In combination, these developments have led to improved accounting for sampling bias, while also maximising the information gained from different observation data sources.

4.5.6 Empirical example: Savannah birds in Tanzania

To fulfil objective 3 and demonstrate the applicability of methodological advances in species distribution modelling to climate vulnerability assessments, we showcase a vulnerability assessment using 40 years of bird observations in Tanzania (Fig. 4.4). We focus our example on savannah specialist birds, a group that has experienced significant levels of climatic and habitat change over the past decades (Ongoma et al. 2018; Ayugi et al. 2021; Nzunda 2022), alongside considerable range shifts (Beale et al. 2013, Chapter 3). We use data integration models to maximise the information derived from two observation data sets (Tanzania Bird Atlas, eBird), and use a spatiotemporal structure to estimate niche curves based on two distinct time periods (1980-1999, 2000-2020). For each of a list of 76 species, we estimate the current range, as a product of the spatial random field, as well as climatic and non-climatic variables and sampling effort (Fig. 4.4A). We then isolate the effect of the multivariate climate alone, to calculate pixel-level suitability change for two climate scenarios considered (SSP2-4.5, SSP5-8.5) (Fig. 4.4A). By accounting for the spatial random field when calculating climate suitability, we account for spatial autocorrelation issues while simultaneously avoiding overprediction outside the species ranges.

We rank species by their average climate vulnerability and find that the region is projected to become more climatically suitable for most species (Fig. 4.4A). This change constitutes up to a 21 percent increase in suitable area, in the case of the bare-eyed thrush (*Turdus tephronotus*) (Fig. 4.4B). However, a small subset of species are projected to experience a decrease in climatically suitable area (Fig. 4.4B), including the rosy-patched bush shrike (*Rhodophoneus cruentus*), with a decrease of approx. 3 percent under the SSP5-8.5 climate scenario (Fig. 4.4B). This projected decrease is larger under the more extreme SSP5-8.5 scenario for all but one of the negatively affected species.

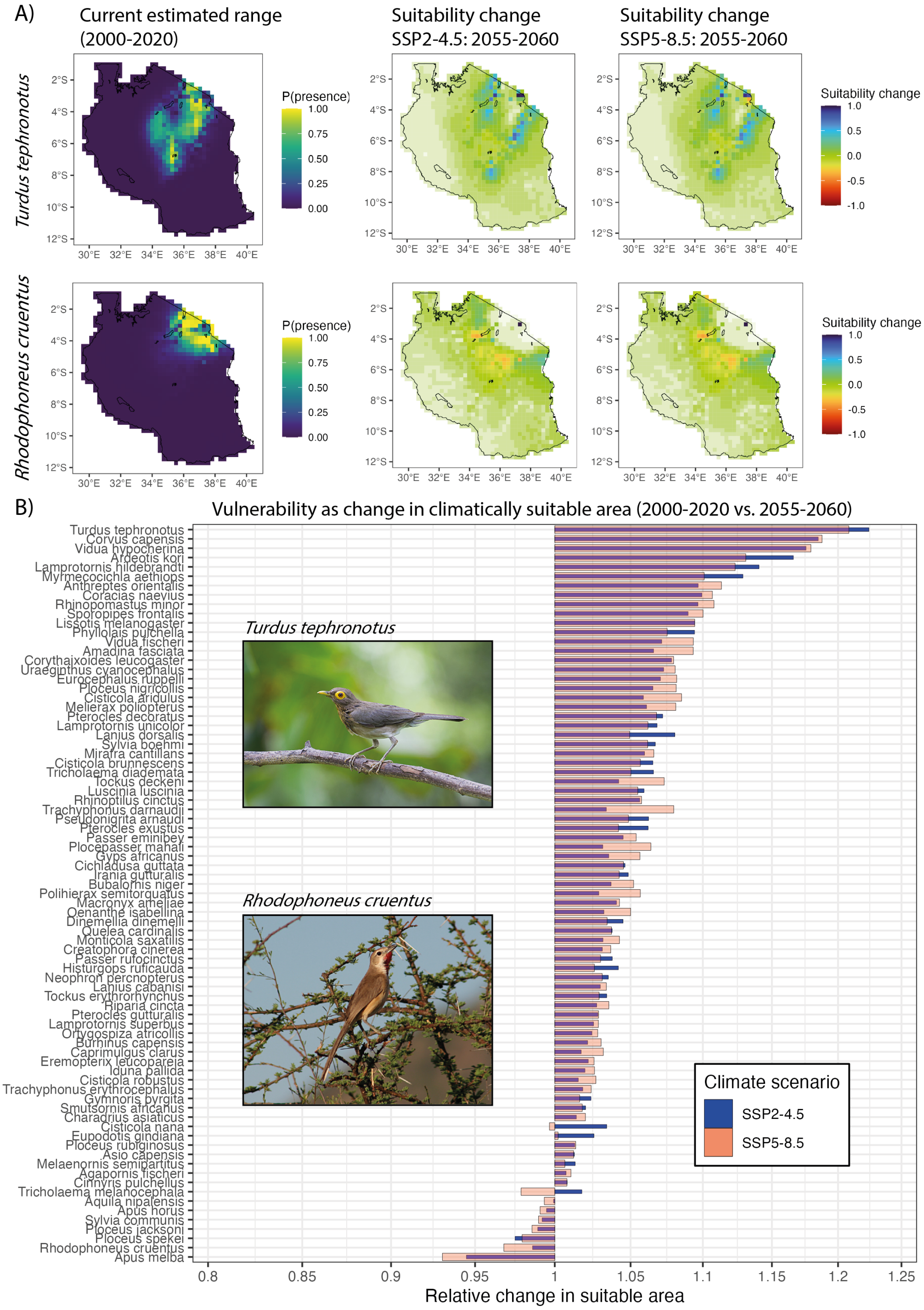

Figure 4.4: *Empirical example for the application of recent advances in distribution modelling to climate change vulnerability assessments. (continued on following page)*

(continued caption) A) Example species, showing the current range estimates as well as change in climatically suitable area for Tanzania, under future climate scenarios SSP2-4.5 and SSP5-8.5. Suitability change maps contain a transparency layer based on quantile values emphasizing pixels where larger changes occurred. B) Species ranked by final vulnerability scores, averaged across the two climate scenarios. Scores are labelled as relative change, where 0 represents no overall change in suitable area, 0.5 represents a halving, and 2 represents a doubling. Highlighted in the photos are the species with a breeding range in Tanzania showing the largest increase (*Turdus tephronotus*) as well as the largest decrease (*Rhodophoneus cruentus*) in climatically suitable area. Photo credits: "Bare-eyed Thrush (5529613751)" by Eleanor Briccetti, CC BY-SA 2.0, via Flickr. "Rosy Patched Bush Shrike, Samburu NR, Kenya" by ChrisHodgesUK, CC BY-SA 3.0, own work. No changes made to original photos.

This approach improves on traditional SDM-based vulnerability assessments in two ways. Firstly, it potentially creates a more reliable estimate of the species' niche curves, by considering two distinct time periods during model fitting. This can help move closer to characterising the fundamental niche, relating species observations to changing environments over time, and hence a wider range of environmental conditions (Myers et al. 2015). Secondly, the spatial random effect structure accounts for unexplained covariates not included in the model, such as biotic interactions that may restrict species distributions beyond any climatic impact. In addition, it avoids overprediction of suitability outside the known species range. However, there are potential caveats. When producing future suitability maps, we use present-day spatial processes. This ignores the fact that landscapes continue changing in the future, and habitat degradation has been shown to significantly compound negative climate change impacts (Travis 2003; Bonebrake et al. 2016; Virkkala 2016). However, accurately forecasting landscape changes beyond just a few years is notoriously difficult (Chaudhuri et al. 2014; Cao et al.

2019), and including present-day spatial processes is no doubt more useful than ignoring this component altogether. In addition, there are theoretical challenges that our modelling approach did not overcome. When estimating future suitability, the niche shape is estimated based on both past and current data, assuming the ecological relationship between presence and climate has not changed over the time period used. Micro-evolutionary adaptation to climate change can occur over relatively short periods of time (Balanyá et al. 2006; Franks et al. 2007), potentially changing the niche shape in the near future. However, these examples stem from species with short life cycles. While evidence for micro-evolutionary adaptation exists in birds (Karell et al. 2011), the effectiveness of this mitigation, and hence bearing on the niche shape, is unclear. Still, suitability forecasts should be viewed critically considering this caveat. Traits might provide complementary information in these cases, for example where they are used to quantify the adaptive capacity of species (Beever et al. 2023), and thereby perhaps the potential for future niche evolution.

4.6 Conclusion

We have demonstrated the fundamental inability of separately assessed SEAC to accurately estimate the true climate change vulnerability of species, alongside uncertainty stemming from subjective decisions in trait-based approaches. Previous vulnerability rankings based on these methods were highly dependent on perceptions of species sensitivity, and failed to reflect true climate vulnerability.

Given the increasing importance of reliable vulnerability rankings under the current climate trajectory, we hope that this study can help practitioners decide on the most appropriate vulnerability framework for their needs. Our findings discourage relying solely on trait-based approaches based on separately assessed SEAC. However this does not exclude the use of traits in vulnerability assessments. Indeed, we believe that traits can play a valuable role in complementing alternative assessments, such as those based on SDMs.

The improved correlative assessment presented here through our empirical example aims to demonstrate how newly developed SDM methods may be used for applied conservation. The flexible nature of the approach means that it is applicable to any species where sufficient geolocated observation data are available, and the models created can be improved as additional observation data are collected. Given the increasing number of observations available for many species, we believe that our approach has broad applicability.

Despite the methodological advances demonstrated here, SDMs are by no means a perfect solution, and theoretical issues not related to analytical challenges remain. Specifically, our empirical example highlights limitations in accounting for the dynamic and complex interactions between species and changing environments. Our models' reliance on static spatial processes and assumptions of constant niche shapes overlooks future landscape changes and potential micro-evolutionary adaptations. This could significantly affect the accuracy of our vulnerability predictions.

The compounded effects of climatic and non-climatic pressures on species vulnerability, not fully addressed here, underscore the necessity for models that can capture these complex interactions. Such improvements are vital for refining vulnerability assessments and guiding conservation strategies amid climate change and habitat degradation. Future research should prioritize the validation of vulnerability rankings and incorporate diverse data sources, including traits and long-term observations, to enhance assessment reliability. This will provide a robust basis for judging the predictive power of SEAC approaches and the applied methodologies in our empirical example. Ultimately, this will contribute to more informed and effective conservation decision-making, ensuring the resilience of biodiversity in an era of unprecedented environmental change.

4.7 Data availability

R code for the theoretical examples can be accessed using the following link: https://doi.org/10.6084/m9.figshare.24764136.v1.

4.8 Acknowledgements

This research was funded by the Natural Environment Research Council (NERC) through the Adapting to the Challenges of a Changing Environment Doctoral Training Partnership (ACCE DTP) program (grant number NE/S00713X). We are extremely grateful to Neil Baker for providing the Tanzania Bird Atlas data, as well as the volunteers who submitted their records to the Tanzania Bird Atlas.

5

Chapter 5: General Discussion

5.1 Summary of thesis findings

In this thesis, I set out to advance our understanding of processes driving habitat degradation and species distribution shifts in Tanzania, drawing more general lessons about species vulnerability assessments where possible. This included analysing long-term trends in degradation in Tanzanian savannas, investigating the explanatory power of traits in relation to range shifts, and critically evaluating a common framework for vulnerability assessments.

In this final chapter, I summarise the methods and findings of each data chapter, followed by an overview of the unique contributions of this thesis to ecological knowledge. I end with suggestions for future studies emerging from the research and limitations of this thesis, as well as concluding remarks.

Chapter 2: Pathways of degradation in rangelands in Northern Tanzania show their loss of resistance, but potential for recovery

In this chapter, I examined mechanisms and correlates of long-term trends in degradation in East-African grasslands, in terms of grazing potential. To do so, I trained machine learning models with remote sensing and field data, allowing me to derive long-term degradation maps for the study area from satellite products. Initially aiming to characterise degradation using bare ground cover and the number of toxic and invasive plants, I discovered the latter to be unreliably estimated and focused instead on bare ground cover alone. I found that degradation emerged due to a decline in resistance to environmental shocks, and that this degradation was associated with lower rainfall and higher human and livestock density. However, I found that even the most degraded sites did not lose their recovery potential, giving hope for restoration provided suitable rainfall continues. Furthermore, I found that, alarmingly, degradation increased across the whole landscape. This increase was lowest for national parks and wildlife management areas, underlining the effectiveness of these management strategies for mitigating current degradation trends.

Chapter 3: Spatio-temporal integrated Bayesian species distribution models reveal lack of broad relationships between traits and range shifts

Here, I investigated the explanatory power of traits in explaining variation in range shifts of species, using 40 years of observation data from Tanzania, and 91 individual study species. Among other remote sensing products, I used bare ground layers produced in Chapter 2 of this thesis. The analysis involved the development of a species distribution modelling approach, using Bayesian models with a spatio-temporal structure, as well as model-based data integration, utilising Atlas as well as citizen science observations. Despite including a wide range of traits and species in the analysis, I found little support for broad trait-range shift relationships across taxa, for either local extinctions, local colonisations, or total change. This result calls into question the usefulness of traits in vulnerability assessments of taxa: where traits are assumed to be a proxy of how species might shift their ranges in the future, our results suggest that this assumption is poorly supported. However, I also found strong species-specific relationships among the results, suggesting that more research into those individual species might help explain why some species respond more than others.

Chapter 4: Separately assessed sensitivity, exposure and adaptive capacity inadequately represent species vulnerability to climate change

In Chapter 4, I critically evaluated a commonly used climate change vulnerability assessment framework, one that is based on separately assessed species sensitivity, exposure, and adaptive capacity. Using theoretical examples and foundational concepts, I show that this framework is fundamentally unable to accurately predict true species vulnerability. This leads me to discourage the use of vulnerability assessments purely based on this framework, such as many trait-based approaches. Using data and methods developed in Chapter 3 of this thesis, I showcase how advances in species distribution modelling can be used to overcome analytical challenges in vulnerability assessments and provide an alternative index.

5.2 Degradation and recovery in East African savannahs

Land degradation is on the rise in Africa. The extent of this trend is made abundantly clear by growing research using remote sensing products (Symeonakis et al. 2004; Bai et al. 2007; Landmann et al. 2014; Kirsten et al.

2023, Chapter 2), including a study in close vicinity to the rangelands investigated in Chapter 2 (Li et al. 2020). Unfortunately, my findings provide further confirmation of this trend: degradation has been steadily increasing in most of the study region over the last 20 years. Since viable pastures are not in limitless supply, a slowdown and reversal of this trend is becoming a necessity if pastoralism is to continue as a viable lifestyle for the people of this region (Bardgett et al. 2021). The need for grassland conservation has been noted for decades (Johnson 1980), but recent anthropogenic trends in East Africa such as agriculture expansion are increasing the urgency of improving the condition of remaining grasslands (Rukundo et al. 2018; Bullock et al. 2021). Identifying the root cause of degradation is the first step in mitigating it, and numerous studies have proposed possible drivers, such as climatic variation (Wang et al. 2017), over-grazing and high fire frequency (Hilker et al. 2014) and nutrient enrichment (Stevens et al. 2004). Based on the identified drivers, management actions can be directed at reducing and reverting degradation, including altering grazing regimes and modifying the vegetation composition (Earl et al. 1996; Heady 2019). However, in practice, the evidence that underpins such management is often rather poor (Rowan et al. 1994; Savari 2022). For example, a key management strategy adopted by thousands of land managers globally is that of 'Holistic Management', developed by Allan Savory, which proposes short but intense grazing to restore rangelands and improve productivity (Savory et al. 1999; Gosnell et al. 2020). Considerable debate exists regarding the effectiveness of this approach (Sherren et al. 2019; Gosnell et al. 2020), but empirical studies showcase potential benefits in some sites (Peel et al. 2018; Hillenbrand et al. 2019). In Chapter

2, I provide a more mechanistic perspective on the causes of degradation, instead of focusing on individual drivers. I demonstrate that degradation is a consequence of repeated environmental shocks over time, and although even the most degraded sites have the potential to recover well, there is insufficient time between shocks to do so. This has important implications for restoration management: my results suggest that the prevention of shocks, coupled with an increase in resistance, can both prevent degradation and support quick recovery, even in the most degraded sites. This contrasts with the view of researchers like Allan Savoury proposing that recovery is not possible without human intervention (Savory et al. 1999). Under the right climatic conditions, rangelands in my study area appear to recover regardless of specific management interventions.

Identifying the factors that increase the resistance of rangelands is an active field of research (Vogel et al. 2012; Hoover et al. 2014; Gillaspy et al. 2023), and my findings underline the importance of these efforts. Using long-term trends, akin to the analysis in Chapter 2, might help identify the effectiveness of interventions aimed at increasing the resistance of rangelands. The prevention of shocks is becoming increasingly challenging. For example, droughts are on the rise due to climate change (Gebremeskel Haile et al. 2019). Indicative of this issue, I show in Chapter 2 that even the most protected land, i.e. national parks, exhibit a gradual long-term increase in degradation, albeit slower than in other areas. It is important to critically evaluate and identify the limits of current management and protection strategies, especially taking into account the complex trajectories of climate forecasts in East Africa (Vizy et al. 2012; Nicholson 2017; Dunning et al. 2018).

Given the ties between recovery and rainfall demonstrated in this thesis, there is a clear need for more research investigating the potential effectiveness of grassland management under a variety of future rainfall scenarios. Linking long-term degradation trends to rainfall at higher spatial and temporal resolution than used in Chapter 2 should provide important insights. Regrowth of grass can occur in as little as 17 days after heavy rainfall events (Post et al. 2020) and greening in as little as two days (Whitecross et al. 2017), and significant spatial heterogeneity occurs in African savannas at scales of 5-25 meters (Augustine 2003). This means that such fine-scale analysis can benefit from daily resolutions at a scale of less than 30 meters. While observations of vegetation greenness at this temporal and spatial scale can feasibly be derived from Sentinel satellite products (Dusseux et al. 2022), higher-resolution rainfall layers might require the use of down-scaled climatic layers, such as those used in microclimate studies (Kearney et al. 2020).

5.3 Predictors of species responses to Anthropocene change

Anthropogenic alteration of vegetation communities and climates is accelerating (Theobald et al. 2020), making it a defining feature of the Anthropocene (Lewis et al. 2015). While my study focused on Tanzania as the study area, my results showing increasing habitat degradation identified in Chapter 2 match a wider global pattern of changing landscapes (Hill et al. 2020a). Studies are showing that these changes compound with climate alteration to create unprecedented pressures on species communities (Travis 2003; Bonebrake et al. 2016; Virkkala 2016), leading to urgency in investigating their responses from a conservation perspective. In this thesis, I provided answers to two key questions in this context: what information might be useful for predicting species responses, and how do we accurately identify the species that might respond more than others?

Due to the enormous diversity of life on earth, conservation plans focused on every individual species are doomed to fail (Cowie et al. 2022). Instead, we often rely on the use of methodologies that are broadly applicable to wider taxonomic groups: researchers frequently assess patterns of responses for phylogenetically diverse groups, sometimes at a global extent (Parmesan et al. 2003; Chen et al. 2011; Lenoir et al. 2015). An appealing alternative to evaluating ecological risks for every species individually is the concept that species with similar functional traits could face similar risks (e.g. Brown et al. 2016). Since traits are not always known at the species level, the identification of relationships between traits and species responses that generalise across taxa would be beneficial. However, in Chapter 3 I provide empirical evidence that assuming such general trends is an oversimplification of the complex processes that drive species responses. In line with recent reviews and meta-analyses (Buckley et al. 2012; MacLean et al. 2017; Beissinger et al. 2021), I found no broad relationships across 57 species and 8 trait categories considered. It emerged that individual, species-specific variation in these relationships was too great for clear trends to surface. I arrived at this finding even after accounting for traditional analytical shortcomings in estimating species ranges, indicating the ecological robustness of this result.

Whereas the lack of broad relationships between traits and distribution changes is the recent conclusion of review studies in this area, the research in Chapter 3 adds to the body of work that tests these relationships empirically (e.g. Reif et al. 2012; Sunday et al. 2015). Importantly though, it sets itself apart by applying improved analytical methods not used in other comparable studies. The analytical steps developed in Chapter 3 are highly flexible and applicable to any species, sessile or mobile, presuming that georeferenced species observations and environmental data, such as climate and land cover, exist. While I provide an important insight into the predictors of savannah bird range shifts, the geographical and taxonomic limitations of Chapter 3 mean that my findings might not necessarily be transferable to other groups with very different life histories, such as fish or plants. However, patterns of contradictory results were found in meta-analyses for both groups (MacLean et al. 2017). A repeat of my study with a different spatial and taxonomic focus is both feasible and valuable as a confirmation of the existence of a wider trend of poor predictive ability of traits, once traditional analytical shortcomings are accounted for. If indeed confirmed, this would help practitioners to make a more informed decision on the most appropriate and economical approach to predicting range shifts, perhaps precluding the use of broad trait categories.

5.4 Prioritising species for conservation in the Anthropocene

A central challenge of our time is the prioritisation of species for conservation action (Pullin et al. 2013; Le Berre et al. 2019). While a staggering number of species are going extinct unnoticed (Régnier et al. 2009; Tedesco et al. 2014), climate change vulnerability assessments (CCVAs) allow us to focus on groups of species that may feasibly be protected, and comparatively assess those most in need of conservation intervention (Foden et al. 2019). Although challenging in practice, examples showcase that declining population trends can indeed be reversed (Kierulff et al. 2012; Brown et al. 2019; Nelson et al. 2019). Since conducting CCVAs as well as consequential conservation management is resource-intensive, and resources made available are limited (Miller et al. 2013; Wiedenfeld et al. 2021), the correct vulnerability ranking of species is crucial. Growing uncertainty about the reliability of different CCVAs in the literature (Lankford et al. 2014; Still et al. 2015; Wheatley et al. 2017), in combination with my finding that traits provide a poor prediction of range change, meant that a critical evaluation is timely. In Chapter 4, I demonstrate theoretically that not all assessments are equal: when assessments are based on separately quantified vulnerability components, they are unable to quantify true species vulnerability reliably.

This finding has important implications for existing vulnerability rankings of species: those that were based on these inadequate assessments should be identified and revised using alternative methods, where possible. Given that such assessments might be part of established methodologies, such as the trait-based approaches used for assessing fish and shellfish by the National Oceanic and Atmospheric Administration (NOAA) (Morrison et al. 2015), this might be challenging. However, the potential for misdirection, and consequential waste of limited conservation resources (Pressey et al. 2017) should justify a critical evaluation backed by my findings in Chapter 4. My results also have a bearing on future assessments. The choice of CCVA methods can be difficult given the number of options (Foden et al. 2019). I provide a theoretical argument that some methods should not be used, narrowing down the list of CCVA frameworks. In addition, the species distribution models I developed in Chapter 3 and applied to vulnerability assessments in Chapter 4 should contribute to making the existing methods a more robust choice.

5.5 Limitations and future directions

5.5.1 Prospects for analytical improvements

Many of the analyses conducted in this thesis are part of rapidly evolving quantitative fields. As such, future studies building on the analytical workflows presented here can benefit from recent methodological advances. For example, in the context of machine-learning-based classification of degradation from satellite images, convolutional neural networks (CNNs) might be particularly well suited to improve model accuracy. Developed for image analysis, CNNs take into account the immediate surroundings of individual pixels (Li et al. 2022), which in a geographical context enables e.g. the recognition of individual plants or patches of agriculture (Maggiori et al. 2017; Kattenborn et al. 2021). They are increasingly adopted in remote sensing analyses, showing promising results for example for land use classification (Castelluccio et al. 2015) as well as grassland degradation more specifically (Pi et al. 2021). Paired with high-resolution imagery provided by increasingly available drones (Simic Milas et al. 2018), CNNs might be well suited to identify encroaching unpalatable and toxic plants, which was not reliably achieved in Chapter 2 of this thesis. A highly accurate classification of such plants would allow for a more nuanced degradation index if paired with a measure of bare ground, while enabling additional analyses, such as quantifying the amount of new biomass that is palatable, as pasture lands recover.

The species distribution models (SDMs) I developed in Chapter 3 provide considerable advances to quantitative ecological practices. By combining data integration methods with spatio-temporally structured hierarchical Bayesian models in R-INLA, I showed how spatial autocorrelation issues can be overcome, while simultaneously using multiple data sources effectively. In practice, however, the use of these models may be limited for data-sparse species, a consequence of taxonomic or geographical bias in the collection of observation data (Beck et al. 2014; Troudet et al. 2017). Joint distribution models may provide a solution in those cases, improving estimates for under-sampled species. In short, joint SDMs specifically model the interdependency of species occurrences, allowing probability estimates of one species being influenced by observations of another (Ovaskainen et al. 2016a; Ovaskainen et al. 2017). This makes them especially useful for species with small sample sizes (Ovaskainen et al. 2011; Ovaskainen et al. 2016b), which might enable the analyses developed in R-INLA in Chapters 3 and 4 to be applied to a wider taxonomic range. In addition, joint SDMs can provide additional ecological information by explicitly quantifying the interdependence of species (Warton et al. 2015; Ovaskainen et al. 2017). Although still rarely used, examples in the literature show the feasibility of fitting joint distribution models in the R-INLA framework (Warton et al. 2015; Sadykova et al. 2017; Niekerk et al. 2021).

5.5.2 Evaluation by comparison

No matter the analytical advances, validation of results should remain a central objective. We live in a time of big data in macroecology, with a key characteristic being the increase in publicly available observation records (Wüest et al. 2020), as well as remote sensing data (Hemati et al. 2021). This presents growing opportunities for evaluation by comparison. While the species distribution models developed in Chapter 3 included validation steps, the most robust test of their predictive abilities will be a comparison to newly collected species observations, a gold standard criterion for distribution models (Araújo et al. 2019a). Continuing development of the methods established in Chapter 4, a comparison of the assessment results I found to be inadequate with fully evaluated iterations of my proposed vulnerability index, will ultimately present the strongest case against these CCVAs. In line with this, Foden et al. (2019) highlighted CCVA validation as a key recommendation for future research. Such validation will become especially important where the methods developed in this thesis are applied to new geographic areas. The machine learning algorithm developed in Chapter 2 was trained for a subsection of Tanzanian savannahs, and hence limited geographic reach. If the analyses were to be repeated for other savannah biomes, in Africa or other continents, evaluation of model performance and potential supplementation with new training data would be crucial.

5.6 Concluding remarks

We are now long past the point of debate regarding the existence of anthropogenic climate and biodiversity alteration. Combating the negative effects of changes through the Anthropocene on habitats and species requires a deep understanding of underlying ecosystem processes. Understanding why landscapes degrade, what predicts species range shifts, and how we can best prioritise species for conservation are important cornerstones of conservation success. In this thesis, I contributed original research to each, moving us a step closer to mediating the inevitable global impacts of anthropogenic environmental change. Embracing technological advances of our time, such as remote sensing, machine learning and species distribution modelling will no doubt play an instrumental role.

The findings from this thesis highlight the urgent need for targeted conservation efforts to address the interconnected challenges of habitat degradation, species distribution shifts, and overexploitation, particularly in savannas. While the focus is on Tanzanian savannas, the implications extend to other ecosystems, like tropical forests, where biodiversity is under threat. These insights call for strategies that not only restore degraded habitats but also incorporate sustainable management and community involvement to counteract the drivers of biodiversity loss. Understanding the complex ecological responses and the ineffectiveness of broad trait-based vulnerability assessments emphasizes the necessity for nuanced, ecosystem-specific conservation approaches that can adapt to the global challenge of preserving biodiversity in the face of anthropogenic changes.

Appendices

A

Appendix 1: Supplementary material for Chapter 2

A.1 Supplementary Tables

Table A.1: Predictor variables used as input for the svr classifier. *L7* Landsat 7 product, *L8* Landsat 8 product, *B1-7* band number in Landsat 7 or 8 products. GEE: Google Earth Engine.

Predictor	Notes
blue	0.45 - 0.52 µm (L7, B1), 0.45 - 0.51 µm (L8, B2)
green	0.52 - 0.60 µm (L7, B2), 0.53 - 0.59 µm (L8, B3)
red	0.63 - 0.69 µm (L7, B3), 0.64 - 0.67 µm (L8, B4)
nir	0.77 - 0.90 µm (L7, B4), 0.85 - 0.88 µm (L8, B5)
swir1	1.55 - 1.75 µm (L7, B5), 1.57 - 1.65 µm (L8, B6)
swir2	2.09 - 2.35 µm (L7, B7), 2.11 - 2.29 µm (L8, B7)
EVI	$\frac{2.5 \times NIR - Red}{NIR + 6 \times Red - 7.5 \times Blue + 1}$
BSI	$\frac{(SWIR1 - Red) - (NIR - Blue)}{(SWIR1 + Red) + (NIR + Blue)}$
MSAVI	$\frac{(2 \times NIR + 1 - \sqrt{(2 \times NIR + 1)^2 - 8 \times (NIR - Red)})}{2}$
EVI, BSI, MSAVI magnitude	cos.hypot(sin).multiply(5) (GEE code)
EVI, BSI, MSAVI phase	sin.atan2(cos).unitScale(-Math.PI, Math.PI) (GEE code)
EVI, BSI, MSAVI val	harmonic_withVar.select(variable).reduce('mean') (GEE code)
CHIRPS total rainfall	May previous year to April of prediction year

Table A.2: Data layers used in creating the rangeland-only mask.

Variable	Threshold	Resolution (Ref. year)	Source (ref.)
Surface water	Occurrence > 0	30 m (1984-2019)	GEE: "JRC/GSW1_2/GlobalSurfaceWater" (Pekel et al. 2016)
Rivers	Permanent water label	90 m (NA)	GEE: "MERIT/Hydro/v1_0_1" (Yamazaki et al. 2019)
Steep areas	Slope $> 45°$	30 m (2000)	GEE: "USGS/SRTMGL1_003" (Farr et al. 2007)
Urban areas	Urban $>=$ 50%	100 m (2019)	GEE: "COPERNICUS/Landcover/100m/ Proba-V/Global" (Buchhorn et al. 2020)
Known crops	Cropland label	30 m (2015)	`https://lpdaac.usgs.gov/products/gfsad30afcev001/` (Xiong et al. 2017)
Forests	Tree cover $> 50\%$	30 m (2000-19)	GEE: "UMD/hansen/global_forest_change_2019_v1_7" (Hansen et al. 2013)
High elevation	Elevation $>$ 2500 m	30 m (NA)	GEE: "USGS/SRTMGL1_003" (Farr et al. 2007)

Table A.3: Total area covered (including non-rangeland), and number of pixels used in the land use analysis in the different land use designation sites considered in the study. NP: National Park (NP), WMA: Wildlife Management Area, CCRO: Certificate of Customary Right of Occupancy, NONE: No official management/protection scheme.

Land use designation	Total area (km^2)	Number of pixels
NP	2944.57	62274
WMA	6715.98	156306
CCRO	1252.27	29979
NONE	20295.9	427246

A.2 Supplementary Figures

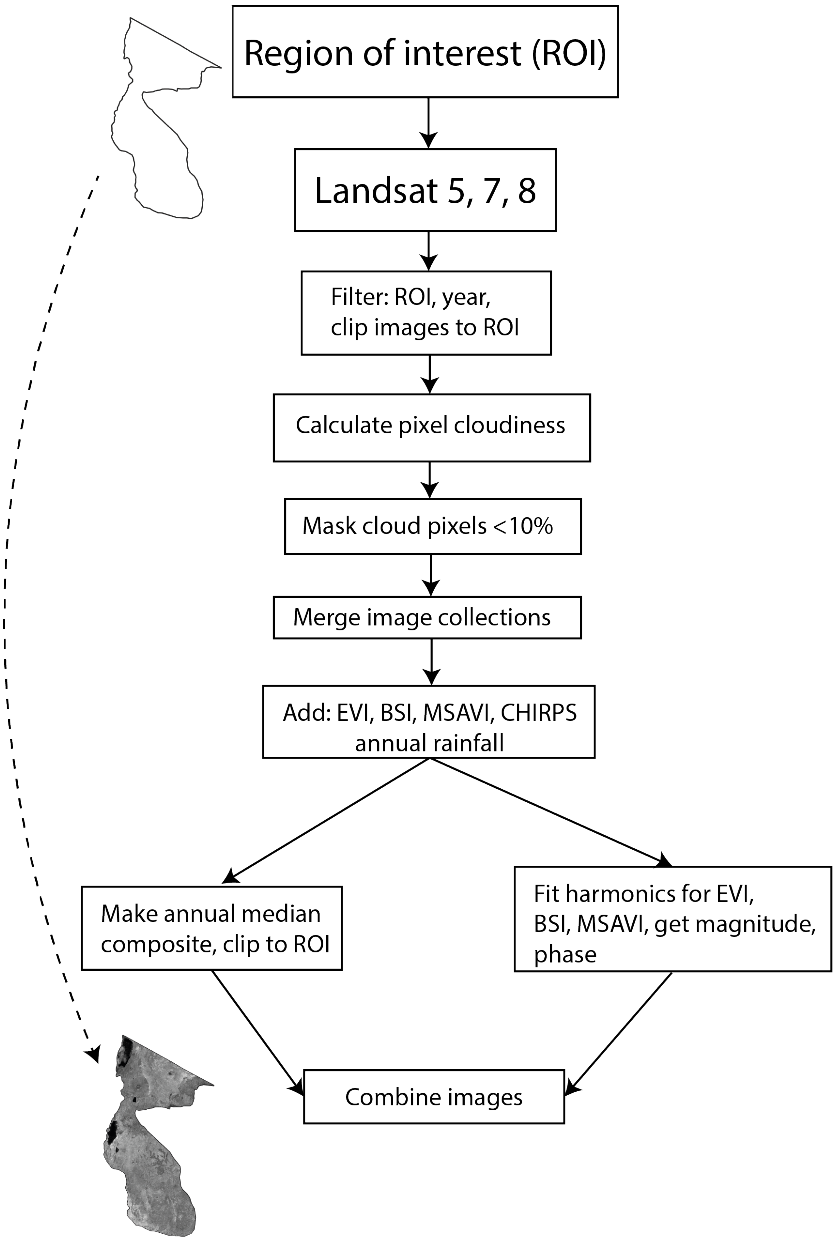
Region of interest (ROI)
Landsat 5, 7, 8
Filter: ROI, year, clip images to ROI
Calculate pixel cloudiness
Mask cloud pixels <10%
Merge image collections
Add: EVI, BSI, MSAVI, CHIRPS annual rainfall
Make annual median composite, clip to ROI
Fit harmonics for EVI, BSI, MSAVI, get magnitude, phase
Combine images

Figure A.1: Conceptual overview of the steps involved in creating annual composite maps for the study area.

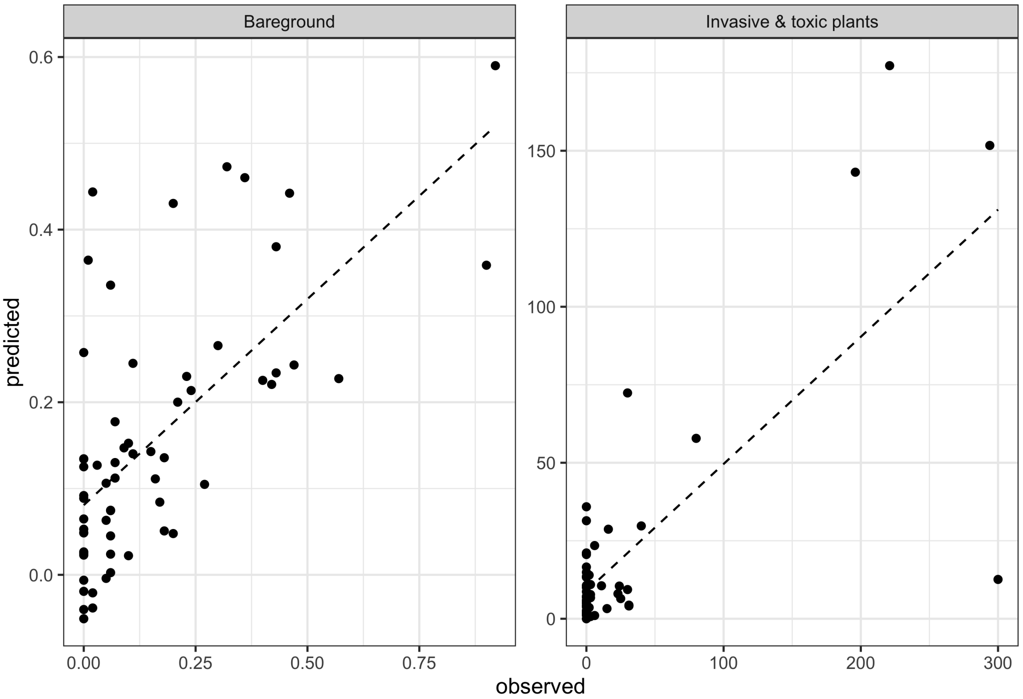

Figure A.2: Validation of degradation scores, observed vs. predicted on 25% of sites not included in modelling for bare ground and number of invasive & toxic plants. Based on the final model, fine-tuned during cross-validation. Dashed lines are trend lines from a linear model on the data.

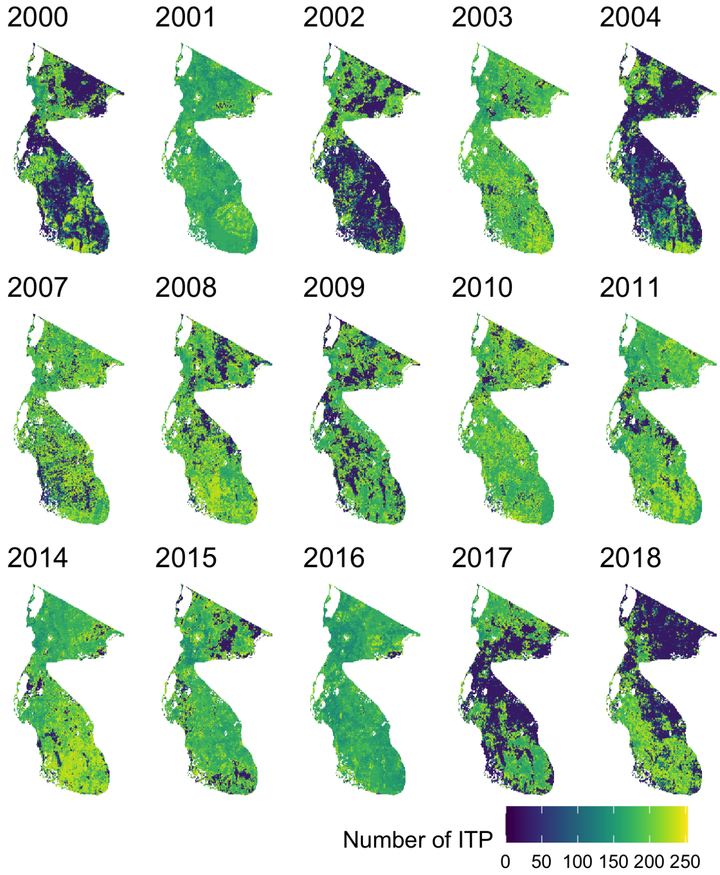
2000
2001
2002
2003
2004
2005
2006
2007
2008
2009
2010
2011
2012
2013
2014
2015
2016
2017
2018
2019
2020
Number of ITP
0
50
100
150
200
250

Figure A.3: Yearly maps of invasive & toxic plant (ITP) cover, based on predictions from the machine learning model. Darker colors correspond to lower ITP cover. The maps were created using R 3.2.2R Core Team 2016.

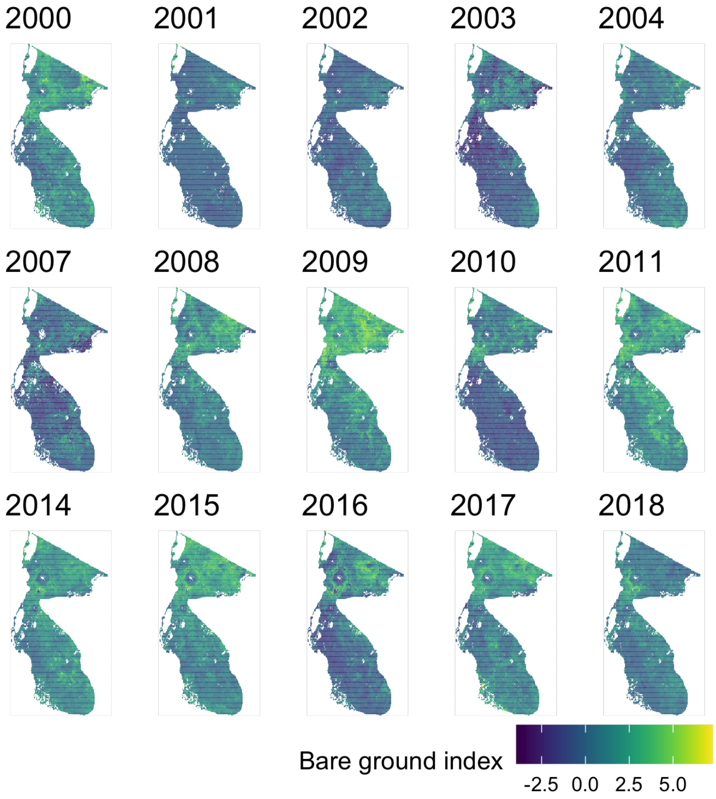
2000
2001
2002
2003
2004
2005
2006
2007
2008
2009
2010
2011
2012
2013
2014
2015
2016
2017
2018
2019
2020
Bare ground index
-2.5
0.0
2.5
5.0

Figure A.4: Yearly maps of bare ground index, based on predictions from the machine learning model, not normalized. Darker colors correspond to a lower bare ground index. The maps were created using R 3.2.2R Core Team 2016.

B

Appendix 2: Supplementary material for Chapter 3

B.1 Supplementary Tables

Table B.1: Environmental covariates included in the species distribution models used to estimate species ranges. Covariates were summarised for the given time frames using a median.

Covariate [units]	Spatial resolution	Time frames covered	Source data	Reference
Annual median rainfall [mm]	5.4 km	1981-1999, 2000-2020	CHIRPS Daily: Climate Hazards Group InfraRed Precipitation With Station Data (Version 2.0 Final)	Funk et al. 2015
Annual median maximum temperature, based on daily maximum near-surface air temperature [°C]	1 km	1981-1999, 2000-2020	'Climatologies at high resolution for the earth's land surface areas' (CHELSA) version 2.1	Karger et al. 2017
Median annual dryspell length [number of continuous days with less than 1 mm of rainfall]	5.4 km	1981-1999, 2000-2020	CHIRPS Daily: Climate Hazards Group InfraRed Precipitation With Station Data (Version 2.0 Final)	Funk et al. 2015
Bare ground cover [bare ground score]	1 km	1990-1999, 2010-2019	Wiethase et al. 2023	Wiethase et al. 2023
Human footprint layer [Combined score]	1 km	1993, 2009	Built environments, crop lands, pasture lands, population density, nightlights, railways, major roadways, navigable waterways	Venter et al. 2016

Table B.2: Taxonomy of the species included in the trait-range shift regression analysis. Numbers in column names represent the total number of unique values in each taxonomic group. Also included are total numbers of detections in the raw observation data, for each species, and each observation data source(eBird and Tanzania Bird Atlas). Taxonomy derived from the National Center for Biotechnology Information (NCBI) database using the 'taxize' package in R (Chamberlain et al. 2013).

Scientific (57)	Common (57)	Family (26)	Order (11)	eBird detections	Atlas detections
Agapornis fischeri	Fischer's Lovebird	Psittacidae	Psittaciformes	376	93
Amadina fasciata	Cut-throat	Estrildidae	Passeriformes	87	91
Anthreptes orientalis	Eastern Violet-backed Sunbird	Nectariniidae	Passeriformes	311	120
Apus horus	Horus Swift	Apodidae	Apodiformes	364	45
Aquila nipalensis	Steppe Eagle	Accipitridae	Accipitriformes	285	78
Ardeotis kori	Kori Bustard	Otididae	Otidiformes	182	55
Bubalornis niger	Red-billed Buffalo-Weaver	Ploceidae	Passeriformes	354	149
Charadrius asiaticus	Caspian Plover	Charadriidae	Charadriiformes	7	46
Cichladusa guttata	Spotted Morning-Thrush	Muscicapidae	Passeriformes	989	171
Cisticola robustus	Stout Cisticola	Cisticolidae	Passeriformes	18	27
Corvus capensis	Cape Crow	Corvidae	Passeriformes	38	23
Corythaixoides leucogaster	White-bellied Go-away-bird	Musophagidae	Musophagiformes	344	103
Creatophora cinerea	Wattled Starling	Sturnidae	Passeriformes	391	150
Dinemellia dinemelli	White-headed Buffalo-Weaver	Ploceidae	Passeriformes	516	138
Eremopterix leucopareia	Fischer's Sparrow-Lark	Alaudidae	Passeriformes	469	181
Eupodotis gindiana	Buff-crested Bustard	Otididae	Otidiformes	42	75
Irania gutturalis	White-throated Robin	Muscicapidae	Passeriformes	37	48
Lamprotornis hildebrandti	Hildebrandt's Starling	Sturnidae	Passeriformes	521	84
Lamprotornis superbus	Superb Starling	Sturnidae	Passeriformes	1770	181
Lanius cabanisi	Long-tailed Fiscal	Laniidae	Passeriformes	524	97
Lanius dorsalis	Taita Fiscal	Laniidae	Passeriformes	115	56
Luscinia luscinia	Thrush Nightingale	Muscicapidae	Passeriformes	259	74
Macronyx aurantiigula	Pangani Longclaw	Motacillidae	Passeriformes	158	39
Melierax poliopterus	Eastern Chanting-Goshawk	Accipitridae	Accipitriformes	209	147
Mirafra cantillans	Singing Bushlark	Alaudidae	Passeriformes	25	37
Monticola saxatilis	Rufous-tailed Rock-Thrush	Muscicapidae	Passeriformes	53	94
Myrmecocichla aethiops	Northern Anteater-Chat	Muscicapidae	Passeriformes	72	29
Oenanthe isabellina	Isabelline Wheatear	Muscicapidae	Passeriformes	60	59
Oenanthe pileata	Capped Wheatear	Muscicapidae	Passeriformes	217	110
Ortygospiza atricollis	Quailfinch	Estrildidae	Passeriformes	29	58
Passer eminibey	Chestnut Sparrow	Passeridae	Passeriformes	182	93
Passer rufocinctus	Kenya Rufous Sparrow	Passeridae	Passeriformes	274	56
Phyllolais pulchella	Buff-bellied Warbler	Cisticolidae	Passeriformes	158	54
Plocepasser mahali	White-browed Sparrow-Weaver	Passeridae	Passeriformes	163	60
Ploceus jacksoni	Golden-backed Weaver	Ploceidae	Passeriformes	850	112
Ploceus nigricollis	Black-necked Weaver	Ploceidae	Passeriformes	117	100
Ploceus rubiginosus	Chestnut Weaver	Ploceidae	Passeriformes	391	92
Ploceus spekei	Speke's Weaver	Ploceidae	Passeriformes	199	32
Poicephalus rufiventris	Red-bellied Parrot	Psittacidae	Psittaciformes	112	38
Polihierax semitorquatus	Pygmy Falcon	Falconidae	Falconiformes	167	90
Pseudonigrita arnaudi	Gray-headed Social-Weaver	Passeridae	Passeriformes	224	133
Pterocles decoratus	Black-faced Sandgrouse	Pteroclididae	Pteroclidiformes	208	92
Pterocles exustus	Chestnut-bellied Sandgrouse	Pteroclididae	Pteroclidiformes	135	52
Pterocles gutturalis	Yellow-throated Sandgrouse	Pteroclididae	Pteroclidiformes	105	66
Quelea cardinalis	Cardinal Quelea	Ploceidae	Passeriformes	108	101
Rhinopomastus minor	Abyssinian Scimitarbill	Phoeniculidae	Bucerotiformes	257	132
Rhinoptilus cinctus	Three-banded Courser	Glareolidae	Charadriiformes	62	46
Rhodophoneus cruentus	Rosy-patched Bushshrike	Malaconotidae	Passeriformes	76	38
Sporopipes frontalis	Speckle-fronted Weaver	Ploceidae	Passeriformes	389	128
Tockus deckeni	Von der Decken's Hornbill	Bucerotidae	Bucerotiformes	434	174
Trachyphonus darnaudii	D'Arnaud's Barbet	Lybiidae	Piciformes	552	138
Tricholaema diademata	Red-fronted Barbet	Lybiidae	Piciformes	130	98
Tricholaema melanocephala	Black-throated Barbet	Lybiidae	Piciformes	105	56
Turdus tephronotus	African Bare-eyed Thrush	Turdidae	Passeriformes	149	51
Uraeginthus cyanocephalus	Blue-capped Cordonbleu	Estrildidae	Passeriformes	378	160
Vidua fischeri	Straw-tailed Whydah	Viduidae	Passeriformes	76	99
Vidua hypocherina	Steel-blue Whydah	Viduidae	Passeriformes	40	69

Table B.3: Samples sizes, as the number of individual species, corresponding to the different levels of categorical traits included in the analyses. Based on a total of 57 study species.

Category	Trait	Description	Sample size
Ecological generalisation	Locomotory niche while foraging	Aerial	2
		Generalist	3
		Insessorial	21
		Terrestrial	31
	Trophic level	Omnivore	11
		Herbivore	21
		Carnivore	25
Movement ability	Migratory ability	Low	42
		Moderate	9
		High	6

B.2 Supplementary Figures

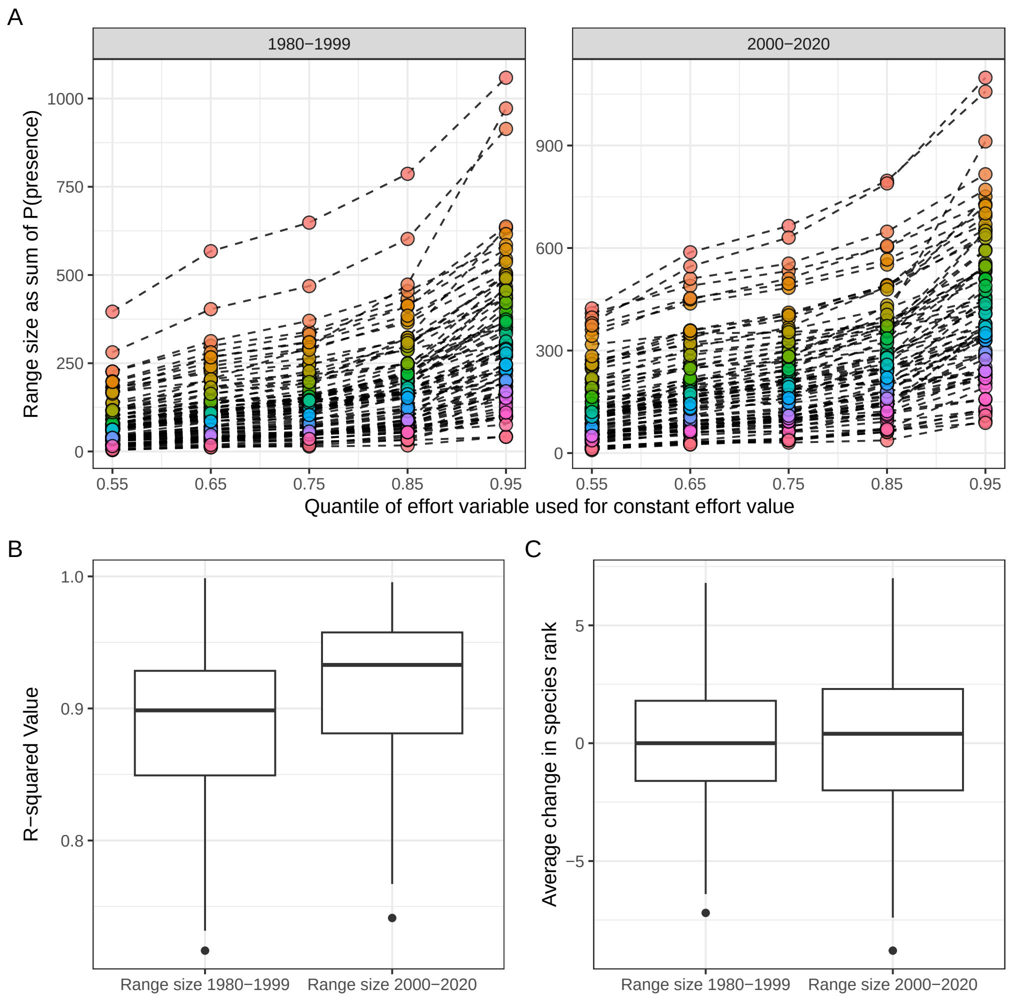

Figure B.1: Plots visualising the effect of the choice of constant sampling effort on the predicted range sizes of species. A) Range size estimates for the 57 species included in the study for the two time periods (1980-1999, 2000-2020), under different sampling effort constants, derived as different quantile values of overall sampling effort. Points are coloured based on the relative rank of each species by range size. Dashed lines connect the range size values within each species. B) Box plots based on r-square values for each species, derived from the four separate range size values of each species in panel A. Average r-square values suggest highly linear relationships for both time periods. *(continued on following page)*

(continued caption) C) Box plots based on the average change in relative range size rank for each species, as sampling effort is varied. Average range change values suggest little to no relative rank change driven by variation in the sampling effort constant.

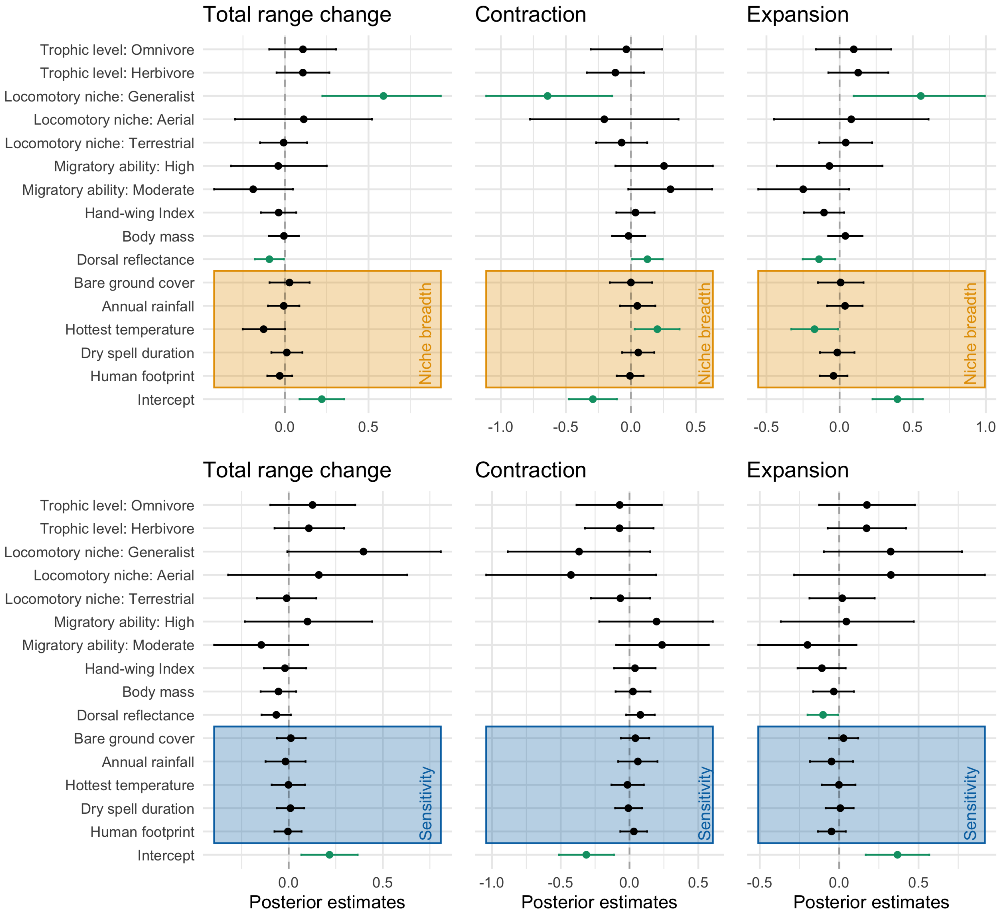

Figure B.2: Parameter estimates and their 95% credible intervals for INLA model results predicting three measures of range shifts: Total range change, meaningful contraction scores, and meaningful expansion scores. Results derived from models containing a phylogenetic random intercept term of family nested in order. Figures A-C are derived from models including human footprint, longest dry spell duration, hottest temperature, annual rainfall, and bare ground cover as niche breadth scores (highlighted in orange). Figures D-F are derived from models including that same set of variables as sensitivity scores (highlighted in blue). *(continued on following page)*

(continued caption) Parameters with credible intervals that do not overlap zero, or credible intervals of other factor levels for categorical variables, may be considered as strong effects in the Bayesian models, and are highlighted in green. For categorical parameters, this signifies that a trait level within a category is statistically different from the reference level. The reference levels are: "Migratory ability: Low", "Locomotory niche: Insessorial" and "Trophic level: Carnivore".

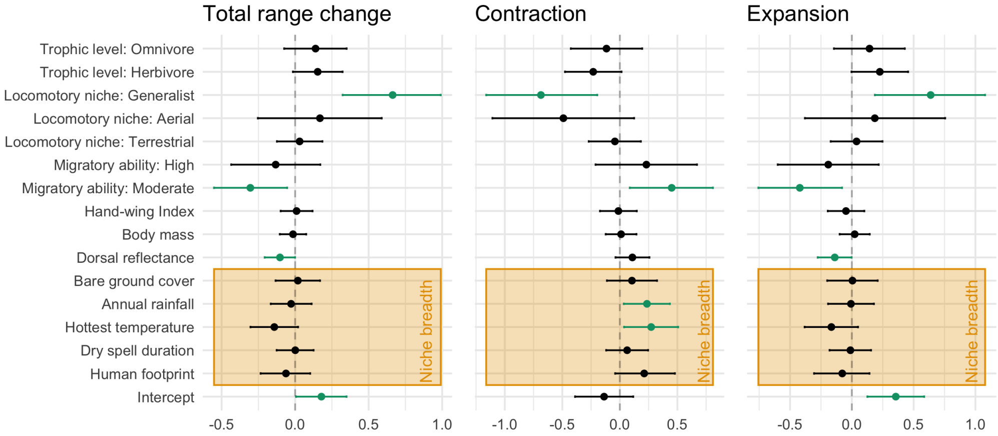

Figure B.3: Parameter estimates and their 95% credible intervals for INLA model results predicting three measures of range shifts: Total range change, meaningful contraction scores, and meaningful expansion scores. Alternative outputs after removing 11 species containing improperly estimated niche shapes (human footprint niche breadth: 8 cases, dry spell duration niche breadth: 3 cases, rainfall niche breadth: 1 case). Parameters with credible intervals that do not overlap zero, or credible intervals of other factor levels for categorical variables, may be considered as strong effects in the Bayesian models, and are highlighted in green. For categorical parameters, this signifies that a trait level within a category is statistically different from the reference level. The reference levels are: "Migratory ability: Low", "Locomotory niche: Insessorial" and "Trophic level: Carnivore".

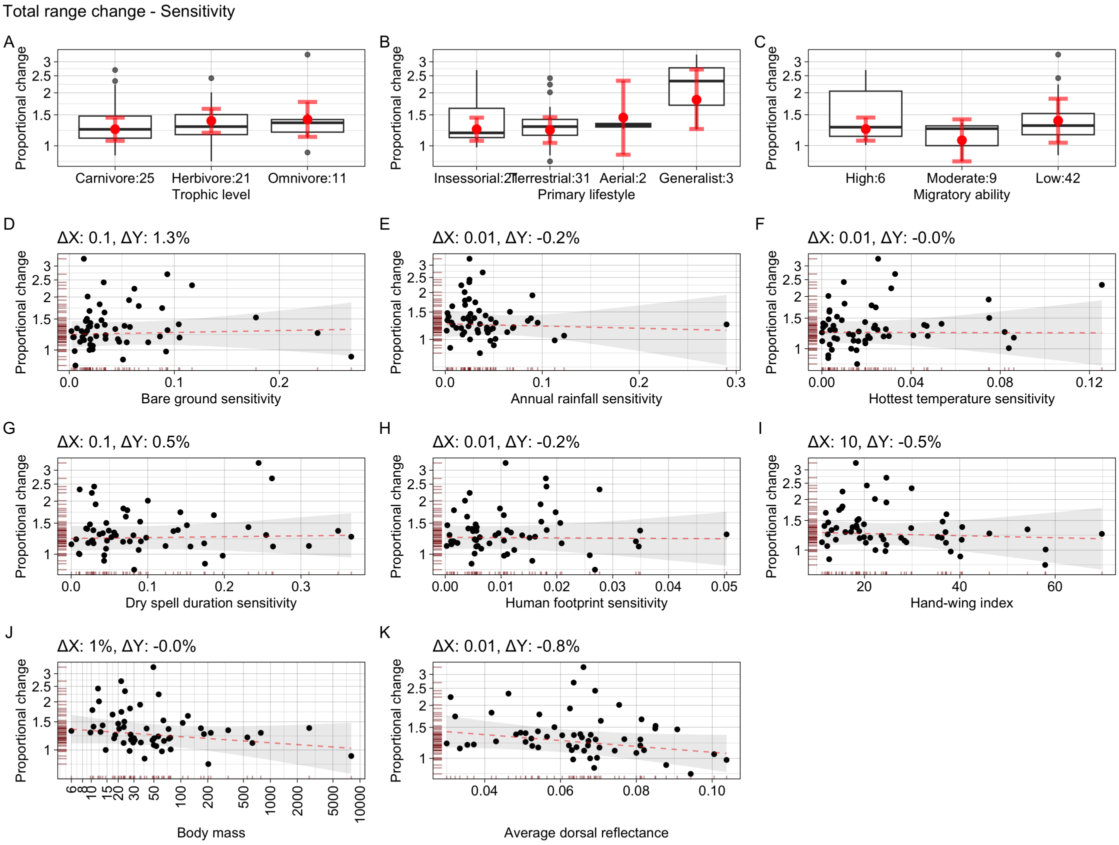

Figure B.4: Effect plots showing the correlations between covariates and total range change, for models containing sensitivity to environmental covariates. Boxplots represent categorical covariates, while scatter plots represent continuous variables. Numbers on x-axis labels represent sample sizes for levels of categorical variables. A score of 1 indicated that no range changes occurred, and a value of 2 indicated that the range size doubled, compared to the initial range. Black points are drawn on the raw data provided to the models, red dashed lines, as well as red points with red error bars are posterior model estimates derived from linear combinations. The rug plots visualise the density of the data points.

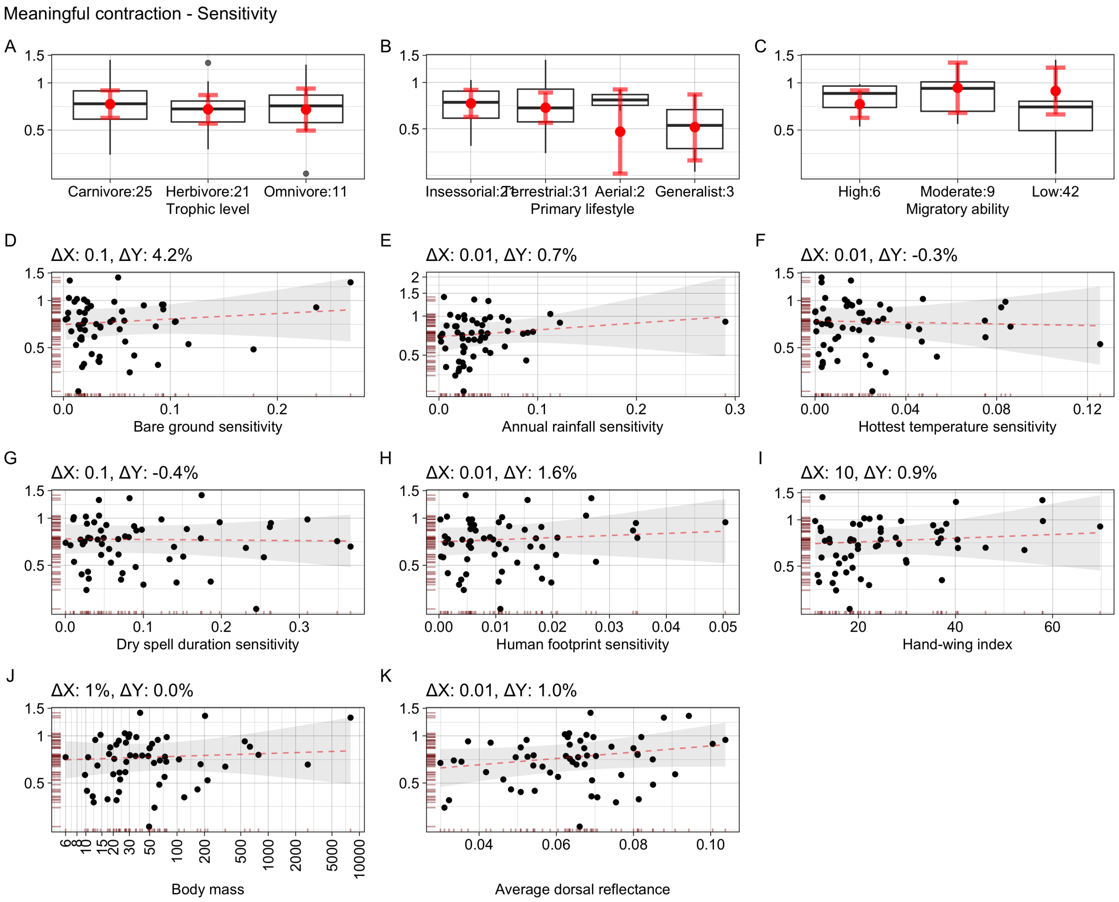

Figure B.5: Effect plots showing the correlations between covariates and meaningful extinction scores, for models containing sensitivity to environmental covariates. Boxplots represent categorical covariates, while scatter plots represent continuous variables. Numbers on x-axis labels represent sample sizes for levels of categorical variables. A score of 1 indicated that changes were exactly as expected from chance (area lost equal to the area of high uncertainty transitions), and a value of 2 indicated that there were twice as many extinctions as expected by chance. A score of 0.5 indicated 50% fewer transitions occurred than expected by chance. Black points are drawn on the raw data provided to the models, red dashed lines, as well as red points with red error bars are posterior model estimates derived from linear combinations. The rug plots visualise the density of the data points.

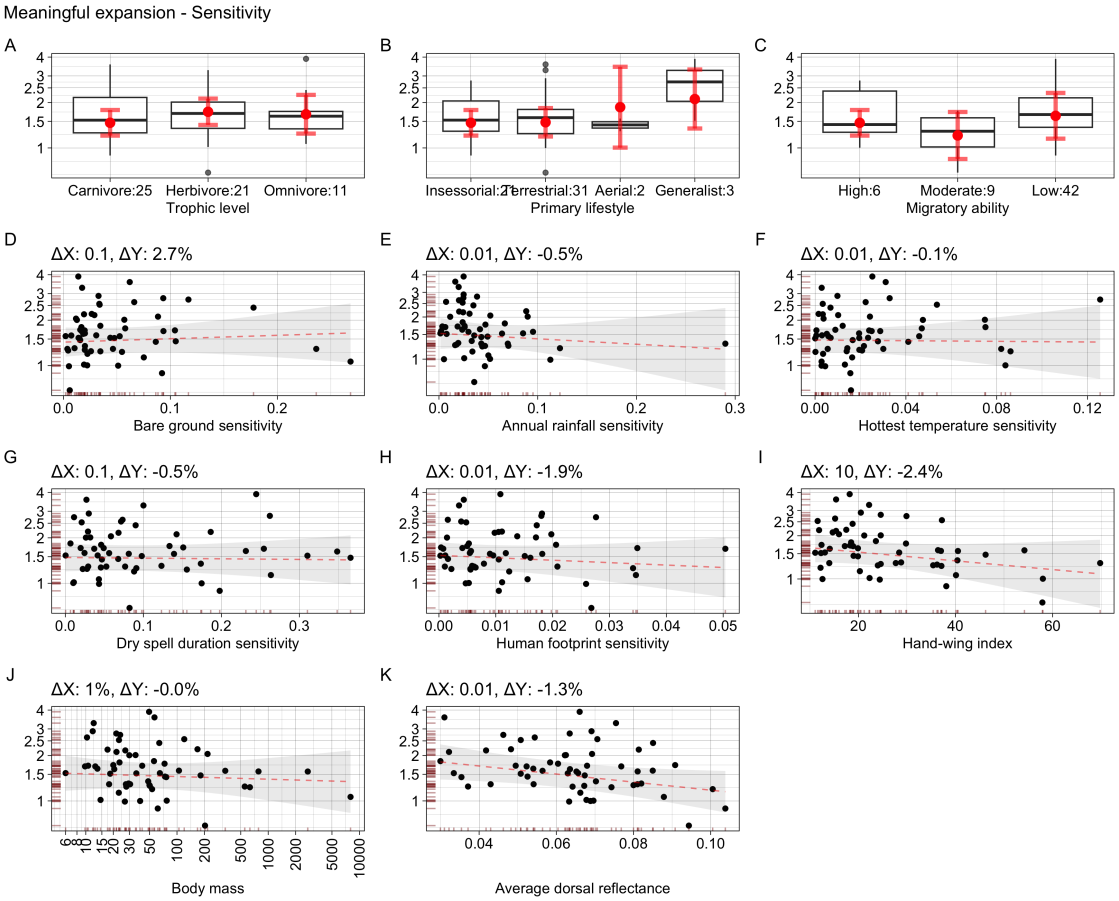

Figure B.6: Effect plots showing the correlations between covariates and meaningful colonisation scores, for models containing sensitivity to environmental covariates. Boxplots represent categorical covariates, while scatter plots represent continuous variables. Numbers on x-axis labels represent sample sizes for levels of categorical variables. A score of 1 indicated that changes were exactly as expected by chance (area colonised equal to the area of high uncertainty transitions), and a value of 2 indicated that there were twice as many colonisations as expected by chance. A score of 0.5 indicated 50% fewer transitions occurred than expected by chance. Black points are drawn on the raw data provided to the models, red dashed lines, as well as red points with red error bars are posterior model estimates derived from linear combinations. The rug plots visualise the density of the data points.

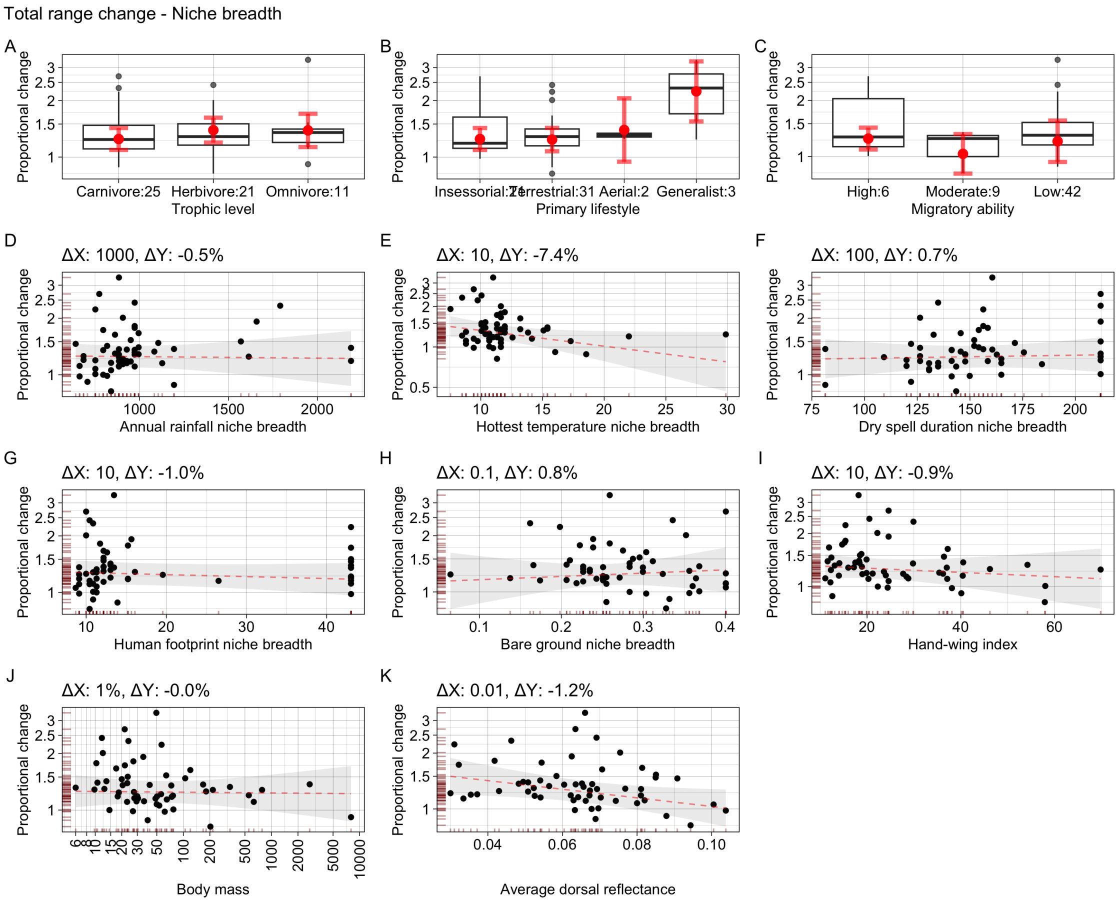

Figure B.7: Effect plots showing the correlations between covariates and total range change, for models containing niche breadth for environmental covariates. Boxplots represent categorical covariates, while scatter plots represent continuous variables. Numbers on x-axis labels represent sample sizes for levels of categorical variables. A score of 1 indicated that no range changes occurred, and a value of 2 indicated that the range size doubled, compared to the initial range. Black points are drawn on the raw data provided to the models, red dashed lines, as well as red points with red error bars are posterior model estimates derived from linear combinations. The rug plots visualise the density of the data points.

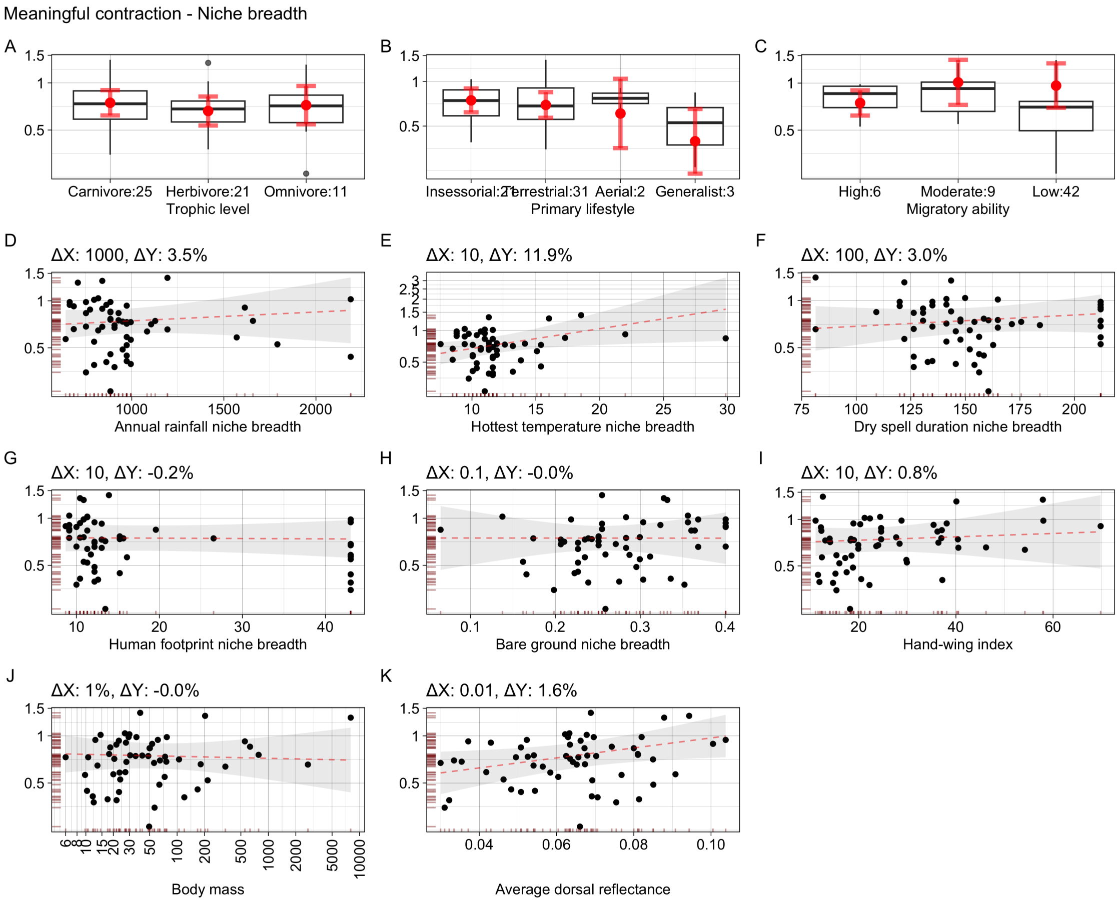

Figure B.8: Effect plots showing the correlations between covariates and meaningful extinction scores, for models containing niche breadth for environmental covariates. Boxplots represent categorical covariates, while scatter plots represent continuous variables. Numbers on x-axis labels represent sample sizes for levels of categorical variables. A score of 1 indicated that changes were exactly as expected from chance (area lost equal to the area of high uncertainty transitions), and a value of 2 indicated that there were twice as many extinctions as expected by chance. A score of 0.5 indicated 50% fewer transitions occurred than expected by chance. Black points are drawn on the raw data provided to the models, red dashed lines, as well as red points with red error bars are posterior model estimates derived from linear combinations. The rug plots visualise the density of the data points.

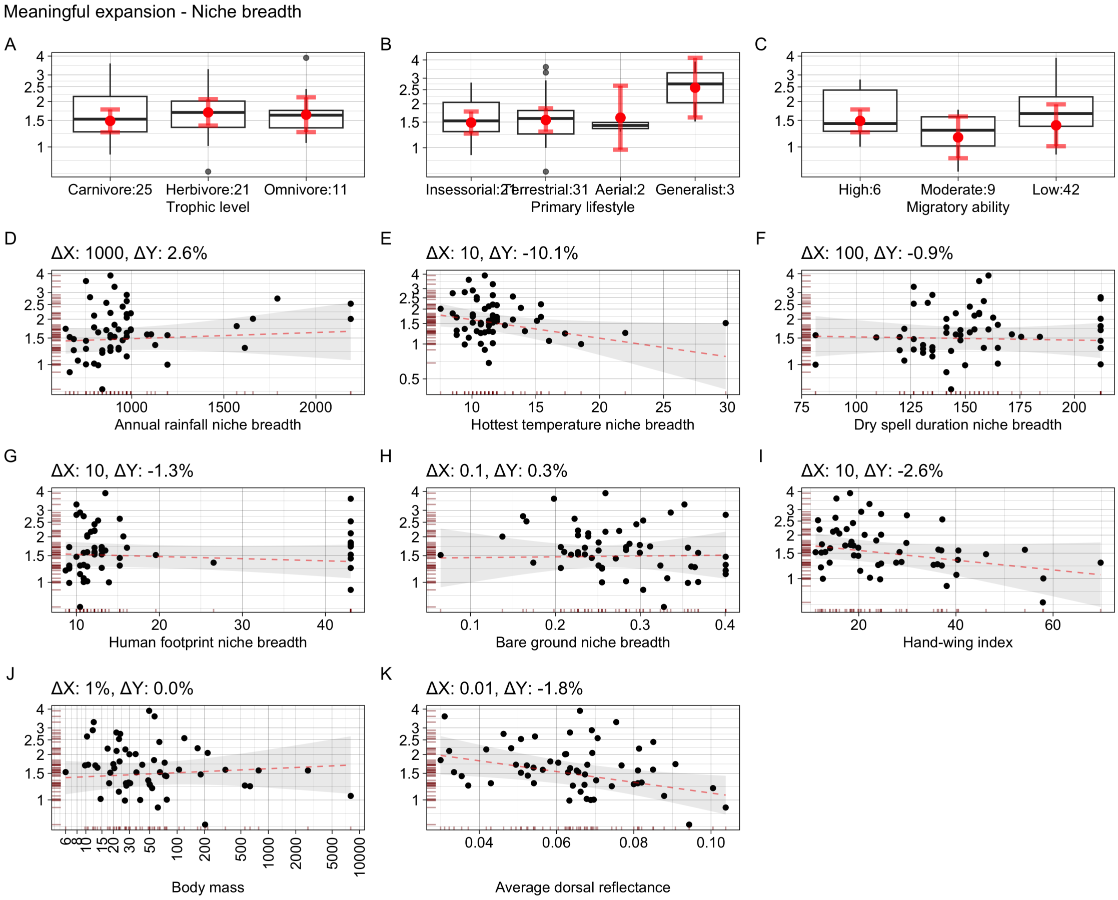

Figure B.9: Effect plots showing the correlations between covariates and meaningful colonisation scores, for models containing niche breadth for environmental covariates. Boxplots represent categorical covariates, while scatter plots represent continuous variables. Numbers on x-axis labels represent sample sizes for levels of categorical variables. A score of 1 indicated that changes were exactly as expected by chance (area colonised equal to the area of high uncertainty transitions), and a value of 2 indicated that there were twice as many colonisations as expected by chance. A score of 0.5 indicated 50% fewer transitions occurred than expected by chance. Black points are drawn on the raw data provided to the models, red dashed lines, as well as red points with red error bars are posterior model estimates derived from linear combinations. The rug plots visualise the density of the data points.

B.3 Methods expanded

B.3.1 Integrated model formulation

We constructed an independent integrated species distribution model (ISDM) for each of the 92 avian species considered for this paper by combining two disparate datasets, by specifying a model-based state-space point process model (as described by Isaac et al. 2020). These integrated models were fit in a Bayesian framework using the integrated nested Laplace approximation methodology (INLA) (Rue et al. 2009) – a computationally efficient method used to approximate a class of latent Gaussian models, through the well-established *R-INLA* package (Martins et al. 2013). The integrated model formulation is based on a hierarchical modelling structure, with an underlying process model that describes how the species observations are distributed across space and time (denoted by the subscript s and t respectively). This process model is characterized by its intensity function, $\lambda(s,t)$, a function of environmental covariates, $\boldsymbol{X}$, and parameters, $\boldsymbol{\theta}$, such that the larger the intensity at a point in space and time, the more abundant the species is.

We furthermore assumed that each of the datasets (Y_i, $i = 1, 2, ...n$) has its own observation model (with likelihood denoted by: $\mathcal{L}(Y_i \mid \boldsymbol{X}, \boldsymbol{\theta}, \phi_i)$ – where ϕ_i denotes dataset specific parameters), which connects the observed species location data to the underlying process model. As a result, this framework differs from conventional data pooling methods, where data are combined into a single observation model; rather we construct individual submodels for each dataset, allowing us to retain the strengths and personalities available in each (Isaac et al. 2020).

By combining these two types of models together, the full likelihood of the integrated model becomes:

$$\mathcal{L}\left(\boldsymbol{Y} \mid \boldsymbol{X}, \boldsymbol{\theta}, \phi\right) \propto p\left(\lambda\left(s\right), \boldsymbol{X}, \phi\right) \cdot \prod_{i=1}^{n} \mathcal{L}\left(Y_i \mid \lambda\left(s, t\right), \theta_i\right), \tag{B.1}$$

analogous to saying the model component of the latent state, multiplied by the product of the likelihoods for the observation models.

B.3.2 Underlying process model

The points are assumed to be distributed across both space and time through a log Gaussian Cox process (LGCP), described by the intensity function, $\lambda\left(s, t\right) = exp\{\eta\left(s, t\right)\}$, where: $\eta\left(s, t\right)$ is a linear predictor for the statistical model. The LCGP is a special type of point process that has an intensity function described by not only covariates $X_{s,t}$, but also by a Gaussian field (GF), $\omega\left(s, t\right)$, used to capture any unmeasured covariates and potential spatial autocorrelation included in the model.

$$\eta\left(s, t\right) = \theta_0 + \sum_{i=1}^{p} \theta_i X_i\left(s, t\right) + \zeta\left(s, t\right), \tag{B.2}$$

where: θ_0 is an intercept term, $X_1, X_2, ..., X_p$ are a collection of covariates, with associated parameters $\theta_1, \theta_2, ..., \theta_p$ and $\zeta\left(s, t\right)$ is a latent process dependent on both space and time. We assume that this latent process evolves across years through first-order auto-correlated effects with parameter $\alpha\,(|\alpha| < 1)$ and spatially-correlated innovations:

$$\zeta\,(s,t) = \alpha\zeta\,(s,t-1) + \omega\,(s,t) \tag{B.3}$$

where: $t = 2, 3, ...T$ are the time periods and $\omega\,(s,t)$ is a temporally independent zero-mean GF with: $\zeta\,(s,t=1) \sim Gaussian\,(0, \sigma_c^2/\,(1-\alpha^2))$, where σ_c^2 denotes the variance component (following Blangiardo et al. 2013, who constructed a spatio-temporal model using the *R-INLA* package (Martins et al. 2013)). This Gaussian field is described by its spatio-temporal covariance function given by:

$$Cov\,(\omega\,(s_i,t)\,, \omega\,(s_j,t')) = \begin{cases} 0 & t \neq t' \\ \sigma_c^2 C\,(h;\nu,\kappa) & t = t' \end{cases} \tag{B.4}$$

where: $i \neq j$ and $C\,(h;\nu,\kappa)$ is the spatial Matérn covariance function:

$$C\,(h;\nu,\kappa) = \frac{1}{\Gamma\,(\nu)\,2^{\nu-1}}\,(\kappa h)^{\nu}\,K_v\,(kh) \tag{B.5}$$

where: Γ is the Gamma function, K_v is the modified bessel function of the second kind, $\kappa > 0$ is a scaling parameter, $\nu > 0$ is a measure of smoothness (typically a fixed value) and $h = \|s_i - s_j\|$ represents the euclidean distance separating the two points (Cressie 2015). The parameter κ is related to the range, ρ (the distance where the spatial correlation is small – chosen as 0.1), where for each ν: $\rho = \sqrt{8\nu}/\kappa$ (Lindgren et al. 2011).

A GF with a Màtern covariance function may be represented by a Gaussian Markov random field (GMRF), and it is therefore computationally efficient to model the spatial structure via the stochastic partial differential equation (SPDE) approach (Lindgren et al. 2011). The SPDE approach is implemented in an easy-to-use method through the *R-INLA* package, which evaluates the continuous GF as a discretely indexed random process, through discretizing the study area Ω into non-intersecting triangles meeting at the edges, called a *spatial mesh* (further details of the method are provided in Cameletti et al. 2013 and Krainski et al. 2019).

Given the linear predictor in equation (B.2), the expected number of points within some area (Ω) for a given time period is given by:

$$\mu\left(\Omega\right) = \int_{\Omega} \lambda\left(s\right) ds. \tag{B.6}$$

The integral provided in equation (B.6) is often intractable, however may be approximated numerically using the finite element method of Simpson et al. 2016: who use integration points after discretizing Ω into triangles, given by:

$$\mu\left(\Omega\right) \approx \sum_{s}^{M} \Phi\left(s\right) \exp\{\eta\left(\Omega\left(s\right)\right)\} \tag{B.7}$$

where: M is the total number of integration points within Ω and $\Phi\left(s\right)$ is the area of the triangle around s. That is, the intensity function is calculated at the integration points; and the rest of the area is interpolated between the three points that form the corners of the surrounding triangles.

B.3.3 Observation models

We considered two disparate datasets for this project: a dataset obtained Tanzanian bird atlas as well as a dataset obtained through the citizen science platform, eBird. Both the Tanzania bird atlas and the eBird data had observations documented in cells across Tanzania. We therefore treated both datasets as detection/non-detection data and subsequently modelled them as Bernoulli random variables in the ISDM. To integrate these data into our inhomogenous-Poisson point process framework, we used a *cloglog* link function, which models the probability that the count of the data at a given space and time point $N(s,t)$ is greater than 0.

$$\begin{aligned} P(N(s,t)) > 0) &= 1 - \exp\{\lambda(s,t)\} \\ &= 1 - \exp\{\exp\{\eta(s,t)\}\}, \end{aligned} \tag{B.8}$$

which would result in the inverse of the *cloglog* function:

$$log(\lambda(s,t)) = log(-log(1 - P(N(s,t) > 0))), \tag{B.9}$$

where: the link function is chosen to link the Bernoulli distribution to a Poisson process (see Kéry et al. 2017).

The linear predictor given in equation (B.2) included a selection of environmental covariates shared between the two datasets (*annual rain*, *hottest temperature*, *max dryspell*, *bare ground cover* and *human footprint*) as well as a shared spatial field. However, we also chose dataset-specific covariates for effort: for the eBird dataset, we used checklist duration, and for the Tanzania bird atlas dataset, we chose the number of unique days any birds had been reported from a cell within the survey periods. In addition, we also included a second spatial field for the eBird dataset, used to reflect spatial variation in sampling effort explained by neither the fixed covariates nor the shared spatial field (Simmonds et al. 2020).

C

Appendix 3: Supplementary material for Chapter 4

C.1 Supplementary Figures

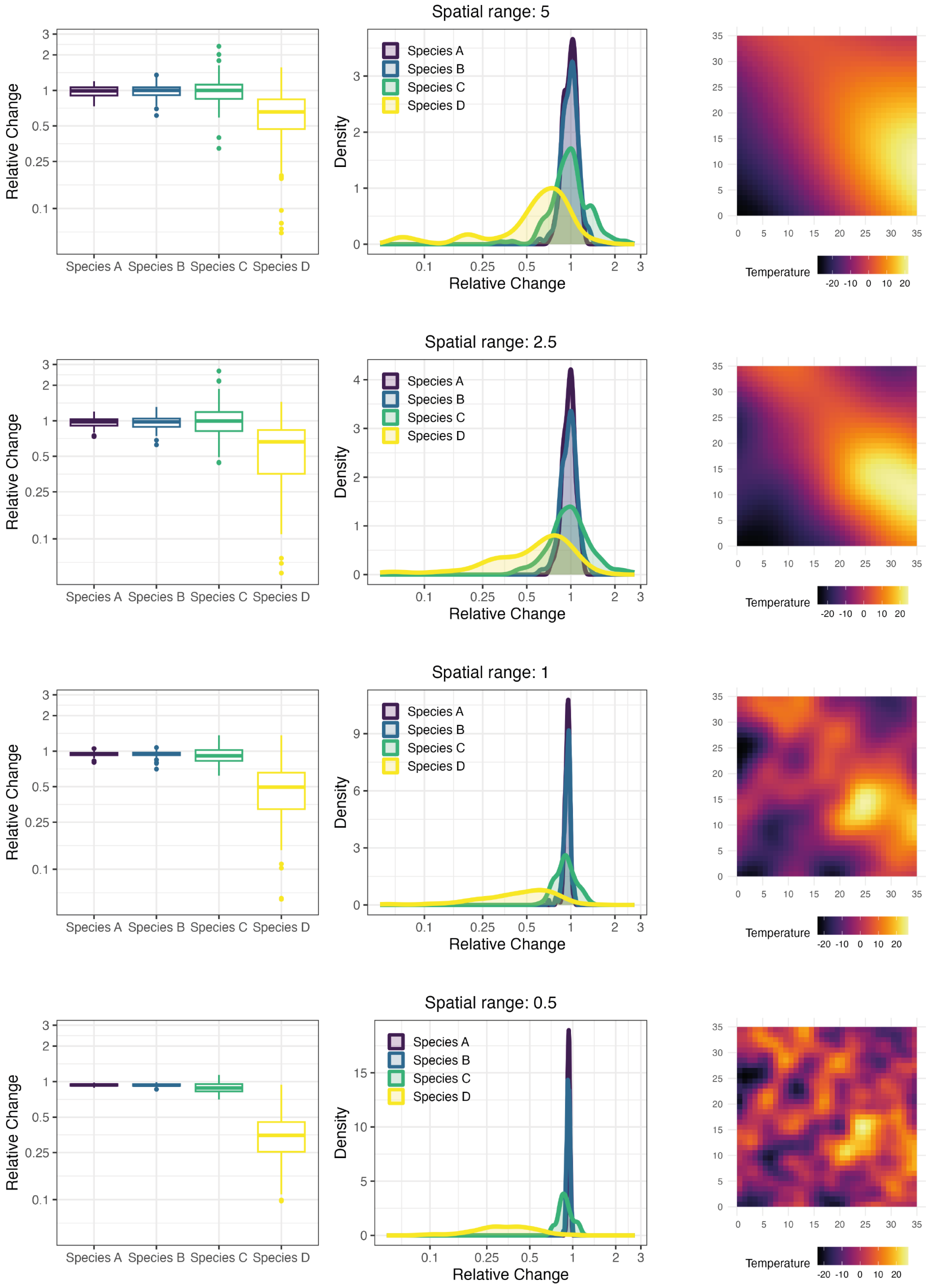

Figure C.1: Effect of range of autocorrelation in the simulated spatial temperature field on true vulnerability rankings of the example species A, B, C and D. *(continued on following page)*

(continued caption) Box plots and density plots are based on vulnerability scores calculated as log-proportional change in range size after exposure of +4 (derived from 100 different simulations of the spatial temperature field). For easier interpretation, scores are labelled as relative change, where 0 represents no overall change in range size, 0.5 represents a halving, and 2 represents a doubling of size. Species D experienced large losses under some simulations, leading to several very small scores; scores were limited to those between -3 and 1 on the log scale for visualisation purposes. Box plots and density curves are based on 100 different simulations of the spatial temperature field. Heat maps show the simulated spatial temperature field under different specifications of the range of the autocorrelation (0.5, 1, 2.5, 5).

References

2012 Population and Housing Census (2013). National Bureau of Statistics, Ministry of Finance.

Abukari, H. and Mwalyosi, R. B. (2018). "Comparing pressures on national parks in Ghana and Tanzania: The case of Mole and Tarangire National Parks". en. In: *Global Ecology and Conservation* 15, e00405.

Adam, E., Mutanga, O., Odindi, J., and Abdel-Rahman, E. M. (2014). "Land-use/cover classification in a heterogeneous coastal landscape using RapidEye imagery: evaluating the performance of random forest and support vector machines classifiers". In: *Int. J. Remote Sens.* 35 (10), pp. 3440–3458.

Adams, B., Iverson, L., Matthews, S., Peters, M., Prasad, A., and Hix, D. M. (2020). "Mapping Forest Composition with Landsat Time Series: An Evaluation of Seasonal Composites and Harmonic Regression". en. In: *Remote Sensing* 12 (4), p. 610.

Addae, B. and Dragićević, S. (2023). "Modelling global deforestation using spherical geographic automata approach". en. In: *ISPRS Int. J. Geoinf.* 12 (8), p. 306.

Adde, A., Casabona i Amat, C., Mazerolle, M. J., Darveau, M., Cumming, S. G., and O'Hara, R. B. (2021). "Integrated modeling of waterfowl distribution in Western Canada using aerial survey and citizen science (eBird) data". en. In: *Ecosphere* 12 (10).

Adhikari, U., Nejadhashemi, A. P., and Woznicki, S. A. (2015). "Climate change and eastern Africa: a review of impact on major crops". en. In: *Food Energy Secur.* 4 (2), pp. 110–132.

Adobe Systems Incorporated (2022). *Adobe Illustrator*. Comp. software.

Akinsanola, A. A., Ongoma, V., and Kooperman, G. J. (2021). "Evaluation of CMIP6 models in simulating the statistics of extreme precipitation over Eastern Africa". en. In: *Atmos. Res.* 254 (105509), p. 105509.

Alabia, I. D., García Molinos, J., Saitoh, S.-I., Hirawake, T., Hirata, T., and Mueter, F. J. (2018). "Distribution shifts of marine taxa in the Pacific Arctic under contemporary climate changes". en. In: *Divers. Distrib.* 24 (11), pp. 1583–1597.

Alananga, S., Makupa, E. R., Moyo, K. J., Matotola, U. C., and Mrema, E. F. (2019). "Land administration practices in Tanzania: A replica of past mistakes". In: *Journal of Property, Planning and Environmental Law.*

Albalawi, E. K. and Kumar, L. (2013). "Using remote sensing technology to detect, model and map desertification: A review". In: *Journal of Food, Agriculture & Environment* 11.

Albouy, C., Delattre, V., Donati, G., Frölicher, T. L., Albouy-Boyer, S., Rufino, M., Pellissier, L., Mouillot, D., and Leprieur, F. (2020). "Global vulnerability of marine mammals to global warming". en. In: *Sci. Rep.* 10 (1), p. 548.

Andersen, E. M. and Steidl, R. J. (2019). "Woody plant encroachment restructures bird communities in semiarid grasslands". en. In: *Biol. Conserv.* 240 (108276), p. 108276.

Anderson, R. P. (2013). "A framework for using niche models to estimate impacts of climate change on species distributions: Niche models and climate change". en. In: *Ann. N. Y. Acad. Sci.* 1297 (1), pp. 8–28.

Andrieu, C. and Thoms, J. (2008). "A tutorial on adaptive MCMC". en. In: *Stat. Comput.* 18 (4), pp. 343–373.

Angelieri, C. C. S., Adams-Hosking, C., Ferraz, K. M. P. M. d. B., Souza, M. P. de, and McAlpine, C. A. (2016). "Using species Distribution Models to predict potential landscape restoration effects on puma conservation". en. In: *PLoS One* 11 (1), e0145232.

Angert, A. L., Crozier, L. G., Rissler, L. J., Gilman, S. E., Tewksbury, J. J., and Chunco, A. J. (2011). "Do species' traits predict recent shifts at expanding range edges?" en. In: *Ecol. Lett.* 14 (7), pp. 677–689.

Arango, A., Pinto-Ledezma, J., Rojas-Soto, O., Lindsay, A. M., Mendenhall, C. D., and Villalobos, F. (2022). "Hand-Wing Index as a surrogate for dispersal ability: the case of the Emberizoidea (Aves: Passeriformes) radiation". In: *Biol. J. Linn. Soc. Lond.* 137 (1), pp. 137–144.

Araújo, M. B., Anderson, R. P., Márcia Barbosa, A., Beale, C. M., Dormann, C. F., Early, R., Garcia, R. A., Guisan, A., Maiorano, L., Naimi, B., O'Hara, R. B., Zimmermann, N. E., and Rahbek, C. (2019a). "Standards for distribution models in biodiversity assessments". en. In: *Sci Adv* 5 (1), eaat4858.

Araújo, M. B., Anderson, R. P., Márcia Barbosa, A., Beale, C. M., Dormann, C. F., Early, R., Garcia, R. A., Guisan, A., Maiorano, L., Naimi, B., O'Hara, R. B., Zimmermann, N. E., and Rahbek, C. (2019b). "Standards for distribution models in biodiversity assessments". en. In: *Sci. Adv.* 5 (1), eaat4858.

Asner, G. P., Elmore, A. J., Olander, L. P., Martin, R. E., and Harris, A. T. (2004). "Grazing Systems, Ecosystem Responses, and Global Change". In: *Annu. Rev. Environ. Resour.* 29 (1), pp. 261–299.

Aubin, I., Boisvert-Marsh, L., Kebli, H., McKenney, D., Pedlar, J., Lawrence, K., Hogg, E. H., Boulanger, Y., Gauthier, S., and Ste-Marie, C. (2018). "Tree vulnerability to climate change: improving exposure-based assessments using traits as indicators of sensitivity". en. In: *Ecosphere* 9 (2), e02108.

Augustine, D. J. (2003). "Spatial heterogeneity in the herbaceous layer of a semi-arid savanna ecosystem". In: *Plant Ecol.* 167 (2), pp. 319–332.

Ayugi, B., Ngoma, H., Babaousmail, H., Karim, R., Iyakaremye, V., Lim Kam Sian, K. T. C., and Ongoma, V. (2021). "Evaluation and projection of mean surface temperature using CMIP6 models over East Africa". en. In: *J. Afr. Earth Sci.* 181 (104226), p. 104226.

Bach, E. M., Baer, S. G., Meyer, C. K., and Six, J. (2010). "Soil texture affects soil microbial and structural recovery during grassland restoration". In: *Soil Biol. Biochem.* 42 (12), pp. 2182–2191.

Bai, Z. G. and Dent, D. L. (2007). "Land degradation and improvement in South Africa. 1: Identification by remote sensing". In.

Bakka, H. (2017). *Mesh Creation including Coastlines.* URL: `https://haakonbakkagit.github.io/btopic104.html` (visited on 05/26/2023).

Bakka, H., Rue, H., Fuglstad, G.-A., Riebler, A., Bolin, D., Illian, J., Krainski, E., Simpson, D., and Lindgren, F. (2018). "Spatial modeling with R-INLA: A review". en. In: *Wiley Interdiscip. Rev. Comput. Stat.* 10 (6), e1443.

Balanyá, J., Oller, J. M., Huey, R. B., Gilchrist, G. W., and Serra, L. (2006). "Global genetic change tracks global climate warming in *Drosophila subobscura*". en. In: *Science* 313 (5794), pp. 1773–1775.

Baldwin, B. (1974). "Behavioural thermoregulation". In: *Heat Loss from Animals and Man: Assessment and Control*, pp. 97–117.

Bardgett, R. D. et al. (2021). "Combatting global grassland degradation". en. In: *Nat. Rev. Earth Environ.* 2 (10), pp. 720–735.

Bateman, B. L., Wilsey, C., Taylor, L., Wu, J., LeBaron, G. S., and Langham, G. (2020). "North American birds require mitigation and adaptation to reduce vulnerability to climate change". en. In: *Conservat Sci and Prac* 2 (8).

Beale, C. M., Baker, N. E., Brewer, M. J., and Lennon, J. J. (2013). "Protected area networks and savannah bird biodiversity in the face of climate change and land degradation". en. In: *Ecol. Lett.* 16 (8), pp. 1061–1068.

Beale, C. M., Brewer, M. J., and Lennon, J. J. (2014). "A new statistical framework for the quantification of covariate associations with species distributions". en. In: *Methods Ecol. Evol.* 5 (5), pp. 421–432.

Beale, C. M. and Lennon, J. J. (2012). "Incorporating uncertainty in predictive species distribution modelling". en. In: *Philos. Trans. R. Soc. Lond. B Biol. Sci.* 367 (1586), pp. 247–258.

Beale, C. M., Lennon, J. J., Yearsley, J. M., Brewer, M. J., and Elston, D. A. (2010). "Regression analysis of spatial data". en. In: *Ecol. Lett.* 13 (2), pp. 246–264.

Beaumont, L. J., Gallagher, R. V., Thuiller, W., Downey, P. O., Leishman, M. R., and Hughes, L. (2009). "Different climatic envelopes among invasive populations may lead to underestimations of current and future biological invasions". en. In: *Divers. Distrib.* 15 (3), pp. 409–420.

Beck, J., Böller, M., Erhardt, A., and Schwanghart, W. (2014). "Spatial bias in the GBIF database and its effect on modeling species' geographic distributions". en. In: *Ecol. Inform.* 19, pp. 10–15.

Beckett, H., Staver, A. C., Charles-Dominique, T., and Bond, W. J. (2022). "Pathways of savannization in a mesic African savanna–forest mosaic following an extreme fire". en. In: *J. Ecol.* 110 (4), pp. 902–915.

Beever, E. A. et al. (2023). "Geographic and taxonomic variation in adaptive capacity among mountain-dwelling small mammals: Implications for conservation status and actions". en. In: *Biol. Conserv.* 282 (109942), p. 109942.

Beissinger, S. R. and Riddell, E. A. (2021). "Why Are Species' Traits Weak Predictors of Range Shifts?" In: *Annu. Rev. Ecol. Evol. Syst.* 52 (1), pp. 47–66.

Belayneh, A. and Tessema, Z. K. (2017). "Mechanisms of bush encroachment and its inter-connection with rangeland degradation in semi-arid African ecosystems: a review". en. In: *J. Arid Land* 9 (2), pp. 299–312.

Belgiu, M. and Drăguț, L. (2016). "Random forest in remote sensing: A review of applications and future directions". en. In: *ISPRS J. Photogramm. Remote Sens.* 114, pp. 24–31.

Bensch, S. (1999). "Is the Range Size of Migratory Birds Constrained by Their Migratory Program?" In: *J. Biogeogr.* 26 (6), pp. 1225–1235.

Bertrand, R., Lenoir, J., Piedallu, C., Riofrío-Dillon, G., Ruffray, P. de, Vidal, C., Pierrat, J.-C., and Gégout, J.-C. (2011). "Changes in plant community composition lag behind climate warming in lowland forests". en. In: *Nature* 479 (7374), pp. 517–520.

Betts, J., Young, R. P., Hilton-Taylor, C., Hoffmann, M., Rodríguez, J. P., Stuart, S. N., and Milner-Gulland, E. J. (2020). "A framework for evaluating the impact of the IUCN Red List of threatened species". en. In: *Conserv. Biol.* 34 (3), pp. 632–643.

Bishop-Taylor, R., Tulbure, M. G., and Broich, M. (2018). "Evaluating static and dynamic landscape connectivity modelling using a 25-year remote sensing time series". en. In: *Landsc. Ecol.* 33 (4), pp. 625–640.

Bivand, R., Rundel, C., Pebesma, E., et al. (2017). "rgeos: interface to geometry engine-open source (GEOS)". In: *R package version 0. 3-26*.

Blangiardo, M. and Cameletti, M. (2015). *Spatial and spatio-temporal Bayesian models with R-INLA*. en. Chichester, West Sussex: John Wiley and Sons, Inc. 1 p.

Blangiardo, M., Cameletti, M., Baio, G., and Rue, H. (2013). "Spatial and spatio-temporal models with R-INLA". en. In: *Spat. Spatiotemporal Epidemiol.* 4, pp. 33–49.

Bled, F., Nichols, J. D., and Altwegg, R. (2013). "Dynamic occupancy models for analyzing species' range dynamics across large geographic scales". en. In: *Ecol. Evol.* 3 (15), pp. 4896–4909.

Böhning-Gaese, K., Halbe, B., Lemoine, N., and Oberrath, R. (2000). "Factors influencing the clutch size, number of broods and annual fecundity of North American and European land birds". en. In: *Evol. Ecol. Res.* 2 (7), pp. 823–839.

Boitani, L., Maiorano, L., Baisero, D., Falcucci, A., Visconti, P., and Rondinini, C. (2011). "What spatial data do we need to develop global mammal conservation strategies?" en. In: *Philos. Trans. R. Soc. Lond. B Biol. Sci.* 366 (1578), pp. 2623–2632.

Bollig, M. and Schulte, A. (1999). "Environmental change and pastoral perceptions: degradation and indigenous knowledge in two African pastoral communities". In: *Hum. Ecol.* 27 (3), pp. 493–514.

Bond, N., Thomson, J., Reich, P., and Stein, J. (2011). "Using species distribution models to infer potential climate change-induced range shifts of freshwater fish in south-eastern Australia". en. In: *Mar. Freshw. Res.* 62 (9), p. 1043.

Bond, W. and Keeley, J. (2005). “Fire as a global ‘herbivore’: the ecology and evolution of flammable ecosystems”. en. In: *Trends Ecol. Evol.* 20 (7), pp. 387–394.

Bonebrake, T. C., Pickett, E. J., Tsang, T. P. N., Tak, C. Y., Vu, M. Q., and Van Vu, L. (2016). “Warming threat compounds habitat degradation impacts on a tropical butterfly community in Vietnam”. en. In: *Glob. Ecol. Conserv.* 8, pp. 203–211.

Booth, T. H. (2017). “Assessing species climatic requirements beyond the realized niche: some lessons mainly from tree species distribution modelling”. en. In: *Clim. Change* 145 (3-4), pp. 259–271.

Borowiec, M. L., Dikow, R. B., Frandsen, P. B., McKeeken, A., Valentini, G., and White, A. E. (2022). “Deep learning as a tool for ecology and evolution”. en. In: *Methods Ecol. Evol.* 13 (8), pp. 1640–1660.

Brawn, J. D., Benson, T. J., Stager, M., Sly, N. D., and Tarwater, C. E. (2016). “Impacts of changing rainfall regime on the demography of tropical birds”. en. In: *Nat. Clim. Chang.* 7 (2), pp. 133–136.

Bright, E. A., Rose, A. N., Urban, M. L., and McKee, J. (2018). *LandScan 2017 High-Resolution Global Population Data Set.* Research rep. Oak Ridge National Lab.(ORNL), Oak Ridge, TN (United States).

Brommer (2008). “Extent of recent polewards range margin shifts in Finnish birds depends on their body mass and feeding ecology”. In: *Ornis Fenn.*

Brooks, T. M., Mittermeier, R. A., Fonseca, G. A. B. da, Gerlach, J., Hoffmann, M., Lamoreux, J. F., Mittermeier, C. G., Pilgrim, J. D., and Rodrigues, A. S. L. (2006). “Global biodiversity conservation priorities”. en. In: *Science* 313 (5783), pp. 58–61.

Brown, B., Chui, M., and Manyika, J. (2010). “Are you ready for the era of ‘big data’?” In: *McKinsey Quarterly.*

Brown, C. J., O’Connor, M. I., Poloczanska, E. S., Schoeman, D. S., Buckley, L. B., Burrows, M. T., Duarte, C. M., Halpern, B. S., Pandolfi, J. M., Parmesan, C., and Richardson, A. J. (2016). “Ecological and methodological drivers of species’ distribution and phenology responses to climate change”. en. In: *Glob. Chang. Biol.* 22 (4), pp. 1548–1560.

Brown, M., Arendse, B., Mels, B., and Lee, A. T. K. (2019). “Bucking the trend: the African Black Oystercatcher as a recent conservation success story”. en. In: *Ostrich* 90 (4), pp. 327–333.

Buchhorn, M., Lesiv, M., Tsendbazar, N.-E., Herold, M., Bertels, L., and Smets, B. (2020). “Copernicus Global Land Cover Layers—Collection 2”. en. In: *Remote Sensing* 12 (6), p. 1044.

Buckley and Kingsolver (2012). "Functional and phylogenetic approaches to forecasting species' responses to climate change". In: *Annu. Rev. Ecol. Syst.*

Bullock, E. L., Healey, S. P., Yang, Z., Oduor, P., Gorelick, N., Omondi, S., Ouko, E., and Cohen, W. B. (2021). "Three decades of land cover change in East Africa". en. In: *Land (Basel)* 10 (2), p. 150.

Butz, R. J. (2009). "Traditional fire management: historical fire regimes and land use change in pastoral East Africa". en. In: *Int. J. Wildland Fire* 18 (4), pp. 442–450.

Camberlin, P. (2018). *Climate of Eastern Africa*. Oxford University Press.

Cameletti, M., Lindgren, F., Simpson, D., and Rue, H. (2013). "Spatio-temporal modeling of particulate matter concentration through the SPDE approach". en. In: *Adv. Stat. Anal.* 97 (2), pp. 109–131.

Cao, C., Dragićević, S., and Li, S. (2019). "Short-term forecasting of land use change using recurrent neural network models". en. In: *Sustain. Sci. Pract. Policy* 11 (19), p. 5376.

Caplat, P., Edelaar, P., Dudaniec, R. Y., Green, A. J., Okamura, B., Cote, J., Ekroos, J., Jonsson, P. R., Löndahl, J., Tesson, S. V. M., and Petit, E. J. (2016). "Looking beyond the mountain: dispersal barriers in a changing world". en. In: *Front. Ecol. Environ.* 14 (5), pp. 261–268.

Caro, T. and Davenport, T. R. B. (2016). "Wildlife and wildlife management in Tanzania". pt. In: *Conserv. Biol.* 30 (4), pp. 716–723.

Castelluccio, M., Poggi, G., Sansone, C., and Verdoliva, L. (2015). "Land use classification in remote sensing images by convolutional neural networks". In: *arXiv [cs.CV]*.

Ceballos, G. and Ehrlich, P. R. (2023). "Mutilation of the tree of life via mass extinction of animal genera". en. In: *Proc. Natl. Acad. Sci. U. S. A.* 120 (39), e2306987120.

Ceballos, G., Ehrlich, P. R., Barnosky, A. D., García, A., Pringle, R. M., and Palmer, T. M. (2015). "Accelerated modern human-induced species losses: Entering the sixth mass extinction". en. In: *Sci. Adv.* 1 (5), e1400253.

Chamberlain, S. A. and Szöcs, E. (2013). "taxize: taxonomic search and retrieval in R". en. In: *F1000Res.* 2, p. 191.

Chaudhuri, G. and Clarke, K. C. (2014). "Temporal accuracy in urban growth forecasting: A study using the SLEUTH model: Temporal accuracy in urban growth forecasting: A study using the SLEUTH model". en. In: *Trans. GIS* 18 (2), pp. 302–320.

Chen, I.-C., Hill, J. K., Ohlemüller, R., Roy, D. B., and Thomas, C. D. (2011). "Rapid range shifts of species associated with high levels of climate warming". en. In: *Science* 333 (6045), pp. 1024–1026.

Chichorro, F., Juslén, A., and Cardoso, P. (2019). "A review of the relation between species traits and extinction risk". en. In: *Biol. Conserv.* 237, pp. 220–229.

Chowdhury, R. R. (2006). "Driving forces of tropical deforestation: The role of remote sensing and spatial models". en. In: *Singap. J. Trop. Geogr.* 27 (1), pp. 82–101.

Cianfrani, C., Broennimann, O., Loy, A., and Guisan, A. (2018). "More than range exposure: Global otter vulnerability to climate change". In: *Biol. Conserv.* 221, pp. 103–113.

Coldrey, K. M., Turpie, J. K., Midgley, G., Scheiter, S., Hannah, L., Roehrdanz, P. R., and Foden, W. B. (2022). "Assessing protected area vulnerability to climate change in a case study of South African national parks". en. In: *Conserv. Biol.* 36 (5), e13941.

Collar, N. J. (1996). "The reasons for Red Data Books". en. In: *Oryx* 30 (2), pp. 121–130.

Colwell, R. K., Brehm, G., Cardelús, C. L., Gilman, A. C., and Longino, J. T. (2008). "Global warming, elevational range shifts, and lowland biotic attrition in the wet tropics". en. In: *Science* 322 (5899), pp. 258–261.

Cooney, C. R., He, Y., Varley, Z. K., Nouri, L. O., Moody, C. J. A., Jardine, M. D., Liker, A., Székely, T., and Thomas, G. H. (2022). "Latitudinal gradients in avian colourfulness". en. In: *Nat Ecol Evol* 6 (5), pp. 622–629.

Côté, I. M. and Darling, E. S. (2010). "Rethinking Ecosystem Resilience in the Face of Climate Change". en. In: *PLoS Biol.* 8 (7), e1000438.

Cotler, H. and Ortega-Larrocea, M. P. (2006). "Effects of land use on soil erosion in a tropical dry forest ecosystem, Chamela watershed, Mexico". In: *Catena* 65 (2), pp. 107–117.

Cowie, R. H., Bouchet, P., and Fontaine, B. (2022). "The Sixth Mass Extinction: fact, fiction or speculation?" en. In: *Biol. Rev. Camb. Philos. Soc.* 97 (2), pp. 640–663.

Crainiceanu, C. M., Ruppert, D., and Wand, M. P. (2005). "Bayesian Analysis for Penalized Spline Regression Using WinBUGS". en. In: *J. Stat. Softw.* 14, pp. 1–24.

Cressie, N. (2015). *Statistics for Spatial Data*. en. Wiley Series in Probability and Statistics. Standards Information Network. 928 pp.

Dai, A. (2011). "Drought under global warming: a review". en. In: *WIREs Climate Change* 2 (1), pp. 45–65.

Dambly, L. I., Isaac, N. J. B., Jones, K. E., Boughey, K. L., and O'Hara, R. B. (2023). "Integrated species distribution models fitted in INLA are sensitive to mesh parameterisation". en. In: *Ecography*.

Dantas, V. d. L., Batalha, M. A., and Pausas, J. G. (2013). "Fire drives functional thresholds on the savanna-forest transition". en. In: *Ecology* 94 (11), pp. 2454–2463.

Daron, D. J. (2018). "Regional climate messages for East Africa". en. In.

Das, P., Zhang, Z., Ghosh, S., Lu, J., Ayugi, B., Ojara, M. A., and Guo, X. (2023). "Historical and projected changes in Extreme High Temperature events over East Africa and associated with meteorological conditions using CMIP6 models". en. In: *Glob. Planet. Change* 222 (104068), p. 104068.

Daskalova, G. N., Myers-Smith, I. H., Bjorkman, A. D., Blowes, S. A., Supp, S. R., Magurran, A. E., and Dornelas, M. (2020). "Landscape-scale forest loss as a catalyst of population and biodiversity change". en. In: *Science* 368 (6497), pp. 1341–1347.

Davis, M. B. and Shaw, R. G. (2001). "Range shifts and adaptive responses to Quaternary climate change". en. In: *Science* 292 (5517), pp. 673–679.

Dawson, T. P., Jackson, S. T., House, J. I., Prentice, I. C., and Mace, G. M. (2011). "Beyond Predictions: Biodiversity Conservation in a Changing Climate". In: *Science* 332 (6025), pp. 53–58.

De Smedt, T., Simons, K., Van Nieuwenhuyse, A., and Molenberghs, G. (2015). "Comparing MCMC and INLA for disease mapping with Bayesian hierarchical models". en. In: *Archives of Public Health; London* 73, p. 1.

Dean, W. (1997). "The distribution and biology of nomadic birds in the Karoo, South Africa". en. In: *J. Biogeogr.* 24 (6), pp. 769–779.

Dean, W. R. J. and Milton, S. J. (2001). "Responses of birds to rainfall and seed abundance in the southern Karoo, South Africa". In: *J. Arid Environ.* 47 (1), pp. 101–121.

Devictor, V., Julliard, R., Couvet, D., and Jiguet, F. (2008). "Birds are tracking climate warming, but not fast enough". en. In: *Proc. Biol. Sci.* 275 (1652), pp. 2743–2748.

Diamond, J. M. and May, R. M. (1977). "Species turnover rates on islands: dependence on census interval". en. In: *Science* 197 (4300), pp. 266–270.

Dickinson, M. G., Orme, C. D. L., Suttle, K. B., and Mace, G. M. (2014). "Separating sensitivity from exposure in assessing extinction risk from climate change". en. In: *Sci. Rep.* 4 (1), p. 6898.

Didan, K. (2015). *MOD13Q1 MODIS/Terra Vegetation Indices 16-Day L3 Global 250m SIN Grid V006 [Data set]*. NASA EOSDIS Land Processes DAAC.

Diek, S., Fornallaz, F., Schaepman, M. E., and De Jong, R. (2017). "Barest pixel composite for agricultural areas using landsat time series". In: *Remote Sensing* 9 (12), p. 1245.

Dormann, C., McPherson, J., Araújo, M., Bivand, R., Bolliger, J., Carl, G., Davies, R., Hirzel, A., Jetz, W., Daniel Kissling, W., Kühn, I., Ohlemüller, R., Peres-Neto, P., Reineking, B., Schröder, B., Schurr, F., and Wilson, R. (2007). "Methods to account for spatial autocorrelation in the analysis of species distributional data: a review". en. In: *Ecography (Cop.)* 30 (5), pp. 609–628.

Dornelas, M., Chase, J. M., Gotelli, N. J., Magurran, A. E., McGill, B. J., Antão, L. H., Blowes, S. A., Daskalova, G. N., Leung, B., Martins, I. S., Moyes, F., Myers-Smith, I. H., Thomas, C. D., and Vellend, M. (2023). "Looking back on biodiversity change: lessons for the road ahead". en. In: *Philos. Trans. R. Soc. Lond. B Biol. Sci.* 378 (1881), p. 20220199.

Dosio, A. (2017). "Projection of temperature and heat waves for Africa with an ensemble of CORDEX Regional Climate Models". en. In: *Clim. Dyn.* 49 (1-2), pp. 493–519.

Drusch, M., Del Bello, U., Carlier, S., Colin, O., Fernandez, V., Gascon, F., Hoersch, B., Isola, C., Laberinti, P., Martimort, P., Meygret, A., Spoto, F., Sy, O., Marchese, F., and Bargellini, P. (2012). "Sentinel-2: ESA's Optical High-Resolution Mission for GMES Operational Services". en. In: *Remote Sens. Environ.* The Sentinel Missions - New Opportunities for Science 120, pp. 25–36.

Dunning, C. M., Black, E., and Allan, R. P. (2018). "Later Wet Seasons with More Intense Rainfall over Africa under Future Climate Change". In: *J. Clim.* 31 (23), pp. 9719–9738.

Dusseux, P., Guyet, T., Pattier, P., Barbier, V., and Nicolas, H. (2022). "Monitoring of grassland productivity using Sentinel-2 remote sensing data". en. In: *Int. J. Appl. Earth Obs. Geoinf.* 111 (102843), p. 102843.

Earl, J. M. and Jones, C. E. (1996). "The need for a new approach to grazing management - is cell grazing the answer?" en. In: *Rangel. J.* 18 (2), p. 327.

Elith, J. and Leathwick, J. R. (2009). "Species distribution models: Ecological explanation and prediction across space and time". en. In: *Annu. Rev. Ecol. Evol. Syst.* 40 (1), pp. 677–697.

Ellis, E. C., Gauthier, N., Klein Goldewijk, K., Bliege Bird, R., Boivin, N., Díaz, S., Fuller, D. Q., Gill, J. L., Kaplan, J. O., Kingston, N., Locke, H., McMichael, C. N. H., Ranco, D., Rick, T. C., Shaw, M. R., Stephens, L., Svenning, J.-C., and Watson, J. E. M. (2021). "People have shaped most of terrestrial nature for at least 12,000 years". en. In: *Proc. Natl. Acad. Sci. U. S. A.* 118 (17), e2023483118.

Engel, M., Mette, T., and Falk, W. (2022). "Spatial species distribution models: Using Bayes inference with INLA and SPDE to improve the tree species choice for important European tree species". In: *For. Ecol. Manage.* 507, p. 119983.

Estrada, A., Morales-Castilla, I., Caplat, P., and Early, R. (2016). "Usefulness of Species Traits in Predicting Range Shifts". en. In: *Trends Ecol. Evol.* 31 (3), pp. 190–203.

Estrada, A., Morales-Castilla, I., Meireles, C., Caplat, P., and Early, R. (2018). "Equipped to cope with climate change: traits associated with range filling across European taxa". en. In: *Ecography (Cop.)* 41 (5), pp. 770–781.

Faisal, A., Dondelinger, F., Husmeier, D., and Beale, C. M. (2010). "Inferring species interaction networks from species abundance data: A comparative evaluation of various statistical and machine learning methods". en. In: *Ecol. Inform.* 5 (6), pp. 451–464.

Faraway, J. J. (2016). *Extending the linear model with R: Generalized linear, mixed effects and nonparametric regression models*. 2nd ed. Chapman & Hall/CRC Texts in Statistical Science. Philadelphia, PA: Chapman & Hall/CRC. 399 pp.

Farr, T. G., Rosen, P. A., Caro, E., Crippen, R., Duren, R., Hensley, S., Kobrick, M., Paller, M., Rodriguez, E., Roth, L., Seal, D., Shaffer, S., Shimada, J., Umland, J., Werner, M., Oskin, M., Burbank, D., and Alsdorf, D. (2007). "The Shuttle Radar Topography Mission". en. In: *Rev. Geophys.* 45 (2), RG2004.

Faurby, S. and Araújo, M. B. (2018). "Anthropogenic range contractions bias species climate change forecasts". en. In: *Nat. Clim. Chang.* 8 (3), pp. 252–256.

Fedrigo, J. K., Ataide, P. F., Filho, J. A., Oliveira, L. V., Jaurena, M., Laca, E. A., Overbeck, G. E., and Nabinger, C. (2018). "Temporary grazing exclusion promotes rapid recovery of species richness and productivity in a long-term overgrazed Campos grassland". en. In: *Restor. Ecol.* 26 (4), pp. 677–685.

Feldman, M. J., Imbeau, L., Marchand, P., Mazerolle, M. J., Darveau, M., and Fenton, N. J. (2021). "Trends and gaps in the use of citizen science derived data as input for species distribution models: A quantitative review". en. In: *PLoS One* 16 (3), e0234587.

Ferkingstad, E., Held, L., and Rue, H. (2017). "Fast and accurate Bayesian model criticism and conflict diagnostics using R-INLA". en. In: *Stat* 6 (1), pp. 331–344.

Fichera, A., King, R., Kath, J., Cobon, D., and Reardon-Smith, K. (2023). "Spatial modelling of agro-ecologically significant grassland species using the INLA-SPDE approach". en. In: *Sci. Rep.* 13 (1), p. 4972.

Finney, D. L., Marsham, J. H., Rowell, D. P., Kendon, E. J., Tucker, S. O., Stratton, R. A., and Jackson, L. S. (2020). "Effects of Explicit Convection on Future Projections of Mesoscale Circulations, Rainfall, and Rainfall Extremes over Eastern Africa". en. In: *J. Clim.* 33 (7), pp. 2701–2718.

Fisher, R. J. and Davis, S. K. (2010). "From Wiens to Robel: A review of grassland-bird habitat selection". en. In: *Wildfire* 74 (2), pp. 265–273.

Foden, W. B., Butchart, S. H. M., Stuart, S. N., Vié, J.-C., Akçakaya, H. R., Angulo, A., DeVantier, L. M., Gutsche, A., Turak, E., Cao, L., Donner, S. D., Katariya, V., Bernard, R., Holland, R. A., Hughes, A. F., O'Hanlon, S. E., Garnett, S. T., Sekercioğlu, C. H., and Mace, G. M. (2013). "Identifying the world's most climate change vulnerable species: a systematic trait-based assessment of all birds, amphibians and corals". en. In: *PLoS One* 8 (6), e65427.

Foden, W. B., Young, B. E., Akçakaya, H. R., Garcia, R. A., Hoffmann, A. A., Stein, B. A., Thomas, C. D., Wheatley, C. J., Bickford, D., Carr, J. A., Hole, D. G., Martin, T. G., Pacifici, M., Pearce-Higgins, J. W., Platts, P. J., Visconti, P., Watson, J. E. M., and Huntley, B. (2019). "Climate change vulnerability assessment of species". en. In: *Wiley Interdiscip. Rev. Clim. Change* 10 (1), e551.

Foley, C. A. H. and Faust, L. J. (2010). "Rapid population growth in an elephant Loxodonta africana population recovering from poaching in Tarangire National Park, Tanzania". In: *Oryx* 44 (2), pp. 205–212.

Forchhammer, M. C., Post, E., and Stenseth, N. C. (1998). "Breeding phenology and climate". en. In: *Nature* 391 (6662), pp. 29–30.

Fortini, L. and Schubert, O. (2017a). "Beyond exposure, sensitivity and adaptive capacity: a response based ecological framework to assess species climate change vulnerability". en. In: *Climate Change Responses* 4 (1), pp. 1–7.

Fortini, L. B. and Dye, K. (2017b). "At a global scale, do climate change threatened species also face a greater number of non-climatic threats?" In: *Global Ecology and Conservation* 11, pp. 207–212.

Franklin, J. (2023). “Species distribution modelling supports the study of past, present and future biogeographies”. en. In: *J. Biogeogr.* 50 (9), pp. 1533–1545.

Franks, S. J., Sim, S., and Weis, A. E. (2007). “Rapid evolution of flowering time by an annual plant in response to a climate fluctuation”. en. In: *Proc. Natl. Acad. Sci. U. S. A.* 104 (4), pp. 1278–1282.

Fremout, T., Thomas, E., Gaisberger, H., Van Meerbeek, K., Muenchow, J., Briers, S., Gutierrez-Miranda, C. E., Marcelo-Peña, J. L., Kindt, R., Atkinson, R., Cabrera, O., Espinosa, C. I., Aguirre-Mendoza, Z., and Muys, B. (2020). “Mapping tree species vulnerability to multiple threats as a guide to restoration and conservation of tropical dry forests”. en. In: *Glob. Chang. Biol.* 26 (6), pp. 3552–3568.

Friedl, M. and Sulla-Menashe, D. (2019). *MCD12Q1 MODIS/Terra+ Aqua Land Cover Type Yearly L3 Global 500m SIN Grid V006*. NASA EOSDIS Land Processes DAAC.

Fuhlendorf, S. D., Fynn, R. W. S., McGranahan, D. A., and Twidwell, D. (2017). “Heterogeneity as the Basis for Rangeland Management”. en. In: *Rangeland Systems: Processes, Management and Challenges*. Ed. by Briske, D. D. Springer Series on Environmental Management. Cham: Springer International Publishing, pp. 169–196.

Funk, C., Peterson, P., Landsfeld, M., Pedreros, D., Verdin, J., Shukla, S., Husak, G., Rowland, J., Harrison, L., Hoell, A., and Michaelsen, J. (2015). “The climate hazards infrared precipitation with stations—a new environmental record for monitoring extremes”. en. In: *Scientific Data* 2 (1), pp. 1–21.

Fynn, R. W. S. and O’Connor, T. G. (2000). “Effect of stocking rate and rainfall on rangeland dynamics and cattle performance in a semi-arid savanna, South Africa”. en. In: *J. Appl. Ecol.* 37 (3), pp. 491–507.

Gallien, L., Douzet, R., Pratte, S., Zimmermann, N. E., and Thuiller, W. (2012). “Invasive species distribution models - how violating the equilibrium assumption can create new insights: Beyond the equilibrium assumption of SDMs”. en. In: *Glob. Ecol. Biogeogr.* 21 (11), pp. 1126–1136.

Galván, I., Rodríguez-Martínez, S., and Carrascal, L. M. (2018). “Dark pigmentation limits thermal niche position in birds”. en. In: *Funct. Ecol.* 32 (6), pp. 1531–1540.

Galvin, K. A. (2009). “Transitions: pastoralists living with change”. In: *Annu. Rev. Anthropol.* 38, pp. 185–198.

Garcia, R. A., Araújo, M. B., Burgess, N. D., Foden, W. B., Gutsche, A., Rahbek, C., and Cabeza, M. (2014). “Matching species traits to projected threats and opportunities from climate change". en. In: *J. Biogeogr.* 41 (4), pp. 724–735.

Gardali, T., Seavy, N. E., DiGaudio, R. T., and Comrack, L. A. (2012). "A climate change vulnerability assessment of California's at-risk birds". en. In: *PLoS One* 7 (3), e29507.

Garnier, S., Ross, N., Rudis, R., Camargo, A. P., Sciaini, M., and Scherer, C. (2023). *viridis(Lite) - Colorblind-Friendly Color Maps for R*. Version 0.6.4.

Gaspard, G., Kim, D., and Chun, Y. (2019). "Residual spatial autocorrelation in macroecological and biogeographical modeling: a review". en. In: *J. Ecol. Environ.* 43 (1), pp. 1–11.

Gebrechorkos, S. H., Hülsmann, S., and Bernhofer, C. (2019a). "Long-term trends in rainfall and temperature using high-resolution climate datasets in East Africa". en. In: *Sci. Rep.* 9 (1), p. 11376.

— (2019b). "Statistically downscaled climate dataset for East Africa". en. In: *Scientific Data* 6 (1), pp. 1–8.

Gebremeskel Haile, G., Tang, Q., Sun, S., Huang, Z., Zhang, X., and Liu, X. (2019). "Droughts in East Africa: Causes, impacts and resilience". en. In: *Earth Sci. Rev.* 193, pp. 146–161.

Genz, A. and Bretz, F. (2009). *Computation of Multivariate Normal and t Probabilities, series Lecture Notes in Statistics*. Heidelberg: Springer-Verlag.

Giannini, T. C., Chapman, D. S., Saraiva, A. M., Alves-dos-Santos, I., and Biesmeijer, J. C. (2013). "Improving species distribution models using biotic interactions: a case study of parasites, pollinators and plants". en. In: *Ecography (Cop.)* 36 (6), pp. 649–656.

Gibson, D. J. (2009). *Grasses and grassland ecology*. en. New York: Oxford University Press. 305 pp.

Gidden, M. J. et al. (2019). "Global emissions pathways under different socioeconomic scenarios for use in CMIP6: a dataset of harmonized emissions trajectories through the end of the century". en. In: *Geosci. Model Dev.* 12 (4), pp. 1443–1475.

Gilbert, M., Nicolas, G., Cinardi, G., Van Boeckel, T. P., Vanwambeke, S. O., Wint, G. R. W., and Robinson, T. P. (2018). "Global distribution data for cattle, buffaloes, horses, sheep, goats, pigs, chickens and ducks in 2010". en. In: *Sci Data* 5 (1), p. 180227.

Gilks, W. R., Richardson, S., and Spiegelhalter, D. (1995). *Markov Chain Monte Carlo in Practice*. Ed. by Gilks, W. R., Richardson, S., and Spiegelhalter, D. Chapman & Hall/CRC Interdisciplinary Statistics. Philadelphia, PA: Chapman & Hall/CRC. 512 pp.

Gillaspy, B. and Green, S. (2023). "Ecological resistance and resilience in rangelands". en. In: *Rangelands* 45 (5), pp. 83–91.

Girvetz, E., Ramirez-Villegas, J., Claessens, L., Lamanna, C., Navarro-Racines, C., Nowak, A., Thornton, P., and Rosenstock, T. S. (2019). "Future Climate Projections in Africa: Where Are We Headed?" In: *The Climate-Smart Agriculture Papers: Investigating the Business of a Productive, Resilient and Low Emission Future*. Ed. by Rosenstock, T. S., Nowak, A., and Girvetz, E. Cham: Springer International Publishing, pp. 15–27.

Gneiting, T., Balabdaoui, F., and Raftery, A. E. (2007). "Probabilistic forecasts, calibration and sharpness". en. In: *J. R. Stat. Soc. Series B Stat. Methodol.* 69 (2), pp. 243–268.

Goldberg, E. E. and Lande, R. (2007). "Species' borders and dispersal barriers". en. In: *Am. Nat.* 170 (2), pp. 297–304.

Goldman, M. J. and Riosmena, F. (2013). "Adaptive Capacity in Tanzanian Maasailand: Changing strategies to cope with drought in fragmented landscapes". en. In: *Glob. Environ. Change* 23 (3), pp. 588–597.

Gorelick, N., Hancher, M., Dixon, M., Ilyushchenko, S., Thau, D., and Moore, R. (2017). "Google Earth Engine: Planetary-scale geospatial analysis for everyone". In: *Remote Sens. Environ.* Big Remotely Sensed Data: tools, applications and experiences 202, pp. 18–27.

Gosnell, H., Grimm, K., and Goldstein, B. E. (2020). "A half century of Holistic Management: what does the evidence reveal?" en. In: *Agric. Human Values* 37 (3), pp. 849–867.

Grant, P. R. (2017). *Ecology and evolution of Darwin's finches (Princeton science library edition): Princeton science library edition*. Princeton Science Library. Princeton, NJ: Princeton University Press. 512 pp.

Grattarola, F., Bowler, D. E., and Keil, P. (2023). "Integrating presence-only and presence–absence data to model changes in species geographic ranges: An example in the Neotropics". en. In: *J. Biogeogr.*

Guo, Q.-H., Hu, T.-Y., Ma, Q., Xu, K.-X., Yang, Q.-L., Sun, Q.-H., Li, Y.-M., Su, Y.-J., and State Key Laboratory of Vegetation and Environmental Change, Institute of Botany, Chinese Academy of Sciences, Beijing 100093, China, University of Chinese Academy of Sciences, Beijing 100049, China (2020). "Advances for the new remote sensing technology in ecosystem ecology research". en. In: *Chin. J. Plant Ecol.* 44 (4), pp. 418–435.

Guo, Q., Hu, Z., Li, S., Li, X., Sun, X., and Yu, G. (2012). "Spatial variations in aboveground net primary productivity along a climate gradient in

Eurasian temperate grassland: effects of mean annual precipitation and its seasonal distribution". en. In: *Glob. Chang. Biol.* 18 (12), pp. 3624–3631.

Gutowsky, L. F. G., Giacomini, H. C., Kerckhove, D. T. de, Mackereth, R., McCormick, D., and Chu, C. (2019). "Quantifying multiple pressure interactions affecting populations of a recreationally and commercially important freshwater fish". en. In: *Glob. Chang. Biol.* 25 (3), pp. 1049–1062.

Gynther, I., Waller, N., and Leung, L. K.-P. (2016). "Confirmation of the extinction of the Bramble Cay melomys *Melomys rubicola* on Bramble Cay, Torres Strait: Results and conclusions from a comprehensive survey in August-September 2014. Unpublished report to the Department of Environment and Heritage Protection, Queensland Government, Brisbane". In.

Haddad, N. M. et al. (2015). "Habitat fragmentation and its lasting impact on Earth's ecosystems". en. In: *Sci Adv* 1 (2), e1500052.

Haji, M. and Bakuza, J. S. (2023). "Climate change vulnerability assessment for the Rondo dwarf Galago in coastal forests, Tanzania". en. In: *Environ. Manage.* 71 (1), pp. 145–158.

Hall, D. G. M., Reeve, M. J., Thomasson, A. J., and Wright, V. F. (1977). *Water retention, porosity and density of field soils*. No. Tech. Monograph N9.

Hannah, L., Midgley, G., Andelman, S., Araújo, M., Hughes, G., Martinez-Meyer, E., Pearson, R., and Williams, P. (2007). "Protected area needs in a changing climate". In: *Frontiers in Ecology and the Environment* 5 (3), pp. 131–138.

Hansen, M. C., Potapov, P. V., Moore, R., Hancher, M., Turubanova, S. A., Tyukavina, A., Thau, D., Stehman, S. V., Goetz, S. J., Loveland, T. R., Kommareddy, A., Egorov, A., Chini, L., Justice, C. O., and Townshend, J. R. G. (2013). "High-Resolution Global Maps of 21st-Century Forest Cover Change". en. In: *Science* 342 (6160), pp. 850–853.

Hare, J. A. et al. (2016). "A vulnerability assessment of fish and invertebrates to climate change on the Northeast U.s. continental shelf". en. In: *PLoS One* 11 (2), e0146756.

Heady, H. (2019). *Rangeland ecology and management*. en. London, England: Routledge. 540 pp.

Hemati, M., Hasanlou, M., Mahdianpari, M., and Mohammadimanesh, F. (2021). "A systematic review of Landsat data for change detection applications: 50 years of monitoring the Earth". en. In: *Remote Sens. (Basel)* 13 (15), p. 2869.

Herkert, J. R. (1994). "The Effects of Habitat Fragmentation on Midwestern Grassland Bird Communities". In: *Ecol. Appl.* 4 (3).

Hernangómez, D. (2023). "Using the tidyverse with terra objects: the tidyterra package". In: *J. Open Source Softw.* 8 (91), p. 5751.

Hickling, R., Roy, D. B., Hill, J. K., Fox, R., and Thomas, C. D. (2006). "The distributions of a wide range of taxonomic groups are expanding polewards: TAXONOMIC GROUPS SHIFTING POLEWARDS". en. In: *Glob. Chang. Biol.* 12 (3), pp. 450–455.

Hijmans, R. J., Bivand, R., Forner, K., Ooms, J., Pebesma, E., and Sumner, M. D. (2023). *Package 'terra'*.

Hilker, T., Natsagdorj, E., Waring, R. H., Lyapustin, A., and Wang, Y. (2014). "Satellite observed widespread decline in Mongolian grasslands largely due to overgrazing". en. In: *Glob. Chang. Biol.* 20 (2), pp. 418–428.

Hill and Guerschman (2020a). "The MODIS Global Vegetation Fractional Cover Product 2001–2018: Characteristics of Vegetation Fractional Cover in Grasslands and Savanna Woodlands". en. In: *Remote Sensing* 12 (3), p. 406.

Hill, M. J. and Guerschman, J. P. (2020b). "The MODIS Global Vegetation Fractional Cover Product 2001–2018: Characteristics of Vegetation Fractional Cover in Grasslands and Savanna Woodlands". en. In: *Remote Sensing* 12 (3), p. 406.

Hillenbrand, M., Thompson, R., Wang, F., Apfelbaum, S., and Teague, R. (2019). "Impacts of holistic planned grazing with bison compared to continuous grazing with cattle in South Dakota shortgrass prairie". en. In: *Agric. Ecosyst. Environ.* 279, pp. 156–168.

Hodgson, D., McDonald, J. L., and Hosken, D. J. (2015). "What do you mean, 'resilient'?" en. In: *Trends Ecol. Evol.* 30 (9), pp. 503–506.

Hoekstra, J. M., Boucher, T. M., Ricketts, T. H., and Roberts, C. (2005). "Confronting a biome crisis: global disparities of habitat loss and protection". en. In: *Ecol. Lett.* 8 (1), pp. 23–29.

Hoffman, T. and Vogel, C. (2008). "Climate change impacts on African rangelands". In: *Rangelands* 30 (3), pp. 12–17.

Hoffmann, A. A. and Sgrò, C. M. (2011). "Climate change and evolutionary adaptation". en. In: *Nature* 470 (7335), pp. 479–485.

Hofner, B., Müller, J., and Hothorn, T. (2011). "Monotonicity-constrained species distribution models". In: *Ecology* 92 (10), pp. 1895–1901.

Holechek, J. L., Cibils, A. F., Bengaly, K., and Kinyamario, J. I. (2017). "Human Population Growth, African Pastoralism, and Rangelands: A Perspective". en. In: *Rangeland Ecol. Manage.* 70 (3), pp. 273–280.

Homewood, K. M. (2004). "Policy, environment and development in African rangelands". In: *Environ. Sci. Policy* 7 (3), pp. 125–143.

Homewood, K. and Rodgers, W. A. (1987). "Pastoralism, conservation and the overgrazing controversy". In: *Conservation in Africa: People, policies and practice*, pp. 111–128.

Hoover, D. L., Knapp, A. K., and Smith, M. D. (2014). "Resistance and resilience of a grassland ecosystem to climate extremes". en. In: *Ecology* 95 (9), pp. 2646–2656.

Horváth, Z., Ptacnik, R., Vad, C. F., and Chase, J. M. (2019). "Habitat loss over six decades accelerates regional and local biodiversity loss via changing landscape connectance". en. In: *Ecol. Lett.* 22 (6), pp. 1019–1027.

Howard, C. et al. (2023). "Local colonisations and extinctions of European birds are poorly explained by changes in climate suitability". en. In: *Nat. Commun.* 14 (1), p. 4304.

Huete, A., Didan, K., Miura, T., Rodriguez, E. P., Gao, X., and Ferreira, L. G. (2002). "Overview of the radiometric and biophysical performance of the MODIS vegetation indices". en. In: *Remote Sens. Environ.* The Moderate Resolution Imaging Spectroradiometer (MODIS): a new generation of Land Surface Monitoring 83 (1), pp. 195–213.

Huggins, C. (2016). "Village land use planning and commercialization of land in Tanzania". In: *LANDac Research Brief* 1.

Hunter, F. D. L., Mitchard, E. T. A., Tyrrell, P., and Russell, S. (2020). "Inter-Seasonal Time Series Imagery Enhances Classification Accuracy of Grazing Resource and Land Degradation Maps in a Savanna Ecosystem". en. In: *Remote Sensing* 12 (1), p. 198.

Hutchinson, G. E. (1957). "Concluding remarks". In: *Cold Spring Harbor symposia on quantitative biology. Vol. 22.* New York, NY: Cold Spring Harbor Laboratory Press, pp. 415–427.

IPCC (2007). *Climate Change 2007 - Impacts, Adaptation and Vulnerability: Working Group II Contribution to the Fourth Assessment Report of the IPCC*. en. Cambridge University Press. 976 pp.

— (2023). "Summary for Policymakers". In: *Climate Change 2022 – Impacts, Adaptation and Vulnerability*. Cambridge University Press, pp. 3–34.

Isaac, N. J. B., Jarzyna, M. A., Keil, P., Dambly, L. I., Boersch-Supan, P. H., Browning, E., Freeman, S. N., Golding, N., Guillera-Arroita, G., Henrys, P. A., Jarvis, S., Lahoz-Monfort, J., Pagel, J., Pescott, O. L., Schmucki, R., Simmonds, E. G., and O'Hara, R. B. (2020). "Data integration for large-scale Models of Species Distributions". en. In: *Trends Ecol. Evol.* 35 (1), pp. 56–67.

Isaac, N. J. B. and Pocock, M. J. O. (2015). "Bias and information in biological records". en. In: *Biol. J. Linn. Soc. Lond.* 115 (3), pp. 522–531.

Jiménez, L. and Soberón, J. (2022). "Estimating the fundamental niche: Accounting for the uneven availability of existing climates in the calibration area". en. In: *Ecol. Modell.* 464 (109823), p. 109823.

Johnson, D. L. (1980). "UNCOD, combatting desertification, and the pastoral nomad". In: *Nomad. People.* (5), pp. 6–10.

Jones, L. A., Mannion, P. D., Farnsworth, A., Valdes, P. J., Kelland, S.-J., and Allison, P. A. (2019). "Coupling of palaeontological and neontological reef coral data improves forecasts of biodiversity responses under global climatic change". en. In: *R. Soc. Open Sci.* 6 (4), p. 182111.

Joyce, L. A., Briske, D. D., Brown, J. R., Polley, H. W., McCarl, B. A., and Bailey, D. W. (2013). "Climate change and North American rangelands: assessment of mitigation and adaptation strategies". In: *Rangeland Ecol. Manage.* 66 (5), pp. 512–528.

Karell, P., Ahola, K., Karstinen, T., Valkama, J., and Brommer, J. E. (2011). "Climate change drives microevolution in a wild bird". en. In: *Nat. Commun.* 2, p. 208.

Karger, D. N., Conrad, O., Böhner, J., Kawohl, T., Kreft, H., Soria-Auza, R. W., Zimmermann, N. E., Linder, H. P., and Kessler, M. (2017). "Climatologies at high resolution for the Earth's land surface areas". en. In: *Sci Data* 4, p. 170122.

Kaswamila, A. (2012). "An analysis of the contribution of community wildlife management areas on livelihood in Tanzania". In: *Sustainable natural resources management*, pp. 139–54.

Kattenborn, T., Leitloff, J., Schiefer, F., and Hinz, S. (2021). "Review on Convolutional Neural Networks (CNN) in vegetation remote sensing". en. In: *ISPRS J. Photogramm. Remote Sens.* 173, pp. 24–49.

Kearney, M. R., Gillingham, P. K., Bramer, I., Duffy, J. P., and Maclean, I. M. D. (2020). "A method for computing hourly, historical, terrain-corrected microclimate anywhere on earth". en. In: *Methods Ecol. Evol.* 11 (1), pp. 38–43.

Kebacho, L. L. (2021). "Large-scale circulations associated with recent interannual variability of the short rains over East Africa". In: *Meteorol. Atmos. Phys.* 134 (1), p. 10.

Kendon, E. J., Stratton, R. A., Tucker, S., Marsham, J. H., Berthou, S., Rowell, D. P., and Senior, C. A. (2019). "Enhanced future changes in wet and dry extremes over Africa at convection-permitting scale". en. In: *Nat. Commun.* 10 (1), p. 1794.

Kéry, M. and Royle, J. A. (2017). "Applied hierarchical modeling in ecology: analysis of distribution, abundance and species richness in R and BUGS". In: *(No Title)*.

Kéry, M., Guillera-Arroita, G., and Lahoz-Monfort, J. J. (2013). "Analysing and mapping species range dynamics using occupancy models". en. In: *J. Biogeogr.* 40 (8), pp. 1463–1474.

Kierulff, M. C. M., Ruiz-Miranda, C. R., Oliveira, P. P. de, Beck, B. B., Martins, A., Dietz, J. M., Rambaldi, D. M., and Baker, A. J. (2012). "The Golden lion tamarin *Leontopithecus rosalia*: a conservation success story: Golden Lion Tamarin: Conservation Success Story". en. In: *Int. Zoo Yearb.* 46 (1), pp. 36–45.

Kiffner, C., Nagar, S., Kollmar, C., and Kioko, J. (2016). "Wildlife species richness and densities in wildlife corridors of Northern Tanzania". en. In: *J. Nat. Conserv.* 31, pp. 29–37.

Kioko, J., Kiringe, J. W., and Seno, S. O. (2012). "Impacts of livestock grazing on a savanna grassland in Kenya". en. In: *J. Arid Land* 4 (1), pp. 29–35.

Kirkpatrick, M. and Barton, N. H. (1997). "Evolution of a species' range". en. In: *Am. Nat.* 150 (1), pp. 1–23.

Kirsten, T., Hoffman, M. T., Bell, W. D., and Visser, V. (2023). "A regional, remote sensing-based approach to mapping land degradation in the Little Karoo, South Africa". en. In: *J. Arid Environ.* 219 (105066), p. 105066.

Kirui, O. K. (2016). "Economics of land degradation and improvement in Tanzania and Malawi". en. In: *Economics of Land Degradation and Improvement – A Global Assessment for Sustainable Development*. Cham: Springer International Publishing, pp. 609–649.

Kling, M. M., Auer, S. L., Comer, P. J., Ackerly, D. D., and Hamilton, H. (2020). "Multiple axes of ecological vulnerability to climate change". en. In: *Glob. Chang. Biol.* 26 (5), pp. 2798–2813.

Koenig, W. D. (1999). "Spatial autocorrelation of ecological phenomena". en. In: *Trends Ecol. Evol.* 14 (1), pp. 22–26.

Kotiaho, J. S., Halme, P., et al. (2018). "The IPBES assessment report on land degradation and restoration". In: *Intergovernmental Science-Policy Platform on Biodiversity and Ecosystem*.

Krainski, E., Gómez-Rubio, V., Bakka, H., Lenzi, A., Castro-Camilo, D., Simpson, D., Lindgren, F., and Rue, H. (2019). *Advanced Spatial Mod-*

eling with Stochastic Partial Differential Equations Using R and INLA. en.

Kumar, D., Pfeiffer, M., Gaillard, C., Langan, L., and Scheiter, S. (2021). "Climate change and elevated CO_2 favor forest over savanna under different future scenarios in South Asia". en. In: *Biogeosciences* 18 (9), pp. 2957–2979.

La Sorte, F. A. and Jetz, W. (2012). "Tracking of climatic niche boundaries under recent climate change: Niche tracking under recent climate change". en. In: *J. Anim. Ecol.* 81 (4), pp. 914–925.

Lake, P. S. (2013). "Resistance, Resilience and Restoration". en. In: *Ecol. Manage. Restor.* 14 (1), pp. 20–24.

Landmann, T. and Dubovyk, O. (2014). "Spatial analysis of human-induced vegetation productivity decline over eastern Africa using a decade (2001–2011) of medium resolution MODIS time-series data". en. In: *Int. J. Appl. Earth Obs. Geoinf.* 33, pp. 76–82.

Lankford, A. J., Svancara, L. K., Lawler, J. J., and Vierling, K. (2014). "Comparison of climate change vulnerability assessments for wildlife". en. In: *Wildl. Soc. Bull.* 38 (2), pp. 386–394.

Lary, D. J., Alavi, A. H., Gandomi, A. H., and Walker, A. L. (2016). "Machine learning in geosciences and remote sensing". In: *Geosci. Front.* 7 (1), pp. 3–10.

Lavergne, S., Thompson, J. D., Garnier, E., and Debussche, M. (2004). "The biology and ecology of narrow endemic and widespread plants: a comparative study of trait variation in 20 congeneric pairs". en. In: *Oikos* 107 (3), pp. 505–518.

Le Berre, M., Noble, V., Pires, M., Médail, F., and Diadema, K. (2019). "How to hierarchise species to determine priorities for conservation action? A critical analysis". en. In: *Biodivers. Conserv.* 28 (12), pp. 3051–3071.

Leão, T. C. C., Reinhardt, J. R., Nic Lughadha, E., and Reich, P. B. (2021). "Projected impacts of climate and land use changes on the habitat of Atlantic Forest plants in Brazil". en. In: *Glob. Ecol. Biogeogr.* 30 (10), pp. 2016–2028.

Lehmann, C. E. R., Archibald, S. A., Hoffmann, W. A., and Bond, W. J. (2011). "Deciphering the distribution of the savanna biome". en. In: *New Phytol.* 191 (1), pp. 197–209.

Leitão, P. J. and Santos, M. J. (2019). "Improving models of species ecological niches: A remote sensing overview". en. In: *Front. Ecol. Evol.* 7, p. 410432.

Lembrechts, J. J., Nijs, I., and Lenoir, J. (2019). "Incorporating microclimate into species distribution models". en. In: *Ecography (Cop.)* 42 (7), pp. 1267–1279.

Lenoir, J. and Svenning, J.-C. (2015). "Climate-related range shifts - a global multidimensional synthesis and new research directions". en. In: *Ecography* 38 (1), pp. 15–28.

Lenth, R. V. (2021). *emmeans: Estimated Marginal Means, aka Least-Squares Means. R package version 1.5.4*. Comp. software.

Lerm, R. E., Ehlers Smith, D. A., Thompson, D. I., and Downs, C. T. (2023). "Human infrastructure, surface water and tree cover are important drivers of bird diversity across a savanna protected area-mosaic landscape". In: *Landsc. Ecol.*

Lewis, S. L. and Maslin, M. A. (2015). "Defining the anthropocene". en. In: *Nature* 519 (7542), pp. 171–180.

Lezama-Ochoa, N., Pennino, M. G., Hall, M. A., Lopez, J., and Murua, H. (2020). "Using a Bayesian modelling approach (INLA-SPDE) to predict the occurrence of the Spinetail Devil Ray (Mobular mobular)". en. In: *Sci. Rep.* 10 (1), p. 18822.

Li, C., Zwiers, F., Zhang, X., Li, G., Sun, Y., and Wehner, M. (2021). "Changes in annual extremes of daily temperature and precipitation in CMIP6 models". In: *J. Clim.* 34 (9), pp. 3441–3460.

Li, W., Buitenwerf, R., Munk, M., Amoke, I., Bøcher, P. K., and Svenning, J.-C. (2020). "Accelerating savanna degradation threatens the Maasai Mara socio-ecological system". In: *Glob. Environ. Change* 60, p. 102030.

Li, Z., Liu, F., Yang, W., Peng, S., and Zhou, J. (2022). "A survey of convolutional neural networks: Analysis, applications, and prospects". en. In: *IEEE Trans. Neural Netw. Learn. Syst.* 33 (12), pp. 6999–7019.

Liao, C., Agrawal, A., Clark, P. E., Levin, S. A., and Rubenstein, D. I. (2020). "Landscape sustainability science in the drylands: mobility, rangelands and livelihoods". en. In: *Landsc. Ecol.* 35 (11), pp. 2433–2447.

Liebmann, B., Bladé, I., Funk, C., Allured, D., Quan, X.-W., Hoerling, M., Hoell, A., Peterson, P., and Thiaw, W. M. (2017). "Climatology and Interannual Variability of Boreal Spring Wet Season Precipitation in the eastern Horn of Africa and Implications for Its Recent Decline". In: *J. Clim.* 30 (10), pp. 3867–3886.

Lind, J., Sabates-Wheeler, R., Caravani, M., Kuol, L. B. D., and Nightingale, D. M. (2020). "Newly evolving pastoral and post-pastoral rangelands of Eastern Africa". en. In: *Pastoralism* 10 (1), p. 24.

Lindgren, F. and Rue, H. (2015). "Bayesian spatial modelling with R-INLA". In: *J. Stat. Softw.* 63 (19), pp. 1–25.

Lindgren, F., Rue, H., and Lindström, J. (2011). "An explicit link between Gaussian fields and Gaussian Markov random fields: the stochastic partial differential equation approach". en. In: *J. R. Stat. Soc. Series B Stat. Methodol.* 73 (4), pp. 423–498.

Lindholm, M., Alahuhta, J., Heino, J., and Toivonen, H. (2021). "Temporal beta diversity of lake plants is determined by concomitant changes in environmental factors across decades". en. In: *J. Ecol.* 109 (2), pp. 819–832.

Lloyd, P. (1999). "Rainfall as a breeding stimulus and clutch size determinant in South African arid-zone birds". en. In: *Ibis* 141 (4), pp. 637–643.

Loarie, S. R., Duffy, P. B., Hamilton, H., Asner, G. P., Field, C. B., and Ackerly, D. D. (2009). "The velocity of climate change". en. In: *Nature* 462 (7276), pp. 1052–1055.

Lobo, J. M., Jiménez-Valverde, A., and Real, R. (2008). "AUC: a misleading measure of the performance of predictive distribution models". en. In: *Glob. Ecol. Biogeogr.* 17 (2), pp. 145–151.

Lobora, A. L., Nahonyo, C. L., Munishi, L. K., Caro, T., Foley, C., and Beale, C. M. (2017). "Modelling habitat conversion in miombo woodlands: Insights from Tanzania". en. In: *J. Land Use Sci.* 12 (5), pp. 391–403.

López-i-Gelats, F., Fraser, E. D. G., Morton, J. F., and Rivera-Ferre, M. G. (2016). "What drives the vulnerability of pastoralists to global environmental change? A qualitative meta-analysis". en. In: *Glob. Environ. Change* 39, pp. 258–274.

Lourenço-de-Moraes, R., Lansac-Toha, F. M., Schwind, L. T. F., Arrieira, R. L., Rosa, R. R., Terribile, L. C., Lemes, P., Fernando Rangel, T., Diniz-Filho, J. A. F., Bastos, R. P., and Bailly, D. (2019). "Climate change will decrease the range size of snake species under negligible protection in the Brazilian Atlantic Forest hotspot". en. In: *Sci. Rep.* 9 (1), p. 8523.

Lyon, B. and DeWitt, D. G. (2012). "A recent and abrupt decline in the East African long rains". en. In: *Geophys. Res. Lett.* 39 (2).

Ma, Y., Wu, H., Wang, L., Huang, B., Ranjan, R., Zomaya, A., and Jie, W. (2015). "Remote sensing big data computing: Challenges and opportunities". en. In: *Future Gener. Comput. Syst.* 51, pp. 47–60.

MacLean, S. A. and Beissinger, S. R. (2017). "Species' traits as predictors of range shifts under contemporary climate change: A review and meta-analysis". en. In: *Glob. Chang. Biol.* 23 (10), pp. 4094–4105.

Maggiori, E., Tarabalka, Y., Charpiat, G., and Alliez, P. (2017). "Convolutional neural networks for large-scale remote-sensing image classification". In: *IEEE Trans. Geosci. Remote Sens.* 55 (2), pp. 645–657.

Manatsa, D. and Behera, S. K. (2013). "On the epochal strengthening in the relationship between rainfall of East Africa and IOD". en. In: *J. Clim.* 26 (15), pp. 5655–5673.

Mansour, K., Mutanga, O., Adam, E., and Abdel-Rahman, E. M. (2016). "Multispectral remote sensing for mapping grassland degradation using the key indicators of grass species and edaphic factors". In: *Geocarto Int.* 31 (5), pp. 477–491.

Manyanza, N. M. and Ojija, F. (2021). "Invasion, Impact and Control Techniques for Invasive Ipomoea hildebrandtii on Maasai Steppe Rangelands". en. In: *NATO Adv. Sci. Inst. Ser. E Appl. Sci.* 17, p. 12.

Martin, T. E. (2004). "Avian Life-History Evolution has an Eminent Past: Does it Have a Bright Future?" en. In: *Auk* 121 (2), pp. 289–301.

Martínez-Minaya, J., Cameletti, M., Conesa, D., and Pennino, M. G. (2018). "Species distribution modeling: a statistical review with focus in spatio-temporal issues". en. In: *Stoch. Environ. Res. Risk Assess.* 32 (11), pp. 3227–3244.

Martins, T. G., Simpson, D., Lindgren, F., and Rue, H. (2013). "Bayesian computing with INLA: New features". en. In: *Comput. Stat. Data Anal.* 67, pp. 68–83.

Mason, S. C., Palmer, G., Fox, R., Gillings, S., Hill, J. K., Thomas, C. D., and Oliver, T. H. (2015). "Geographical range margins of many taxonomic groups continue to shift polewards". In: *Biol. J. Linn. Soc. Lond.* 115 (3), pp. 586–597.

Maxwell, A. E., Warner, T. A., and Fang, F. (2018). "Implementation of machine-learning classification in remote sensing: an applied review". en. In: *Int. J. Remote Sens.* 39 (9), pp. 2784–2817.

McCain, C. M. and Garfinkel, C. F. (2021). "Climate change and elevational range shifts in insects". en. In: *Curr Opin Insect Sci* 47, pp. 111–118.

McClure, M. M. et al. (2023). "Vulnerability to climate change of managed stocks in the California Current large marine ecosystem". en. In: *Front. Mar. Sci.* 10, p. 1103767.

McKinney, M. L. (1997). "How do rare species avoid extinction? A paleontological view". en. In: *The Biology of Rarity*, pp. 110–129.

McNeill, J. R. (2016). *The great acceleration: An environmental history of the anthropocene since 1945*. London, England: Harvard University Press. 224 pp.

Medina, I., Newton, E., Kearney, M. R., Mulder, R. A., Porter, W. P., and Stuart-Fox, D. (2018). "Reflection of near-infrared light confers thermal protection in birds". en. In: *Nat. Commun.* 9 (1), p. 3610.

Mendes, P., Velazco, S. J. E., Andrade, A. F. A. d., and De Marco Júnior, P. (2020). "Dealing with overprediction in species distribution models: How adding distance constraints can improve model accuracy". en. In: *Ecol. Modell.* 431 (109180), p. 109180.

Menéndez-Guerrero, P. A., Green, D. M., and Davies, T. J. (2020). "Climate change and the future restructuring of Neotropical anuran biodiversity". en. In: *Ecography (Cop.)* 43 (2), pp. 222–235.

Middleton, N. (2018). "Rangeland management and climate hazards in drylands: dust storms, desertification and the overgrazing debate". en. In: *Nat. Hazards* 92 (1), pp. 57–70.

Midgley, G. F. and Bond, W. J. (2015). "Future of African terrestrial biodiversity and ecosystems under anthropogenic climate change". en. In: *Nat. Clim. Chang.* 5 (9), pp. 823–829.

Millenium Ecosystem Assessment Board (2005). *Ecosystems and Human Well-Being: Wetlands and Water: Synthesis*. Washington, DC: Island Press.

Miller, F. and Bowen, K. (2013). "Questioning the assumptions: the role of vulnerability assessments in climate change adaptation". en. In: *Impact Assess. Proj. Apprais.* 31 (3), pp. 190–197.

Miller, J. A. (2012). "Species distribution models: Spatial autocorrelation and non-stationarity". en. In: *Prog. Phys. Geogr.* 36 (5), pp. 681–692.

Milling, C. R., Rachlow, J. L., Chappell, M. A., Camp, M. J., Johnson, T. R., Shipley, L. A., Paul, D. R., and Forbey, J. S. (2018). "Seasonal temperature acclimatization in a semi-fossorial mammal and the role of burrows as thermal refuges". en. In: *PeerJ* 6, e4511.

Mmassy, E. C. (2017). "Ecology and Conservation Challenges of the Kori bustard (*Ardeotis kori struthiunculus*) in the Serengeti National Park, Tanzania". Trondheim, Norwegian University of Science and Technology.

Møller, J., Syversveen, A. R., and Waagepetersen, R. P. (1998). "Log Gaussian Cox Processes". en. In: *Scand. Stat. Theory Appl.* 25 (3), pp. 451–482.

Moncrieff, G. R., Scheiter, S., Langan, L., Trabucco, A., and Higgins, S. I. (2016). "The future distribution of the savannah biome: model-based and biogeographic contingency". en. In: *Philos. Trans. R. Soc. Lond. B Biol. Sci.* 371 (1703).

Moore, D. C. and Singer, M. J. (1990). "Crust formation effects on soil erosion processes". en. In: *Soil Sci. Soc. Am. J.* 54 (4), pp. 1117–1123.

Moore, N., Alagarswamy, G., Pijanowski, B., Thornton, P., Lofgren, B., Olson, J., Andresen, J., Yanda, P., and Qi, J. (2012). "East African food security as influenced by future climate change and land use change at local to regional scales". In: *Clim. Change* 110 (3), pp. 823–844.

Morera-Pujol, V., Mostert, P. S., Murphy, K. J., Burkitt, T., Coad, B., McMahon, B. J., Nieuwenhuis, M., Morelle, K., Ward, A. I., and Ciuti, S. (2023). "Bayesian species distribution models integrate presence-only and presence–absence data to predict deer distribution and relative abundance". en. In: *Ecography* 2023 (2).

Morrison, W. E., Nelson, M. W., Howard, J. F., Teeters, E. J., Griffis, R., Hare, J. A., Scott, J. D., and Alexander, M. A. (2015). *Methodology for assessing the vulnerability of marine fish and shellfish species to a changing climate.*

Moudrý, V., Cord, A. F., Gábor, L., Laurin, G. V., Barták, V., Gdulová, K., Malavasi, M., Rocchini, D., Stereńczak, K., Prošek, J., Klápště, P., and Wild, J. (2023). "Vegetation structure derived from airborne laser scanning to assess species distribution and habitat suitability: The way forward". en. In: *Divers. Distrib.* 29 (1), pp. 39–50.

Mountrakis, G., Im, J., and Ogole, C. (2011). "Support vector machines in remote sensing: A review". en. In: *ISPRS J. Photogramm. Remote Sens.* 66 (3), pp. 247–259.

Msoffe, F., Mturi, F. A., Galanti, V., Tosi, W., Wauters, L. A., and Tosi, G. (2007). "Comparing data of different survey methods for sustainable wildlife management in hunting areas: the case of Tarangire–Manyara ecosystem, northern Tanzania". en. In: *Eur. J. Wildl. Res.* 53 (2), pp. 112–124.

Muñoz, P., Gonzalez-Roglich, M., Negre, M., MBA-Mebiame, R., Malerba, D., and Cuesta Leiva, J. A. (2019). *Land degradation, poverty and inequality.*

Mworia, J., Kinyamario, J., and John, E. (2008). "Impact of the invader *Ipomoea hildebrandtii* on grass biomass, nitrogen mineralisation and determinants of its seedling establishment in Kajiado, Kenya". en. In: *Afr. J. Range Forage Sci.* 25 (1), pp. 11–16.

Myers, C. E., Stigall, A. L., and Lieberman, B. S. (2015). "PaleoENM: applying ecological niche modeling to the fossil record". en. In: *Paleobiology* 41 (2), pp. 226–244.

Naimi, B., Skidmore, A. K., Groen, T. A., and Hamm, N. A. S. (2011). "Spatial autocorrelation in predictors reduces the impact of positional uncertainty in occurrence data on species distribution modelling: Spatial autocorrelation and positional uncertainty". en. In: *J. Biogeogr.* 38 (8), pp. 1497–1509.

Nelson, N. J., Briskie, J. V., Constantine, R., Monks, J., Wallis, G. P., Watts, C., and Wotton, D. M. (2019). "The winners: species that have benefited from 30 years of conservation action". en. In: *J. R. Soc. N. Z.* 49 (3), pp. 281–300.

Ngondya, I. B., Treydte, A. C., Ndakidemi, P. A., and Munishi, L. K. (2017). "Invasive plants: ecological effects, status, management challenges in Tanzania and the way forward". In: *Journal of Biodiversity and Environmental Sciences (JBES)* 10 (3), pp. 204–217.

Nicholson, S. E. (2015). "Long-term variability of the East African 'short rains' and its links to large-scale factors". en. In: *Int. J. Climatol.* 35 (13), pp. 3979–3990.

— (2017). "Climate and climatic variability of rainfall over eastern Africa". fr. In: *Rev. Geophys.* 55 (3), pp. 590–635.

Niekerk, J. van, Bakka, H., Rue, H., and Schenk, O. (2019). "New frontiers in Bayesian modeling using the INLA package in R". In: *arXiv:1907.10426 [stat]*.

Niekerk, J. van, Bakka, H., and Rue, H. (2021). "Competing risks joint models using R-INLA". en. In: *Stat. Modelling* 21 (1-2), pp. 56–71.

Nikulin, G., Lennard, C., Dosio, A., Kjellström, E., Chen, Y., Hänsler, A., Kupiainen, M., Laprise, R., Mariotti, L., Maule, C. F., Meijgaard, E. van, Panitz, H.-J., Scinocca, J. F., and Somot, S. (2018). "The effects of 1.5 and 2 degrees of global warming on Africa in the CORDEX ensemble". In: *Environ. Res. Lett.* 13 (6), p. 065003.

NTRI (2016). *Maps — Ntri - Northern Tanzania Rangelands Initiative*. en-US. URL: `https://www.ntri.co.tz/maps/` (visited on 03/29/2021).

Nwanganga, F. and Chapple, M. (2020). *Practical machine learning in R*. en. 1st ed. Indianapolis: John Wiley and Sons.

Nwilo, P. C., Olayinka, D. N., Okolie, C. J., Emmanuel, E. I., Orji, M. J., and Daramola, O. E. (2020). "Impacts of land cover changes on desertification in northern Nigeria and implications on the Lake Chad Basin". en. In: *J. Arid Environ.* 181 (104190), p. 104190.

Nychka, D., Furrer, R., Paige, J., and Sain, S. (2021). *fields: Tools for Spatial Data*. Comp. software. Version 15.2.

Nzunda, E. F. (2022). "Grassland loss in Tanzania: Causes, consequences and control". en. In: *Asian Journal of Research in Education and Social Sciences* 4 (2), pp. 20–38.

Nzunda, E. F. and Midtgaard, F. (2019). “Deforestation and loss of bushland and grassland primarily due to expansion of cultivation in mainland Tanzania (1995–2010)”. In: *J. Sustainable For.* 38 (6), pp. 509–525.

O’Loughlin, J., Witmer, F. D. W., Linke, A. M., Laing, A., Gettelman, A., and Dudhia, J. (2012). “Climate variability and conflict risk in East Africa, 1990-2009”. en. In: *Proc. Natl. Acad. Sci.* 109 (45), pp. 18344–18349.

O’Neill, B. C., Kriegler, E., Ebi, K. L., Kemp-Benedict, E., Riahi, K., Rothman, D. S., Ruijven, B. J. van, Vuuren, D. P. van, Birkmann, J., Kok, K., Levy, M., and Solecki, W. (2017). “The roads ahead: Narratives for shared socioeconomic pathways describing world futures in the 21st century”. en. In: *Glob. Environ. Change* 42, pp. 169–180.

Oba, G. and Lusigi, W. J. (1987). *An overview of drought strategies and land use in African pastoral systems*. Agricultural Administration Unit, Overseas Development Institute.

Obiri, J. F. (2011). “Invasive plant species and their disaster-effects in dry tropical forests and rangelands of Kenya and Tanzania”. en. In: *Jàmbá: Journal of Disaster Risk Studies* 3 (2), pp. 417–428.

Ogega, O. M., Koske, J., Kung’u, J. B., Scoccimarro, E., Endris, H. S., and Mistry, M. N. (2020). “Heavy precipitation events over East Africa in a changing climate: results from CORDEX RCMs”. en. In: *Clim. Dyn.* 55 (3-4), pp. 993–1009.

Ongoma, V., Chen, H., Gao, C., Nyongesa, A. M., and Polong, F. (2018). “Future changes in climate extremes over Equatorial East Africa based on CMIP5 multimodel ensemble”. In: *Nat. Hazards* 90 (2), pp. 901–920.

Ovaskainen, O., Abrego, N., Halme, P., and Dunson, D. (2016a). “Using latent variable models to identify large networks of species-to-species associations at different spatial scales”. en. In: *Methods in Ecology and Evolution* 7 (5), pp. 549–555.

Ovaskainen, O., Roy, D. B., Fox, R., and Anderson, B. J. (2016b). “Uncovering hidden spatial structure in species communities with spatially explicit joint species distribution models”. en. In: *Methods in Ecology and Evolution* 7 (4), pp. 428–436.

Ovaskainen, O. and Soininen, J. (2011). “Making more out of sparse data: hierarchical modeling of species communities”. en. In: *Ecology* 92 (2), pp. 289–295.

Ovaskainen, O., Tikhonov, G., Norberg, A., Guillaume Blanchet, F., Duan, L., Dunson, D., Roslin, T., and Abrego, N. (2017). “How to make more out of community data? A conceptual framework and its implementation as models and software”. en. In: *Ecol. Lett.* 20 (5), pp. 561–576.

Owen-Smith, N., Page, B., Teren, G., and Druce, D. J. (2019). *Megabrowser impacts on woody vegetation in savannas.* en.

Panetta, A. M., Stanton, M. L., and Harte, J. (2018). "Climate warming drives local extinction: Evidence from observation and experimentation". en. In: *Sci Adv* 4 (2), eaaq1819.

Pang, C.-C., Ma, X. K.-K., Hung, T. T.-H., and Hau, B. C.-H. (2018). "Early ecological succession on landslide trails, Hong Kong, China". en. In: *Écoscience* 25 (2), pp. 153–161.

Parmesan, C. et al. (2023). "Terrestrial and freshwater ecosystems and their services". In: *Climate Change 2022 – Impacts, Adaptation and Vulnerability.* Ed. by Singh, B. Cambridge University Press, pp. 197–378.

Parmesan, C., Ryrholm, N., Stefanescu, C., Hill, J. K., Thomas, C. D., Descimon, H., Huntley, B., Kaila, L., Kullberg, J., Tammaru, T., Tennent, W. J., Thomas, J. A., and Warren, M. (1999). "Poleward shifts in geographical ranges of butterfly species associated with regional warming". en. In: *Nature* 399 (6736), pp. 579–583.

Parmesan, C. and Yohe, G. (2003). "A globally coherent fingerprint of climate change impacts across natural systems". en. In: *Nature* 421 (6918), pp. 37–42.

Pearson, R. G., Stanton, J. C., Shoemaker, K. T., Aiello-Lammens, M. E., Ersts, P. J., Horning, N., Fordham, D. A., Raxworthy, C. J., Ryu, H. Y., McNees, J., and Akçakaya, H. R. (2014). "Life history and spatial traits predict extinction risk due to climate change". en. In: *Nat. Clim. Chang.* 4 (3), pp. 217–221.

Peel, M. and Stalmans, M. (2018). "The effect of Holistic Planned Grazing™ on African rangelands: a case study from Zimbabwe". en. In: *Afr. J. Range Forage Sci.* 35 (1), pp. 23–31.

Pekel, J.-F., Cottam, A., Gorelick, N., and Belward, A. S. (2016). "High-resolution mapping of global surface water and its long-term changes". en. In: *Nature* 540 (7633), pp. 418–422.

Pellegrini, A. F. A., Socolar, J. B., Elsen, P. R., and Giam, X. (2016). "Trade-offs between savanna woody plant diversity and carbon storage in the Brazilian Cerrado". en. In: *Glob. Chang. Biol.* 22 (10), pp. 3373–3382.

Peterson, A. T. (2001). "Predicting species' geographic distributions based on ecological niche modeling". en. In: *Condor* 103 (3), p. 599.

Pettorelli, N., Ryan, S., Mueller, T., Bunnefeld, N., Jedrzejewska, B., Lima, M., and Kausrud, K. (2011). "The Normalized Difference Vegetation Index (NDVI): unforeseen successes in animal ecology". In: *Clim. Res.* 46 (1), pp. 15–27.

Pham, T. D., Le, N. N., Ha, N. T., Nguyen, L. V., Xia, J., Yokoya, N., To, T. T., Trinh, H. X., Kieu, L. Q., and Takeuchi, W. (2020). "Estimating Mangrove Above-Ground Biomass Using Extreme Gradient Boosting Decision Trees Algorithm with Fused Sentinel-2 and ALOS-2 PALSAR-2 Data in Can Gio Biosphere Reserve, Vietnam". en. In: *Remote Sensing* 12 (5), p. 777.

Phiri, D., Simwanda, M., Salekin, S., Nyirenda, V., Murayama, Y., and Ranagalage, M. (2020). "Sentinel-2 data for land cover/use mapping: A review". en. In: *Remote Sens. (Basel)* 12 (14), p. 2291.

Pi, W., Du, J., Bi, Y., Gao, X., and Zhu, X. (2021). "3D-CNN based UAV hyperspectral imagery for grassland degradation indicator ground object classification research". en. In: *Ecol. Inform.* 62 (101278), p. 101278.

Piot, B. and Bacuez, F. (2021). *A major range extension of Horus Swift Apus horus, north-west to Senegal.*

Pörtner, H. O., Roberts, D. C., Tignor, M., Poloczanska, E. S., Mintenbeck, K., Alegría, A., Craig, M., Langsdorf, S., Löschke, S., Möller, V., Okem, A., and Rama, B., eds. (2022). *IPCC, 2022: Climate Change 2022: Impacts, Adaptation and Vulnerability. Contribution of Working Group II to the Sixth Assessment Report of the Intergovernmental Panel on Climate Change*. en. Cambridge University Press, Cambridge, UK and New York, NY, USA: Cambridge University Press.

Post, A. K. and Knapp, A. K. (2020). "The importance of extreme rainfall events and their timing in a semi-arid grassland". en. In: *J. Ecol.* 108 (6), pp. 2431–2443.

Potapov, P., Turubanova, S., Hansen, M. C., Tyukavina, A., Zalles, V., Khan, A., Song, X.-P., Pickens, A., Shen, Q., and Cortez, J. (2022). "Global maps of cropland extent and change show accelerated cropland expansion in the twenty-first century". en. In: *Nat. Food* 3 (1), pp. 19–28.

Powers, R. P. and Jetz, W. (2019). "Global habitat loss and extinction risk of terrestrial vertebrates under future land-use-change scenarios". en. In: *Nat. Clim. Chang.* 9 (4), pp. 323–329.

Pressey, R. L., Weeks, R., and Gurney, G. G. (2017). "From displacement activities to evidence-informed decisions in conservation". en. In: *Biol. Conserv.* 212, pp. 337–348.

Prins, H. H. T. and Loth, P. E. (1988). "Rainfall Patterns as Background to Plant Phenology in Northern Tanzania". In: *J. Biogeogr.* 15 (3), pp. 451–463.

Pulliam, H. R. (1988). "Sources, Sinks, and Population Regulation". In: *Am. Nat.* 132 (5), pp. 652–661.

Pullin, A. S., Sutherland, W., Gardner, T., Kapos, V., and Fa, J. E. (2013). "Conservation priorities: identifying need, taking action and evaluating success". In: *Key Topics in Conservation Biology 2*. Oxford: John Wiley & Sons, pp. 1–22.

Purvis, A., Cardillo, M., Grenyer, R., and Collen, B. (2005). "Correlates of extinction risk: phylogeny, biology, threat and scale". In: *Phylogeny and conservation*. Ed. by Purvis, A., Gittleman, J. L., and Brooks, T. Cambridge: Cambridge University Press, p. 295.

QGIS Development Team (2022). *QGIS Geographic Information System*. Version 3.14. QGIS Association.

Qi, J., Chehbouni, A., Huete, A. R., Kerr, Y. H., and Sorooshian, S. (1994). "A modified soil adjusted vegetation index". en. In: *Remote Sens. Environ.* 48 (2), pp. 119–126.

R Core Team (2016). *R: A language and environment for statistical computing*. Vienna, Austria.

— (2021). *R: A language and environment for statistical computing*. Vienna, Austria.

— (2023). *R: A Language and Environment for Statistical Computing*. Comp. software. Version 4.3.2.

Radchuk, V. et al. (2019). "Adaptive responses of animals to climate change are most likely insufficient". en. In: *Nat. Commun.* 10 (1), p. 3109.

Radosavljevic, A. and Anderson, R. P. (2014). "Making better Maxent models of species distributions: complexity, overfitting and evaluation". en. In: *J. Biogeogr.* 41 (4), pp. 629–643.

Rahmonov, O. and Oles, W. (2010). "Vegetation succession over an area of a medieval ecological disaster. The case of the Bledów Desert, Poland". In: *Erdkunde* 64 (3), pp. 241–255.

Ramos, J. E., Tam, J., Aramayo, V., Briceño, F. A., Bandin, R., Buitron, B., Cuba, A., Fernandez, E., Flores-Valiente, J., Gomez, E., Jara, H. J., Ñiquen, M., Rujel, J., Salazar, C. M., Sanjinez, M., León, R. I., Nelson, M., Gutiérrez, D., and Pecl, G. T. (2022). "Climate vulnerability assessment of key fishery resources in the Northern Humboldt Current System". en. In: *Sci. Rep.* 12 (1), p. 4800.

Rapinel, S., Mony, C., Lecoq, L., Clément, B., Thomas, A., and Hubert-Moy, L. (2019). "Evaluation of Sentinel-2 time-series for mapping floodplain grassland plant communities". en. In: *Remote Sens. Environ.* 223, pp. 115–129.

Raup, D. M. and Sepkoski Jr, J. J. (1982). "Mass extinctions in the marine fossil record". en. In: *Science* 215 (4539), pp. 1501–1503.

Redding, D. W., Lucas, T. C. D., Blackburn, T. M., and Jones, K. E. (2017). "Evaluating Bayesian spatial methods for modelling species distributions with clumped and restricted occurrence data". en. In: *PLoS One* 12 (11), e0187602.

Régnier, C., Fontaine, B., and Bouchet, P. (2009). "Not knowing, not recording, not listing: numerous unnoticed mollusk extinctions". en. In: *Conserv. Biol.* 23 (5), pp. 1214–1221.

Reif, J. and Flousek, J. (2012). "The role of species' ecological traits in climatically driven altitudinal range shifts of central European birds". en. In: *Oikos* 121 (7), pp. 1053–1060.

Rejmánek, M. (2018). "Vascular plant extinctions in California: A critical assessment". en. In: *Divers. Distrib.* 24 (1), pp. 129–136.

Reside, A. E., VanDerWal, J., Garnett, S. T., and Kutt, A. S. (2016). "Vulnerability of Australian tropical savanna birds to climate change". en. In: *Austral Ecol.* 41 (1), pp. 106–116.

Riddell, E. A., Iknayan, K. J., Hargrove, L., Tremor, S., Patton, J. L., Ramirez, R., Wolf, B. O., and Beissinger, S. R. (2021). "Exposure to climate change drives stability or collapse of desert mammal and bird communities". en. In: *Science* 371 (6529), pp. 633–636.

Righetto, A. J., Faes, C., Vandendijck, Y., and Ribeiro, P. J. (2020). "On the choice of the mesh for the analysis of geostatistical data using R-INLA". In: *Communications in Statistics - Theory and Methods* 49 (1), pp. 203–220.

Riginos, C. and Herrick, J. E. (2010). "Monitoring rangeland health: a guide for pastoralists and other land managers in eastern Africa". In: *Version II*.

Rikimaru, A., Roy, P. S., and Miyatake, S. (2002). "Tropical forest cover density mapping". In: *Trop. Ecol.*, pp. 39–47.

Rinnan, D. S. and Lawler, J. (2019). "Climate-niche factor analysis: a spatial approach to quantifying species vulnerability to climate change". en. In: *Ecography* 42 (9), pp. 1494–1503.

Rivera, O. R. de, Blangiardo, M., López-Quílez, A., and Martín-Sanz, I. (2019). "Species distribution modelling through Bayesian hierarchical approach". en. In: *Theor. Ecol.* 12 (1), pp. 49–59.

Robin, X., Turck, N., Hainard, A., Tiberti, N., Lisacek, F., Sanchez, J.-C., and Müller, M. (2011). "pROC: an open-source package for R and S+ to analyze and compare ROC curves". en. In: *BMC Bioinformatics* 12, p. 77.

Rodrigues, A. S. L., Pilgrim, J. D., Lamoreux, J. F., Hoffmann, M., and Brooks, T. M. (2006). "The value of the IUCN Red List for conservation". en. In: *Trends Ecol. Evol.* 21 (2), pp. 71–76.

Rodríguez, J. P., Brotons, L., Bustamante, J., and Seoane, J. (2007). "The Application of Predictive Modelling of Species Distribution to Biodiversity Conservation". In: *Diversity and Distributions* 13 (3), pp. 243–251.

Roques, K. G., O'Connor, T. G., and Watkinson, A. R. (2001). "Dynamics of shrub encroachment in an African savanna: relative influences of fire, herbivory, rainfall and density dependence". en. In: *J. Appl. Ecol.* 38 (2), pp. 268–280.

Rose, M. B., Velazco, S. J. E., Regan, H. M., and Franklin, J. (2023). "Rarity, geography, and plant exposure to global change in the California Floristic Province". en. In: *Glob. Ecol. Biogeogr.* 32 (2), pp. 218–232.

Rowan, R. C., Ladewig, H. W., and White, L. D. (1994). "Perceptions vs. Recommendations: A rangeland decision-making dilemma". In: *J. Range Manag.* 47 (5), p. 344.

Rowell, D. P., Booth, B. B. B., Nicholson, S. E., and Good, P. (2015). "Reconciling Past and Future Rainfall Trends over East Africa". en. In: *J. Clim.* 28 (24), pp. 9768–9788.

Royall, R. M. (1986). "The Effect of Sample Size on the Meaning of Significance Tests". In: *Am. Stat.* 40 (4), pp. 313–315.

Ruaro, R. et al. (2019). "Climate change will decrease the range of a keystone fish species in La Plata River Basin, South America". en. In: *Hydrobiologia* 836 (1), pp. 1–19.

Rue, H., Martino, S., and Chopin, N. (2009). "Approximate Bayesian inference for latent Gaussian models by using integrated nested Laplace approximations". en. In: *J. R. Stat. Soc. Series B Stat. Methodol.* 71 (2), pp. 319–392.

Rukundo, E., Liu, S., Dong, Y., Rutebuka, E., Asamoah, E. F., Xu, J., and Wu, X. (2018). "Spatio-temporal dynamics of critical ecosystem services in response to agricultural expansion in Rwanda, East Africa". en. In: *Ecol. Indic.* 89, pp. 696–705.

Ruppert, J. C., Harmoney, K., Henkin, Z., Snyman, H. A., Sternberg, M., Willms, W., and Linstädter, A. (2015). "Quantifying drylands' drought resistance and recovery: the importance of drought intensity, dominant life history and grazing regime". en. In: *Glob. Chang. Biol.* 21 (3), pp. 1258–1270.

Russell, S., Tyrrell, P., and Western, D. (2018). "Seasonal interactions of pastoralists and wildlife in relation to pasture in an African savanna ecosystem". en. In: *J. Arid Environ.* 154, pp. 70–81.

Sadykova, D., Scott, B. E., De Dominicis, M., Wakelin, S. L., Sadykov, A., and Wolf, J. (2017). "Bayesian joint models with INLA exploring marine mobile predator-prey and competitor species habitat overlap". en. In: *Ecol. Evol.* 7 (14), pp. 5212–5226.

Saether, B. E. (1988). "Pattern of covariation between life-history traits of European birds". en. In: *Nature* 331 (6157), pp. 616–617.

Sallu, S. M., Twyman, C., and Stringer, L. C. (2010). "Resilient or Vulnerable Livelihoods? Assessing Livelihood Dynamics and Trajectories in Rural Botswana". en. In: *Ecology and Society* 15 (4).

Savari, M. (2022). "Explaining the ranchers' behavior of rangeland conservation in western Iran". en. In: *Front. Psychol.* 13, p. 1090723.

Savory, A. and Butterfield, J. (1999). "Holistic management: a new framework for decision making". In.

Scaramuzza, P. and Barsi, J. (2005). "Landsat 7 scan line corrector-off gap-filled product development". In: *Proceeding of Pecora*. Vol. 16, pp. 23–27.

Schaub, M., Martinez, N., Tagmann-Ioset, A., Weisshaupt, N., Maurer, M. L., Reichlin, T. S., Abadi, F., Zbinden, N., Jenni, L., and Arlettaz, R. (2010). "Patches of Bare Ground as a Staple Commodity for Declining ground-foraging Insectivorous Farmland Birds". en. In: *PLoS One* 5 (10). Ed. by Evans, D. M., e13115.

Scholes, R. J. and Archer, S. R. (1997). "Tree-grass interactions in savannas". en. In: *Annu. Rev. Ecol. Syst.* 28 (1), pp. 517–544.

Scoones, I. (1995). "Exploiting heterogeneity: habitat use by cattle in dryland Zimbabwe". In: *J. Arid Environ.* 29, pp. 221–237.

Şekercioğlu, Ç. H., Schneider, S. H., Fay, J. P., and Loarie, S. R. (2008). "Climate change, elevational range shifts, and bird extinctions". en. In: *Conserv. Biol.* 22 (1), pp. 140–150.

Selemani, I. S. (2018). "Ecological implications of bush encroachment on foraging behavior of dairy cows and goats at SUA farm, Morogoro, Tanzania". en. In: *Trop. grassl.-Forrajes trop.* 6 (3), pp. 169–176.

Selemani, I. S. et al. (2014). "Communal rangelands management and challenges underpinning pastoral mobility in Tanzania: a review". In: *Livestock Res. Rural Dev.* 26 (78), pp. 1–12.

Senyatso, K. J., Collar, N. J., and Dolman, P. M. (2013). "Assessing range-wide conservation status change in an unmonitored widespread African bird species". en. In: *Divers. Distrib.* 19 (2), pp. 106–119.

Shabani, F., Kumar, L., and Ahmadi, M. (2016). "A comparison of absolute performance of different correlative and mechanistic species distribution models in an independent area". en. In: *Ecol. Evol.* 6 (16), pp. 5973–5986.

Sherren, K. and Kent, C. (2019). "Who's afraid of Allan Savory? Scientometric polarization on Holistic Management as competing understandings". en. In: *Renew. Agric. Food Syst.* 34 (1), pp. 77–92.

Shongwe, M. E., Oldenborgh, G. J. van, Hurk, B. van den, and Aalst, M. van (2011). "Projected Changes in Mean and Extreme Precipitation in Africa under Global Warming. Part II: East Africa". en. In: *J. Clim.* 24 (14), pp. 3718–3733.

Sicacha-Parada, J., Steinsland, I., Cretois, B., and Borgelt, J. (2021). "Accounting for spatial varying sampling effort due to accessibility in Citizen Science data: A case study of moose in Norway". In: *Spatial Statistics* 42, p. 100446.

Sih, A., Jonsson, B. G., and Luikart, G. (2000). "Habitat loss: ecological, evolutionary and genetic consequences". en. In: *Trends Ecol. Evol.* 15 (4), pp. 132–134.

Simic Milas, A., Cracknell, A. P., and Warner, T. A. (2018). "Drones – the third generation source of remote sensing data". en. In: *Int. J. Remote Sens.* 39 (21), pp. 7125–7137.

Simmonds, E. G., Jarvis, S. G., Henrys, P. A., Isaac, N. J. B., and O'Hara, R. B. (2020). "Is more data always better? A simulation study of benefits and limitations of integrated distribution models". en. In: *Ecography* 43 (10), pp. 1413–1422.

Simpson, D., Illian, J. B., Lindgren, F., Sørbye, S. H., and Rue, H. (2016). "Going off grid: computationally efficient inference for log-Gaussian Cox processes". en. In: *Biometrika* 103 (1), pp. 49–70.

Simpson, D., Rue, H., Riebler, A., Martins, T. G., and Sørbye, S. H. (2017). "Penalising Model Component Complexity: A Principled, Practical Approach to Constructing Priors". en. In: *Statistical Science* 32 (1), pp. 1–28.

Singh, J. S. (2002). "The biodiversity crisis: A multifaceted review". In: *Curr. Sci.* 82 (6), pp. 638–647.

Sirami, C., Brotons, L., and Martin, J.-L. (2008). "Spatial extent of bird species response to landscape changes: colonisation/extinction dynamics at the community-level in two contrasting habitats". en. In: *Ecography (Cop.)* 31 (4), pp. 509–518.

Skarpe, C. (1991). "Impact of Grazing in Savanna Ecosystems". In: *Ambio* 20 (8), pp. 351–356.

— (1992). "Dynamics of savanna ecosystems". en. In: *J. Veg. Sci.* 3 (3), pp. 293–300.

Smit, I. P. J. and Prins, H. H. T. (2015). "Predicting the Effects of Woody Encroachment on Mammal Communities, Grazing Biomass and Fire Frequency in African Savannas". en. In: *PLoS One* 10 (9). Ed. by Crowther, M. S., e0137857.

Stahl, U., Reu, B., and Wirth, C. (2014). "Predicting species' range limits from functional traits for the tree flora of North America". In: *Proc. Natl. Acad. Sci.* 111 (38), pp. 13739–13744.

Staver, A. C., Archibald, S., and Levin, S. A. (2011). "The Global Extent and Determinants of Savanna and Forest as Alternative Biome States". en. In: *Science* 334 (6053), pp. 230–232.

Stein, H., Maganga, F. P., Odgaard, R., Askew, K., and Cunningham, S. (2016). "The Formal Divide: Customary Rights and the Allocation of Credit to Agriculture in Tanzania". en. In: *J. Dev. Stud.* 52 (9), pp. 1306–1319.

Stevens, C. J., Dise, N. B., Mountford, J. O., and Gowing, D. J. (2004). "Impact of nitrogen deposition on the species richness of grasslands". en. In: *Science* 303 (5665), pp. 1876–1879.

Stevens, N., Lehmann, C. E. R., Murphy, B. P., and Durigan, G. (2017). "Savanna woody encroachment is widespread across three continents". en. In: *Glob. Chang. Biol.* 23 (1), pp. 235–244.

Still, S. M., Frances, A. L., Treher, A. C., and Oliver, L. (2015). "Using two climate change vulnerability assessment methods to prioritize and manage rare plants: A case study". en. In: *Nat. Areas J.* 35 (1), pp. 106–121.

Strien, A. J. van, Swaay, C. A. M. van, Strien-van Liempt, W. T. F. H. van, Poot, M. J. M., and WallisDeVries, M. F. (2019). "Over a century of data reveal more than 80% decline in butterflies in the Netherlands". In: *Biol. Conserv.* 234, pp. 116–122.

Strimas-Mackey, M., Hochachka, W. M., Ruiz-Gutierrez, V., Robinson, O. J., Miller, E. T., Auer, T., Kelling, S., Fink, D., and Johnston, A. (2023). *Best Practices for Using eBird Data. Version 2.0.* URL: `https://ebird.github.io/ebird-best-practices/`,`https://doi.org/10.5281/zenodo.3620739`.

Stringer, L. C., Reed, M. S., Dougill, A. J., Seely, M. K., and Rokitzki, M. (2007). "Implementing the UNCCD: Participatory challenges". en. In: *Nat. Resour. Forum* 31 (3), pp. 198–211.

Stuart-Fox, D., Newton, E., and Clusella-Trullas, S. (2017). "Thermal consequences of colour and near-infrared reflectance". en. In: *Philos. Trans. R. Soc. Lond. B Biol. Sci.* 372 (1724).

Sullivan, B. L., Wood, C. L., Iliff, M. J., Bonney, R. E., Fink, D., and Kelling, S. (2009). "eBird: A citizen-based bird observation network in the biological sciences". In: *Biol. Conserv.* 142 (10), pp. 2282–2292.

Sullivan, B. L. et al. (2014). "The eBird enterprise: An integrated approach to development and application of citizen science". In: *Biol. Conserv.* 169, pp. 31–40.

Sunday, J. M., Pecl, G. T., Frusher, S., Hobday, A. J., Hill, N., Holbrook, N. J., Edgar, G. J., Stuart-Smith, R., Barrett, N., Wernberg, T., Watson, R. A., Smale, D. A., Fulton, E. A., Slawinski, D., Feng, M., Radford, B. T., Thompson, P. A., and Bates, A. E. (2015). "Species traits and climate velocity explain geographic range shifts in an ocean-warming hotspot". en. In: *Ecol. Lett.* 18 (9), pp. 944–953.

Symeonakis, E. and Drake, N. (2004). "Monitoring desertification and land degradation over sub-Saharan Africa". en. In: *Int. J. Remote Sens.* 25 (3), pp. 573–592.

Szpakowski, D. and Jensen, J. (2019). "A review of the applications of remote sensing in fire ecology". en. In: *Remote Sens. (Basel)* 11 (22), p. 2638.

Tayleur, C. M., Devictor, V., Gaüzère, P., Jonzén, N., Smith, H. G., and Lindström, Å. (2016). "Regional variation in climate change winners and losers highlights the rapid loss of cold-dwelling species". en. In: *Divers. Distrib.* 22 (4), pp. 468–480.

Taylor, B. M. and Diggle, P. J. (2014). "INLA or MCMC? A tutorial and comparative evaluation for spatial prediction in log-Gaussian Cox processes". en. In: *J. Stat. Comput. Simul.* 84 (10), pp. 2266–2284.

Tedesco, P. A., Bigorne, R., Bogan, A. E., Giam, X., Jézéquel, C., and Hugueny, B. (2014). "Estimating how many undescribed species have gone extinct: Estimating Undescribed species extinctions". en. In: *Conserv. Biol.* 28 (5), pp. 1360–1370.

Thaiyah, A. G., Nyaga, P. N., Maribei, J. M., Ngatia, T. A., Kamau, J. P. M., and Kinyuru, J. M. (2011). "Acute, sub-chronic and chronic toxicity of Solanum incanum L in sheep in Kenya". In: *Kenya Veterinarian* 35 (1), pp. 1–8.

Theobald, D. M., Kennedy, C., Chen, B., Oakleaf, J., Baruch-Mordo, S., and Kiesecker, J. (2020). "Earth transformed: detailed mapping of global human modification from 1990 to 2017". en. In: *Earth Syst. Sci. Data* 12 (3), pp. 1953–1972.

Thiollay, J.-M. (2006). "Large Bird Declines with Increasing Human Pressure in Savanna Woodlands (Burkina Faso)". en. In: *Biodivers. Conserv.* 15 (7), pp. 2085–2108.

Thomas, C. D., Hill, J. K., Anderson, B. J., Bailey, S., Beale, C. M., Bradbury, R. B., Bulman, C. R., Crick, H. Q. P., Eigenbrod, F., Griffiths, H. M., Kunin, W. E., Oliver, T. H., Walmsley, C. A., Watts, K., Worsfold, N. T., and Yardley, T. (2011). "A framework for assessing threats and benefits to species responding to climate change". In: *Methods in Ecology and Evolution* 2 (2), pp. 125–142.

Thrasher, B., Wang, W., Michaelis, A., Melton, F., Lee, T., and Nemani, R. (2022). "NASA global daily downscaled projections, CMIP6". en. In: *Sci. Data* 9 (1), p. 262.

Thuiller, W. (2004). "Patterns and uncertainties of species' range shifts under climate change". en. In: *Glob. Chang. Biol.* 10 (12), pp. 2020–2027.

Thurman, L. L., Stein, B. A., Beever, E. A., Foden, W., Geange, S. R., Green, N., Gross, J. E., Lawrence, D. J., LeDee, O., Olden, J. D., Thompson, L. M., and Young, B. E. (2020). "Persist in place or shift in space? Evaluating the adaptive capacity of species to climate change". en. In: *Front. Ecol. Environ.* 18 (9), pp. 520–528.

Tilman, D. and Downing, J. A. (1994). "Biodiversity and stability in grasslands". en. In: *Nature* 367 (6461), pp. 363–365.

Tingley, R., Vallinoto, M., Sequeira, F., and Kearney, M. R. (2014). "Realized niche shift during a global biological invasion". en. In: *Proc. Natl. Acad. Sci. U. S. A.* 111 (28), pp. 10233–10238.

Tobias, J. A. et al. (2022). "AVONET: morphological, ecological and geographical data for all birds". en. In: *Ecol. Lett.* 25 (3), pp. 581–597.

Tobler, W. R. (1970). "A computer movie simulating urban growth in the Detroit region". In: *Econ. Geogr.* 46, p. 234.

Touboul, J. D., Staver, A. C., and Levin, S. A. (2018). "On the complex dynamics of savanna landscapes". en. In: *Proc. Natl. Acad. Sci. U. S. A.* 115 (7), E1336–E1345.

Trainor, A. M., Schmitz, O. J., Ivan, J. S., and Shenk, T. M. (2014). "Enhancing species distribution modeling by characterizing predator-prey interactions". en. In: *Ecol. Appl.* 24 (1), pp. 204–216.

Travis, J. M. J. (2003). "Climate change and habitat destruction: a deadly anthropogenic cocktail". en. In: *Proc. Biol. Sci.* 270 (1514), pp. 467–473.

Trisos, C. H., Merow, C., and Pigot, A. L. (2020). "The projected timing of abrupt ecological disruption from climate change". en. In: *Nature* 580 (7804), pp. 496–501.

Triviño, M., Cabeza, M., Thuiller, W., Hickler, T., and Araújo, M. B. (2013). "Risk assessment for Iberian birds under global change". In: *Biol. Conserv.* 168, pp. 192–200.

Troudet, J., Grandcolas, P., Blin, A., Vignes-Lebbe, R., and Legendre, F. (2017). "Taxonomic bias in biodiversity data and societal preferences". en. In: *Sci. Rep.* 7 (1), p. 9132.

Tyukavina, A., Potapov, P., Hansen, M. C., Pickens, A. H., Stehman, S. V., Turubanova, S., Parker, D., Zalles, V., Lima, A., Kommareddy, I., Song, X.-P., Wang, L., and Harris, N. (2022). "Global trends of forest loss due to fire from 2001 to 2019". In: *Front. Remote Sens.* 3, p. 825190.

Urban, M. C. (2015). "Accelerating extinction risk from climate change". en. In: *Science* 348 (6234), pp. 571–573.

Vågen, T.-G., Winowiecki, L. A., Tondoh, J. E., Desta, L. T., and Gumbricht, T. (2016). "Mapping of soil properties and land degradation risk in Africa using MODIS reflectance". en. In: *Geoderma* 263, pp. 216–225.

Valencia, J. B., Mesa, J., León, J. G., Madriñán, S., and Cortés, A. J. (2020). "Climate Vulnerability Assessment of the Espeletia Complex on Páramo Sky Islands in the Northern Andes". In: *Front. Ecol. Evol.* 8, p. 309.

Van der Colff, D., Kumschick, S., Foden, W., Raimondo, D., Botella, C., Staden, L. von, and Wilson, J. R. U. (2023). "Drivers, predictors, and probabilities of plant extinctions in South Africa". en. In: *Biodivers. Conserv.* 32 (13), pp. 4313–4336.

Van Der Veken, S., Bellemare, J., Verheyen, K., and Hermy, M. (2007). "Life-history Traits Are Correlated with Geographical Distribution Patterns of Western European Forest Herb Species". In: *J. Biogeogr.* 34 (10), pp. 1723–1735.

Velazco, S. J. E., Ribeiro, B. R., Laureto, L. M. O., and De Marco Júnior, P. (2020). "Overprediction of species distribution models in conservation planning: A still neglected issue with strong effects". en. In: *Biol. Conserv.* 252 (108822), p. 108822.

Veldhuis, M. P., Ritchie, M. E., Ogutu, J. O., Morrison, T. A., Beale, C. M., Estes, A. B., Mwakilema, W., Ojwang, G. O., Parr, C. L., Probert, J., Wargute, P. W., Hopcraft, J. G. C., and Olff, H. (2019). "Cross-boundary human impacts compromise the Serengeti-Mara ecosystem". en. In: *Science* 363 (6434), pp. 1424–1428.

Venter, O., Sanderson, E. W., Magrach, A., Allan, J. R., Beher, J., Jones, K. R., Possingham, H. P., Laurance, W. F., Wood, P., Fekete, B. M., Levy, M. A., and Watson, J. E. M. (2016). "Global terrestrial Human Footprint maps for 1993 and 2009". en. In: *Sci Data* 3, p. 160067.

Vermote, E. (2015). "MOD09A1 MODIS/terra surface reflectance 8-day L3 global 500m SIN grid V006". In: *NASA EOSDIS Land Processes DAAC* 10.

Vié, J.-C., Hilton-Taylor, C., Pollock, C., Ragle, J., Smart, J., Stuart, S. N., and Tong, R. (2009). "The IUCN Red List: a key conservation tool". In: *Wildlife in a changing world–An analysis of the 2008 IUCN Red List of Threatened Species*, p. 1.

Vierich, H. I. D. and Stoop, W. A. (1990). "Changes in West African Savanna agriculture in response to growing population and continuing low rainfall". en. In: *Agric. Ecosyst. Environ.* 31 (2), pp. 115–132.

Villero, D., Pla, M., Camps, D., Ruiz-Olmo, J., and Brotons, L. (2017). "Integrating species distribution modelling into decision-making to inform conservation actions". en. In: *Biodivers. Conserv.* 26 (2), pp. 251–271.

Virkkala, R. (2016). "Long-term decline of southern boreal forest birds: consequence of habitat alteration or climate change?" en. In: *Biodivers. Conserv.* 25 (1), pp. 151–167.

Visser, M. E., Holleman, L. J. M., and Gienapp, P. (2006). "Shifts in caterpillar biomass phenology due to climate change and its impact on the breeding biology of an insectivorous bird". en. In: *Oecologia* 147 (1), pp. 164–172.

Vizy, E. K. and Cook, K. H. (2012). "Mid-twenty-first-century Changes in Extreme Events over Northern and Tropical Africa". In: *J. Clim.* 25 (17), pp. 5748–5767.

Vogel, A., Scherer-Lorenzen, M., and Weigelt, A. (2012). "Grassland resistance and resilience after drought depends on management intensity and species richness". en. In: *PLoS One* 7 (5), e36992.

Wainwright, C. M., Finney, D. L., Kilavi, M., Black, E., and Marsham, J. H. (2021). "Extreme rainfall in East Africa, October 2019–January 2020 and context under future climate change". In: *Weather* 76 (1), pp. 26–31.

Walz, Y., Janzen, S., Narvaez, L., Ortiz-Vargas, A., Woelki, J., Doswald, N., and Sebesvari, Z. (2021). "Disaster-related losses of ecosystems and their services. Why and how do losses matter for disaster risk reduction?" en. In: *Int. J. Disaster Risk Reduct.* 63 (102425), p. 102425.

Wang, S., Chen, W., Xie, S. M., Azzari, G., and Lobell, D. B. (2020). "Weakly Supervised Deep Learning for Segmentation of Remote Sensing Imagery". en. In: *Remote Sensing* 12 (2), p. 207.

Wang, X., Yue, Y., and Faraway, J. J. (2018). *Bayesian Regression Modeling with INLA*. en. 1st ed. Chapman and Hall/CRC.

Wang, Z., Deng, X., Song, W., Li, Z., and Chen, J. (2017). "What is the main cause of grassland degradation? A case study of grassland ecosystem service in the middle-south Inner Mongolia". In: *Catena* 150, pp. 100–107.

Ward, A. I. (2005). "Expanding ranges of wild and feral deer in Great Britain". en. In: *Mamm. Rev.* 35 (2), pp. 165–173.

Warton, D. I., Blanchet, F. G., O'Hara, R. B., Ovaskainen, O., Taskinen, S., Walker, S. C., and Hui, F. K. C. (2015). "So many variables: Joint modeling in community ecology". en. In: *Trends Ecol. Evol.* 30 (12), pp. 766–779.

Waters, C. N. and Turner, S. D. (2022). "Defining the onset of the Anthropocene". en. In: *Science* 378 (6621), pp. 706–708.

Western, D., Mose, V. N., Worden, J., and Maitumo, D. (2015). "Predicting Extreme Droughts in Savannah Africa: A Comparison of Proxy and Direct Measures in Detecting Biomass Fluctuations, Trends and Their Causes". en. In: *PLoS One* 10 (8), e0136516.

Wheatley, C. J., Beale, C. M., Bradbury, R. B., Pearce-Higgins, J. W., Critchlow, R., and Thomas, C. D. (2017). "Climate change vulnerability for species-Assessing the assessments". en. In: *Glob. Chang. Biol.* 23 (9), pp. 3704–3715.

Wheatley, C. J., Beale, C. M., White, P. C. L., Villaseñor, A., Sanchez, A., Cunningham, C. A., and Hill, J. K. (2023). "Revising vulnerability assessments of montane birds in the colombian páramo to account for threats from climate change". en. In: *Biodivers. Conserv.*, pp. 1–16.

Whitecross, M. A., Witkowski, E. T. F., and Archibald, S. (2017). "Savanna tree-grass interactions: A phenological investigation of green-up in relation to water availability over three seasons". en. In: *S. Afr. J. Bot.* 108, pp. 29–40.

Wickham, H. (2011). "ggplot2". en. In: *Wiley Interdiscip. Rev. Comput. Stat.* 3 (2), pp. 180–185.

Wiedenfeld, D. A. et al. (2021). "Conservation resource allocation, small population resiliency, and the fallacy of conservation triage". en. In: *Conserv. Biol.* 35 (5), pp. 1388–1395.

Wiens, J. J. (2016). "Climate-related Local Extinctions Are Already Widespread among Plant and Animal Species". en. In: *PLoS Biol.* 14 (12), e2001104.

Wiethase, J. H., Critchlow, R., Foley, C., Foley, L., Kinsey, E. J., Bergman, B. G., Osujaki, B., Mbwambo, Z., Kirway, P. B., Redeker, K. R., Hartley, S. E., and Beale, C. M. (2023). "Pathways of degradation in rangelands in Northern Tanzania show their loss of resistance, but potential for recovery". en. In: *Sci. Rep.* 13 (1), p. 2417.

Wiethase, J. H., Mostert, P. S., Cooney, C. R., O'Hara, R. B., and Beale, C. M. (2024). "Spatio-temporal integrated Bayesian species distribution models reveal lack of broad relationships between traits and range shifts". en. In: *Glob. Ecol. Biogeogr.*, e13819.

Williams, J. E. and Blois, J. L. (2018). "Range shifts in response to past and future climate change: Can climate velocities and species' dispersal capabilities explain variation in mammalian range shifts?" en. In: *J. Biogeogr.* 45 (9), pp. 2175–2189.

Williams, S. E., Shoo, L. P., Isaac, J. L., Hoffmann, A. A., and Langham, G. (2008). "Towards an integrated framework for assessing the vulnerability of species to climate change". en. In: *PLoS Biol.* 6 (12), pp. 2621–2626.

Willis, S. G., Foden, W., Baker, D. J., Belle, E., Burgess, N. D., Carr, J. A., Doswald, N., Garcia, R. A., Hartley, A., Hof, C., Newbold, T., Rahbek, C., Smith, R. J., Visconti, P., Young, B. E., and Butchart, S. H. M. (2015). "Integrating climate change vulnerability assessments from species distribution models and trait-based approaches". en. In: *Biol. Conserv.* 190 (C), pp. 167–178.

Wilsey, C., Taylor, L., Bateman, B., Jensen, C., Michel, N., Panjabi, A., and Langham, G. (2019). "Climate policy action needed to reduce vulnerability of conservation-reliant grassland birds in North America". en. In: *Conservat Sci and Prac* 1 (4), e21.

Wisz, M. S. et al. (2013). "The role of biotic interactions in shaping distributions and realised assemblages of species: implications for species distribution modelling". en. In: *Biol. Rev. Camb. Philos. Soc.* 88 (1), pp. 15–30.

Wonkka, C. L., Twidwell, D., Franz, T. E., Taylor, C. A., and Rogers, W. E. (2016). "Persistence of a Severe Drought Increases Desertification but not Woody Dieback in Semiarid Savanna". en. In: *Rangeland Ecol. Manage.* 69 (6), pp. 491–498.

Wüest, R. O., Zimmermann, N. E., Zurell, D., Alexander, J. M., Fritz, S. A., Hof, C., Kreft, H., Normand, S., Cabral, J. S., Szekely, E., Thuiller, W., Wikelski, M., and Karger, D. N. (2020). "Macroecology in the age of Big Data – Where to go from here?" en. In: *J. Biogeogr.* 47 (1), pp. 1–12.

Wulder, M. A. et al. (2019). "Current status of Landsat program, science, and applications". en. In: *Remote Sens. Environ.* 225, pp. 127–147.

Wynne, R. H. and Campbell, J. B. (2011). *Introduction to remote sensing, fifth edition*. Not Avail. 667 pp.

Xiong, J., Thenkabail, P. S., Tilton, J. C., Gumma, M. K., Teluguntla, P., Congalton, R. G., Yadav, K., Dungan, J., Oliphant, A. J., and Poehnelt, J. (2017). "NASA Making Earth System Data Records for Use in Research Environments (MEaSUREs) Global Food Security-support Analysis Data (GFSAD) Cropland Extent 2015 Africa 30 m V001". In.

Yalcin, S. and Leroux, S. J. (2017). "Diversity and suitability of existing methods and metrics for quantifying species range shifts". en. In: *Glob. Ecol. Biogeogr.* 26 (6), pp. 609–624.

Yamazaki, D., Ikeshima, D., Sosa, J., Bates, P. D., Allen, G. H., and Pavelsky, T. M. (2019). "MERIT Hydro: A High-Resolution Global Hydrography Map Based on Latest Topography Dataset". en. In: *Water Resour. Res.* 55 (6), pp. 5053–5073.

Yang, L., Zhang, X., Liang, S., Yao, Y., Jia, K., and Jia, A. (2018). "Estimating Surface Downward Shortwave Radiation over China Based on the Gradient Boosting Decision Tree Method". en. In: *Remote Sensing* 10 (2), p. 185.

Yang, X., Wang, Y., Si, X., and Feng, G. (2020). "Species traits linked with range shifts of Chinese birds". In: *Glob. Ecol. Conserv.* 21, e00874.

Yang, Y., Fang, J., Ma, W., and Wang, W. (2008). "Relationship between variability in aboveground net primary production and precipitation in global grasslands". en. In: *Geophys. Res. Lett.* 35 (23).

Zeileis, A. and Grothendieck, G. (2005). "zoo: S3 Infrastructure for Regular and Irregular Time Series". In: *arXiv:math/0505527*. Comment: 24 pages, 5 figures.

Zhang, G. (2020). "Spatial and temporal patterns in volunteer data contribution activities: A case study of eBird". en. In: *ISPRS Int. J. Geoinf.* 9 (10), p. 597.

Zhou, Y., Varquez, A. C. G., and Kanda, M. (2019). "High-resolution global urban growth projection based on multiple applications of the SLEUTH urban growth model". en. In: *Sci. Data* 6 (1), p. 34.

Zurell, D., Fritz, S. A., Rönnfeldt, A., and Steinbauer, M. J. (2023). "Predicting extinctions with species distribution models". en. In: *Camb. prisms Extinction* 1 (e8).